

**SYNTHESIS AND PROPERTIES OF NEW CARBOSILANE  
COPOLYMERS AND SYMMETRICAL BIS(ALKOXY- BENZYLIDENE)-  
1,5-NAPHTHALENE DIMERS BASED ON BISPHENOL  
SCHIFF BASE MONOMERS**

**WISAM NAJI ATIYAH AL-MEHANA**

**FACULTY OF SCIENCE  
UNIVERSITY OF MALAYA  
KUALA LUMPUR**

**2015**

**SYNTHESIS AND PROPERTIES OF NEW CARBOSILANE  
COPOLYMERS AND SYMMETRICAL BIS(ALKOXY- BENZYLIDENE)-  
1,5-NAPHTHALENE DIMERS BASED ON BISPHENOL  
SCHIFF BASE MONOMERS**

**WISAM NAJI ATIYAH AL-MEHANA**

**THESIS SUBMITTED IN FULFILLMENT OF THE REQUIREMENTS  
FOR THE DEGREE OF DOCTOR OF PHILOSOPHY**

**DEPARTMENT OF CHEMISTRY  
FACULTY OF SCIENCE  
UNIVERSITY OF MALAYA  
KUALA LUMPUR**

**2015**

**UNIVERSITY OF MALAYA**  
**ORIGINAL LITERARY WORK DECLARATION**

Name of Candidate: WISAM NAJI ATIYAH AL-MEHANA

Registration/ Matric No: SHC100012

Name of Degree: DOCTOR OF PHILOSOPHY

Title of Project Paper/Research Report/Dissertation/Thesis:

Synthesis and properties of new carbosilane copolymers and symmetrical bis(alkoxy-benzylidene)-1,5-naphthalene dimers based on bisphenol schiff base monomers

Field of Study: Polymer chemistry

I do solemnly and sincerely declare that:

- (1) I am the sole author/writer of this work.
- (2) This work is original.
- (3) Any use of any work in which copyright exists was done by way of fair dealing and for permitted purposes and any excerpt or extract from, or reference to or reproduction of any copyright work has been disclosed expressly and sufficiently and the title of the work and its authorship have been acknowledged in this work.
- (4) I do not have any actual knowledge nor ought I reasonably to know that the making of this work constitutes an infringement of any copyright work.
- (5) I hereby assign all and every rights in the copyright to this work to the University of Malaya ("UM"), who henceforth shall be owner of the copyright in this work and that any reproduction or use in any form or by any means whatsoever is prohibited without the written consent of UM having been first had and obtained.
- (6) I am fully aware that if in the course of making this work I have infringed any copyright whether intentionally or otherwise, I may be subject to legal action or any other action as may be determined by UM.

Candidate's Signature:

Date:

Witness's Signature:

Name:

Date:

Designation:

## ABSTRAK

Satu siri baru kopolimer karbosilana bisfenol azina dengan kumpulan-kumpulan pengganti yang berbeza (penderma- dan/atau penarik-elektron) (**Pa1-Pa6**) telah berjaya disintesis melalui tindak balas polikondensasi menggunakan bis(klorometil) dimetilsilana. Berat molekul purata-nombor kopolimer adalah antara 2322 dan 9805, dan indeks polisebaran antara 1.04 dan 2.1. Monomer menunjukkan keterlarutan yang baik dalam DMSO dan DMF dan kopolimer mempamerkan keterlarutan yang sangat baik dalam pelarut organik umum (THF,  $\text{CHCl}_3$  dan DMF) tetapi tidak larut dalam pelarut yang mengandungi kumpulan hidroksil ( $\text{CH}_3\text{OH}$  dan  $\text{C}_2\text{H}_5\text{OH}$ ). Semua kopolimer menunjukkan kestabilan terma yang baik dengan suhu pada kehilangan berat 10% yang lebih tinggi daripada  $265.96^\circ\text{C}$  di bawah nitrogen. Kopolimer mempamerkan penyerapan UV-vis yang kuat dalam DMF cair dengan  $\lambda_{\text{maks}}$  pada 318-351 nm dan keputusan foto-pondarcahayaan menunjukkan foto-pondarcahayaan sederhana di kawasan biru dengan  $\lambda_{\text{maks}}$  pada 416-422 nm. Daripada pengukuran voltammetri siklik (CV) jurang jalur elektrokimia ( $E_g$ ) yang dikira berada di bawah 2.00 eV. Pengaruh kumpulan pengganti terhadap berat molekul dan semua sifat fizikal telah dikaji. Selepas polikarbosilana baru berasaskan monomer bisfenol azina berkonjugat penuh berjaya disintesis, polikarbosilana baru yang berkonjugasi lebih tinggi telah disintesis (**Pb1-Pb7**) berasaskan bes bis-Schiff 1,4-fenilena dan 1,5-naftalena. Berat molekul purata-nombor kopolimer adalah antara 2401 dan 7414, dan indeks polisebaran antara 1.21 and 2.04. Kopolimer mempamerkan keterlarutan yang baik dalam pelarut organik umum

(THF,  $\text{CHCl}_3$  dan DMF) dan keterlarutan separa dalam pelarut yang mengandungi kumpulan hidroksil ( $\text{CH}_3\text{OH}$  dan  $\text{C}_2\text{H}_5\text{OH}$ ). Semua kopolimer menunjukkan kestabilan terma lebih tinggi berbanding dengan kopolimer karbosilana yang mengandungi azina dengan suhu pada kehilangan berat 10% yang lebih tinggi daripada  $324^\circ\text{C}$  di bawah nitrogen. Kopolimer mempamerkan penyerapan UV-vis kuat dalam DMF cair, di mana kopolimer yang mengandungi 1,4-fenilena muncul sebagai dua puncak pada  $\lambda_{\text{maks}}$  pada 287-365 nm dan kopolimer yang mengandungi 1,5-naftalena muncul sebagai tiga puncak pada  $\lambda_{\text{maks}}$  273-363 nm. Keputusan foto-pendarcahayaan menunjukkan pendarcahayaan sederhana di kawasan biru dengan  $\lambda_{\text{maks}}$  pada 416-429 nm. HOMO dan LUMO telah disiasat untuk kopolimer ini untuk menganggarkan jurang jalurnya. Jurang jalur elektrokimia ( $E_g$ ) yang dikira berada antara 2.23-2.54 eV. Di samping itu, dua siri baru dimer homolog bersimetri, N,N-bis(4-alkoksi-benzilidena)-1,5-naftalenadiimina yang dikumpulkan sebagai siri (c) dan N,N-bis(3-metoksi-4-alkoksi-benzilidena)-1,5-naftalenadiimina yang dikumpulkan sebagai siri (d) dengan kumpulan alkil hujung sama sekata tetapi berbeza panjangnya iaitu dari butil hingga oktadakil telah disintesis dan dicirikan. Sifat mesomorfik sebatian ini telah disiasat melalui pengimbasan pembezaan kalorimetri dan mikroskopi polarisasi optik. Suatu kelakuan fasa-peralihan yang pelbagai diperhatikan bagi anggota siri (c) yang boleh dikaitkan dengan konformasi molekul yang mungkin. Sebatian dengan panjang rantai dalam lingkungan  $\text{C}_6\text{H}_{13}$  hingga  $\text{C}_{12}\text{H}_{33}$  menunjukkan fasa smektik C manakala  $\text{C}_{14}\text{H}_{29}$  dan  $\text{C}_{16}\text{H}_{33}$  mempamerkan fasa smektik dan nematik. Dimer yang mengandungi moiety butil dan

oktadekil tidak mempamerkan sifat mesogenik. Manakala, siri (d) tidak menunjukkan sebarang fasa hablur cecair disebabkan oleh pengaruh kumpulan metoksi pada molekul. Semua sebatian dalam siri (c) mempunyai kestabilan termal yang tinggi dan tidak menunjukkan penguraian ketara di bawah 400°C dalam keadaan nitrogen. Keputusan UV-vis menunjukkan puncak kuat pada 281-283 nm dan puncak lemah pada 362-363 nm dan puncak pendarfluor sebatian yang terhasil adalah dalam kawasan merah pada 516-518 nm. Struktur kimia sebatian yang disintesis telah disahkan melalui FT-IR,  $^1\text{H}$ ,  $^{13}\text{C}$  NMR, 2D NMR dan kristalografi X-Ray.

## ABSTRACT

A series of new carbosilane bisphenol azine copolymers with different substituted groups (electron-donating and/or withdrawing) (**Pa1-Pa6**) were successfully synthesized by polycondensation reaction using bis(chloromethyl) dimethylsilane. The number-average molecular weights of the copolymers were between 2322 and 9805, and the polydispersity index between 1.04 and 2.10. The monomers showed good solubility in DMSO and DMF except for **a5** and **a6** which required high temperature to dissolve and the copolymers exhibited excellent solubility in common organic solvents (THF, CHCl<sub>3</sub> and DMF) but insoluble in hydroxyl-group containing solvents (CH<sub>3</sub>OH and C<sub>2</sub>H<sub>5</sub>OH). All the copolymers showed good thermal stabilities with their temperatures at 10% weight loss being higher than 265.96°C under nitrogen. The copolymers exhibited strong UV-vis absorptions in dilute DMF with  $\lambda_{\text{max}}$  at 318-351 nm and photoluminescence results showed a medium photoluminescence in the blue region with  $\lambda_{\text{max}}$  at 416-422 nm. From cyclic voltammetry (CV) measurements the electrochemical band gaps ( $E_g$ ) calculated were below 2.00 eV. The influence of the substitution groups on the molecular weight and all the physical properties was studied.

After successfully synthesized the new polycarbosilanes based on the full conjugated bisphenol azine monomers, newly higher conjugation of polycarbosilanes were synthesised (**Pb1-Pb7**) based on 1,4-phenylene and 1,5-naphthalene bis-Schiff base. The number-average molecular weights of the copolymers were between 2401 and 7414, and the polydispersity index between 1.21 and 2.04. The copolymers exhibited

excellent solubility in common organic solvents (THF, CHCl<sub>3</sub> and DMF) and partially dissolving in hydroxyl-group containing solvents (CH<sub>3</sub>OH and C<sub>2</sub>H<sub>5</sub>OH). All the copolymers showed higher thermal stabilities compared to the carbosilane copolymers containing azines with their temperatures at 10% weight loss being higher than 324°C under nitrogen. The copolymers exhibited strong UV-vis absorptions in dilute DMF, where the copolymers containing 1,4-phenylene appeared as two peaks at  $\lambda_{\text{max}}$  287-365 nm and the copolymers containing 1,5-naphthalene appeared as three peaks at  $\lambda_{\text{max}}$  273-363 nm. Photoluminescent results showed a medium photoluminescence in the blue region with  $\lambda_{\text{max}}$  at 416-429 nm. The HOMO and LUMO were investigated for these copolymers to estimate the band gaps. In addition, two new series of homologous symmetrical dimers *N,N*-bis(4-alkoxy-benzylidene)-1,5-naphthalenediimine grouped as series (c) and *N,N*-bis(3-methoxy-4-alkoxy-benzylidene)-1,5-naphthalenediimine grouped as series (d) with different lengths of terminal alkyl groups of even parity ranging from butyl to octadecyl were synthesized and characterized. The mesomorphic properties of these compounds were investigated via differential scanning calorimetry and optical polarizing microscopy. A diversified phase-transition behavior was observed for the members of series (c) which could be attributed to the possible molecular conformations. Compounds with chain length in a range of C<sub>6</sub>H<sub>13</sub> to C<sub>12</sub>H<sub>25</sub> showed smectic C phase while C<sub>14</sub>H<sub>29</sub> and C<sub>16</sub>H<sub>33</sub> displayed smectic and nematic phase. The dimers containing butyl and octadecyl moiety did not display mesogenic properties. Meanwhile, series (d) did not exhibit any liquid crystalline phase due to the effect of

methoxy group on molecule. All of the compounds in the first series (**c1-c8**) have high thermal stability and did not show significant decomposition below 400°C in nitrogen atmosphere. UV-Vis results showed strong peak at 281-283 nm and weak peak at 362–363 nm and fluorescent peak of the resultant compound was in the red region at 516–518 nm. The chemical structures of synthesized compounds were confirmed by FT-IR,  $^1\text{H}$ ,  $^{13}\text{C}$  NMR, 2D NMR and X-Ray crystallography.

University of Malaya

## ACKNOWLEDGMENTS

It was impossible to write this thesis without the great help and support of the kind people around me, to only some of whom it is possible to give particular, mention here, for those people, whose names may not appear here, their efforts and help will still be in mind forever.

With a deep sense of gratitude and respect, I would like to thank my supervisor Professor Dr. Rosiyah Yahya for her guidance, support and encouragement to my work until the end this thesis. Special thanks and grateful will go to Dr. Raied Mustafa Shakir for all advices, helpful discussions and his opinions.

I would like to extend my thanks and gratitude to Dr. Faridah Sunsudin and Mr. Zulkifli Abu Hasan for the valuable assistance provided for completion of this thesis. Also I wish to express my appreciation to NMR staff, Miss Norzalida Zakaria, Dara Fiona, Suwing eh Vit, Mr. Fateh Ngaliman and Nordin Mohamad. I would like to acknowledge the financial, academic and technical support of the University of Malaya especially for the UM research grants PS372/2010B and ERGS/2012A for the financial support.

Furthermore I would like to thank Dr. Rusnah for her advice. Also great thanks to Assoc. Prof. Dr Lo Ko Mun for X-ray analysis. I sincerely thank all my friends for all support they have provided me during this research, especially Dr. Noordini Mohamad, Abu Ubaidah Alsadon, Tammar Hussein Ali, Ali Jaffar Witwit, Ali Mohamad Abdulamir, and Ahmad Danial. Furthermore, I will remember for everyone in my group and my PhD colleagues in the Department of Chemistry for the real brotherhood and friendship that they showed me along the period of PhD study.

Love and respect without limits to my father, mother, my beloved wife Dr. Manar, my sweet heart son Ali Wisam, my sisters and brothers especially my brother Dr. Hussain whose have given me their unequivocal support throughout, as always, for which my mere expression of thanks likewise does not suffice.

University of Malaya

## TABLE OF CONTENTS

ABSTRAK .....	ii
ABSTRACT .....	v
ACKNOWLEDGMENTS .....	viii
TABLE OF CONTENTS .....	x
LIST OF FIGURES .....	xv
LIST OF TABLES .....	xix
LIST OF APPENDICES .....	xxiv
<b>CHAPTER 1 : INTRODUCTION AND LITERATURE REVIEW .....</b>	<b>1</b>
<b>1.1 Introduction .....</b>	<b>1</b>
<b>1.2 Types of silicon-containing polymers .....</b>	<b>4</b>
1.2.1 Polysiloxane .....	4
1.2.2 Polysiloles .....	6
1.2.3 Polysilanes .....	7
1.2.4 Polysilazines.....	8
1.2.5 Polysilynes .....	9
1.2.6 Polysilylacetylenes.....	9
1.2.6 Polycarbosilanes.....	11
<b>1.3 Schiff base containing polymers .....</b>	<b>16</b>
1.3.1 Synthesis of Schiff base polymers .....	19
1.3.1.1 Polymerization of Schiff base compounds by polycondensation reaction.....	19
1.3.1.2 Polymerization of Schiff base monomers by chemical and electro- chemical oxidation .....	22
1.3.2 Some properties of Schiff base containing polymer.....	23
1.3.2.1 Thermal properties.....	23
1.3.2.2 Mechanical properties.....	24
<b>1.4 Motivation .....</b>	<b>25</b>
<b>1.5 Objectives of this research thesis.....</b>	<b>25</b>

<b>CHAPTER 2 : EXPERIMENTAL</b> .....	<b>28</b>
<b>2.1 Materials</b> .....	<b>28</b>
<b>2.2 Synthesis of monomers</b> .....	<b>29</b>
2.2.1 Synthesis of azine monomers ( <b>a1-a6</b> ) .....	29
2.2.2 Synthesis of bisphenol bis-Schiff base monomers containing 1, 4-phenylene ( <b>b1-b4</b> ) .....	33
2.2.3 Synthesis of bisphenol bis-Schiff base monomers containing 1,5-naphthalene ( <b>b5-b8</b> ).....	35
<b>2.3 Synthesis of copolymers</b> .....	<b>39</b>
Synthesis of copolymer, <b>Pa1</b> .....	40
Synthesis of copolymer, <b>Pa2</b> .....	40
Synthesis of copolymer, <b>Pa3</b> .....	41
Synthesis of copolymer, <b>Pa4</b> .....	41
Synthesis of copolymer, <b>Pa5</b> .....	42
Synthesis of copolymer, <b>Pa6</b> .....	42
Synthesis of copolymers, <b>Pb1</b> .....	43
Synthesis of copolymer, <b>Pb2</b> .....	43
Synthesis of copolymer, <b>Pb3</b> .....	44
Synthesis of copolymer, <b>Pb4</b> .....	44
Synthesis of copolymer, <b>Pb5</b> .....	45
Synthesis of copolymer, <b>Pb6</b> .....	45
Synthesis of copolymer, <b>Pb7</b> .....	46
<b>2.4 Characterization methods and instrumentation</b> .....	<b>46</b>
2.4.1 Fourier Transform Infrared Spectroscopy (FTIR).....	46
2.4.2 Nuclear Magnetic Resonance Spectroscopy ( <sup>1</sup> H NMR, <sup>13</sup> C NMR and 2D NMR).....	47
2.4.3 Thin Layer Chromatography (TLC).....	48
2.4.4 Gel Permeation Chromatography (GPC) .....	48
2.4.5 Thermogravimetric Analysis (TGA) .....	49
2.4.6 Differential Scanning Calorimetry (DSC).....	49
2.4.7 Polarised Optical Microscopy (POM).....	50
2.4.8 X-Ray Crystallography .....	50

2.4.9	Ultraviolet-Visible (UV-Visible) and Photoluminescence Spectroscopies .....	51
2.4.10	Electrochemical measurement.....	51

### **CHAPTER 3 : CARBOSILANE COPOLYMERS BASED ON BISPHENOL AZINE**

#### **MONOMERS ..... 53**

##### **3.1 Introduction ..... 53**

##### **3.2 Results and discussion ..... 53**

###### 3.2.1 Synthesis route of bisphenol azine monomers (**a1-a6**) ..... 53

###### 3.2.2 Characterizations of the azine monomers ..... 54

###### 3.2.2.1 Fourier transform infrared (FTIR) ..... 55

###### 3.2.2.2 <sup>1</sup>H NMR..... 57

###### 3.2.2.3 <sup>13</sup>C NMR..... 58

###### 3.2.2.4 The 2DNMR..... 60

###### 3.2.2.5 X-ray crystallography..... 62

###### 3.2.2 Carbosilane bisphenol azine copolymers (**Pa1-Pa6**)..... 66

###### 3.2.3 Mechanism of Williamson etherification ..... 67

###### 3.2.4 Characterization of copolymers ..... 68

###### 3.2.4.1 FTIR ..... 68

###### 3.2.4.2 <sup>1</sup>H NMR..... 69

###### 3.2.4.3 <sup>13</sup>C NMR..... 70

###### 3.2.4.4 Gel permeation chromatography (GPC) ..... 71

##### **3.3 Physical properties ..... 74**

###### 3.3.1 Thermal properties ..... 74

###### 3.3.2 Optical properties..... 76

###### 3.3.3 Electrochemical properties..... 78

### **CHAPTER 4 : CARBOSILANE COPOLYMERS BASED ON BISPHENOL BIS-SCHIFF**

#### **BASE MONOMERS ..... 82**

##### **4.1 Introduction ..... 82**

<b>4.2 Results and discussion .....</b>	<b>82</b>
4.2.1 Synthetic route of bisphenol bis-Schiff base monomers (Schiff base formation) .....	82
4.2.1.1 Synthesis of Schiff base monomers containing 1,4-phenylene.....	83
4.2.1.2 Characterization of Schiff base monomers containing 1,4-phenylene.....	84
4.2.1.3 Synthesis of bis-Schiff base monomers containing 1,5-naphthalene .....	89
4.2.1.4 Characterization of Schiff base containing 1,5-naphthalene.....	90
4.2.2 Carbonosilane bisphenol bis-Schiff base copolymers .....	94
4.2.3 Characterization of copolymers .....	96
4.2.3.1 FTIR .....	96
4.2.3.2 <sup>1</sup> H NMR.....	97
4.2.3.3 <sup>13</sup> C NMR.....	98
4.2.3.4 Gel permeation chromatography (GPC) .....	98
<b>4.3 Physical properties .....</b>	<b>99</b>
4.3.1 Thermal degradation properties of copolymers.....	99
4.3.2 Optical properties.....	101
4.3.3 Electrochemical properties.....	103
 <b>CHAPTER 5: LIQUID CRYSTAL OF SYMMETRICAL DIMERS BASED ON BISPHENOL BIS-SCHIFF BASE.....</b>	 <b>106</b>
<b>5.1 Introduction .....</b>	<b>106</b>
<b>5.2 Historical development of liquid crystals.....</b>	<b>108</b>
<b>5.3 Types of liquid crystals.....</b>	<b>110</b>
5.3.1 Calamitic liquid crystals.....	111
5.3.1.1 Nematic Phase .....	113
5.3.1.2 Smectic phase .....	113
<b>5.4 Structure-mesomorphic properties relationship.....</b>	<b>114</b>
5.4.1 Influence of mesogenic core on mesomorphic properties .....	115
5.4.2 Influence of terminal unit on mesomorphic properties .....	116
5.4.3 Influence of linking unit on mesomorphic properties .....	118

5.4.4	Influence of lateral unit on mesomorphic properties.....	119
<b>5.5</b>	<b>Liquid crystals with Schiff bases .....</b>	<b>119</b>
<b>5.6</b>	<b>Experimental.....</b>	<b>121</b>
5.6.1	Synthesis of symmetrical dimers.....	121
5.6.2	Synthesis of the symmetrical dimers containing 4,4'-(naphthalene 1,5-diylbis(azan-1-yl-1-ylidene))bis(methan-1-yl-1-ylidene) diphenol ( <b>b8</b> ).....	122
5.6.3	Synthesis of the symmetrical dimers containing 4,4'-(naphthalene 1,5-diylbis(azan-1-yl-1-ylidene))bis(methan-1-yl-1-ylidene)bis(2methoxyphenol) ( <b>b5</b> ).....	125
<b>5.7</b>	<b>Results and discussion .....</b>	<b>129</b>
5.7.1	Characterization of the symmetrical dimers.....	131
5.7.1.1	FTIR .....	131
5.7.1.2	<sup>1</sup> H NMR.....	132
5.7.1.3.	<sup>13</sup> C NMR.....	134
5.7.2	Thermal degradation properties .....	136
5.7.3	Optical properties .....	138
5.7.4	Thermal behavior and textural observation.....	140
<b>CHAPTER 6 :</b>	<b>CONCLUSIONS AND SUGGESTION FOR FUTURE STUDIES .....</b>	<b>148</b>
<b>6.1</b>	<b>Conclusions.....</b>	<b>148</b>
<b>6.2</b>	<b>Suggestion for further research.....</b>	<b>151</b>
<b>REFERENCES</b>	<b>.....</b>	<b>152</b>
<b>APPENDICES</b>	<b>.....</b>	<b>171</b>

## LIST OF FIGURES

Figure 1.1: Basic structures of organosilicon polymers[3] .....	3
Figure 1.2 : Structure of polysiloxane.....	5
Figure 1.3 : (a) Siloxane polymer used in tubing and catheters for medical applications[19].....	6
Figure 1.4 : Synthesis of polysiloles .....	7
Figure 1.5 : Synthesis of polysilanes[43].....	8
Figure 1.6: Complex oligomer of polysilazane[47] .....	9
Figure 1.7: Synthesis of polysilylacetylene[68].....	11
Figure 1.8 : Synthesis of poly carbosilane[71] .....	12
Figure 1.9 : Synthesis of disilacyclobutanes[76] .....	13
Figure 1.10 : Synthesis of polycarbosilane with high molecular weight[76].....	13
Figure 1.11: Synthesis of poly carbosilane by the ring opening polymerization method[77] ...	14
Figure 1.12 : Synthesis of polycarbosilane containing anthracene moiety[78] .....	15
Figure 1.13 : General structure of Schiff base .....	16
Figure 1.14 : (a) Polyazomethines, (b) Poly(p-phenylenevinylene), (c) Polyazines[110]. .....	18
Figure 1.15: The structures of the Schiff base monomers used in polymerization by chemical and electrochemical oxidation[129]. .....	23
Figure 3.1 : General synthetic route of bisphenol azine monomer .....	54
Figure 3.2 : FTIR spectrum of monomer <b>a2</b> .....	56
Figure 3.3 : <sup>1</sup> H NMR spectrum of monomer <b>a3</b> .....	58
Figure 3.4 : <sup>13</sup> C NMR spectrum of monomer <b>a3</b> .....	59
Figure 3.5: HMQC expansion region of monomer <b>a2</b> .....	60
Figure 3.6 : The HMBC spectrum of monomers <b>a2</b> .....	61
Figure 3.7 : The molecular structure of 4,4 -(1E,1 E)-1,2-diylidenebis(methan-1-yl-1-ylidene) bis(2-ethoxyphenol) showing 50% probability displacement ellipsoids. Hydrogen atoms are drawn as spheres of arbitrary radius. ....	62

Figure 3.8 : A view of the two-dimensional supramolecular network in the title compound showing the O—H•••N hydrogen bonds (in red dotted lines).....	63
Figure 3.9 : Ellipsoidal plot of the molecular structure of <b>a4</b> with 50% probability. ....	64
Figure 3.10 : Ellipsoidal plot of the molecular structure of <b>a5</b> with 50% probability. ....	64
Figure 3.11 : Synthetic route of copolymers ( <b>Pa1-Pa6</b> ).....	66
Figure 3.12 : (a) <b>Pa2</b> (b) <b>Pa4</b> (c) <b>Pa6</b> .....	67
Figure 3.13 : Mechanism of the Williamson etherification of copolymers .....	68
Figure 3.14 : FTIR spectrum of copolymer <b>Pa3</b> .....	69
Figure 3.15 : <sup>1</sup> H NMR spectrum of copolymer <b>Pa2</b> .....	70
Figure 3.16: <sup>13</sup> C NMR spectrum of copolymer <b>Pa3</b> .....	71
Figure 3.17 : Raw GPC chromatogram of copolymer <b>Pa3</b> .....	72
Figure 3.18 : The suggesting mechanism of donating substituent group of copolymer <b>Pa2</b> .....	73
Figure 3.19 : The suggesting mechanism of copolymer <b>Pa1</b> .....	74
Figure 3.20 : TGA curves of copolymer ( <b>Pa2</b> ) with its derivative .....	76
Figure 3.21 : UV-Vis absorption spectral traces of the selected copolymers ( <b>Pa1, Pa3, and Pa5</b> ) .....	77
Figure 3.22 : Photoluminescence emission spectral of copolymers <b>Pa1, Pa3 and Pa4</b> .....	78
Figure 3.23: Cyclic voltammogram of <b>Pa2</b> in CH <sub>3</sub> CN at scan rate 50 mV s <sup>-1</sup> .....	81
Figure 4.1 : Reaction mechanism of Schiff base.....	83
Figure 4.2 : Synthetic route of Schiff base monomers containing 1,4-phenylene group.....	84
Figure 4.4 : <sup>13</sup> C NMR spectrum of monomer <b>b2</b> .....	88
Figure 4.5 : Synthetic route of bis-Schiff base monomers containing 1,5-naphthalene .....	89
Figure 4.6 : <sup>1</sup> H NMR spectrum of compound <b>b5</b> .....	92
Figure 4.7 : <sup>13</sup> C NMR spectrum of monomer <b>b5</b> .....	94
Figure 4.8 : Synthetic route of copolymers ( <b>Pb1-Pb7</b> ).....	95
Figure 4.9 : (a) <b>Pb2</b> copolymer (b) <b>Pb4</b> copolymer (c) <b>Pb7</b> copolymer .....	96

Figure 4.10: $^1\text{H}$ NMR spectrum of copolymer <b>Pb2</b> .....	97
Figure 4.11 : $^{13}\text{C}$ NMR spectrum of copolymer <b>Pb2</b> .....	98
Figure 4.12 : TGA curves for copolymer ( <b>Pb3</b> ) at a heating rate of $10^\circ\text{C}/\text{min}$ .....	101
Figure 4.13 : UV-vis absorption spectral traces of the copolymers <b>Pb2</b> and <b>Pb5</b> .....	102
Figure 4.14 : Photoluminescence emission spectral of copolymers <b>Pb2</b> , <b>Pb5</b> and <b>Pb6</b> .....	103
Figure 4.15 : Cyclic voltammogram of <b>Pb3</b> in $\text{CH}_3\text{CN}$ at scan rate $50 \text{ mV s}^{-1}$ .....	105
Figure 5.1 : A comparison of the ordering of the crystal, liquid crystal and liquid states. ....	106
5.5.2 : Structure of cholesteryl benzoate with two melting points.....	108
Figure 5.3 : Molecular structure of MBBA.....	109
Figure 5.4 : Classification of liquid crystals .....	111
Figure 5.5 : Basic structure of typical calamitic liquid crystals .....	112
Figure 5.6 : Texture and molecular arrangement of nematic liquid crystals.....	113
Figure 5.7 : Molecular arrangements of (a) smectic A (b) smectic C.....	114
Figure 5.8 : The structures of thermotropic liquid crystals with core unit of (a) monophenyl, (b) biphenyl and (c) phenyl benzoate[205].....	116
Figure 5.9 : Studied compound [208] .....	117
Figure 5.10 : Azo benzothiazole compound[209].....	117
Figure 5.11 : Synthesis of compounds containing azomethine and ester.....	118
Figure 5.12 : Structure of symmetrical dimer containing bis-Schiff base linking group[217].	120
Figure 5.13 : A series of Schiff base compound containing naphthalene group[227]. ....	120
Figure 5.14 : General structures of the symmetrical dimers of series (c) and (d).....	121
Figure 5.14 : Synthetic route of symmetrical dimers.....	130
Figure 5.16: FT-IR spectra of the symmetrical dimers (a) <b>c2</b> , (b) <b>c4</b> and (c) <b>c6</b> .....	131
Figure 5.17 : $^1\text{H}$ NMR spectrum of monomer containing naphthalene <b>b8</b> .....	133
Figure 5.18 : $^1\text{H}$ NMR spectrum of dimer containing naphthalene <b>c2</b> .....	134
Figure 5.19 : $^{13}\text{C}$ NMR spectrum of dimer containing naphthalene <b>b8</b> .....	135

Figure 5.20 : $^{13}\text{C}$ NMR spectrum of dimer containing naphthalene <b>c2</b> .....	136
Figure 5.21 : (a) Thermograms of <b>c2</b> , <b>c4</b> , <b>c6</b> and <b>c7</b> , (b) DTG of <b>c2</b> , <b>c4</b> , <b>c6</b> and <b>c7</b> . .....	138
Figure 5.22 : UV-Vis absorption spectra of compounds <b>c3</b> , <b>c5</b> and <b>c7</b> .....	140
Figure 5.23 : PL spectra of compounds <b>c3</b> , <b>c5</b> , and <b>c7</b> in THF solution.....	140
Figure 5.24 : (a) The crystal texture on cooling taken at 79°C, (b) schlieren texture of smectic C at 128°C while (c) is showing schlieren texture for nematic phase on cooling at 158°C for compound <b>c6</b> .....	142
Figure 5.25 : DSC trace of compound <b>c4</b> .....	143
Figure 5.26 : DSC trace of compound <b>c6</b> .....	144
Figure 5.27 : Thermotropic behaviors as a function of alkyl chain length for series (c) and (d). .....	144
Figure 5.28 : DSC trace of compound <b>d6</b> .....	145

## LIST OF TABLES

Table 1.1: Some dicarbonyl and diamine compounds used for synthesis of polyimines.....	19
Table 3.1 : Details of the synthesized bisphenol azine monomers .....	54
Table 3.2 : Some of the important FT-IR spectra data of azine monomers .....	56
Table 3.3: <sup>1</sup> H NMR data of azine monomers ( <b>a1-a6</b> ).....	58
Table 3.4: <sup>13</sup> C NMR data of bisphenol azine monomers ( <b>a1-a6</b> ) .....	59
Table 3.5 : Crystal data and structure refinement for <b>a4</b> and <b>a5</b> .....	65
Table 3.6 : Hydrogen bonds for <b>a4</b> and <b>a5</b> [Å and deg.] .....	65
Table 3.7: Percentage yield and characteristics of the synthesized copolymers.....	71
Table 3.8 : Thermal properties of copolymers.....	75
Table 3.9 : UV-Vis Absorption and PL emission spectral data of copolymers .....	78
Table 3.10 : Electrochemical data of the copolymers.....	80
Table 4.1 : Details of the synthesized bisphenol bis-Schiff base monomers containing 1,4- phenylene group .....	84
Table 4.2 : Some of the important FTIR spectra data of monomers.....	85
Table 4.3: <sup>1</sup> H NMR data of monomers ( <b>b1-b4</b> ).....	86
Table 4.4 : <sup>13</sup> C NMR data of monomers ( <b>b1-b4</b> ).....	88
Table 4.5 : Details of the synthesized bisphenol bis-Schiff base monomers containing 1,5- naphthalene group .....	90
Table 4.6 : Some of the important FTIR spectra data of monomers.....	91
Table 4.7 : <sup>1</sup> H NMR data of monomers ( <b>b5-b8</b> ).....	92
Table 4.8 : <sup>13</sup> C NMR data of monomers ( <b>b5-b8</b> ).....	93
Table 4.9 : Details of the synthesized copolymers containing bisphenol bis-Schiff base monomers ( <b>Pb1-Pb7</b> ).....	95
Table 4.10 : Yields, colors and characteristics of the synthesized copolymers .....	99
Table 4.11 : Thermal properties of copolymers ( <b>Pb1-Pb7</b> ).....	100

Table 4.12 : UV-vis Absorption and photoluminescence emission spectral data of copolymers. .....	103
Table 4.13 : Electrochemical results of the copolymers ( <b>Pb1-Pb7</b> ).....	105
Table 5.1 : <sup>1</sup> H NMR chemical shifts of dimers (c1-c8) .....	133
Table 5.2 : <sup>13</sup> C NMR chemical shifts of compounds (c1-c8).....	135
Table 5.3 : Thermal analysis data of the symmetrical dimers (c1-c8). .....	137
Table 5.4 : UV-vis absorption and PL emission spectral data of the symmetrical dimer (c1-c8) .....	139
Table 5.5 : Phase transitions, Temperature and transition enthalpy changes for compounds (c1– c8) and (d6 and d7).....	141
Table 2.1: GPC calibration data for 4 <sup>th</sup> order non-linear Fitting vial standard molecular .....	202

## LIST OF ABBRIVATIONS AND SYMBOLS

ATR	Attenuated total reflectance
$\text{CDCl}_3$	Deuterated Chloroform
$\text{CH}_3\text{CN}$	Acetonitrile
$\text{CH}_3\text{COOH}$	Glacial acetic acid
$\text{CHCl}_3$	Chloroform
CV	Cyclic Voltmetry
DMAC	N,N-dimethylacetamide
DMF	N,N-dimethylformamide
DMSO	Dimethyl sulfoxide
$\text{DMSO-d}^6$	Deuterated dimethyl sulfoxide
DSC	Differential Scanning Calorimetry
$E_g$	Band gap
FT-IR	Fourier Transform Infrared Spectroscopy
GPC	Gel Permeation Chromatography
$\text{H}_2\text{SO}_4$	Sulphuric acid
HCl	Chloride acid
HMBC	Heteronuclear Multiple-Bond Correlation
HMPA	Hexamethyl phosphoramide

HMQC	Heteronuclear Multiple-Quantum Correlation
HOMO	Highest Occupied Molecular Orbital
$K_2CO_3$	Potassium carbonate
LC	Liquid crystalline
LUMO	Lowest Unoccupied Molecular Orbital
M.p.	Melting point
Mn	Number average molecular weight
MBBA	N-(4-methoxybenzylidene)-4-butylaniline
Mw	Weight average molecular weight
NMP	N-methylpyrrolidone
NMR	Nuclear Magnetic Resonance Spectroscopy
PAMs	Polyazomethines
PAZs	Polyazines
PDFMS	Polydifluorosilylene methylene
PDI	Polysdispersity index
PIS	Polyimines
POM	Polarised Optical Microscopy
ppm	Parts per million
ROP	Ring opening polymerization

$T_d$	Decomposition temperature
TFDSCB	1,1,3,3-tetrafluoro-1,3-disilacyclobutane
$T_g$	Glass transition temperature
TGA	Thermogravimetric Analysis
THF	Tetrahydrofuran
TLC	Thin Layer Chromatography
TMS	Tetramethylsilane
UV-vis	Ultra Violet Visible
$ZnCl_2$	Zinc chloride

## LIST OF APPENDICES

APPENDIX A: $^1\text{H}$ NMR Figures.....	173
APPENDIX B: $^{13}\text{C}$ NMR Figures .....	187
APPENDIX C: TGA Figures .....	202
APPENDIX D: Calibration of GPC.....	203

University of Malaya

# CHAPTER 1 : INTRODUCTION AND LITERATURE REVIEW

## 1.1 Introduction

The development in science and synthesis of new materials are equally significant, thus continuously we need new materials for development. In addition, the advancement of technology requires design and synthesis of new materials. Significant progress in all fields of technology depends almost entirely on the rate at which useful new materials can be synthesized and designed. Polymer material is one major of the classical areas in the field of materials science. This field is very important because of their broad application in modern life such as medicine, electronics technology, elastomers, films, structural materials and the wide range of fibre.

Polymers are very-long-chain macromolecules made by linking together smaller compounds, called monomers, through covalent bonds. The long-chain character of the polymer makes these materials different compared to other small molecules. This character allows the chain to become entangled in the solid state or in solution or for specific macromolecular structures, to become lined up in regular arrays in the solid state. The characteristics of these materials give rise to solid state materials properties, such as elasticity, strength, film forming, or fiber-forming qualities properties, that are not found in the system of small molecules.

Polymers can be classified into two large categories, biopolymers and synthetic polymers. Biopolymers are polymers that occur naturally in organisms, examples are DNA, RNA, proteins, and polysaccharides. Synthetic polymers are materials that can be prepared in laboratory with specific properties which is very important in commercial products in today's economy.

Silicon-containing polymers are one of the important synthetic polymers which have wide spectrum applications. In fact, the significance of pure grade silicon compound is

important for the entire electronic industry, especially for computers, etc. as we could say we are living in a "Silicon Age" in comparison to the "Bronze Age" or the "Ceramic Age" of the past. Silicon-based materials, consisting of backbones and surface-capped atoms or pendants, have been considered in the field of both chemistry and physics. In the former, the focus has been on inorganic silicon materials (amorphous silicon, crystalline silicon, nanoparticles and porous silicon). Nitrogen containing silicon namely silicon nitride has become a progressively important industrial product[1] and organic silicon materials such as polyorganosilanes, polysilanes, oligosilicones, polysilylenes and cyclosilanes are shown to exhibit interesting physical properties[2].

There are many types of polymers containing silicon depending on the atom that is attached directly to the silicon atom as shown in Figure 1.1, i.e. polysiloxanes or silicones 1, polycarbosilanes or poly(silylene methylenes) 2, polysilazanes 3, polysilanes 4, polysilynes 5, poly(silylene ethenes) 6, poly(silylene ethynes) 7, poly(silylene butadiyenes) 8, poly(silylene phenylenes) 9, and poly(silyleneheteroarylenes) 10[3]. These materials have unique optoelectronic properties which are attributed to the conjugation occurring along the silicon main chain; hence, they are extremely sensitive to the polymer conformation and to the substituent attached to the polymer backbone.

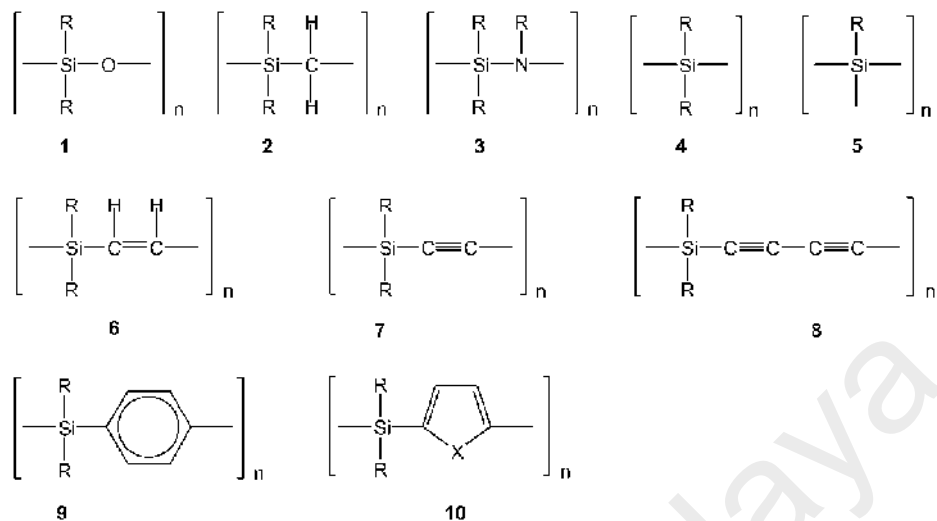


Figure 1.1: Basic structures of organosilicon polymers[3]

Currently, there is a growing interest in oligomers and polymers whose backbone is composed of an alternating arrangement of an organosilane unit and a  $\pi$ -conjugated unit. Their unique properties ascribed to the interaction between the  $\sigma$ -orbital of the oligosilane units and the  $\pi$ -orbital ( $\sigma$ -conjugation), and also to  $\pi$ -donation from the silicon units to the  $\pi$ -systems can lead to their potential use as highly functionalized materials such as photoresists, organic semiconductors in their doped states, and heat-resistant materials[4]. Furthermore, it has been demonstrated that the substitution of silicon into a  $\pi$ -electron system in these compounds enhances the luminescent properties[5] and thus, several attempts have been made to prepare Si- $\pi$  alternating polymers, which constitute a new class of organic photo and electroluminescent materials as mention in this chapter.

On the other hand, polymers having extended  $\pi$ -conjugated units are usable as excellent hole-transporting materials in multi-layered light emitting devices. In those polymers, the electron-donating organosilanylne units would elevate the HOMO energy levels of the  $\pi$ -conjugated units to enhance hole affinity of the polymers. Also, polymers with highly conjugated chains occupy significant position in the development

of new materials in the last few years because of their broad variety of properties and applications. Many works have been reported on high conjugated systems of type polyphenylene vinylenes, polyphenylene, polyactetylene, polyaniline, polypyrrole, or polythiophene[6-11].

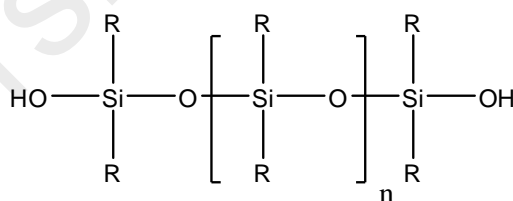
## **1.2 Types of silicon-containing polymers**

There have been considerable interests in the chemistry of silicon-containing polymers that can use as functional materials. To date, several types of containing-silicone polymers have been synthesized and studied depending on the atom that has been attached directly to the silicon atom in the backbone of the polymers. Each of these polymers has certain physical properties and applications. In this chapter, we will describe some of the most important types of these polymers.

### **1.2.1 Polysiloxane**

Polysiloxanes or (silicones) contain silicon atom attach to the oxygen atom (Si-O) in the main chain. Currently, siloxane polymers are the most important and unique materials among inorganic and semi-inorganic polymers due to their unique physical and chemical properties. The unique properties of polysiloxane arise from the unusual features of the backbone. For instance, the unsubstituted O atom and the substituted Si atom differ greatly in size, giving the polymer a very irregular cross section. This influences the way the chains are packed in the bulk, amorphous state, which in turn, gives the polymer the unusual equation-of-state properties (such as compressibilities). In addition, the chemical characteristics and the nature of the bonding of typical side groups between these atoms give the chains a very low surface free energy and consequently, unusual and desirable surface properties. For this reason polysiloxanes are used as waterproofing garments, mould-release agents and biomedical materials. Furthermore, siloxane backbones display a number of remarkable configurational

characteristics due to the bond angles around the O atom being much larger than those around the Si atom, which makes the planar all trans form of the chain approximate a series of closed polygons[12]. A broad range of applications for polysiloxanes have been studied because the polymers have good thermal, oxidative, biological and chemical stabilities and are commercially readily available[13]. For example, highly thermal stability[14] of these polymers make them very important for their use in high temperature applications such as heat transfer agents and high performance elastomers[12]. Taking advantage of the inertness of siloxane polymer, polysiloxanes have been developed for many medical applications such as artificial organ, prostheses, vitreous substitutes in the eyes, tubing and catheters, and object for facial reconstruction[15-19], as well as contact lenses, artificial skin, and drug-delivery system utilize their high permeability [20-22]. Beside, polysiloxanes have many non-medical applications which include electrical insulator, anti-foaming agent, adhesive, protective coating, microlithographic[23-27] and liquid crystal materials[28]. Figure 1.2 shows the general structure of polysiloxane.



R= Organic moiety

Figure 1.2 : Structure of polysiloxane

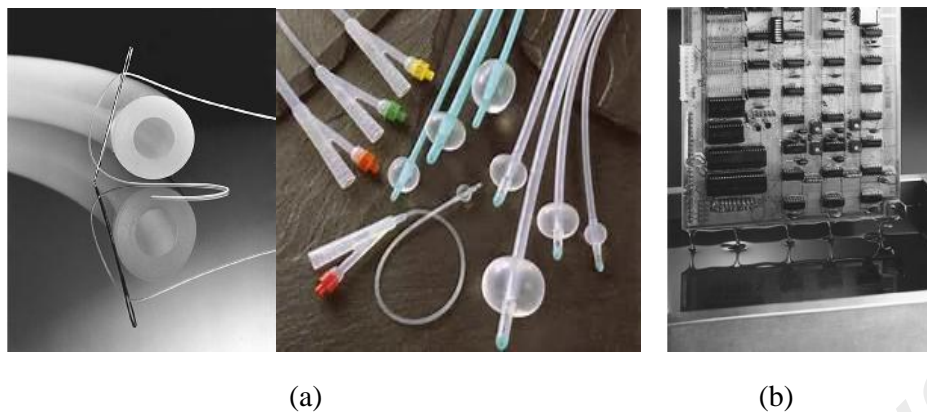


Figure 1.3 : (a) Siloxane polymer used in tubing and catheters for medical applications[19]

(b) An electronic circuit board being given a protective polysiloxane coating[29].

### 1.2.2 Polysiloles

Polysiloles are a relatively new type of silicon-containing polymers consisting of a five-membered silacycle in their back bone which may structurally be viewed as cyclopentadiene derivative with its carbon bridge replaced by a silicon atom, hence the name silacyclopentadiene[30]. This type of silicon-containing polymer has recently received a lot of interest because of the unique aspects of their synthesis and reaction chemistry as well as the novel photophysical and electronic properties such as high fluorescent efficiency[31], strong electron affinity[32], thermal stability[30], chemical stability and photostability, as well the relatively small energy band gap between their LUMO and HOMO level and the predictable unusual electronic behavior due to the orbital interaction between the  $\sigma^*$ -orbital of the silole silicon atom and the  $\sigma^*$ -orbital of the pentadiene fragment[32, 33]. These novel properties make siloles ideal candidates for components in light emitting devices[34, 35]. Siloles have also been investigated as chemical sensors for nitroaromatic and other types of explosives[36].

In 1999, Honglea Shon *et al.*[37] prepared the first compound of polysilole homopolymer whereby silicon in atom in the polymer chain is also part of silole ring.

This polymer was easily obtained by reduction of 1,1-dichlorotetraphenylsilole with lithium, sodium or potassium in THF, as shown in Figure 1.4, to get the polysilole of a moderate molecular weight,  $M_n=5500$  with polydispersity= 1.1.

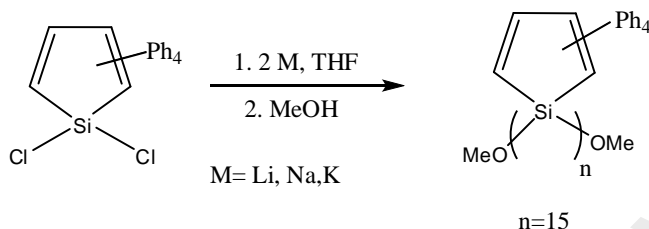


Figure 1.4 : Synthesis of polysiloles

### 1.2.3 Polysilanes

Polysilanes are polymers based on inorganic elements which contain Si-Si catenation in the backbone thus allowing extensive electron delocalization to take place. This delocalization of the sigma-electrons in the Si-Si moiety in the main chain leads to unique physical properties such as conductivity, strong electronic absorption, electroluminescence, photoconductivity, photosensitivity, and so on, which are crucial for many technological applications of polysilanes[12, 38, 39]. Furthermore, the nature of the organic groups attached to silicon atoms in the main chain plays a very important role in determining the properties of this type of polymer. Polysilanes have a broad applications such as photoconducting[40], photoinitiators, precursors to silicon carbide, photoresists for microelectronics[12], electrical conducting[41] and nonlinear optical materials[42].

The first clear description of a polymeric product involving catenated silicon atom was described in a classic paper by Burkhard in 1949[43]. He prepared poly(dimethylsilane)  $[\text{Me}_2\text{Si}]_n$  by combining 450 g of sodium metal with 700 g of  $\text{Me}_2\text{SiCl}_2$  and one liter of benzene, sealed them in an autoclave and heated the mixture

(200°C) under high pressure to produce the polysilane polymer. Figure 1.5 shows the preparation of polysilanes polymer.

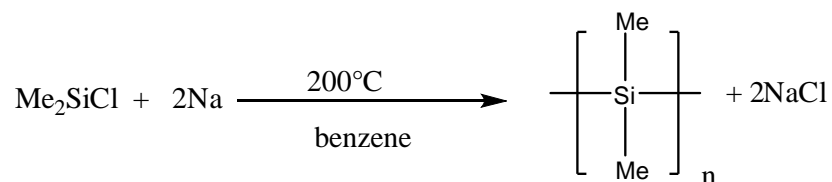


Figure 1.5 : Synthesis of polysilanes[43]

#### 1.2.4 Polysilazines

Polysilazines are an important class of silicon-containing polymers that contain silicon and nitrogen atom on their main chain. Since each silicon atom is bound to two separate nitrogen atoms and each nitrogen atom bound to two silicon atoms, both rings and chains of the formula  $[\text{R}_1\text{R}_2\text{Si-NR}_3]_n$  occur. There are two common designs of these types of polymers which is dependent on R in the formula; if all substituents R are H atoms the polymer is called polyperhydrosilazane, perhydropolysilazanes or inorganic polysilazane with formula  $[\text{H}_2\text{Si-NH}]_n$ . If all the substituents R bound to silicon atom are hydrocarbons, the polymer will be polyorganosilazanes or polycarbosilazines[43]. The most important application for polysilazines are for use in ceramic materials, where the polysilazines have been shown to be very good polymeric precursors (after pyrolyzed) to silicon nitride or SiNC ceramic material due to the toughness, strength, good stability to aggressive chemicals, and high thermal stability of these materials[44, 45].

The first synthesis of polyorganosilazane was described in 1964 by Kruger and Rochow[46]. Chlorosilane was reacted with ammonia in a dry organic solvent at high temperatures with catalyst to yield high molecular weight polymer. In 1974, Varbeek and Winter[47, 48] prepared a complex oligomer, as shown in Figure 1.6, by reacting methylamine or ammonia with methyltrichlorosilane. This species could be melt-spun

to form preceramic fibers which, when cross-linked, pyrolyzed to amorphous silico-carbo-nitride fibers.

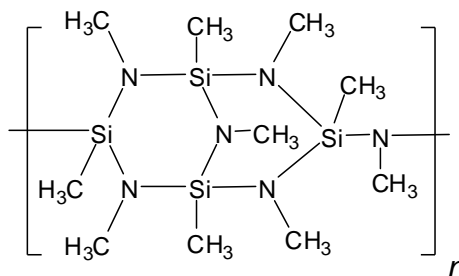


Figure 1.6: Complex oligomer of polysilazane[47]

### 1.2.5 Polysilynes

Polysilynes are relatively new class of silicon-containing polymers which in each silicon is bonded via silicon-silicon bond to the main chain, and attach to one R substituent ( $[\text{RSi}]_n$  R=Alkyl) to yield silicon-based network backbone polymers. These materials have been recently studied and investigated because of their  $\pi$ -conjugated three-dimensional network backbone which displays many physical and chemical properties such as optical, electronic and preceramic[49-51]. They have also been studied as low band-gap energy semiconducting silicon-based materials[52], photo-patternable thin-film waveguide[53, 54], photoresists for 193 nm photolithography[55], models for luminescent properties of amorphous silicon[56]. Polysilynes have also been studied as precursors for silicon-based ceramics, such as silicon carbide[57], amorphous silicon films[58], silica, and mixture of these three[59].

### 1.2.6 Polysilylacetylenes

Polysilylacetylenes are polymers that consist of the acetylene and silicon-containing unit in the backbone. These types of acetylenes containing silicon polymers have been the subject of intensive research interest in the recent years[60]. In the particular, types that contain  $\pi$ -conjugated silylacetylene systems functionalized with

phenylene, biphenylene anthrylene or oligothiénylene bridges together with Si residues in the backbone have been extensively investigated with regards to their applications in electro- and optical devices[61, 62]. They have been shown to display unique electric and optical properties such as semiconducting properties in their doped state, high hole-transporting for electroluminescence, photoresists and red shifted UV absorptions[60, 63, 64]. Additionally, they have also been studied for enhancing the thermal stability of the polymers[65, 66], and Homrighausen and Keller have successfully synthesized high temperature elastomers of these polymers[67].

M. Yan *et al*[68] in 2006 had synthesized various novel polymers that contain diacetylene moieties and nitrogen atoms in the main chain by aminolysis and condensation of the corresponding  $\alpha, \omega$ -dichlorodiorganosilylenediacetylene oligomers as shown in Figure 1.7. The synthesized polysilylacetylene showed high thermal stability and excellent properties due to the conjugated silicon-containing polymer besides exhibiting good optical and electrical properties. The presence of nitrogen atom in the polymer main chain also enhances the other properties of these polymers such as solubility, flexibility and processability. Due to their highly heat-resistant and processable light-weight, polysilylacetylenes show high potential for applications in the aerospace and microelectronic[67].

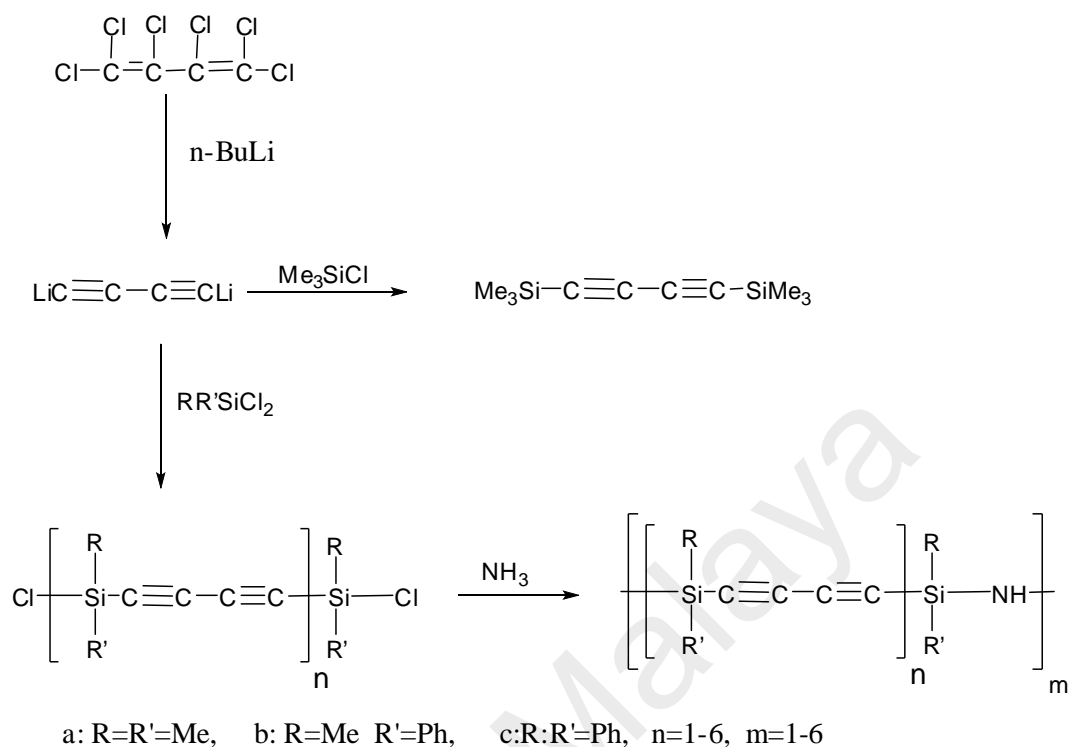


Figure 1.7: Synthesis of polysilylacetylene[68]

### 1.2.6 Polycarbosilanes

Carbosilane chemistry (as an inherent part of organometallic chemistry) is one of the most rapidly developing fields of science. These polymers are a wide class of silicon-containing polymers in which silicon atom is attached to carbon atom in the main chain of the polymer. In nature, there are many well-known polymeric and inorganic compounds containing silicon. However, since Kipping's pioneer work at the beginning of the 20<sup>th</sup> century, researchers have oriented their focus on materials containing silicon and carbon in the main chain of the polymers, rather than on purely organic or inorganic polymers. Recently, carbosilane copolymers have garnered the interest of researchers due to their enhanced material properties, which cannot be attained by inorganic polymers based on silicon alone or organic polymers based on carbon alone. The uniqueness of polycarbosilanes has centered on their high thermal stability, good electrical resistance, low surface tension, release and lubricating

properties, high hydrophobicity, low glass transition, and low toxicity for natural environment[69, 70].

In 1975, Yajima *et al.* prepared the most important member of this family by the thermolysis of poly(dimethylsilane),  $[\text{Me}_2\text{Si}]_n$  at  $450^\circ\text{C}$  under argon atmosphere to yield  $[(\text{H})(\text{CH}_3)\text{SiCH}_2]_n$ . Figure 1.8 displays the synthesis of polycarbosilane from polysilanes. The significance of this polymer come from the fact that it can be spun into fibers, cross-linked by heating in air at around  $300^\circ\text{C}$  and transformed by pyrolysis at  $1200^\circ\text{C}$  under nitrogen to silicon carbide fibers impregnated with silicon carbide crystallites[71-75]. This pioneering work has in fact inspired much of the research on polycarbosilanes.

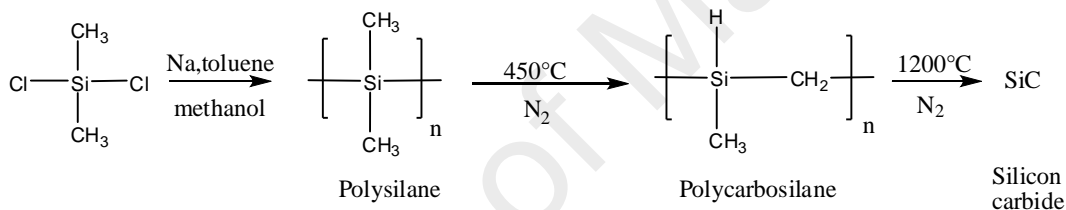


Figure 1.8 : Synthesis of poly carbosilane[71]

Interrante *et al.* in 1990's developed an elegant synthetic route for polymers containing alternate  $\text{R}_2\text{Si}$  and  $\text{CH}_2$  units. These polymers are called poly-(silylenemethylene)s or polysilaethylenes. The new route to prepare these polymers was by using a platinum ( $\text{H}_2\text{PtCl}_6$ )-catalyzed ring-opening polymerization of the four-membered 1,3-disilacyclobutanes. These monomeric inorganic rings can be formed in many ways. Thus, the reduction of  $\text{Cl}(\text{OEt})_2\text{SiCH}_2\text{Cl}$  with magnesium produce an alkoxydisilacyclobutane as intermediate product and then converted to the corresponding tetrachloro derivative by treatment with acetylchloride. The chlorine atoms on the silicon can be replaced by alkyl moieties by the corresponding Grignard reagent. These disilacyclobutanes have been found to be ideal substrate for ring-opening

polymerization[76]. Figure 1.9 shows the preparation of disilacyclobutanes by using Grignard reagent.

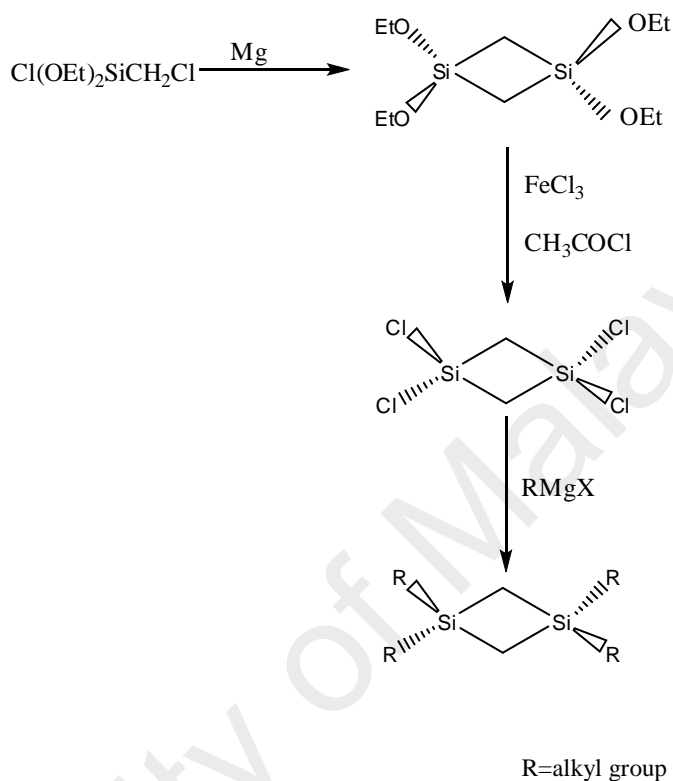


Figure 1.9 : Synthesis of disilacyclobutanes[76]

Tetrachlorodisilacyclobutane can be ring-opened to produce the polymeric  $[\text{Cl}_2\text{SiCH}_2]_n$  derivative. By reducing this polymer with  $\text{LiAlH}_4$  can afford  $[\text{H}_2\text{SiCH}_2]_n$  with a high molecular weight of approximately 80,000 as illustrated in Figure 1.10.

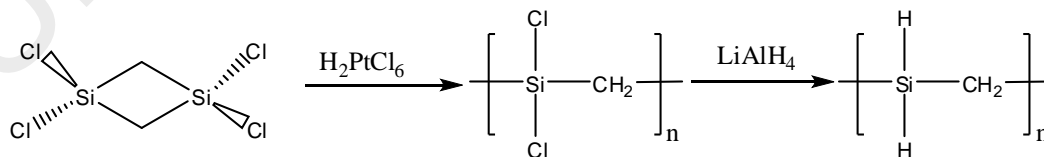


Figure 1.10 : Synthesis of polycarbosilane with high molecular weight[76]

Lienhard *et al.* in 1997 successfully prepared monosilicon analog of polydifluorosilylenemethylene (PDFSM),  $[\text{F}_2\text{SiCH}_2]_n$ , by a different method. This

polymer was prepared by the ring opening polymerization (ROP) of disilacyclobutanes. Two different approaches, both involving ROP of a disilacyclobutane monomer were used. In the first approach, the 1,1,3,3-tetraethoxydisilacyclobutane was polymerized directly by ROP using a platinum complex as a catalyst to afford the linear polymer polydiethoxysilylenemethylene followed by reaction with excess  $\text{BF}_3 \cdot \text{Et}_2\text{O}$  to afford PDFMS with high molecular weight of about 22000/5800 ( $M_w/M_n$ ). Figure 1.11 displays the synthesis of polycarbosilane by the first approach of ring opening polymerization.

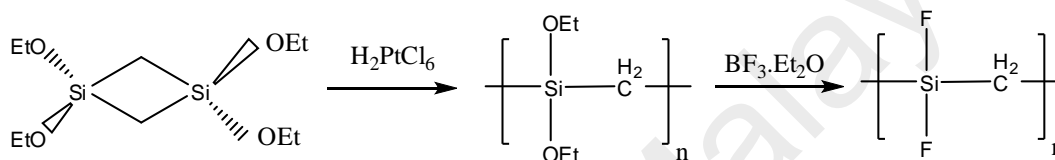


Figure 1.11: Synthesis of poly carbosilane by the ring opening polymerization method[77]

The second approach simply reversed the order of these fluorination and ROP reactions beginning with the same tetraethoxydisilacyclobutane as starting material. In this approach, solvent and neat  $\text{BF}_3 \cdot \text{Et}_2\text{O}$  as the fluorinating agent were employed for the first reaction to produce 1,1,3,3-tetrafluoro-1,3-disilacyclobutane (TFDSCB) in very good yield (70%). The pure TFDSCB was then subjected to polymerization process at  $120^\circ\text{C}$  by using a platinum complex catalyst in a hydrocarbon solvent[77].

In 2000, Sacarescu G. *et al.* [78] synthesized a new class of polycarbosilane containing anthracene moiety with good yield and good molecular weight through the coupling reaction of dimethyldichlorosilanes, methylphenyl-dichlorosilanes, methyldichlorosilanes with dichlorodihydrodisilaanthracene using sodium dispersion in toluene and equimolar reactants ratios as shown in Figure 1.12. In the first stage, in the presence of a large excess of sodium organometallic derivative, the coupling reactions have led to dichlorodihydroanthracene oligosilanes with low molecular weights. In the second

stage, the disproportionation reactions in the presence of the remaining organometallic compound and in an inert atmosphere and room temperature, have led to substituted polycarbosilanes with increasing molecular weights. The molecular weight and the organic moieties content in polycarbosilanes were strongly dependent on the amount of the organometallic derivative in the reaction mixture.

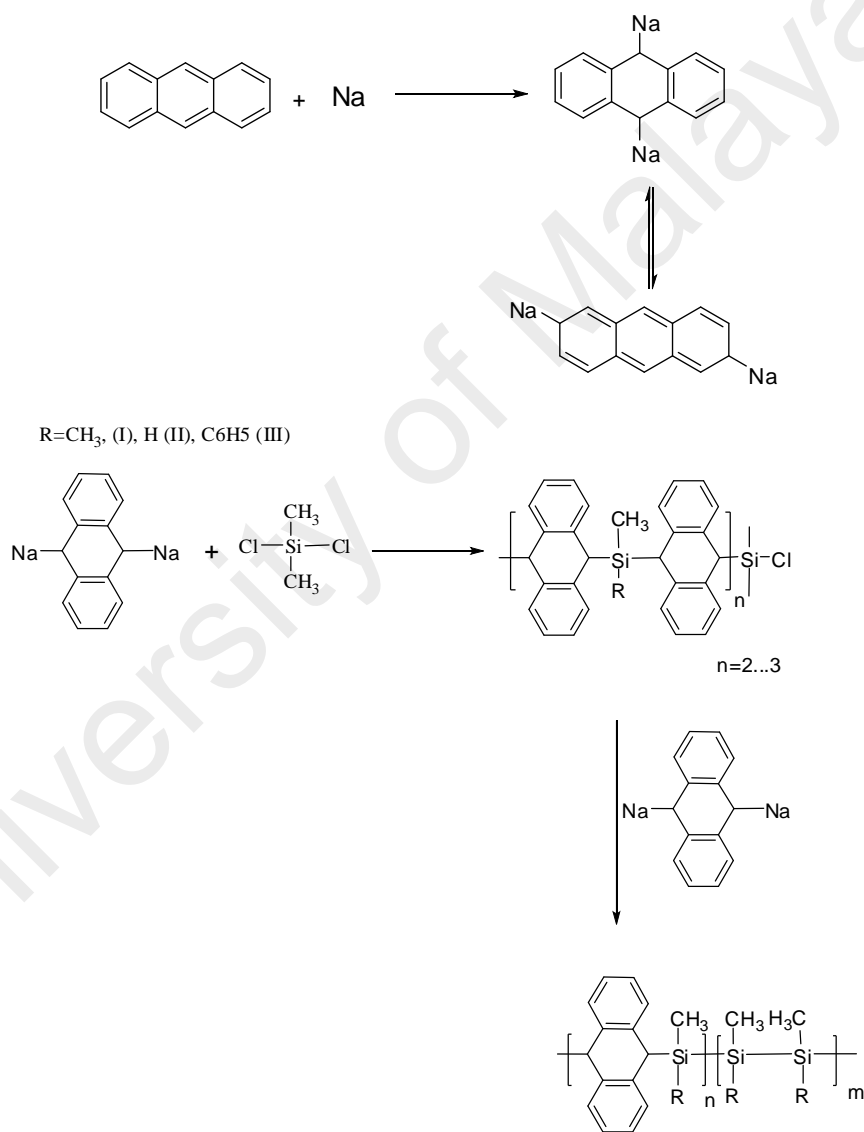
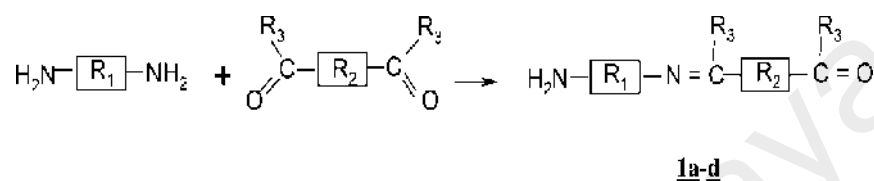


Figure 1.12 : Synthesis of polycarbosilane containing anthracene moiety[78]

### 1.3 Schiff base containing polymers

Polymers containing Schiff base are a class of polymer family which has been less reviewed and are known as polyimines (PIs). The polymers are synthesized by polycondensation reaction between hydrazine or diamine with diketone or dialdehyde to obtain one of the following structures (1a-d), Figure 1.13.



R<sub>1</sub>, R<sub>2</sub> and R<sub>3</sub> can be:

R <sub>1</sub>	R <sub>2</sub>	R <sub>3</sub>	Polymer
<i>n=1</i>	Aryl or alkyl	H	<u>1a</u>
Aryl or alkyl	Aryl or alkyl	H	<u>1b</u>
<i>n=1</i>	Aryl or alkyl	Aryl or alkyl	<u>1c</u>
Aryl or alkyl	Aryl or alkyl	Aryl or alkyl	<u>1d</u>

Figure 1.13 : General structure of Schiff base

These polymers are also known as polyazines (PAZs, 1a) or polyazomethines (PAMs, 1b) when hydrazine and diamines, respectively, are used in reactions with dialdehyde compounds and polyketazines (1c) or polyketamines (1d) when diketones are used as dicarbonyl compounds in reaction with hydrazine or diamines. Schiff bases with aryl substituents are more readily synthesized and more stable than those containing aliphatic aldehyde which is relatively unstable and readily polymerizable. The reason of the stability of aryl containing azomethine is due to the effective conjugation of the aryl moiety which makes these compounds more stable. Due to variation in their structures and molecular properties these types of compounds have been widely investigated. The unique combination of an unsaturated carbon-nitrogen double bond and the formation of pseudoaromatic rings (six-membered rings with the presence of double bonds) enables this intramolecular bond to be exceptionally strong

in some cases[79, 80]. The intramolecular hydrogen bonds are useful model systems due to their thermodynamic and structural stabilities, which allow study of proton transfer depending on temperature or solvent polarity[81]. Furthermore, proton transfer process is important in the mechanisms of various chemical reactions, including enzyme catalysis[82, 83], photochromic[84] and thermochromic[85] properties of Schiff bases and also the mechanism of proton transport in biological systems[86]. Investigations of such hydrogen bonds and related molecular features are interesting for understanding of various biologically and technically relevant properties at the microscopic level.

Generally, Schiff base materials have attracted much interest as they are found to have potential in biological and pharmaceutical applications such as anticancer[87], HIV-1[88], antioxidants[89], antimicrobial[90-92], antiparasitic[93], antibacterial and antifungal[94]. Furthermore, in industrial field, these compounds exhibited wide physical properties like liquid crystal [95-98] for liquid crystal displays, good thermal stability for use as solid stationary phase in gas chromatography[99], pigments and dyes, catalysts, as hole transport materials for organic electronic devices[100], intermediates in organic synthesis and as polymer stabilizers[101]. In modern technology, it is used for the preparation of nonlinear optical (NLO) materials[102].

Schiff base polymers date back to 1923, where Adams *et al.*[103] synthesized the first polymer containing Schiff base by a polycondensation reaction between benzidine and di-anisidine with isophthalaldehyde and terephthalaldehyde. Many researchers had tried to synthesize Schiff base polymers. In 1935 Steingkopf and Eger[104] reacted hydrazine with terephthalaldehyde and isophthalaldehyde in the molten state to yield an infusible and insoluble product. In 1950s Marval and Hill[105] tried the synthesis of PIs by solution polycondensation of aromatic dialdehydes with *o*-phenylenediamine and hydrazine by using different solvents such as acetic acid, benzene and dimethylacetamide as reaction media. However, this polymerization

process failed as the product precipitated out of the reaction media very rapidly, leading to very low molecular weight polymer; which was insoluble in all solvents except in concentrated sulfuric acid. In late 1960s and early 1970s, PIs started to be the subject of a systematic study beginning with the pioneering work of D' Alelio *et al.*[106, 107] as a result of the strong interest in thermally stable polymers for aircraft applications. They synthesized many polyazomethines in various reaction schemes, including the melt polymerization of aromatic diamines with aromatic dialdehydes and the amine with carbonyl. In the last few years, classes of these polymers have been developed. For example, aromatic PAMs, Figure 1.14 (a), are used as isoelectronic with poly(p-phenylenevinylene) and, Figure 1.14 (b), are used as electroluminescent[108, 109] polymer while PAZ, Figure 1.14 (c), synthesized from hydrazine and glyoxal, is a nitrogen containing analog of polyacetylene, in which the latter is considered as the most known conducting organic polymer[110]. However, unlike polyacetylene which is unstable, PAZ is thermally stable and is not oxidized in air.

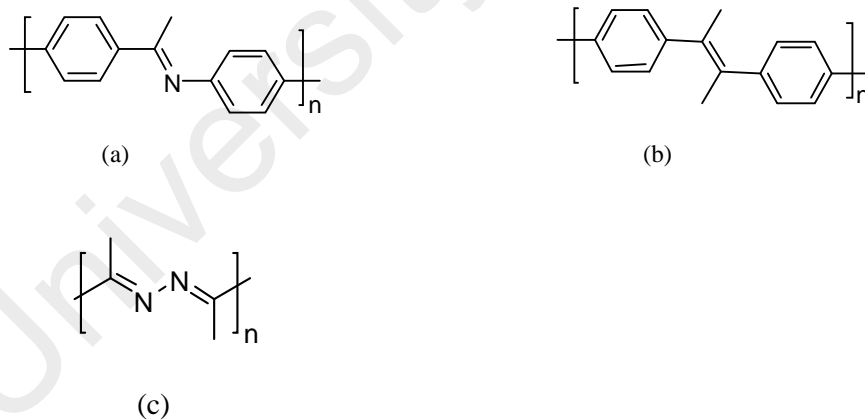


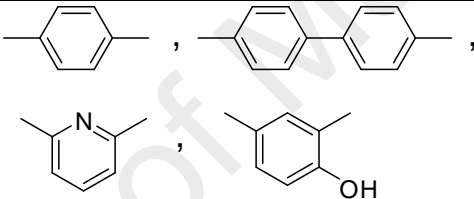
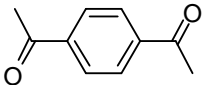
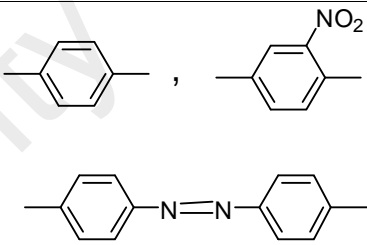
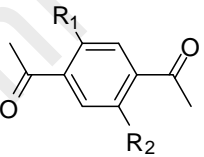
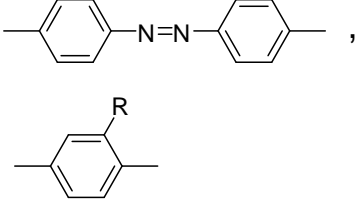
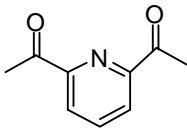
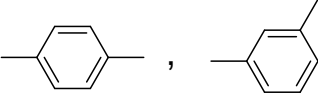
Figure 1.14 : (a) Polyazomethines, (b) Poly(p-phenylenevinylene), (c) Polyazines[110].

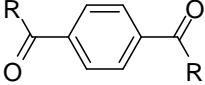
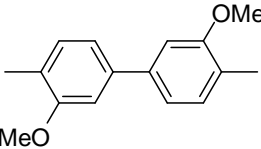
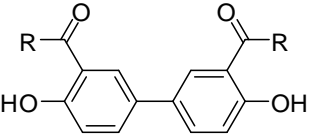
### 1.3.1 Synthesis of Schiff base polymers

#### 1.3.1.1 Polymerization of Schiff base compounds by polycondensation reaction.

Polymers containing Schiff base have been synthesized by polycondensation reaction of dicarbonyl and diamine materials and their derivatives. Table 1.1 displays some structures of the main diamine and dicarbonyl materials that can be used for preparing of PAMs.

Table 1.1: Some dicarbonyl and diamine compounds used for synthesis of polyimines

Dicarbonyl	NH <sub>2</sub> -R-NH <sub>2</sub>	References
1. 		[111, 112]
2. 		[113, 114]
3.  R <sub>1</sub> , R <sub>2</sub> = CH <sub>3</sub> , OCH <sub>3</sub> R <sub>1</sub> = H, R <sub>2</sub> = Cl, OH, CH <sub>3</sub>	 R = H, Cl, CH <sub>3</sub> , OCH <sub>3</sub>	[114-116]
4. 		[116]

<p>5.</p>  <p>R=CH<sub>3</sub></p>		<p>[117, 118]</p>
<p>6.</p>  <p>R=CH<sub>3</sub>, Ph</p>		<p>[119]</p>

Generally, polycondensation reaction can be achieved by using a suitable solvent with catalyst as well can be performed by the melt but by using the melt polycondensation of such monomers is difficult to control where side reactions will be obtained and consequently produce undesirable yields.

Low yields of Schiff base polymers were obtained by solution polycondensation reaction using methanol, ethanol or water as solvent and Lewis acid as catalyst due to establishment of equilibrium. To overcome this problem, use of other solvents such as toluene and benzene have been suggested, which will allow the removal of the water formed as a result of polycondensation reaction by azeotropic distillation. The condensation reaction will be accelerated by azeotropic distillation of water, leading to higher yields, yet it will not influence the degree of polycondensation. The low yield is because Schiff base containing polymers precipitate out of the solution during the reaction of polycondensation as the structure of the polymers have a rigid backbone chain in the reaction media resulting in low solubility of the polymers[120].

Better yields of Schiff base polymers can be obtained when polar aprotic solvents such as N,N-dimethylacetamide (DMAc), tetrahydrofuran (THF), N,N

dimethyl- formamide (DMF), dimethylsulfoxide (DMSO), N-methylpyrrolidone (NMP), or hexamethylphosphoramide (HMPA), or protic solvents, such as m-cersol or p-chlorophenol are used, due to the high solubility of the polymer in these polar solvents[120]. In addition, higher molecular weight polymers can be obtained from polycondensation reaction by adding lithium chloride or calcium chloride, as these salts can enhance the solubility of the growing macromolecular chain in the polycondensation system and maintain it in solution until higher polycondensation degree is obtained. Furthermore, the ability of calcium chloride as a dehydrating agent eliminates water in the polycondensation reaction by absorbing it; and thus accordingly resulting in the equilibrium favouring the formation of the polymer[120]. Phosphorous pentoxide can also be employed as dehydrating agent for this type of reaction.

The polycondensation reaction uses a few drops of acid as catalyst such as sulphuric acid ( $H_2SO_4$ ), hydrochloric acid (HCl), glacial acetic acid ( $CH_3COOH$ ) and p-toluenesulfonic acid. In addition, salt can be utilized as catalyst such as zinc chloride ( $ZnCl_2$ ) but it may leave traces which make the salt acts as a dopant. In addition, there are some cases of polycondensation performed without any catalyst. In this research, ammonia solution was used as catalyst to prepare the azines monomers and few drops of glacial acetic acid to prepare the Schiff base containing 1,5-naphthalene monomers. No catalyst was used in the case of Schiff base containing 1,4-phenylene[120].

The first step of polycondensation starts by attacking the nucleophilic amine group on the carbonyl bond resulting in dehydration of the tetrahedral intermediate. Therefore, the electrophilicity of the carbonyl and the nucleophilicity of diamine are important in terms of rate of reaction. As a general rule, the reactivity of diamine derivative compounds decreases in the same order as their basicity: hydrazine > aliphatic diamine > aromatic diamine, whereas in the case of bis-carbonyl compounds

the order is: dialdehyde > diketone > quinone[120]. A highly exothermic reaction is obtained from the polycondensation reaction of aromatic dialdehydes with aliphatic diamines, which proceeds rapidly in solution to high conversions[121, 122], whereas in the case of polycondensation of quinines more particular conditions are required.

### ***1.3.1.2 Polymerization of Schiff base monomers by chemical and electrochemical oxidation***

There is another method for the synthesis of Schiff base polymers by chemical or electrochemical oxidation from monomers containing aryl groups derived from naphthalene, furan, thiophene, pyrrole, etc... connected by azine or imine linkages in the backbone[123-127]. This type of reaction involves a single electron transfer oxidation of the aromatic rings to the cation-radical followed by their coupling at the radical sites with elimination of two protons. Through the chemical and electrochemical processing oxidation will be realized. The best advantage of generating the active species by electrochemical polymerization is by controlling the rate of initiation and the active centers concentration. In fact, this type of polymerization is fast, simple and possible to be performed under potentiostatic, galvanostatic, and cyclic voltammetric conditions.

Numerous inorganic oxidants have been used for the polymerization of monomers containing Schiff base groups such as:  $(\text{NH}_4)_2\text{S}_2\text{O}_8$ ,  $\text{FeCl}_3$  hydrate ( $\text{FeCl}_3 \cdot 6\text{H}_2\text{O}$ ),  $\text{FeCl}_3$  anhydrous,  $\text{Cu}(\text{ClO}_4)_2$ , etc. The first two oxidants can polymerized monomer containing pyrrole only as they possess low oxidation potential ( 0.8 against  $\text{Ag}/\text{Ag}^+$  electrode), whereas thiophene (1.6 eV) derivatives require stronger oxidants[128]. The syntheses of these monomers have been performed by using catalyzed condensation of an aromatic, aliphatic, as well heteroaromatic dialdehyde with aliphatic or aromatic diamine[129]. Figure 1.15 presents some examples of Schiff

base monomers, which have been used in polymerization by chemical and electrochemical oxidations involving cation-radical.

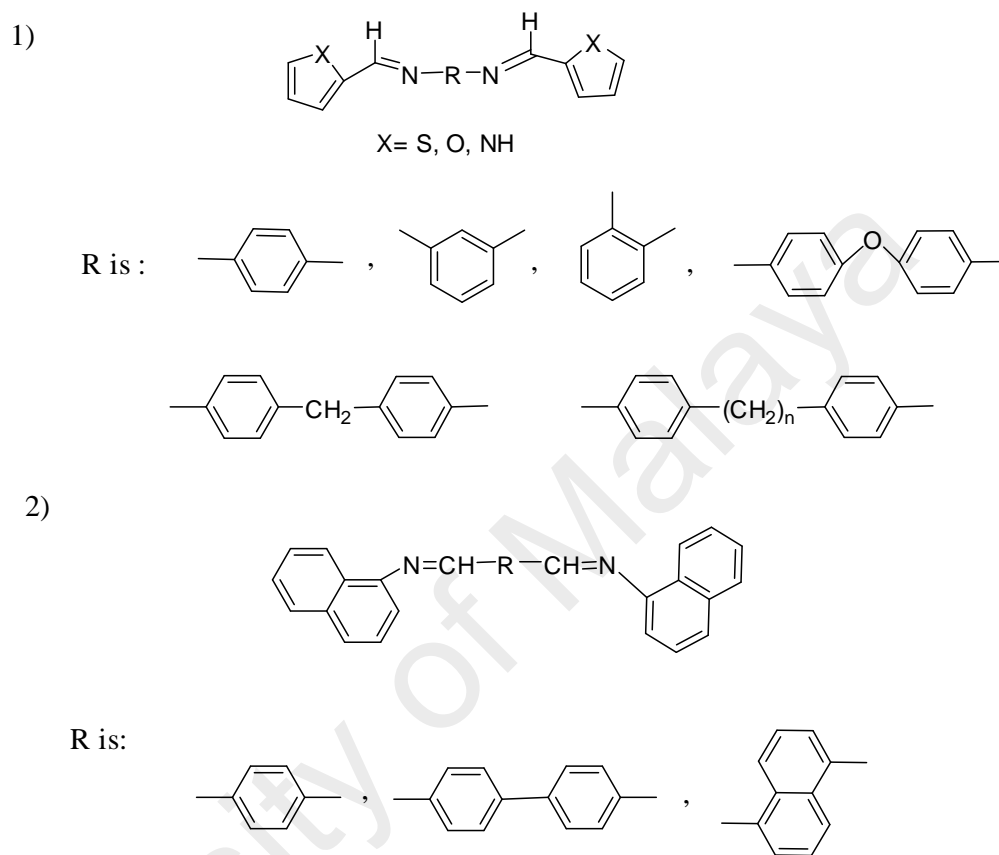


Figure 1.15: The structures of the Schiff base monomers used in polymerization by chemical and electrochemical oxidation[129].

### 1.3.2 Some properties of Schiff base containing polymer

#### 1.3.2.1 Thermal properties

All Schiff base containing polymers show a significant thermal stability. Even non-conjugated polymers synthesized from terephthaldehyde and aliphatic diamines have high thermal stabilities of about 250°C in air and 300°C in nitrogen[107]. Fully conjugated Schiff base containing polymers are yellow to orange to red to brown to black colored products, with thermal stabilities up to 430–480°C in air and 500–550°C in nitrogen. They are also resistant to radiation and their stability is shown to be

independent of dose rate and nature of the ionizing radiation. The first step of decomposition for the polyazomethine is nitrogen elimination followed by formation of stable polyenes, which subsequently decomposes[106].

### **1.3.2.2 Mechanical properties**

Aromatic polyazomethines are rigid rod molecules with high anisotropy in their optical, electrical, and thermomechanical properties. Melt spinning of their thermotropic mesophases having a spontaneous alignment of the molecules in the flow direction led to high-strength and high stiffness fibers[130]. The properties can be further improved by thermal annealing in a relaxed state at temperatures near, but below the flow temperature as a result of the PIs tendency to increase molecular weight and crystallinity[130]. These fibers have been used for reinforcement of thermoplastic polymers (polyamides, polycarbonates, polyacrylates, etc.)[131-133]. The rigid rod segment of the polyimine can also be introduced in the matrix of a thermoplastic polymer by in situ polycondensation of aromatic dialdehyde and diamine where molecular composites and blends with high-strength properties have been obtained[134]. The presence of imine hard segment in a soft polymer chain introduces liquid crystalline behavior and improves mechanical properties of the resultant segmented copolymer.

Semiflexible polyimines containing hydroxyl groups in the ortho position of the imine bond can be coordinated with metal ions the main effect of this coordination result an increase of the mechanical properties and intermolecular cohesive forces of the fibers[135].

## 1.4 Motivation

In the research work, we attempt to develop and synthesize new materials that have properties combining those of different classical materials. In particular, one of the most promising approaches to the development of new materials that combine the advantage of organic compounds (bisphenol Schiff bases) that contain full conjugated structure with those of inorganic (silicon) is to devise copolymer that have a backbone of inorganic atoms to which are attached to the organic moiety. The effect of substituted groups (electron-withdrawing and donating) attached with aromatic ring on molecular weight and properties of polymer were studied, together with their thermal stability, optical and electrochemical properties. In addition, liquid crystal properties were investigated for some of bisphenol bis-Schiff base monomers by reacted with bromoalkyl to produce symmetrical dimers and confirmed by differential scanning calorimetry (DSC) and optical polarized microscopy (OPM). The obtained materials were characterized using FT-IR,  $^1\text{H-NMR}$ ,  $^{13}\text{C NMR}$ , X-Ray single crystal and GPC analyses. TGA technique was used to determine the stabilities of thermal degradation. Optical properties were determined by using UV-vis spectra and the fluorescence spectra of the copolymers were measured to determine the maximal emission intensities. The HOMO-LUMO levels and electrochemical band gap values were studied by using Circle voltammetry (CV) technique.

## 1.5 Objectives of this research thesis

The scope of this work covers the synthesis and characterization aspects of the full conjugated azine monomers, monomers containing Schiff base group and copolymers containing silicon moiety besides Schiff base group thus far unreported in the literature. In addition, a newly symmetrical dimers based on bis phenol bis-Schiff bases containing 1,5-naphthalene were synthesized, characterized and studied their liquid crystal properties. The research objectives can be summarized as follows:

1. To synthesize full conjugated azine monomers derived from condensation reaction of hydrazine sulfate with different types of 4-hydroxybenzaldehyde and its derivatives.
2. To synthesize full conjugated bis-Schiff base monomers derived from condensation reaction of 1,4-phenylene diamine and 1,5-naphthalenediamine with 4-hydroxybenzaldehyde and its derivative to form higher conjugated monomers.
3. To copolymerize the synthesized monomers with bis(chloromethyl) dimethylsilane by polycondensation reaction using Williamson's reaction to yield copolymers containing silicon in the main backbone and good molecular weight.
4. To study the influence of electron-donating and electron-withdrawing substituted groups attached to the phenyl ring on molecular weight, optical and electrochemical properties.
5. To synthesize two series of symmetrical dimers containing 1,5-naphthalene moiety and investigate the properties of liquid crystal.
6. To characterize the monomers, copolymers and symmetrical dimers synthesized structurally by several analytical techniques such as:
  - Fourier transform infrared spectroscopy (FT-IR)
  - Nuclear magnetic resonance spectroscopy (FT-NMR)
  - single crystal x-ray crystallography
  - Gel permeation chromatography (GPC)
7. To investigate the thermal stability, liquid crystal properties, opto and electro chemical properties of the synthesized compounds by several types of techniques such as:
  - Differential scanning calorimetry (DSC)

- Optical polarized microscopy (OPM)
- Thermal gravimetric analysis (TGA)
- UV-Vis and fluorescence spectroscopy
- Cyclic voltammetry (CV)

University of Malaya

## CHAPTER 2 : EXPERIMENTAL

### 2.1 Materials

The chemicals used for the synthesise work were: 4-hydroxybenzaldehyde (Acros, 99%), Vanillin (Acros, 97%), hydrazinium sulfate (Merck, 99%), 3-ethoxy-4-hydroxybenzaldehyde (Merck, 97%), 3,5-dimethoxy-4-hydroxy-benzaldehyde (Sigma Aldrich, 97%), 3-nitro-4-hydroxybenzaldehyde (Merck, 95%), 4-hydroxy-3-methoxy-5-nitrobenzaldehyde (Merck, 99%), *p*-phenylenediamine (Acros, 99%), 1,5-naphthalenediamine (Merck, 95%), bis(chloromethyl)dimethylsilane (Sigma-Aldrich, 97%), Potassium carbonate ( $K_2CO_3$ ) (Riendemenn Schmit Chemicals), 1-bromoalkane (1-bromobutane, 1-bromohexane, 1-bromooctane, 1-bromodecane, 1-bromododecane, 1-bromotetradecane, 1-bromohexadecane and 1-bromooctadecane) (Merck, 95%), sodium sulfate (Riendemenn Schmit Chemicals, 99%). Purities of materials were examined by using a thin layer chromatography (Silica gel TLC) plate's (Merck) and the spot located with UV light and iodine vapor. All the chemicals were used directly from the freshly opened bottles without further purification, except for *p*-phenylenediamine and 1,5-naphthalenediamine which were recrystallized from toluene and dried under reduced pressure prior to use.

Ethanol (95%), absolute ethanol (99.8%), *N,N*-dimethylformamide (DMF), ethyl acetate, acetonitrile, glacial acetic acid, acetone, tetrahydrofuran (THF), methanol, and Deuterated NMR solvents used were of reagent-grade and purchased from Sigma Aldrich, Riendemann schimidt chemicals, Acros and Merck. DMF was distilled and keep under molecular sieve prior to use.

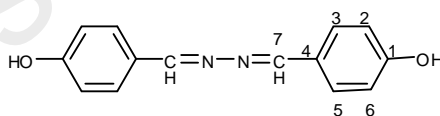
## 2.2 Synthesis of monomers

In this research, several polymerizable monomers with different types of substituent groups were synthesized. The procedure, synthetic route and chemical structure as characterized by FT-IR,  $^1\text{H}$  NMR,  $^{13}\text{C}$  NMR are listed below for all the monomers.

### 2.2.1 Synthesis of azine monomers (a1-a6)

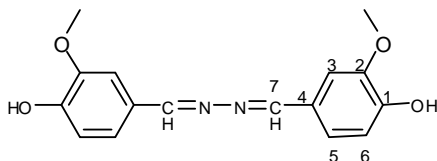
The azine monomers were synthesized according to literature[136, 137], with some modifications. In a 250 mL two-necked reaction flask equipped with a magnetic stirrer, a solution of 19.7 mmol of hydrazine sulphate in 10 mL water and 1.3 mL of concentrated ammonium solution were stirred until a clear solution was obtained. To this solution, 9.8 mmol of aldehyde in 10 mL of ethanol was added dropwise and the mixture stirred for 3 h at ambient temperature. A solid product filtered, dried and crystallized from suitable solvent to obtain the yellow crystals.

#### Synthesis of 4,4'-hydrazine-1,2-diylidenebis(methan-1-yl-1-ylidene)diphenol (a1)[138]



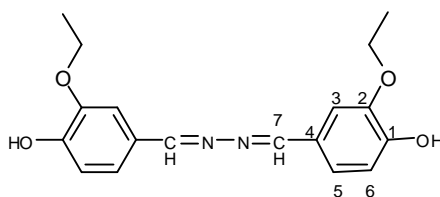
1.65 g of hydrazine sulphate with 3 g of 4-hydroxybenzaldehyde was reacted according to the general synthesis of azine. The yellow solid product was purified by crystallization from ethanol. Mp: 284-285°C, yield 81.3%. IR,  $\nu_{\text{max}}$  3481.4 (OH), 3045 ( $\text{C}_{\text{ar}}\text{-H}$ ), 1618 (C=N), 1586-1505 (C-C).  $^1\text{H}$  NMR,  $\delta$  (ppm, DMSO- $d_6$ , 400 MHz): 6.84 (d, 4H, J = 8.5,  $\text{H}_{2,6}$ ), 7.67 (d, 4H, J = 8.8,  $\text{H}_{3,5}$ ), 8.54 (s, 2H,  $\text{H}_7$ ), 10.06 (s, 2H, OH),  $^{13}\text{C}$  NMR,  $\delta$  (ppm, DMSO- $d_6$ , 100 MHz): 116.3 (4C,  $\text{C}_{2,6}$ ), 125.63 (2C,  $\text{C}_4$ ), 130.66 (4C,  $\text{C}_{3,5}$ ), 160.8 (2C,  $\text{C}_1$ ), 160.96 (2C,  $\text{C}_7$ ).

**Synthesis of 4,4'-(1E,1'E)-hydrazine-1,2-diylidenebis(methan-1-yl-1-ylidene)bis(2-methoxyphenol) (a2)**



1.28 g of hydrazine sulphate with 3 g of 4-hydroxy-3-methoxybenzaldehyde was reacted according to general synthesis of azines[139]. The yellow solid product was purified by crystallization from ethanol. Mp: 178°C [136]; obtained 175-176°C, yield 82%. IR,  $\nu$ , 3479 (OH), 3070 ( $C_{ar}$ -H), 2919.6 ( $C-H_{alph}$ ), 1624( $C=N$ ), 1512-1600 (C-C) and 1257 ( $-OCH_3$ )  $cm^{-1}$ ,  $^1H$  NMR, (ppm, DMSO- $d^6$ , 400 MHz): 3.80 (s, 6H, O- $CH_3$ ), 6.86 (d, 2H, J = 7.76,  $H_6$ ), 7.23 (dd, 2H, J = 8.24;1.8,  $H_5$ ), 7.43 (s, 2H,  $H_3$ ), 8.55 (s, 2H,  $H_7$ ), 9.67 (s, 2H, -OH),  $^{13}C$  NMR, (ppm, DMSO- $d^6$ , 100 MHz): 56 (2C,  $OCH_3$ ), 110.3 (2C,  $C_3$ ), 116.2 (2C,  $C_6$ ), 124.9 (2C,  $C_5$ ), 126.6 (2C,  $C_4$ ), 148.5 (2C,  $C_2$ ), 150.4 (2C,  $C_1$ ), 161.1 (2C,  $C_7$ ).

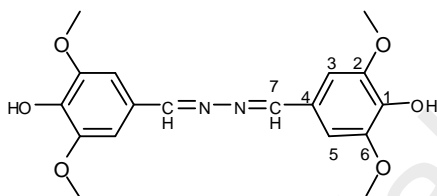
**Synthesis of 4,4'-(1E,1'E)-hydrazine-1,2-diylidenebis(methan-1-yl-1-ylidene)bis(2-ethoxyphenol) (a3)**



1.17 g of hydrazine sulphate with 3 g of 4-hydroxy-3-ethoxybenzaldehyde was reacted according to general synthesis of azines. The product was pale yellow solid precipitate, which was purified by crystallization from THF and recrystallized from acetonitrile to obtain a single crystal. Mp: 204-205°C, yield 80.3%. IR,  $\nu$ , 3617.5 (OH) 3034 ( $C_{ar}$ -H), 2928-2876.6 ( $C-H_{alph}$ ), 1628 ( $C=N$ ), 1597-1509 (C-C) and 1267 ( $O-CH_2CH_3$ )  $cm^{-1}$ ,  $^1H$  NMR, (ppm, DMSO- $d^6$ , 400 MHz): 1.33 (t, 6H, J = 6.9 x(2) O- $CH_2CH_3$ ),

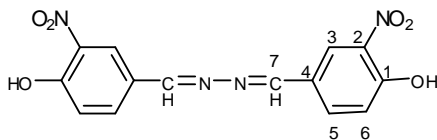
4.03 (q, 4H, J = 7x(3) O-CH<sub>2</sub>), 6.85 (d, 2H, J = 8.1, H<sub>6</sub>), 7.21 (dd, 2H, J = 8.2; 1.7, H<sub>5</sub>), 7.40 (d, 2H, J = 1.8, H<sub>3</sub>), 8.52 (s, 2H, H<sub>7</sub>), 9.58 (s, 2H, OH), <sup>13</sup>C NMR, (ppm, DMSO-d<sup>6</sup>, 100 MHz): 15.2 (2C, O-CH<sub>2</sub>CH<sub>3</sub>), 64 (2C, OCH<sub>2</sub>), 111.9 (2C, C<sub>3</sub>), 116.3 (2C, C<sub>6</sub>), 123.8 (2C, C<sub>5</sub>), 126.1 (2C, C<sub>4</sub>), 147.6 (2C, C<sub>2</sub>), 150.6 (2C, C<sub>1</sub>), 161.2 (2C, C<sub>7</sub>).

**Synthesis of 4,4'-(1E,1'E)hydrazine-1,2-diylidenebis(methan-1-y1-1-ylidene)bis(2,5-dimethoxyphenol) (a4)**



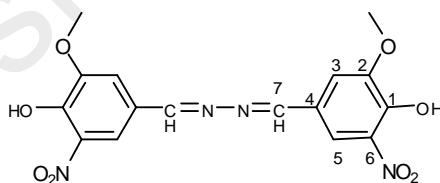
3 g of 4-hydroxy-2,5 dimethoxybenzaldehyde with 1.08 g of hydrazine sulphate were reacted according to general synthesis of azine. The resultant was a yellow solid product, purified by crystallization from ethanol and recrystallized by acetonitrile to obtain single crystal. Mp: 214-215 °C, yield 78.8%. IR, , 3480 (OH), 3012 (C<sub>ar</sub>-H), 2936 (C-H<sub>aliph</sub>), 1621 (C=N), 1588-1498 (C-C) and 1219.3 (O-CH<sub>3</sub>) cm<sup>-1</sup>, <sup>1</sup>H NMR, (ppm, DMSO-d<sup>6</sup>, 400 MHz): 3.79 (s, 12H, -OCH<sub>3</sub>), 7.12 (s, 4H, H<sub>3,5</sub>), 8.55 (s, 2H, H<sub>7</sub>), 9.02 (s, 2H, OH), <sup>13</sup>C NMR, (ppm, DMSO-d<sup>6</sup>, 100 MHz): 56.56 (4C, OCH<sub>3</sub>), 106.36 (4C, C<sub>3,5</sub>), 124.8 (2C, C<sub>4</sub>), 139.4 (2C, C<sub>2,6</sub>), 148.6 (4C, C<sub>1</sub>), 161.4 (2C, C<sub>7</sub>).

**Synthesis 4,4'-(1E,1'E)-hydrazine-1,2-diylidenebis(methan-1-yl-1-ylidene)bis(2-nitrophenol) (a5)**



2 g of 4-hydroxy-3-nitrobenzaldehyde with 0.76 g of hydrazine sulphate were reacted according to general procedure of azine. The yellow solid product was purified by crystallization from ethanol. Mp: 257-258°C, yield 80.1%. IR,  $\nu$ , 3570.3(OH), 3074 ( $C_{ar}$ -H), 1620 (C=N) and 1571-1488 (C-C) and 1251 (OCH<sub>3</sub>)  $cm^{-1}$ . <sup>1</sup>H NMR, (ppm, DMSO-d<sup>6</sup>, 400 MHz): 7.30 (d, 2H, J = 8.8, H<sub>6</sub>), 8.11 (dd, 2H, J = 8.8, 2.2, H<sub>5</sub>), 8.42 (d, 2H, J = 2.2, H<sub>3</sub>), 8.75 (s, 2H, H<sub>7</sub>). <sup>13</sup>C NMR, (ppm, DMSO-d<sup>6</sup>, 100 MHz): 120.3 (2C, C<sub>6</sub>), 125.64 (2C, C<sub>3</sub>), 126.34 (2C, C<sub>4</sub>), 134.43 (2C, C<sub>5</sub>), 137.61 (2C, C<sub>2</sub>), 150.4 (2C, C<sub>1</sub>), 161 (2C, C<sub>7</sub>).

**Synthesis of 2,2'-dinitro-5,5'-dimethoxy-4,4'-[hydrazinediylidenebis(methanylylidene)] diphenol (a6)**



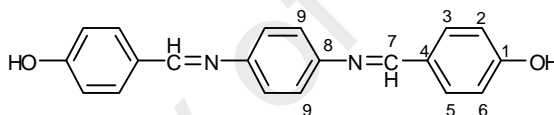
2 g of 4-hydroxy-3-nitrobenzaldehyde with 0.66 g of hydrazine sulphate were reacted as according to procedure of azine. The yellow solid product was purified by crystallization from ethanol. Mp: 269-270°C, yield 72.9%. IR,  $\nu$ , 3561(OH), 3083 ( $C_{ar}$ -H), 2953-2833 (C-H<sub>alph</sub>), 1625 (C=N), 1598-1504 (C-C) and 1253 (O-CH<sub>3</sub>)  $cm^{-1}$ . <sup>1</sup>H NMR, (ppm, DMSO-d<sup>6</sup>, 400 MHz): 3.91 (s, 6H, OCH<sub>3</sub>), 7.66 (d, 2H, J=1.2, H<sub>3</sub>), 7.92 (d, 2H, J=1.7, H<sub>5</sub>), 8.65 (s, 2H, H<sub>7</sub>). <sup>13</sup>C NMR, (ppm, DMSO-d<sup>6</sup>, 100 MHz): 75.11

(2C, OCH<sub>3</sub>), 112.98 (2C, C<sub>3</sub>), 118.87 (2C, C<sub>5</sub>), 124.24 (2C, C<sub>4</sub>), 137.59 (2C, C<sub>6</sub>), 146.7 (2C, C<sub>2</sub>), 150.68 (2C, C<sub>1</sub>), 160.51 (2C, C<sub>7</sub>).

## 2.2.2 Synthesis of bisphenol bis-Schiff base monomers containing 1, 4-phenylene (b1-b4)

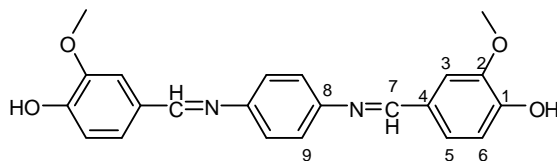
A minimum methanolic solution of *p*-phenylenediamine (9.2 mmol) was added dropwise to a stirred 30 mL methanolic solution of 4-hydroxybenzaldehyde and its derivative (19.7 mmol). The reaction mixture was then refluxed at 80°C for 4 h. The resultant product was filtered, washed with distilled water and crystallized twice from methanol. Thereafter the solid products were dried in oven.

### Synthesis of 4,4'-(1,4-phenylenebis(azan-1-yl-1-ylidene))bis(methan-1-yl-1-ylidene) diphenol. (b1)



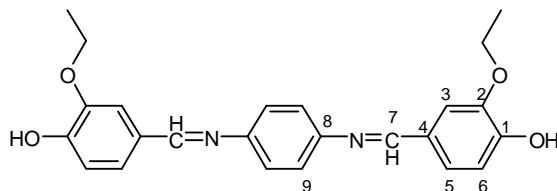
4-hydroxybenzaldehyde (2 g) with *p*-phenylenediamine (0.9 g) were reacted according to procedure of Schiff base containing 1,4-phenylene. The yellow solid product was purified by crystallization from methanol. Mp: 275-277°C, yield 79.3%. IR, , 3489 (OH), 3067 (C<sub>ar</sub>-H), 1618 (C=N), 1505-1525 (C=C<sub>ar</sub>) cm<sup>-1</sup>, <sup>1</sup>H NMR, (ppm, DMSO-d<sup>6</sup>, 400 MHz): 6.88 (d, 4H, J=8.2, H<sub>2,6</sub>), 7.25 (s, 4H, H<sub>9</sub>), 7.77 (d, 4H, J=8.2, H<sub>3,5</sub>), 8.50 (s, 2H, H<sub>7</sub>), 10.13 (s, 2H, OH), <sup>13</sup>C NMR, (ppm, DMSO-d<sup>6</sup>, 100 MHz): 116.19 (4C, C<sub>2,6</sub>), 122.33 (4C, C<sub>9</sub>), 128.15 (2C, C<sub>4</sub>), 131.16 (4C, C<sub>3,5</sub>), 149.82 (2C, C<sub>8</sub>), 159.71 (2C, C<sub>1</sub>), 161.08 (2C, C<sub>7</sub>).

**Synthesis of 4,4'-(1,4-phenylenebis(azan-1-yl-1-ylidene))bis(methan-1-yl-1-ylidene) bis(2-methoxyphenol) (b2)**



1.08 g of *p*-phenylenediamine with 3 g of 4-hydroxy-3-methoxybenzaldehyde was reacted according to general synthesis of Schiff base containing 1, 4-phenylene. The resultant was a yellow solid product which was purified by crystallization from methanol. Mp: 198-19°C, yield 79.3, IR, , 3528 (OH), 3058 (C<sub>ar</sub>-H), 2934-2848 (C-H<sub>alph</sub>), 1619 (C=N), 1508-1593 (C-C<sub>ar</sub>) and 1273 (O-CH<sub>3</sub>) cm<sup>-1</sup>, <sup>1</sup>H NMR, (ppm, DMSO-d<sup>6</sup>, 400 MHz): 3.48 (s, 6H, -OCH<sub>3</sub>), 6.90 (d, 2H, J= 8.1, H<sub>6</sub>), 7.27 (s, 4H, H<sub>9</sub>), 7.33 (d, 2H, J= 8.1, H<sub>5</sub>), 7.53 (s, 2H, H<sub>3</sub>), 8.50 (s, 2H, H<sub>7</sub>), 9.76 (s, 2H, -OH), <sup>13</sup>C NMR, (ppm, DMSO-d<sup>6</sup>, 100 MHz): 56.06 (2C, -OCH<sub>3</sub>), 110.84 (2C, C<sub>3</sub>), 115.81 (2C, C<sub>6</sub>), 122.59 (4C, C<sub>9</sub>), 124.62 (2C, C<sub>5</sub>), 128.5 (2C, C<sub>4</sub>), 148.5 (2C, C<sub>8</sub>), 149.76 (2C, C<sub>2</sub>), 150.67 (2C, C<sub>1</sub>), 159.9 (2C, C<sub>7</sub>).

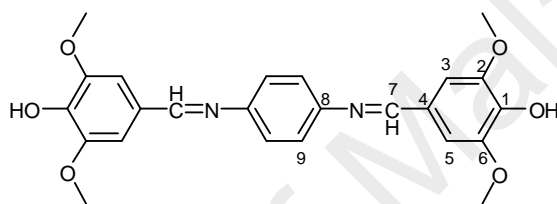
**Synthesis of 4,4'-(1,4-phenylenebis(azan-1-yl-1-ylidene))bis(methan-1-yl-1-ylidene) bis(2-ethoxyphenol) (b3)**



0.64 g of *p*-phenylenediamine with 2 g of 4-hydroxy-3-ethoxybenzaldehyde was reacted according to general synthesis of Schiff base containing 1,4-phenylene. The product was a yellow solid product which was purified by crystallization from ethyl acetate. Mp: 172-173°C, yield 79.3%, IR, , 3579 (OH), 3043 (C<sub>ar</sub>-H), 2944-2861 (C-H<sub>alph</sub>), 1624 (C=N), 1505-1585 (C-C<sub>ar</sub>) and 1267 (O-CH<sub>3</sub>) cm<sup>-1</sup>. <sup>1</sup>H NMR, (ppm,

DMSO-d<sup>6</sup>, 400 MHz): 1.36 (t, 6H, J=7, -OCH<sub>2</sub>-CH<sub>3</sub>), 4.08 (q, 4H, J=6.8, O-CH<sub>2</sub>), 6.90 (d, 2H, J=8.3, H<sub>6</sub>), 7.25 (s, 4H, H<sub>9</sub>), 7.34 (d, 2H, J=9.1, H<sub>5</sub>), 7.50 (s, 2H, H<sub>3</sub>), 8.48 (s, 2H, H<sub>7</sub>), 9.66 (s, 2H, -OH), <sup>13</sup>C NMR, (ppm, DMSO-d<sup>6</sup>, 100 MHz): 15.25 (2C, -OCH<sub>2</sub>CH<sub>3</sub>), 64.36 (2C, -OCH<sub>2</sub>), 112.18 (2C, C<sub>3</sub>), 115.89 (2C, C<sub>6</sub>), 122.35 (4C, C<sub>9</sub>), 124.44 (2C, C<sub>5</sub>), 128.54 (2C, C<sub>4</sub>), 147.6 (2C, C<sub>8</sub>), 149.76 (2C, C<sub>2</sub>), 150.89 (2C, C<sub>1</sub>), 159.94 (2C, C<sub>7</sub>).

**Synthesis of 4,4'-(1,4-phenylenebis(azan-1-yl-1-ylidene))bis(methan-1-yl-1-ylidene) bis (2-5methoxyphenol) (b4)**



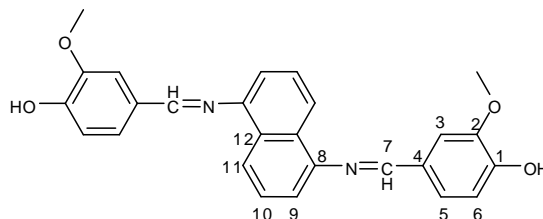
0.6 g of *p*-phenylenediamine with 2 g of 4-hydroxy-3,5-dimethoxybenzaldehyde was reacted according to general synthesis of Schiff base containing 1,4-phenylene. The product was a brown solid product which was purified by crystallization from methanol. Mp: 215-216°C, yield 72.2%. IR, , 3519 (OH), 3031 (C<sub>ar</sub>-H), 2921-2869 (C-H<sub>aliph</sub>), 1622 (C=N), 1502-1579 (C-C<sub>ar</sub>) and 1254 (O-CH<sub>3</sub>) cm<sup>-1</sup>. <sup>1</sup>H NMR, (ppm, DMSO-d<sup>6</sup>, 400 MHz): 3.81 (s, 12H, -OCH<sub>3</sub>), 7.21 (s, 4H, H<sub>3,5</sub>), 7.25 (s, 4H, H<sub>9</sub>), 8.48 (s, 2H, H<sub>7</sub>), 9.06 (s, 2H, -OH), <sup>13</sup>C NMR, (ppm, DMSO-d<sup>6</sup>, 100 MHz): 56.56 (4C, OCH<sub>3</sub>), 106.72 (4C, C<sub>3,5</sub>), 122.37 (4C, C<sub>9</sub>), 127.24 (2C, C<sub>4</sub>), 139.69 (2C, C<sub>8</sub>), 148.6 (4C, C<sub>2,6</sub>), 149.75 (2C, C<sub>1</sub>), 161.4 (2C, C<sub>7</sub>).

**2.2.3 Synthesis of bisphenol bis-Schiff base monomers containing 1,5-naphthalene (b5-b8)**

A minimum methanolic solution of 1,5-naphthalenediamine (0.64 g, 4x10<sup>-3</sup> mol) was added dropwise to a stirred 30 mL methanolic solution containing 5 drops of glacial acetic acid and 4-hydroxybenzaldehyde (1 g, 8x10<sup>-3</sup> mol). The reaction mixture was

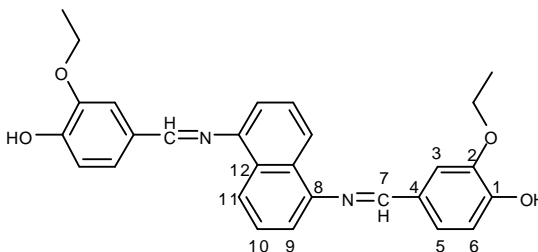
refluxed at 90°C for 6 h. The resultant product was filtered, washed with distilled water and crystallized twice from methanol. Thereafter the product was dried in oven.

**Synthesis of 4,4'-(naphthalene-1,5-diylbis(azan-1-yl-1-ylidene))bis(methan-1-yl-1-ylidene)bis(2methoxyphenol) (b5)**



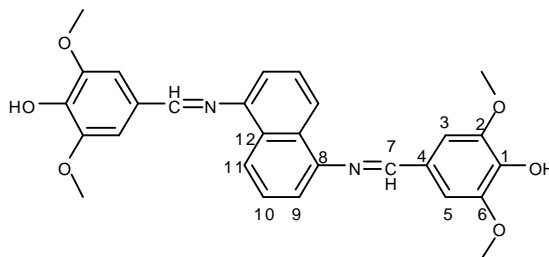
3 g of 4-hydroxy-3-methoxybenzaldehyde with 1.56 g of 1,5-naphthalene-diamine were reacted according to general synthesis of bisphenol containing 1,5-naphthalene. The greenish yellow solid product was purified by crystallization from methanol. Mp: 195-197°C, yield 76.4, IR,  $\nu$ , 3456 (OH), 3014 ( $C_{ar}-H$ ), 2939-2851 ( $C-H_{alph}$ ), 1624 (C=N), 1522-1579 (C- $C_{ar}$ ) and 1258 (O- $CH_3$ )  $cm^{-1}$ .  $^1H$  NMR, (ppm, DMSO- $d_6$ , 400 MHz): 4.89 (s, 6H,  $OCH_3$ ), 6.94 (d, 2H,  $J=8.2$ ,  $H_6$ ), 7.17 (d, 2H,  $J=7.0$ ,  $H_5$ ), 7.44(d, 2H,  $J=8.1$ ,  $H_9$ ), 7.5 (t, 2H,  $J=7.8$ ,  $H_{10}$ ), 7.68 (s, 2H,  $H_3$ ), 8.14 (d, 2H,  $J=8.2$ ,  $H_{11}$ ), 8.53 (s, 2H,  $H_7$ ), 9.82 (s, 2H, -OH),  $^{13}C$  NMR, (ppm, DMSO- $d_6$ , 100 MHz): 55.67 (2C,- $OCH_3$ ), 110.9 (2C,  $C_3$ ), 113.55 (2C,  $C_9$ ), 115.57 (2C,  $C_6$ ), 1.21 ( 2C,  $C_5$ ) 124.37 (2C,  $C_{11}$ ), 126.1 (2C,  $C_{10}$ ) 128.2 (2C,  $C_{12}$ ), 129.1 (2C,  $C_4$ ), 148.2 (2C,  $C_8$ ), 148.9 (2C,  $C_2$ ), 150.5 (2C,  $C_1$ ), 161.2 (2C,  $C_7$ ).

**Synthesis of 4,4'-(naphthalene-1,5-diylbis(azan-1-yl-1-ylidene))bis(methan-1-yl-1-ylidene)bis(3 ethoxyphenol) (b6)**



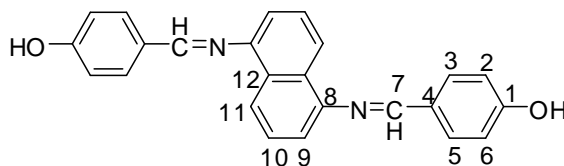
3 g of 4-hydroxy-3-ethoxybenzaldehyde with 1.41 g of 1,5-naphthalenediamine were reacted according to general synthesis of bisphenol containing 1,5-naphthalene. The product was a yellow solid product which was purified by crystallization from ethanol. Mp: 207-208°C, yield 81.4%. IR, , 3412 (OH), 3054 (C<sub>ar</sub>-H), 2979-2875 (C-H<sub>alph</sub>), 1632 (C=N), 1511-1600 (C-C<sub>ar</sub>) and 1267 (O-CH<sub>3</sub>) cm<sup>-1</sup>. <sup>1</sup>H NMR, (ppm, DMSO-d<sup>6</sup>, 400 MHz): 1.38 (t, 6H, J=7, -OCH<sub>2</sub>CH<sub>3</sub>), 4.14 (q, 4H, J=6.8, OCH<sub>2</sub>), 6.95 (d, 2H, J=8.1, H<sub>6</sub>), 7.17 (d, 2H, J=7.3, H<sub>5</sub>), 7.44 (d, 2H, J=8.1, H<sub>9</sub>) 7.5 (t, 2H, J=7.8, H<sub>10</sub>), 7.65 (s, 2H, H<sub>3</sub>), 8.12 (d, 2H, J=8.3, H<sub>11</sub>), 8.52 (s, 2H, H<sub>7</sub>), 9.75 (s, 2H, -OH), <sup>13</sup>C NMR, (ppm, DMSO-d<sup>6</sup>, 100 MHz): 15.26 (2C, OCH<sub>2</sub>CH<sub>3</sub>), 64.44 (2C, -OCH<sub>2</sub>), 112.61 (2C, C<sub>3</sub>), 113.95 (2C, C<sub>9</sub>), 116.05 (2C, C<sub>6</sub>), 1.21.39 (2C, C<sub>5</sub>) 124.64 (2C, C<sub>11</sub>), 126.52 (2C, C<sub>10</sub>) 128.63 (2C, C<sub>12</sub>), 129.54 (2C, C<sub>4</sub>), 147.76 (2C, C<sub>8</sub>), 149.31 (2C, C<sub>2</sub>), 151.1 (2C, C<sub>1</sub>), 161 (2C, C<sub>7</sub>).

**Synthesis of 4,4'-(naphthalene-1,5-diylbis(azan-1-yl-1-ylidene))bis(methan-1-yl-1-ylidene)bis(2,5 dimethoxyphenol) (b7)**



3 g of 4-hydroxy-3,5-dimethoxybenzaldehyde with 1.29 g of 1,5-naphthalenediamine were reacted according to general synthesis of bisphenol containing 1,5-naphthalene. The product was a yellowish green solid product which purified by crystallization from methanol. Mp: 281-282 C, yield 76.2%. IR, , 3389 (OH), 3066 ( $C_{ar}$ -H), 2961-2851 ( $C-H_{aliph}$ ), 1618 ( $C=N$ ), 1506-1590 ( $C-C_{ar}$ ) and 1269 (O- $CH_3$ )  $cm^{-1}$ .  $^1H$  NMR, (ppm, DMSO- $d_6$ , 400 MHz): 3.85 (s, 12H,  $OCH_3$ ), 7.18 (d, 2H,  $J=7.3$ ,  $H_9$ ), 7.37 (s, 4H,  $H_{3,5}$ ), 7.43 (d, 2H,  $J=8.1$ ,  $H_9$ ), 7.52 (t, 2H,  $J=7.8$ ,  $H_{10}$ ), 8.14 (d, 2H,  $J=8.3$ ,  $H_{11}$ ), 8.54 (s, 2H,  $H_7$ ), 9.18 (s, 2H, OH),  $^{13}C$  NMR, (ppm, DMSO- $d_6$ , 100 MHz): 56.63 (4C, - $OCH_3$ ), 107 (4C,  $C_{3,5}$ ), 114 (2C,  $C_9$ ), 121.46 (2C,  $C_{11}$ ), 126.5 (2C,  $C_{10}$ ), 128 (2C,  $C_{12}$ ), 129 (2C,  $C_4$ ), 139.9 (2C,  $C_8$ ), 148.6 (4C,  $C_{2,6}$ ), 149.2 (2C,  $C_1$ ), 161.2 (2C,  $C_7$ ).

**Synthesis of 4,4'-(naphthalene-1,5-diylbis(azan-1-yl-1-ylidene))bis(methan-1-yl-1-ylidene)diphenol (b8)**



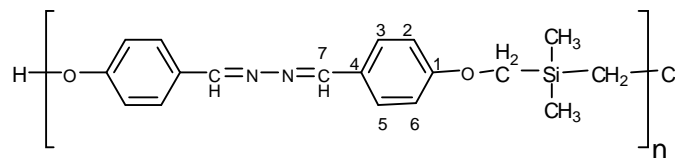
3 g of 4-hydroxybenzaldehyde with 1.92 g of 1,5-naphthalenediamine were reacted according to general synthesis of bisphenol containing 1,5-naphthalene. Yellow solid, Mp: 267-268°C, yield 83.3%. IR, , 3423 (OH), 3036 ( $C_{ar}$ -H), 2965-2889 (C-

H<sub>alph</sub>), 1626 (C=N), 1513-1592 (C-C<sub>ar</sub>) and 1261 (O-CH<sub>3</sub>) cm<sup>-1</sup>. <sup>1</sup>H NMR, (ppm, DMSO-d<sup>6</sup>, 400 MHz): 6.95 (d, 4H, J=8.5, H<sub>2</sub>), 7.20 (d, 2H, J=6.8, H<sub>9</sub>), 7.51 (t, 2H, J=7.8x(2), H<sub>10</sub>), 7.92 (d, 4H, J=8.5, H<sub>3</sub>), 8.14 (d, 2H, J=8.5, H<sub>11</sub>), 8.58 (s, 2H, H<sub>7</sub>), 10.20 (s, 2H, -OH), <sup>13</sup>C NMR, (ppm, DMSO-d<sup>6</sup>, 100 MHz): 113.90 (2C, C<sub>9</sub>), 116.28 (4C, C<sub>2</sub>), 121.34 (2C, C<sub>11</sub>), 126.51 (2C, C<sub>4</sub>), 128.26 (2C, C<sub>10</sub>), 129.58 (2C, C<sub>12</sub>), 131.46 (4C, C<sub>3</sub>), 149.31 (2C, C<sub>8</sub>), 160.77 (2C, C<sub>1</sub>), 161.34 (2C, C<sub>7</sub>).

### 2.3 Synthesis of copolymers

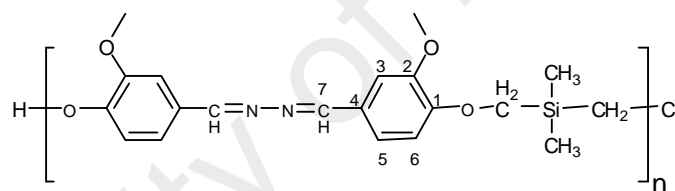
A 100 mL three-neck round-bottomed flask, equipped with a condenser, a septum, nitrogen inlet-outlet and magnetic stirrer, was charged under nitrogen with bisphenol (3.33 mmol) dissolved in 20 mL of dried DMF containing anhydrous K<sub>2</sub>CO<sub>3</sub>, (6.81 mmol). The solution of monomers and solvent will be N<sub>2</sub> purged for 20 min prior to the start of the reaction. The solution was stirred and heated at 40°C for 30 min. When the reaction is ready to be started, bis(chloromethyl)dimethylsilane (3.3 mmol) was introduced with a syringe through a septum dropwise within 30 min. After refluxing for 24 h under stirring at 80°C, another batch of bis(chloromethyl)-dimethylsilane (1.65 mmol) was added dropwise under the same conditions for another 24 h. After cooling, the resulting solution was extracted with CHCl<sub>3</sub>; the organic layer was washed with brine for three times and dried under MgSO<sub>4</sub> or Na<sub>2</sub>SO<sub>4</sub>. The excess solvent was evaporated under reduced pressure thereafter the residue was dried under vacuum for 24 h. The resultant product was a glassy solid compound.

### Synthesis of copolymer, Pa1



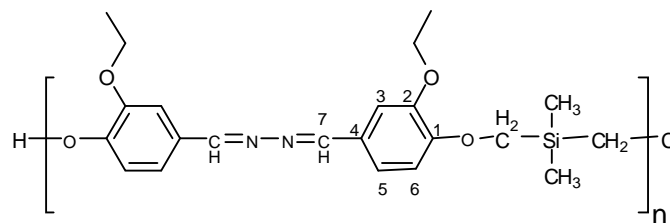
The resultant product was a glassy yellow transparent compound: yield 51.91%, IR, , 3449 (OH), 3020 ( $C_{ar}$ -H), 2936-2851 ( $C-H_{aliph}$ ), 1619 ( $C=N$ ), 1566-1509 ( $C-C$ ), 1259 ( $OCH_2$ ), 1248 ( $OCH_3$ ) and 849 ( $Si-CH_3$ )  $cm^{-1}$ .  $^1H$  NMR, (ppm,  $CDCl_3$ , 400 MHz): -0.1-0.38 (6H,  $Si-CH_3$ ), 3.34-3.41 (2H,  $OCH_2Si$ ), 6.9-7.38 (8H,  $H_{ar}$ ), 8.4 (2H,  $H_7$ ).  $^{13}C$  NMR, (ppm,  $CDCl_3$ , 100 MHz) -1.6-3.92 (2C,  $SiCH_3$ ), 61.1 (1C,  $OCH_2Si$ ), 116.9 (4C,  $C_{2,6}$ ), 126.1 (2C,  $C_4$ ), 131.23 (2C,  $C_{3,5}$ ), 159.54 (2C,  $C_1$ ), 161 (2C,  $C_7$ ).

### Synthesis of copolymer, Pa2



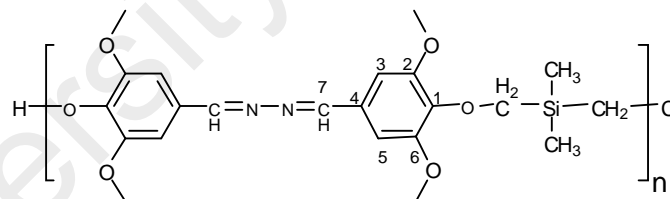
The resultant product was a glassy yellow transparent compound: yield 69.21%, IR, , 3460 (OH), 3003 ( $C_{ar}$ -H), 2955-2831 ( $C-H_{aliph}$ ), 1622.7 ( $C=N$ ), 1597-1503 ( $C-C$ ), 1271 ( $OCH_2$ ), 1251 ( $OCH_3$ ) and 830 ( $Si-CH_3$ )  $cm^{-1}$ .  $^1H$  NMR, (ppm, acetone- $d^6$ , 400 MHz): -0.20-0.05 (6H,  $Si-CH_3$ ), 3.34-3.67 (8H,  $OCH_2Si$  &  $OCH_3 \times (2)$ ), 6.63-7.26 (6H,  $H_{ar}$ ), 8.13-8.29 (2H,  $H_7$ ).  $^{13}C$  NMR, (ppm,  $DMSO-d^6$ , 100 MHz): -5.42-1.52 (2C,  $SiCH_3$ ), 55.91-56.28 (2C,  $OCH_3$ ), 59.76 (1C,  $OCH_2Si$ ), 109.64-110.18 (2C,  $C_3$ ), 111.96-112.59 (2C,  $C_6$ ), 123.99 (2C,  $C_5$ ), 127.02-127.27 (2C,  $C_4$ ), 149.53 (2C,  $C_2$ ), 153.81 (2C,  $C_1$ ), 161.24 (2C,  $C_7$ ).

### Synthesis of copolymer, Pa3



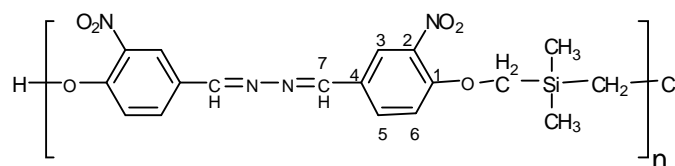
The obtained product was a glassy yellow transparent compound: yield 71.3%, IR,  $\nu$ , 3584.6 (OH), 3004 ( $C_{ar}$ -H), 2994-2890 ( $C-H_{aliph}$ ), 1622 (C=N), 1597-1502 (C-C) 1282 ( $OCH_2$ ), 1249 (O- $CH_3$ ) 796 ( $SiCH_3$ )  $cm^{-1}$ .  $^1H$  NMR, (ppm,  $CDCl_3$ , 400 MHz): -0.28-0.03 (6H,  $SiCH_3$ ), 1.08 (6H,  $OCH_2CH_3$ ), 1.34 (2H,  $SiCH_2Cl$ ), 3.55 (2H,  $OCH_2Si$ ), 3.73-3.84 (4H,  $OCH_2CH_3$ ), 6.67-7.15 (6H,  $H_{ar}$ ), 8.22(2H,  $H_7$ ).  $^{13}C$  NMR, (ppm,  $CDCl_3$ , 100 MHz): -4.97-1.71 (2C,  $CH_3Si$ ), 15.83 (2C,  $OCH_2CH_3$ ), 60.71(1C,  $OCH_2Si$ ), 65.66 (2C,  $OCH_2CH_3$ ), 112.49 (2C,  $C_3$ ), 113.05 (2C,  $C_6$ ), 124.76-124.88 (2C,  $C_5$ ), 128.15-128.73 (2C,  $C_4$ ), 150.26 (2C,  $C_2$ ), 155.22 (2C,  $C_1$ ), 162.39 (2C,  $C_7$ ).

### Synthesis of copolymer, Pa4



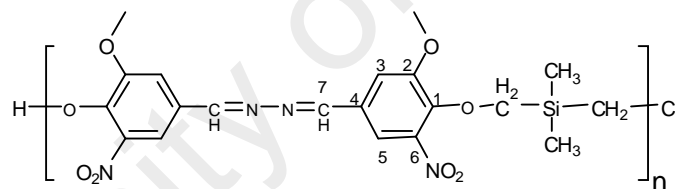
The obtained product was glassy yellow transparent compound, yield 68.6%, IR,  $\nu$ , 3477 (OH), 3009 ( $C_{ar}$ -H), 2928- 2865 ( $C-H_{aliph}$ ), 1619 (C=N), 1581-1498 (C-C), 1268 ( $OCH_2$ ), 1249 (O- $CH_3$ ) 822 ( $SiCH_3$ )  $cm^{-1}$ ,  $^1H$  NMR, (ppm,  $DMSO-d_6$ , 400 MHz): -0.25-0.07 (m, 6H,  $CH_3Si$ ), 3.61-3.68 (m, 14H,  $OCH_2Si$  &  $OCH_3$  (x4)), 6.98 ( $s_{br}$ , 4H,  $H_{3,5}$ ), 8.44 ( $s_{br}$ , 2H,  $H_7$ ),  $^{13}C$  NMR, (ppm,  $DMSO-d_6$ , 100 MHz): -6.10-0.94 (2C,  $CH_3Si$ ), 55.93 (4C,  $OCH_3$ ), 65.82 (1C,  $OCH_2Si$ ), 105.75-106.88 (4C,  $C_{3,5}$ ), 128.98 (2C,  $C_4$ ), 142.41 (2C,  $C_{2,6}$ ), 153.17 (4C,  $C_1$ ), 161.46 (2C,  $C_7$ ).

### Synthesis of copolymer, Pa5



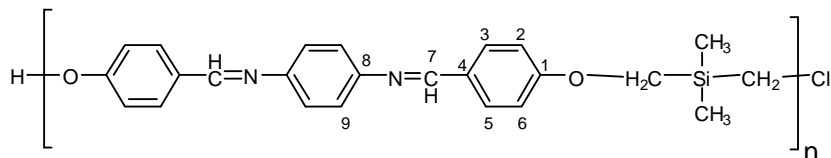
The product was orange in color: yield 68.6%, IR,  $\nu$ , 3564 (OH), 3062 ( $C_{ar}$ -H), 2951-2887 ( $C-H_{aliph}$ ), 1613 (C=N), 1564-1493 (C-C), 1278 (OCH<sub>2</sub>), 1251 (O-CH<sub>3</sub>), 817 (SiCH<sub>3</sub>)  $cm^{-1}$ . <sup>1</sup>H NMR, (ppm, CDCl<sub>3</sub>, 400 MHz): 0.05-0.32 (6H, SiCH<sub>3</sub>), 3.96 (2H, OCH<sub>2</sub>Si), 7.09-8.27 (6H, H<sub>ar</sub>), 8.50-5.52 (2H, H<sub>7</sub>). <sup>13</sup>C NMR, (ppm, CDCl<sub>3</sub>, 100 MHz): -6.13-1.10 (2C, SiCH<sub>3</sub>), 56.91 (1C, OCH<sub>2</sub>Si), 113.81 (2C, C<sub>6</sub>), 125.68 (2C, C<sub>3</sub>), 126.75 (2C, C<sub>4</sub>), 134.04 (2C, C<sub>5</sub>), 140 (2C, C<sub>2</sub>), 154.93 (2C, C<sub>1</sub>), 159.85 (2C, C<sub>7</sub>).

### Synthesis of copolymer, Pa6



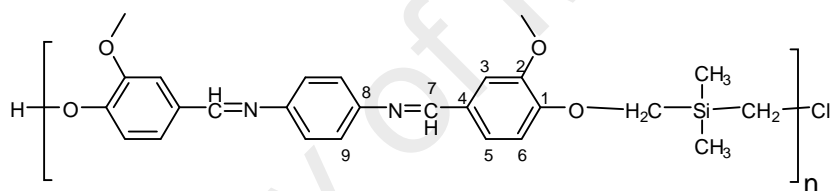
The product was glassy red color, yield 59.6%, IR,  $\nu$ , 3561 (OH), 3083 ( $C_{ar}$ -H), 2953-2833 ( $C-H_{aliph}$ ), 1625 (C=N), 1598-1504 (C-C) 1272 (OCH<sub>2</sub>), 1253 (O-CH<sub>3</sub>) 784 (SiCH<sub>3</sub>)  $cm^{-1}$ , <sup>1</sup>H NMR, (ppm, CDCl<sub>3</sub>, 400 MHz): 0.07-0.22 (6H, SiCH<sub>3</sub>), 3.93-4.03 (8H, OCH<sub>3</sub> & OCH<sub>2</sub>Si), 7.20-7.61 (4H, H<sub>ar</sub>), 8.47 (2H, H<sub>7</sub>), <sup>13</sup>C NMR, (ppm, CDCl<sub>3</sub>, 100 MHz): -7.17-0.0 (2C, SiCH<sub>3</sub>), 55.52 (2C, OCH<sub>3</sub>), 66.07 (1C, OCH<sub>2</sub>Si), 112.54 (2C, C<sub>3</sub>), 116.57 (2C, C<sub>5</sub>), 128.33 (2C, C<sub>4</sub>), 143.56 (2C, C<sub>6</sub>), 153.44 (2C, C<sub>2</sub>), 159.01 (2C, C<sub>1</sub>), 164.01 (2C, C<sub>7</sub>).

### Synthesis of copolymers, Pb1



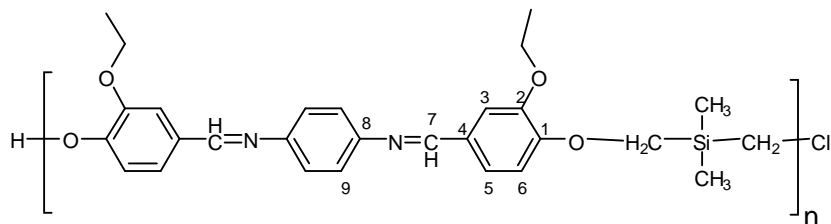
The resultant product was a glassy yellow transparent compound, yield 49.32%, IR,  $\nu$ , 3456 (OH), 3008 ( $C_{ar}$ -H), 1621 (C=N), 1566-1509 (C-C), 1272 ( $OCH_2$ ), 1258 ( $OCH_3$ )  $cm^{-1}$ .  $^1H$  NMR, (ppm,  $CDCl_3$ , 400 MHz): 0.29-0.43 (6H, Si- $CH_3$ ), 3.49-3.61 (2H,  $OCH_2Si$ ), 6.84 -7.61 (12H,  $H_{ar}$ ), 8.42 (2H,  $H_7$ ).  $^{13}C$  NMR, (ppm,  $CDCl_3$ , 100 MHz): -0.9-4.46 (2C, Si $CH_3$ ), 59.6 (1C,  $OCH_2Si$ ), 115.15 (4C,  $C_{2,6}$ ), 119.1 (4C,  $C_9$ ), 125.8 (2C,  $C_4$ ), 131.68 (2C,  $C_{3,5}$ ), 140.21 (2C,  $C_8$ ), 160.21 (2C,  $C_1$ ), 162.69 (2C,  $C_7$ ).

### Synthesis of copolymer, Pb2



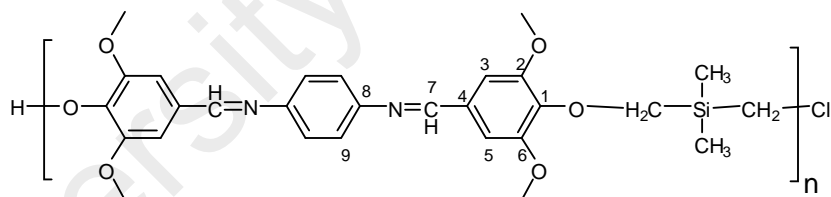
The obtained product was a glassy brown compound, yield 61.41%, IR,  $\nu$ , 3568 (OH), 3043 ( $C_{ar}$ -H), 2961-2849 ( $C-H_{aliph}$ ), 1623 (C=N), 1591-1519 (C-C), 1268 ( $OCH_2$ ), 1254 (O- $CH_3$ )  $cm^{-1}$ .  $^1H$  NMR, (ppm,  $CDCl_3$ , 400 MHz): 0.04-0.26 (6H, Si- $CH_3$ ), 3.78-3.81 (2H,  $OCH_2Si$ ), 3.84 (6H, &  $OCH_3$  (2)), 6.59-7.55 (10H,  $H_{ar}$ ), 8.42 (2H,  $H_7$ ), 9.37(2H, OH),  $^{13}C$  NMR, (ppm, acetone- $d_6$ , 100 MHz): -6.68-0.62 (2C, Si $CH_3$ ), 55.22-55.61 (2C,  $OCH_3$ ), 59.42 (1C,  $OCH_2Si$ ), 110.22 (2C,  $C_3$ ), 112.22 (2C,  $C_6$ ), 121.88 (4C,  $C_9$ ), 124.12(2C,  $C_5$ ), 129.86 (2C,  $C_4$ ), 149.94 (2C,  $C_8$ ), 151.84 (2C,  $C_2$ ), 154.21 (2C,  $C_1$ ), 158.86 (2C,  $C_7$ ).

### Synthesis of copolymer, Pb3



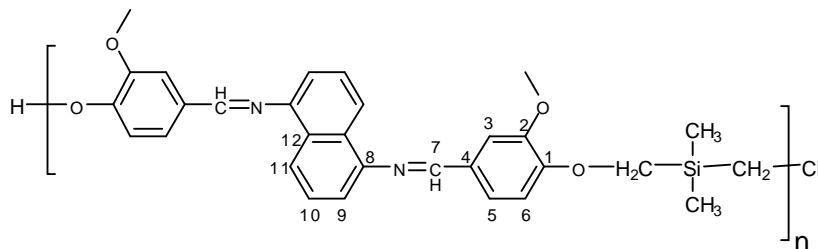
The obtained product was a dark brown compound, yield 64.11%, IR,  $\nu$ , 3562 (OH), 3079 ( $C_{ar}$ -H), 2939-2863 ( $C-H_{aliph}$ ), 1623 ( $C=N$ ), 1598-1504 ( $C-C$ ), 1267 ( $OCH_2$ ), 1244 ( $O-CH_3$ )  $cm^{-1}$ ,  $^1H$  NMR, (ppm,  $CDCl_3$ , 400 MHz): -0.28-0.04 (6H,  $Si-CH_3$ ), 1.07 (6H,  $OCH_2CH_3$ ), 3.57-3.74 (m, 6H,  $OCH_2Si$  &  $OCH_2CH_3$  ( $\times 2$ )), 6.34-7.20 (m, 10H,  $H_{ar}$ ), 8.00- 8.03 (2H,  $H_7$ ),  $^{13}C$  NMR, (ppm,  $CDCl_3$ , 100 MHz): 0.86 - 1.18 (2C,  $SiCH_3$ ), 15.03 (2C,  $OCH_2CH_3$ ), 59.89 (2C,  $OCH_2CH_3$ ), 64.75 (1C,  $OCH_2Si$ ), 111.53 (2C,  $C_3$ ), 115.68 (2C,  $C_6$ ), 121.89 (4C,  $C_9$ ), 124.42 (2C,  $C_5$ ), 129.53 (2C,  $C_4$ ), 148.89 (2C,  $C_8$ ), 149.40 (2C,  $C_2$ ), 154.42 (2C,  $C_1$ ), 159.37 (2C,  $C_7$ ).

### Synthesis of copolymer, Pb4



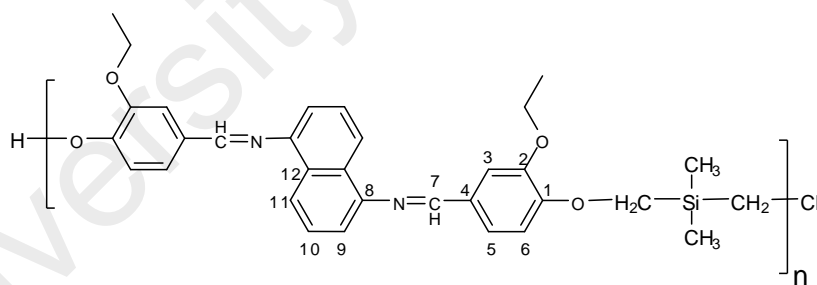
The obtained product was a dark brown compound, yield 59.5%, IR,  $\nu$ , 3559 (OH), 3079 ( $C_{ar}$ -H), 2948-2849 ( $C-H_{aliph}$ ), 1623 ( $C=N$ ), 1589-1518 ( $C-C$ ), 1269 ( $OCH_2$ ), 1248 ( $O-CH_3$ )  $cm^{-1}$ ,  $^1H$  NMR, (ppm,  $CDCl_3$ , 400 MHz): 0.02-0.26 (6H,  $SiCH_3$ ), 3.69-3.98 (14H,  $OCH_2Si$  &  $OCH_3$  ( $\times 4$ )), 7.03-7.19 (8H,  $H_{ar}$ ), 8.3 (2H,  $H_7$ ),  $^{13}C$  NMR, (ppm,  $CDCl_3$ , 100 MHz): -0.87-1.14 (2C,  $SiCH_3$ ), 56.26 (4C,  $OCH_3$ ), 66.83-68.42 (1C,  $OCH_2Si$ ), 105.88-107.08 (2C,  $C_{3,5}$ ), 122.39 (4C,  $C_9$ ), 131.37 (2C,  $C_4$ ), 146.17 (2C,  $C_8$ ), 153.68 (4C,  $C_2$ ), 153.86 (2C,  $C_1$ ), 159.50 (2C,  $C_7$ ).

### Synthesis of copolymer, Pb5



The obtained product was a dark brown compound, yield 56.2%, IR,  $\nu$ , 3566 (OH), 3069 ( $C_{ar}$ -H), 2933-2859 ( $C-H_{aliph}$ ), 1622 (C=N), 1588-1519 (C-C), 1266 ( $OCH_2$ ), 1247 (O-CH<sub>3</sub>)  $cm^{-1}$ ,  $^1H$  NMR, (ppm, acetone- $d^6$ , 400 MHz): 0.01-0.31 (6H,  $CH_3Si$ ), 3.89 (6H,  $OCH_3$ ), 3.95 (2H,  $OCH_2Si$ ), 6.39-7.43 (8H,  $H_{ar}$ ), 7.61-7.71 (m, 2H,  $H_3$ ), 8.14 (d, 2H,  $H_{11}$ ), 8.36 (m, 2H,  $H_7$ ),  $^{13}C$  NMR, (ppm, acetone- $d^6$ , 100 MHz): -3.92-1.03 (2C,  $SiCH_3$ ), 59.92(2C,  $OCH_2CH_3$ ), 64.84 (1C,  $OCH_2Si$ ), 108.65-114.20 (6C,  $C_{3,6,9}$ ), 119.64 (2C,  $C_5$ ), 123.54-126.59 (6C,  $C_{10,11,12}$ ), 131.12 (2C,  $C_4$ ), 149.54 (2C,  $C_8$ ), 149.15 (2C,  $C_2$ ), 157.25 (2C,  $C_1$ ), 160.01 (2C,  $C_7$ ).

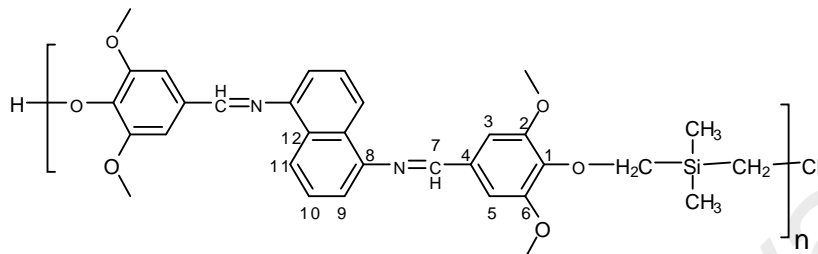
### Synthesis of copolymer, Pb6



The obtained product was a brownish black compound, yield 57.01%, IR,  $\nu$ , 3569 (OH), 3059 ( $C_{ar}$ -H), 2943-2861 ( $C-H_{aliph}$ ), 1620 (C=N), 1579-1504 (C-C), 1271 ( $OCH_2$ ), 1239 (O-CH<sub>3</sub>)  $cm^{-1}$ ,  $^1H$  NMR, (ppm,  $CDCl_3$ , 400 MHz): -0.29-0.09 (6H,  $CH_3Si$ ), 0.91-1.05 (6H,  $OCH_2CH_3$ ), 3.38-3.88 (6H,  $OCH_2Si$  &  $OCH_2CH_3$  (x2)), 6.24-8.18 (12H,  $H_{ar}$ ),  $^{13}C$  NMR, (ppm, acetone- $d^6$ , 100 MHz): -6.30-1.03 (2C,  $SiCH_3$ ), 14.76 (2C,  $OCH_2CH_3$ ), 59.92 (2C,  $OCH_2CH_3$ ), 64.54-64.84 (1C,  $OCH_2Si$ ), 108.77-

113.80 (6C, C<sub>3,6,9</sub>), 119.64 (2C, C<sub>5</sub>), 124.41-126.64 (6C, C<sub>10,11,12</sub>), 130.78 (2C, C<sub>4</sub>), 149.72 (2C, C<sub>8</sub>), 149.86 (2C, C<sub>2</sub>), 157.28 (2C, C<sub>1</sub>), 159.91 (2C, C<sub>7</sub>).

### Synthesis of copolymer, Pb7



The obtained product was a brownish black compound, yield 51.6%, IR,  $\nu$ , 3559 (OH), 3061 (C<sub>ar</sub>-H), 2941-2853 (C-H<sub>aliph</sub>), 1622 (C=N), 1589-1523 (C-C), 1268 (OCH<sub>2</sub>), 1251 (O-CH<sub>3</sub>) cm<sup>-1</sup>, <sup>1</sup>H NMR, (ppm, CDCl<sub>3</sub>, 400 MHz): -0.22-0.06 (6H, SiCH<sub>3</sub>), 3.63 (12H, OCH<sub>3</sub> (x4)), 3.76 (2H, OCH<sub>2</sub>Si), 6.76 (2H, H<sub>9</sub>), 6.91-6.96 (4H, H<sub>3,5</sub>), 7.16 (2H, H<sub>8</sub>), 7.88 (2H, H<sub>11</sub>), 8.12 (2H, H<sub>7</sub>), <sup>13</sup>C NMR, (ppm, CDCl<sub>3</sub>, 100 MHz): -5.95-1.18 (2C, SiCH<sub>3</sub>), 56.37 (4C, OCH<sub>3</sub>), 66.88 (1C, OCH<sub>2</sub>Si), 106.00-106.35 (4C, C<sub>3,5</sub>), 113.63 (2C, C<sub>9</sub>), 121 (2C, C<sub>11</sub>), 125.97 (2C, C<sub>10</sub>), 129.33 (2C, C<sub>12</sub>), 131.53 (2C, C<sub>4</sub>), 143.72 (2C, C<sub>8</sub>), 149.24 (2C, C<sub>2,6</sub>), 153.74 (2C, C<sub>1</sub>), 160.26 (2C, C<sub>7</sub>).

## 2.4 Characterization methods and instrumentation

The synthesized monomers, copolymers and symmetrical dimers were characterized and confirmed by using instruments as described in the following section.

### 2.4.1 Fourier Transform Infrared Spectroscopy (FTIR)

Infrared spectroscopy is one of the most important techniques for study and identifying types of chemical bonds (functional groups) that are either inorganic or organic by producing an infrared absorption spectrum that is like a molecular “fingerprint”. It is also possible to apply it in the chemical study of polymers, spills, coatings and contaminants[140].

The FT-IR was determined by a Spotlight 400 PerkinElmer spectrometer at room temperature with 16 scans using attenuated total reflectance (ATR) technique. The region of the wavelength was recorded from 650-4000  $\text{cm}^{-1}$ . Background effects due to atmospheric water and carbon dioxide were subtracted.

#### **2.4.2 Nuclear Magnetic Resonance Spectroscopy ( $^1\text{H}$ NMR, $^{13}\text{C}$ NMR and 2D NMR)**

Nuclear Magnetic Resonance spectroscopy (NMR) has become the most excellent analytical technique for identifying and determining the structure of compounds[141]. Of all the spectroscopic methods, it is the only one for which a full analysis and interpretation of the entire spectrum is normally estimated. Although larger amounts of sample are needed compared to mass spectroscopy, NMR is non-destructive, and with modern instruments good data may be obtained from samples weighing less than a milligram.

The proton nuclear magnetic resonance  $^1\text{H}$  NMR and  $^{13}\text{C}$  NMR spectra were recorded with a Lambda 400 MHz spectrometer, a JEOL-ECA 100 MHz spectrometer and AVN 600 MHz spectrometer. Samples were dissolved in suitable solvent to obtain a clear solution. Commonly used solvents include dimethyl sulfoxide- $\text{d}^6$  (DMSO- $\text{d}^6$ ), chloroform- $\text{d}_1$  ( $\text{CDCl}_3$ ) and acetone- $\text{d}^6$ . Concentrations were maintained at 2.5% (w/v) and 15% (w/v) for the  $^1\text{H}$  NMR and  $^{13}\text{C}$  NMR analyses respectively. Tetramethylsilane (TMS) was used as standard for chemical shift at 0 ppm, and the deuterated solvents ( $\text{CDCl}_3$ ) display typical peaks at 7.26 ppm and 1.7 ppm for  $^1\text{H}$  NMR and 77.0 ppm for  $^{13}\text{C}$  NMR. In addition, the (DMSO- $\text{d}^6$ ) peaks appear at 3.34 ppm and 2.4 for  $^1\text{H}$  NMR and 40.6 ppm for  $^{13}\text{C}$  NMR. Acetone- $\text{d}^6$  peaks are observed at 2.17 ppm for  $^1\text{H}$  NMR and 29.9 ppm for  $^{13}\text{C}$  NMR.

### 2.4.3 Thin Layer Chromatography (TLC)

TLC was used to examine and purifies the sample as well as monitoring the progress of the reaction by using aluminium-backed silica-gel plates under short-wave ultra violet light or iodine vapours. Initially the sample was dissolved in an appropriate solvent and placed at 0.5 cm from bottom of the TLC plate. Mixture of hexane and ethyl acetate was prepared with a ratio of 3:1 respectively which acted as the mobile phase. The TLC evaporation chamber was lined with a folded piece of filter paper to create uniform and saturated atmosphere of solvent vapour. In addition, this can be used to avoid evaporation of solvent. The moving of the solvent was monitored until approximately 0.5 cm from the top of TLC plate, followed by removing the TLC plate and examined by using short-wave ultra violet light which usually shows only one spot if the compound is pure.

### 2.4.4 Gel Permeation Chromatography (GPC)

Molecular weight distribution is one of the basic characteristic of polymers because it can significantly affect the properties of polymers such as thermal stability and other mechanical and physical properties. The average molecular weights and polydispersities (PDI) of polymers were measured by gel permeation chromatography GPC also called size exclusion chromatography (SEC)[142]. GPC analysis was conducted using a Waters 2414 refractive index detector coupled with a Waters 717 plus Autosampler and Waters 600 Controller. Polystyrene (PS) standards were used as reference and (THF) as the eluent, at a flow rate of 1 cm<sup>3</sup>/min at room temperature. A weight of 5 mg of the sample was dissolved in 5 mL of THF followed by filtration through a Waters GHP Acrodisc that has a minispikes diameter of 13 mm and a pore size of 0.45 µm (to avoid any undissolved particulates pass through the column) into small vial of about 1 mL capacity. Running time for each sample was 55 minutes and the

volume of injection was 100  $\mu\text{l}$  for each vial. The calibration curves of GPC are shown in appendix.

#### **2.4.5 Thermogravimetric Analysis (TGA)**

TGA is one of an important technique for determining thermal stability of polymers. The most widely used TGA technique is based on continuous measurement of weight on a very sensitive balance called a thermobalance (a sensitive balance) as sample temperature is increased in air or in an inert atmosphere. Data are recorded as a thermogram of weight versus temperature[142].

In this research, thermal stability of the synthesized copolymers were obtained using a PerkinElmer Pyris-Diamond TG/DTA thermobalance under a steady flow of nitrogen atmosphere at a heating rate of 20°C/min starting from 50°C to 900°C. The sample weight used was between 5-10 mg for all the materials. The processing of the data was performed using the instrument's built in Pyris v9.1.0.0203 software.

#### **2.4.6 Differential Scanning Calorimetry (DSC)**

DSC is an accurate analytical technique that allows determination of glass transition temperature ( $T_g$ ) and analyses the enthalpy changes of the sample.  $T_g$  is defined as a change in the heat capacity as the polymer matrix passes from the glassy state to the rubbery state. The polymer sample and an inert reference are heated in a nitrogen atmosphere and thermal transitions in the sample are measured and detected.

In this study, thermal transition temperature of the synthesized materials was performed using a PerkinElmer DSC instrument in nitrogen atmosphere and calibrated with an indium standard. The scan rate and temperature for both heating and cooling were set accordingly for the various samples. The nitrogen flow during heating and cooling was 3 mL/minutes. 5-10 mg of samples were weighed accurately and transferred to a 45  $\mu\text{L}$  aluminium crucible. The crucible was pressed tightly with a cover

by using the sealing press. The same empty crucible was utilized as a reference and then placed into the compartment of the DSC instruments. After the scanning was completed, the sample was removed from the compartment and preceded to another sample. The processing of the data was performed using the instrument's built in Pyris v9.1.0.0203 software.

#### **2.4.7 Polarised Optical Microscopy (POM)**

The liquid crystalline behaviour was performed by polarised optical microscopy (OPM) using Mettler Toledo FP82HT hot stage (Mettler Toledo Inc, Switzerland) viewed with an Olympus BX51 microscope fitted with crossed polarizing filters. The images were obtained by an Olympus camera that was connected to a microscope, and the magnification factors of the images were 10 and 20. The image was obtained by using a microscope with a small amount of sample covered with a small glass slip. The sample was heated on a hot stage until isotropic temperature (clear point) at a rate of 3°C/min. When the sample was melted the glass cover was pressed gently by a wooden stick to obtain a thin film of the sample followed by cooling at 3°C/min before the mesophase image was obtained with good texture.

#### **2.4.8 X-Ray Crystallography**

X-ray crystallography is a technique used for studying and determining the atomic and molecular structure of a crystal, in which the atoms cause a beam of X-ray to diffract into many specific directions. Three dimensional pictures of the density of electrons within the crystal were obtained by measuring the intensities and angles of these diffracted beams. From the electron density, it is possible to determine the mean positions of the atoms in the crystal.

The crystal structure determination was carried out on a Bruker Smart APEXII CCD area detector diffractometer equipped with graphite mono-chromatised Mo-K

( $\lambda = 0.71073 \text{ \AA}$ ) radiation. The program *APEX2* (Bruker 2009) was used for collecting frames of data, indexing of reflections and determination of lattice parameters, *SAINT* (Bruker 2009) for absorption correction, and *SHELXS97* and *SHELXL97* (Sheldrick 2008) for structural solution.

#### **2.4.9 Ultraviolet-Visible (UV-Visible) and Photoluminescence Spectroscopies**

Ultraviolet-visible absorption spectroscopy is used to study the changes in electronic energy level within the molecule arising due to transfer of electron from  $\pi$ - or non-bonding orbitals as well detection and quantitative measurement of chromophores that undergo  $n \rightarrow \pi^*$  or  $\pi \rightarrow \pi^*$  transitions. Due to its sensitivity, UV-vis spectroscopy has been particularly useful in identifying and analysing in polymeric materials. In addition, UV-vis provides information on  $\pi$ -electron systems, conjugated unsaturations, aromatic compounds and conjugated non-bonding electron systems[143].

UV-vis absorption measurement was performed on a Cary 60 UV-VIS spectrophotometer at room temperature. The copolymer solution of concentration  $1 \times 10^{-6} \text{ M}$  in DMF was prepared and distilled DMF was used as a blank and placed in clear quartz cuvettes. The sample was scanned at 200 nm to 800 nm with medium scan rate. Fluorescence spectra were obtained through a Cary Eclipse spectrophotometer and the copolymer was also measured from 200 nm to 600 nm.

#### **2.4.10 Electrochemical measurement**

The electrochemical properties were measured using a potentiostat/galvanostat (AUTOLAB/PGSTAT 302N) which was run by general purpose Electrochemical system software (GPES). The experiments were achieved in a 0.1 M tetrabutylammonium perchlorate ( $\text{Bu}_4\text{NClO}_4$ ) (TBAP) as a supporting electrolyte in an anhydrous acetonitrile ( $\text{CH}_3\text{CN}$ ) using a thin film coated on an indium-tin-oxide (ITO) glass substrate as working electrode at room temperature. The cyclic voltammetric

curves were referenced to an AgCl/Ag reference electrode and the scan rate was 50 mV/s in a potential range of -2.0 V to +2.0 V.

University of Malaya

## **CHAPTER 3 : CARBOSILANE COPOLYMERS BASED ON BISPHENOL AZINE MONOMERS**

### **3.1 Introduction**

As mentioned in Chapter 1, silicon containing polymer and Schiff base containing polymer have a wide spectrum applications and many interesting physical properties. In this chapter, the syntheses of new copolymers that have combined silicon moiety together with full conjugated structure of bisphenol containing bis-Schiff base monomers are presented. Some of their physical properties which could elucidate the application of these new copolymers are also described.

### **3.2 Results and discussion**

New polycarbosilanes was successfully synthesized based on full conjugation bisphenol azine monomers with different substituted groups. The synthesized materials were characterized and identified by FTIR,  $^1\text{H}$  NMR,  $^{13}\text{C}$  NMR, 2D NMR, X-ray crystallography, and GPC for the synthesized copolymers.

#### **3.2.1 Synthesis route of bisphenol azine monomers (a1-a6)**

Full conjugation bisphenol azine monomers were successfully synthesized with different substituents groups at ortho position of the phenol group. These monomers were synthesized through the condensation reaction of 4-hydroxybenzaldehyde and their substituted derivatives with hydrazine sulphate in the presence of concentrated ammonium solution as a catalyst to produce high yield. The synthetic route of bisphenol azine monomers is illustrated in Figure 3.1. The substituted groups, yields, melting points and the molecular formulae of the synthesized monomers are tabulated in Table 3.1.

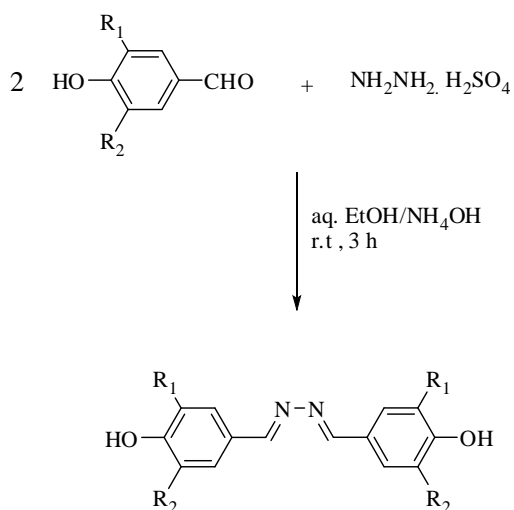


Figure 3.1 : General synthetic route of bisphenol azine monomer

Table 3.1 : Details of the synthesized bisphenol azine monomers

Monomer	R <sub>1</sub>	R <sub>2</sub>	Yield (%)	Mp. (°C)	Molecular Formula
<b>a1</b>	H	H	81.3	284-285	C <sub>14</sub> H <sub>12</sub> N <sub>2</sub> O <sub>2</sub>
<b>a2</b>	H	OCH <sub>3</sub>	82.9	175-176	C <sub>16</sub> H <sub>16</sub> N <sub>2</sub> O <sub>4</sub>
<b>a3</b>	H	OCH <sub>2</sub> CH <sub>3</sub>	80.4	204-205	C <sub>18</sub> H <sub>20</sub> N <sub>2</sub> O <sub>4</sub>
<b>a4</b>	OCH <sub>3</sub>	OCH <sub>3</sub>	78.8	214-215	C <sub>18</sub> H <sub>20</sub> N <sub>2</sub> O <sub>6</sub>
<b>a5</b>	H	NO <sub>2</sub>	71.1	257-258	C <sub>14</sub> H <sub>10</sub> N <sub>4</sub> O <sub>6</sub>
<b>a6</b>	OCH <sub>3</sub>	NO <sub>2</sub>	72.9	269-270	C <sub>16</sub> H <sub>14</sub> N <sub>4</sub> O <sub>6</sub>

The monomers showed good solubility in DMF and DMSO at room temperature except for (**a5**) and (**a6**) which require high temperature due to the presence of NO<sub>2</sub> moiety[144].

### 3.2.2 Characterizations of the azine monomers

The synthesized monomers (**a1-a6**) were characterized by FTIR, <sup>1</sup>H NMR, <sup>13</sup>C NMR. 2D NMR (HSQC and HMBC) was used for further identification of compound (**a2**). Three single crystals of compounds **a3**, **a4** and **a5** were analysed by X-ray crystallography. The results were in agreement with the proposed structures.

### 3.2.2.1 Fourier transform infrared (FTIR)

The aromatic compounds display significant characteristic infrared bands in five regions of the mid-infrared spectrum. The C-H stretching bands of aromatic materials exist in the frequencies 3100-3000  $\text{cm}^{-1}$  range, so making them easy to distinguish from those produced by aliphatic C-H moieties which appear in the frequencies between 2850-2950  $\text{cm}^{-1}$ . A series of overtone and weak combination bands as well as the pattern of the overtone bands reflects the substitution pattern of the aromatic ring which appear in the frequencies of 2000-1700  $\text{cm}^{-1}$ . Skeletal vibrations, representing C=C stretching, absorb in the frequencies of 1600-1430  $\text{cm}^{-1}$  range. In-plane bending and out-of plane bending for C-H bending bands appear in the frequencies range of 1257-1000  $\text{cm}^{-1}$  and 900-690  $\text{cm}^{-1}$  respectively. The bands of the out-of-plane bending vibrations of benzene ring are strong and characteristic of the number of hydrogen atoms in the aromatic compounds, and hence can be used to give the substitution pattern[145].

The main infrared bands and their assignments for the synthesized azine monomers (**a1-a6**) are tabulated in Table 3.2. There are similarities in the IR spectra of the azine monomers, except for some slight variations in the shifts and intensities of vibration peaks due to different substituted groups attached to the benzene ring. The O-H stretching bands of the bisphenol monomers appear within the frequencies of 3476-3617  $\text{cm}^{-1}$  with observed weak absorption bands for all monomers which is attributed to the presence of strong intramolecular hydrogen bonding O-H...N. The characteristic frequencies appeared in the spectra of all monomers in the range of 3012-3083  $\text{cm}^{-1}$  assignable to C-H stretching band and the characteristic frequencies presented in the range of 2913-2952  $\text{cm}^{-1}$  are assignable to C-H aliphatic stretching band. Strong intensity absorption peaks appeared in the frequencies of 1618-1628  $\text{cm}^{-1}$  region assignable to Schiff base moiety(C=N)[146, 147]. On the other hand, the ether moiety

absorbed strongly in the frequencies range of 1251-1275  $\text{cm}^{-1}$ . With disappearance of the carbonyl group of the aldehyde and the amine of hydrazinium sulphate which appeared in the frequencies of 1720-1800  $\text{cm}^{-1}$ , and appearance of a new peaks due to formation of imine group at 1618-1628  $\text{cm}^{-1}$  as well the other expected peaks such as OH at 3479-3617  $\text{cm}^{-1}$  confirm the proposed structure. Figure 3.2 shows the FTIR of monomer **a2** which is typical for all the monomers.

Table 3.2 : Some of the important FT-IR spectra data of azine monomers

Monomer	O-H	C-H <sub>ar</sub>	C-H <sub>aliph</sub>	C=N	C=C <sub>ar</sub>	O-C
<b>a1</b>	3481	3045	-	1618	1586-1505	-
<b>a2</b>	3479	3070	2919	1624	1512-1600	1257
<b>a3</b>	3617	3034	1929	1628	1509-1597	1275
<b>a4</b>	3480	3012	2936	1621	1494-1588	1254
<b>a5</b>	3570	3074	-	1620	1488-1571	1251
<b>a6</b>	3561	3083	2953	1625	1598-1504	1253

= stretching , aliph= aliphatic, ar= aromatic

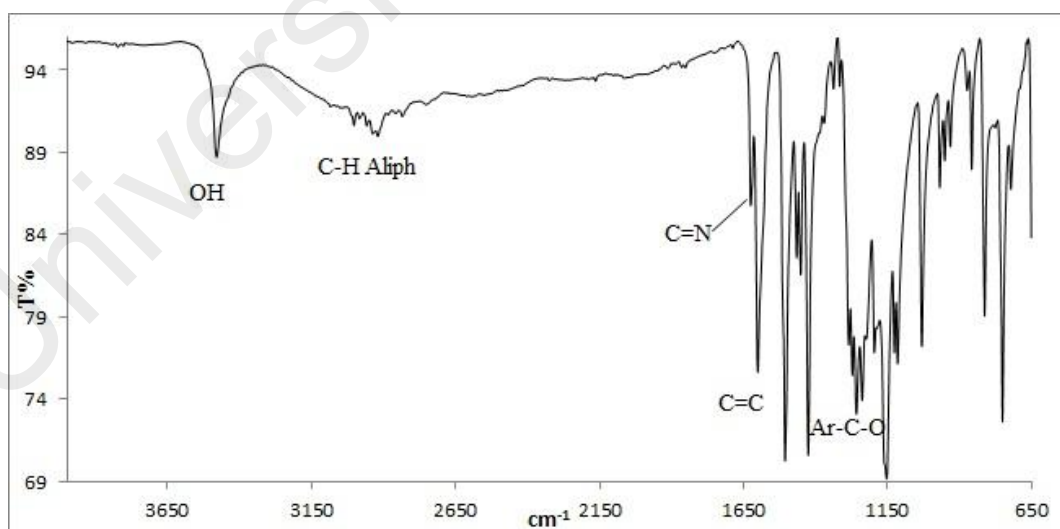


Figure 3.2 : FTIR spectrum of monomer **a2**

### 3.2.2.2 <sup>1</sup>H NMR

The structures and purities of all the synthesized azine monomers (**a1-a6**) were confirmed by <sup>1</sup>H NMR analysis. The <sup>1</sup>H NMR spectrum and structure of (**a3**) azine monomer with its molecular structure are shown in Figure 3.3. The results are tabulated in Table 3.3.

The <sup>1</sup>H NMR spectra shows the disappearance of the aldehyde, (CHO) and amino group (NH<sub>2</sub>) in all monomers. Beside, a new sharp singlet peak at the region of 8.52-8.75 ppm with an integration equivalent to two protons corresponding to the azomethine group (C=N) is exhibited by all the monomers[148, 149]. The H<sub>3</sub> shows doublet peaks in the region of 6.76-8.42 ppm with a coupling constant range of 1.3-1.6 MHz that could be attributed to 1,3 splitting [150], except for monomers (**a2**) and (**a4**) which give singlet peak. Double doublets are observed for H<sub>5</sub> due to two protons in the region of 7.12-8.11 ppm with a coupling constants of 8.2-8.8 MHz and 1.7-2.2MHz which are attributed to 1,2 and 1,3 splitting [150]. In the region of 6.84-7.30 ppm, the doublet signals for two protons are assigned for H<sub>6</sub> proton. The signals observed in the region of 3.79-4.02 ppm correspond to methoxy group protons attached to benzene[151]. For (**a3**) monomers, a quartet peak in the region of 4.02 ppm and a tertiary peak in the region of 1.33 ppm due to O-CH<sub>2</sub> and O-CH<sub>2</sub>CH<sub>3</sub> group respectively are displayed. A singlet peak in the range of 9.02-10.06 ppm attributed to proton of (OH) group is shown by some compounds only. The difficulty in observing this peak in the other compounds could be because of the replacement of most of the hydrogen atoms of OH by deuterium of DMSO solvent as well formation of strong intramolecular hydrogen bonding O-H...N.

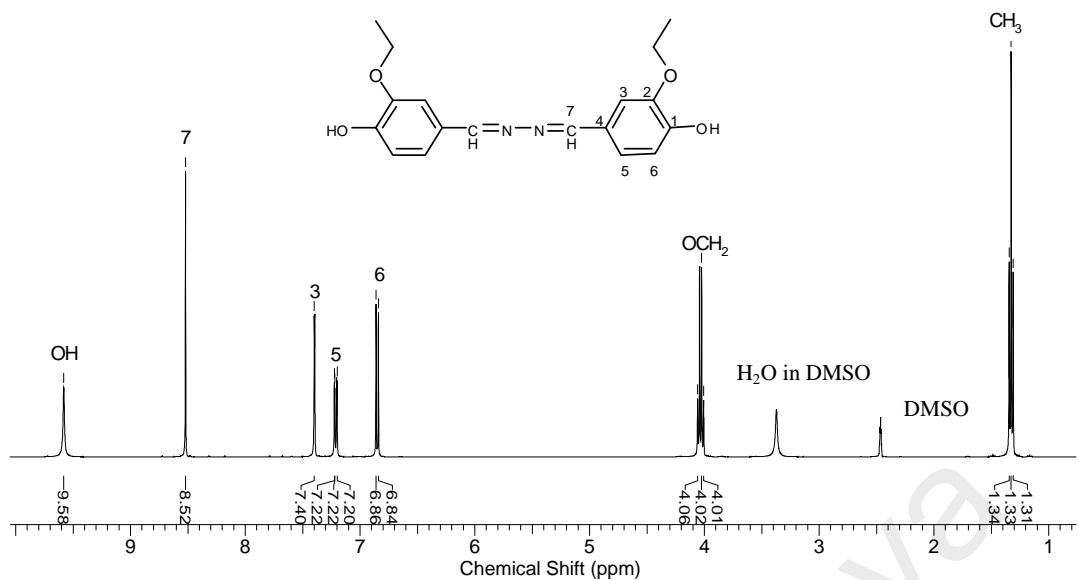


Figure 3.3 :  $^1\text{H}$  NMR spectrum of monomer **a3**

Table 3.3:  $^1\text{H}$  NMR data of azine monomers (**a1-a6**)

Type of proton	Chemical shift (ppm)
O-CH <sub>3</sub>	3.79- 4.02
CH <sub>2</sub> CH <sub>3</sub>	1.33
Ar-H 2 <sup>th</sup> position	6.84
Ar-H 3 <sup>th</sup> position	6.76-8.42
Ar-H 5 <sup>th</sup> position	7.12-8.11
Ar-H 6 <sup>th</sup> position	6.84-7.30
C=N 7 <sup>th</sup> position	8.52-8.75
Ar-OH 1 <sup>th</sup> position	9.02-10.06

### 3.2.2.3 $^{13}\text{C}$ NMR

The most significant peak of  $^{13}\text{C}$  NMR is observed at 160.96-161.4 ppm which is attributed to the azomethine (C=N) carbon atom of azine monomer[152]. The C<sub>1</sub> which is attached to OH phenol is observed down field in the region of 148.6-160.8 ppm. In addition, C<sub>2</sub> appears in a broad shift range of shifting within the region of 116.3-148.5 ppm depending on the substituted moieties that is attached with this carbon. For example, when the substituted group is NO<sub>2</sub> the C<sub>1</sub> will appear in the region of 137 ppm while when the moiety is OCH<sub>3</sub> the shifting will be toward low field in the region

of 146-148 ppm. The C<sub>3</sub> carbon gives signal in the region of 106.36-130.66 ppm and C<sub>4</sub> carbon gives signal in the region of 124.24-126.34 ppm while C<sub>5</sub> carbon is assignable in the region of 106.36-143.34 ppm. Figure 3.4 displays <sup>13</sup>C NMR spectrum of monomers (**a3**) and Table 3.4 shows <sup>13</sup>C NMR results of the bisphenol azine monomers (**a1-a6**).

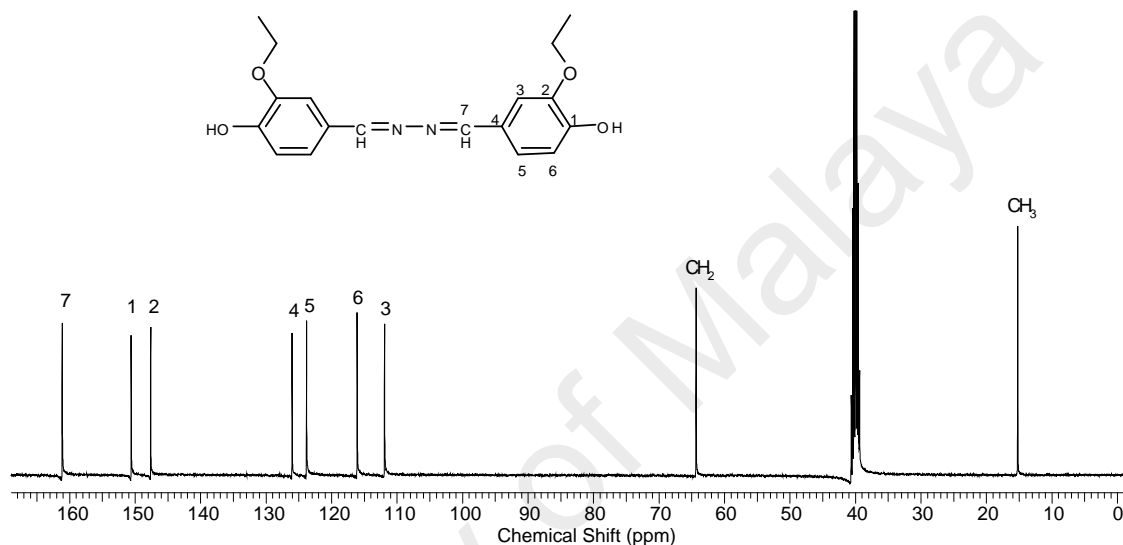


Figure 3.4: <sup>13</sup>C NMR spectrum of monomer **a3**

Table 3.4: <sup>13</sup>C NMR data of bisphenol azine monomers (**a1-a6**)

Type of carbon	Chemical shift (ppm)
OCH <sub>2</sub> , O-CH <sub>3</sub>	56 -75.11
CH <sub>3</sub>	15.2
Ar-C 2 <sup>th</sup> position	116.3-148.5
Ar-C 3 <sup>th</sup> position	106.36-130.66
Ar-C 5 <sup>th</sup> position	106.36-143.34
Ar-C 6 <sup>th</sup> position	116.2-139.4
Ar-C 4 <sup>th</sup> position	124.24-126.34
C=N 7 <sup>th</sup> position	160-160.96
Ar-OH 1 <sup>th</sup> position	148.6-160.8

### 3.2.2.4 The 2DNMR

There are three peaks in  $^{13}\text{C}$  NMR spectra of monomers in the range of 145-160 ppm which are attributed to  $\text{C}_1\text{-OH}$ ,  $\text{C}_2\text{-OR}$  and  $\text{C=N}$ . These three peaks are difficult to distinguish due to the similarity of their shifts. To overcome on this problem 2DNMR (HMQC and HMBC) was utilized to resolve this confusion. Monomer (**a2**) was used as an example to illustrate this problem.

As shown in Figure 3.5, the HMQC spectra exhibited the correlation between  $\text{H}_7$  and  $\text{C}_7$  and confirmed that the peak at 161 ppm belongs to  $\text{C}_7$  ( $\text{CH=N}$ ). The HMQC also demonstrated the correlation between  $\text{H}_3$  and  $\text{C}_3$  at 6.85-110 ppm. The correlation between  $\text{H}_5\text{-C}_5$  at 7.23-124 and that  $\text{H}_6\text{-C}_6$  are shown in Figure 3.6.

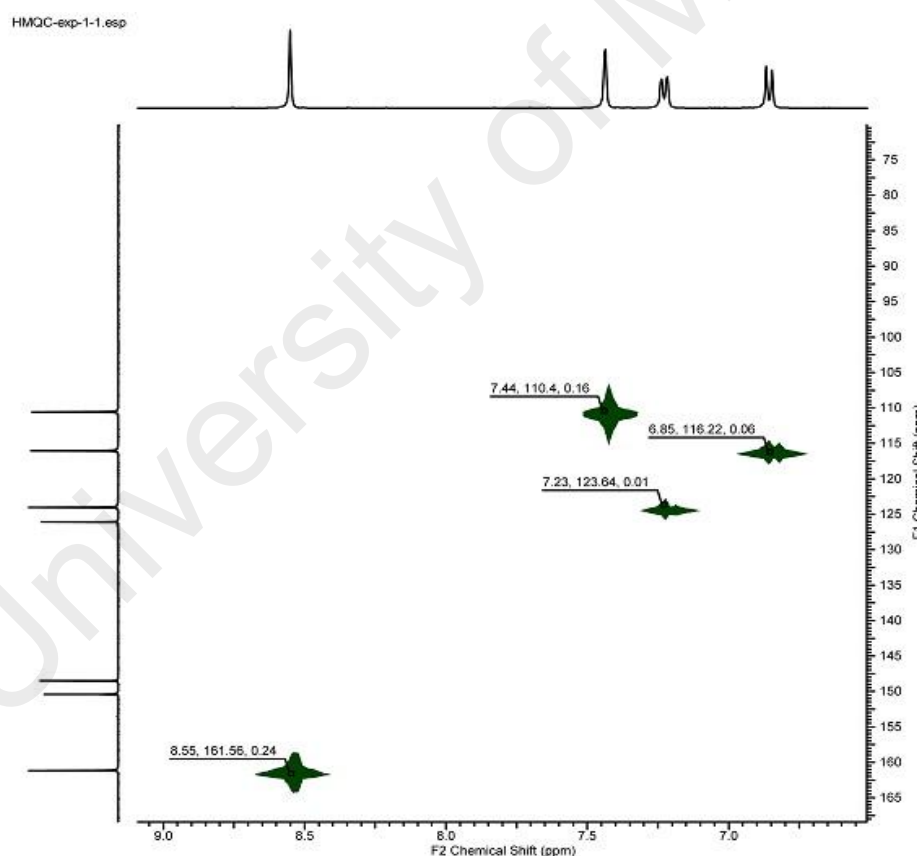


Figure 3.5: HMQC expansion region of monomer **a2**

Distinguishing between  $C_1$  (C-OH) and  $C_2$  (C-OCH<sub>3</sub>) was also a problem as their peaks appeared very close to each other due to the similarity in their electronegativities. Thus, the HMBC was used to resolve the confusion between these groups where the HMBC will show the strong correlation through the long distance coupling  $J_3$  and also the weak correlation through  $J_2$ .

The correlation of OCH<sub>3</sub> proton with carbon at 148 ppm as  $J_3$  and the correlation of OH proton with C<sub>6</sub> and carbon at 148 ppm as  $J_3$  clarify that the carbon at 148 ppm belongs to C<sub>2</sub> and the carbon at 150 ppm belongs to C<sub>1</sub>. The other correlations are depicted in Figure 3.6.

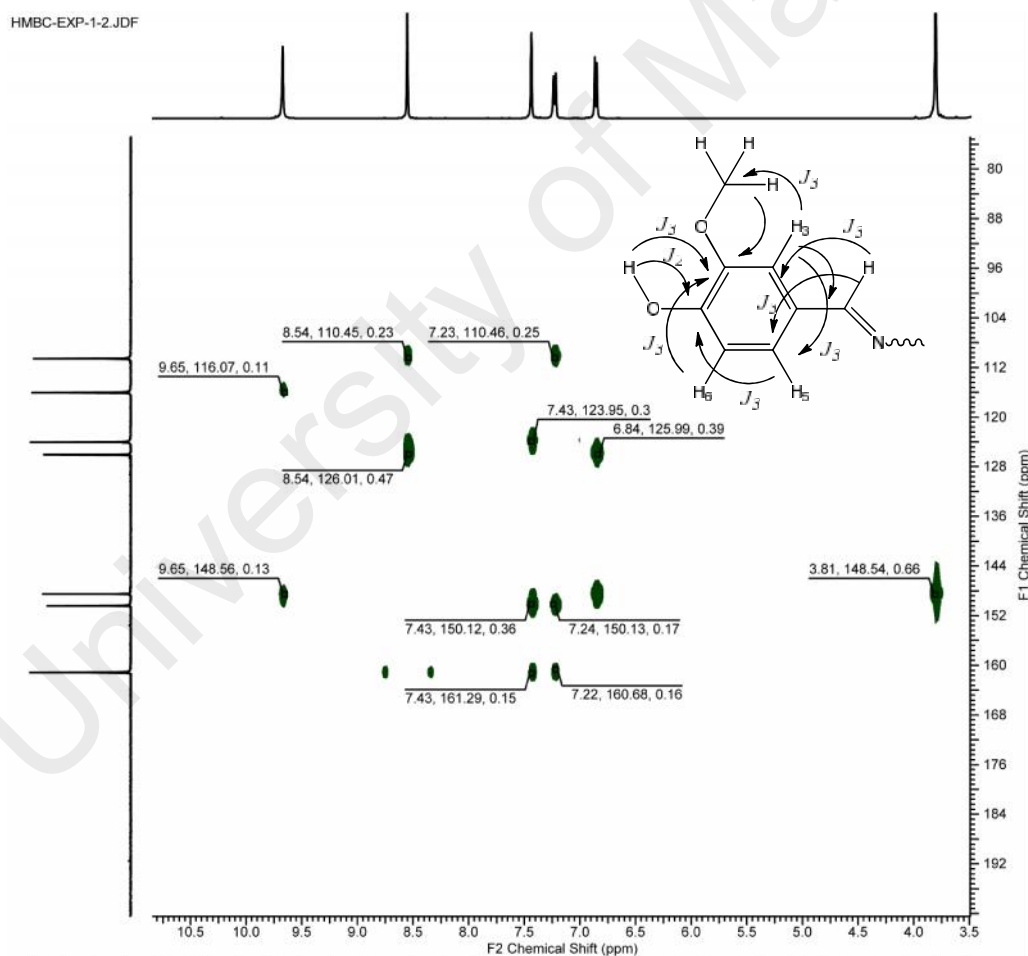


Figure 3.6 : The HMBC spectrum of monomers **a2**

### 3.2.2.5 X-ray crystallography

The molecular structure of compounds **a3**, **a4** and **a5** were characterized by X-ray crystallography where the monomer **a4** ( $C_{18}H_{20}N_2O_4$ ) is centrosymmetric around the central azine bond [ $N1-N1^i = 1.416(2) \text{ \AA}$ ; symmetry operation  $i: -x + 2, -y + 1, -z + 1$ ], with the *E* configuration around the  $N1=C1$  bond [ $1.284(1) \text{ \AA}$ ]. In the crystal structure of the title compound in Figure 3.7, the molecules are linked together by  $O-H\cdots N$  hydrogen bonds [ $O2-H2\cdots N1^{ii} = 2.7782(12) \text{ \AA}$ ; symmetry operation  $ii: 3/2 - x, 1/2 + y, 1/2 + z$ ] resulting in the formation of a two-dimensional supramolecular network which propagated parallel to the *bc* plane.  $C-H\cdots\pi$  interaction is also present;  $C8-H8b\cdots Cg1^{iii} = 2.71 \text{ \AA}$  where  $Cg1$  is the centroid of the ring  $C2 - C7$ , [symmetry code: (iii)  $-1 + x, y, z$ ]. In contrast to the title compound, the methoxy substituted analogue[153] consists of two asymmetric units with the presence of additional intermolecular  $O-H\cdots O$  hydrogen bonds with the adjacent asymmetric unit[154].

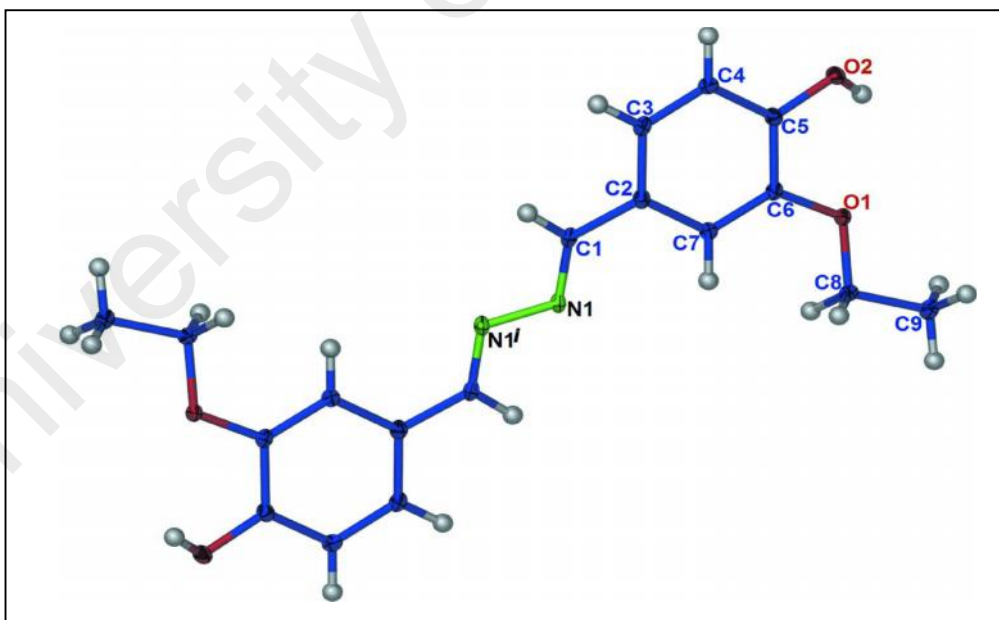


Figure 3.7 : The molecular structure of 4,4-(1*E*,1*E*)-1,2-diylidenebis(methan-1-yl-1-ylidene)bis(2-ethoxyphenol) showing 50% probability displacement ellipsoids. Hydrogen atoms are drawn as spheres of arbitrary radius.

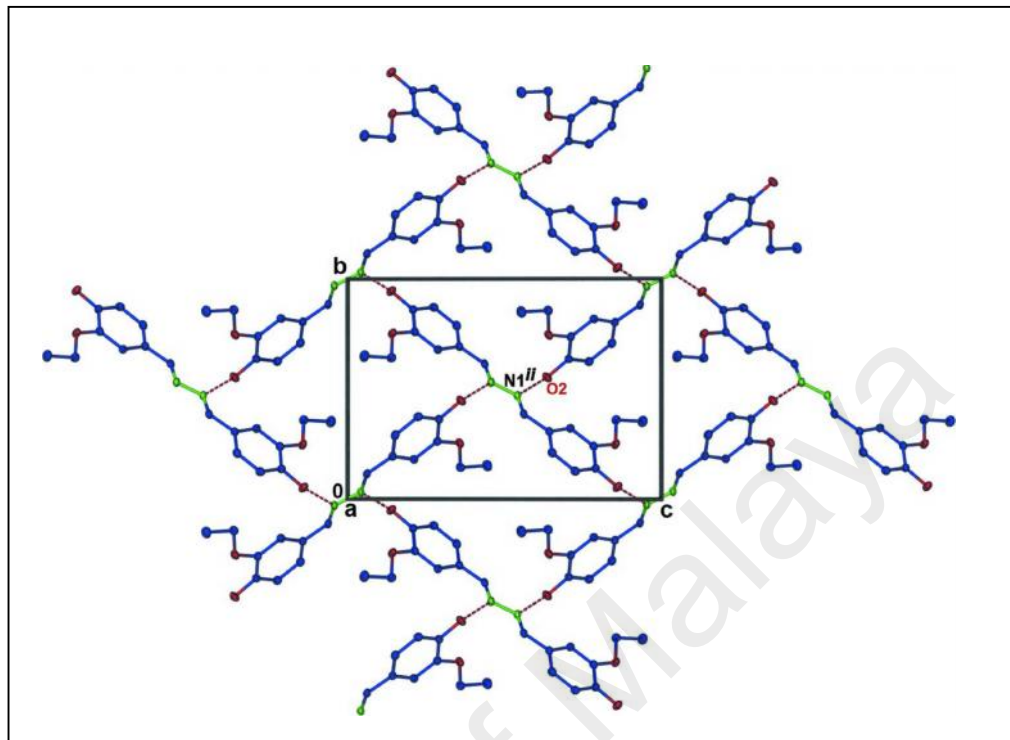


Figure 3.8 : A view of the two-dimensional supramolecular network in the title compound showing the O—H...N hydrogen bonds (in red dotted lines)

The X-ray structures of **(a4)** and **(a5)** are given in Figures 3.9 and 3.10, respectively. The two compounds are isostructural in which the overall structure is centrosymmetric with the mid-point of the central N-N bond located on an inversion centre. The configuration around the C=N bond is *E*. All the molecules are approximately planar (excluding the hydrogen atoms and the methoxy and nitro substituents), with a small r.m.s deviation from planarity of 0.0229 and 0.0446. In the crystal structure of **(a4)**, the presence of a water molecule in the crystal structure gives rise to extensive hydrogen bonding interactions between the hydroxyl substituent and the methoxy substituents with the water molecule (Table 3.5). On the other hand, in the absence of water molecule in the crystal structure of **(a5)**, hydrogen bonding interactions are only confined to the hydroxyl and nitro substituents (Table 3.6).

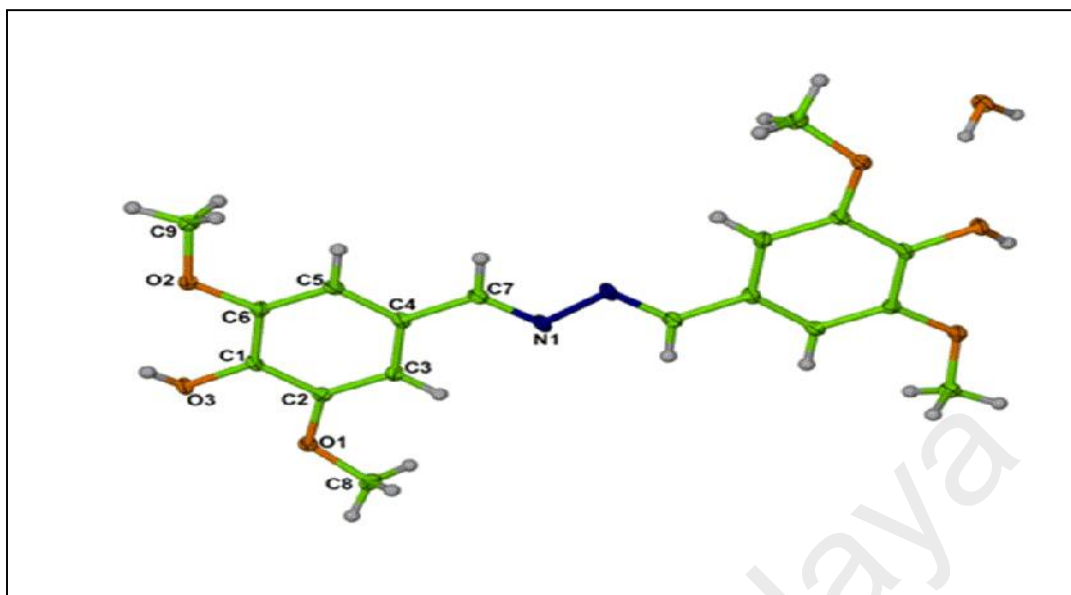


Figure 3.9 : Ellipsoidal plot of the molecular structure of **a4** with 50% probability.

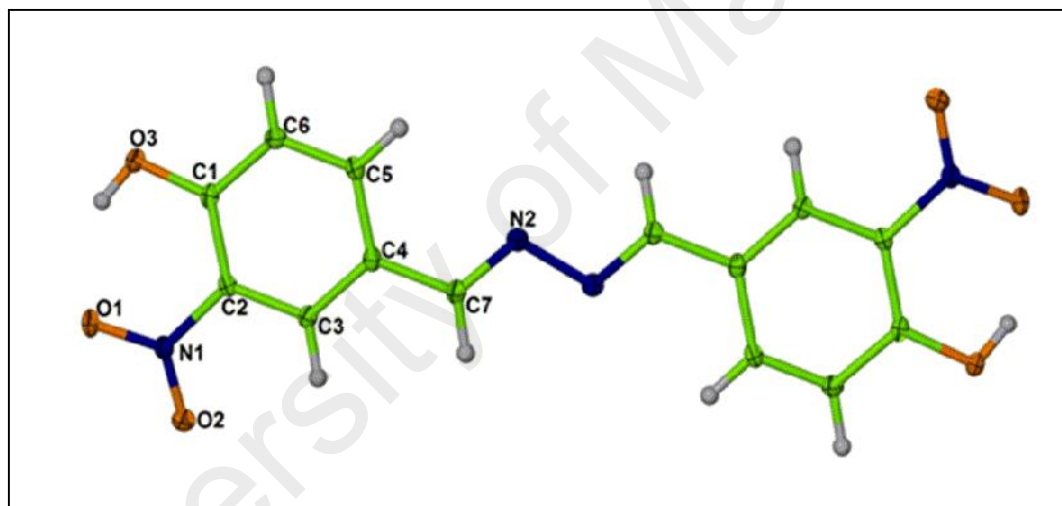


Figure 3.10 : Ellipsoidal plot of the molecular structure of **a5** with 50% probability.

Table 3.5 : Crystal data and structure refinement for **a4** and **a5**

Compound code	(a4)	(a5)
Empirical formula	C <sub>18</sub> H <sub>24</sub> N <sub>2</sub> O <sub>8</sub>	C <sub>14</sub> H <sub>10</sub> N <sub>2</sub> O <sub>4</sub>
Formula weight	396.39	270.24
Temperature	100(2) K	100(2) K
Crystal system, space group	monoclinic, <i>C2/c</i>	monoclinic, <i>P2(1)/c</i>
Unit cell dimensions	a = 29.588(5) Å b = 4.6103(9) Å c = 14.009(3) Å α = 90° β = 91.512(12)° γ = 90°	a = 6.8666(2) Å b = 12.0354(4) Å c = 8.2270(3) Å α = 90° β = 94.381(2)° γ = 90°
Volume	1910.3(6) Å <sup>3</sup>	677.91(4) Å <sup>3</sup>
Z, Calculated density	4, 1.378 Mg/m <sup>3</sup>	2, 1.324 Mg/m <sup>3</sup>
Absorption coefficient	0.109 mm <sup>-1</sup>	0.099 mm <sup>-1</sup>
F(000)	840	280
Crystal size	0.23 x 0.30 x 0.07 mm	0.20 x 0.18 x 0.10 mm
Theta range for data collection	2.75 to 26.00°	2.98 to 27.50°
Limiting indices	-36 ≤ h ≤ 36, -5 ≤ k ≤ 5, -17 ≤ l ≤ 17	8 ≤ h ≤ 8, -15 ≤ k ≤ 15, -10 ≤ l ≤ 10
Reflections collected / unique	7645 / 1882 [R(int) = 0.0359]	6261 / 1552 [R(int) = 0.0232]
Completeness to theta = 26.00	99.9 %	99.9 %
Data / restraints / parameters	1882 / 0 / 138	1552 / 0 / 108
Goodness-of-fit on F <sup>2</sup>	1.063	1.063
Final R indices [I > 2σ(I)]	R1 = 0.0349, wR2 = 0.0943	R1 = 0.0367, wR2 = 0.0952
R indices (all data)	R1 = 0.0416, wR2 = 0.1004	R1 = 0.0425, wR2 = 0.0992
Largest diff. peak and hole	0.254 and -0.220 e. Å <sup>-3</sup>	0.356 and -0.480 e. Å <sup>-3</sup>

Table 3.6 : Hydrogen bonds for **a4** and **a5** [Å and deg.]

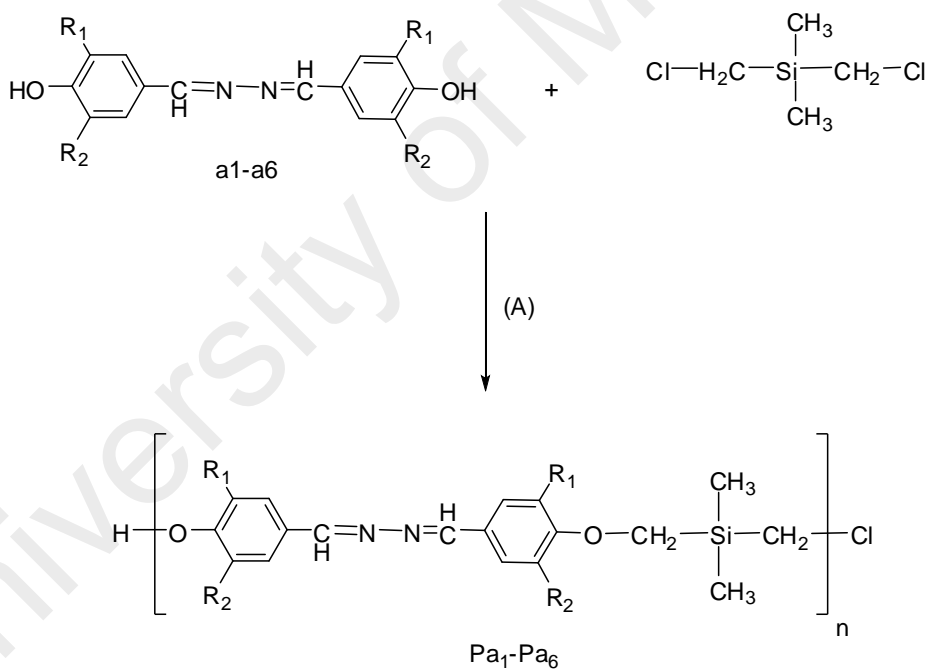
D-H...A	d(D-H)	d(H...A)	d(D...A)	<(DHA)
<b>Monomer (a4)</b>				
O(3)-H(3O)...O(4)#2	0.84	1.81	2.6131(14)	159.0
O(4)-H(4B)...O(3)#2	0.88(2)	1.99(2)	2.8680(15)	178(2)
O(4)-H(4A)...O(1)	0.88(2)	2.33(2)	3.0084(15)	134.2(18)
O(4)-H(4A)...O(3)	0.88(2)	2.20(2)	3.0098(15)	154.0(18)
<b>Monomer (a5)</b>				
O(3)-H(3O)...O(1)	0.82(2)	1.89(2)	2.6068(15)	145(2)
O(3)-H(3O)...O(1)#3	0.82(2)	2.36(2)	2.9762(14)	133(2)
O(3)-H(3O)...N(1)	0.82(2)	2.48(2)	2.9259(15)	115.7(18)

Symmetry transformations used to generate equivalent atoms:

#1 -x,-y+1,-z #2 -x+1,-y+1,-z+2 #3 -x+1/2,y+1/2,-z+3/2

### 3.2.2 Carbosilane bisphenol azine copolymers (Pa1-Pa6)

A new carbosilane bisphenol azine copolymers (**Pa1-Pa6**) were synthesized through the polycondensation reaction of bis(chloromethyl)dimethylsilane and the synthesized monomers (**a1-a6**) in presence of dry  $K_2CO_3$  as proton acceptor. The synthetic route of copolymers is illustrated in Figure 3.11. The etherification process occurs by adding two batches of bis(chloromethyl)dimethylsilane to enhance the molecular weight of the copolymers where by adding two batch of bis(chloromethyl)dimethylsilane will increase the molecular weight to double. The synthesized copolymers are subjected to Williamson etherification (details are described in Section 3.2.3).



(A) Dry DMF, Dry  $K_2CO_3$ , Reflux 48 h (2 batches)

Figure 3.11 : Synthetic route of copolymers (**Pa1-Pa6**)

From our investigation, DMF is found to be the best solvent in the polymerization process. It gave good Mw at low temperatures and faster reaction. Furthermore, this solvent was able to ensure good homogeneity of the reaction medium

and an easier separation of the final product. Other solvents such as acetone, acetonitrile and pyridine did not give the same results. For example, the  $M_w$  for polymerization of **a2** in DMF was 6870 whereas; the polymerization of the same monomer for 72-96 h in acetone, acetonitrile and pyridine gave  $M_w$  of 3400, 3674 and 4225 respectively. As such, all the monomers were polymerized by using DMF as solvent.

All the copolymers are observed to become gummy at high temperature and it will be glassy-like below 100°C. Figure 3.12 shows a few selected samples of the azine copolymers. The copolymers exhibited excellent solubility in common organic solvents (THF,  $\text{CHCl}_3$  and DMF) but insoluble in hydroxyl-group containing solvents (methanol and ethanol).

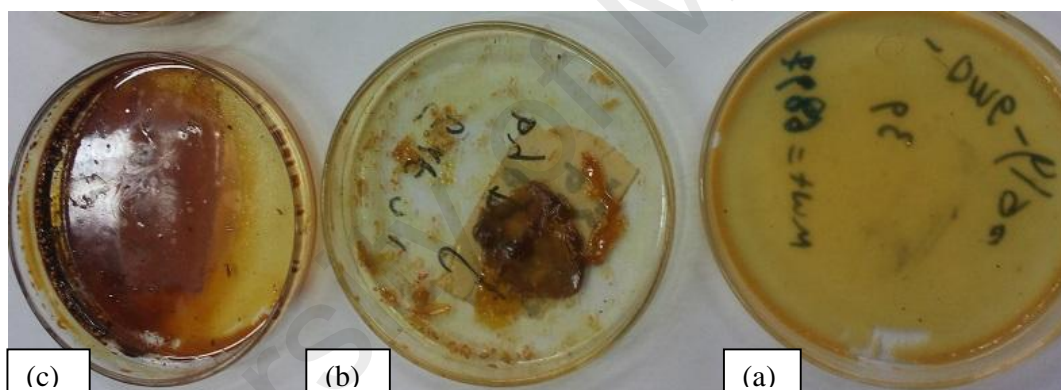


Figure 3.12 : (a) **Pa2** (b) **Pa4** (c) **Pa6**

### 3.2.3 Mechanism of Williamson etherification

Williamson etherification is a  $\text{S}_{\text{N}}2$  reaction between an alkyl halide  $\text{R-X}$  and a phenoxide  $\text{Ar-O}^-$  ion to yield an ether,  $\text{Ar-O-R}$ . In planning the Williamson ether synthesis, it is essential to use a combination of reactants that maximizes nucleophilic substitution and minimizes any competing  $\beta$ -elimination[155]. Yields of Williamson reaction depend usually on the halide that is attached to alkyl or aryl group, where the highest yield is obtained when the halide displaces a methyl or a primary carbon and the yield is low in a displacement from secondary halides due to the competing of  $\beta$ -

elimination. For tertiary halides the etherification fails to be carried out as  $\beta$ -elimination by an E2 mechanism is an exclusive reaction[155].

The first step of Williamson's reaction starts with deprotonated of an phenyl hydroxide by the addition of base, usually potassium hydroxide or  $K_2CO_3$ . In the second step, a primary alkyl halide is added and SN2 reaction occurs in which the phenoxide undergoes the nucleophilic attack to displace the halide.

The Schiff base monomers are subjected to Williamson etherification with the suitable chloroalkylsilane in the presence of  $K_2CO_3$ . The proposed mechanism for Williamson etherification is shown in Figure 3.13.

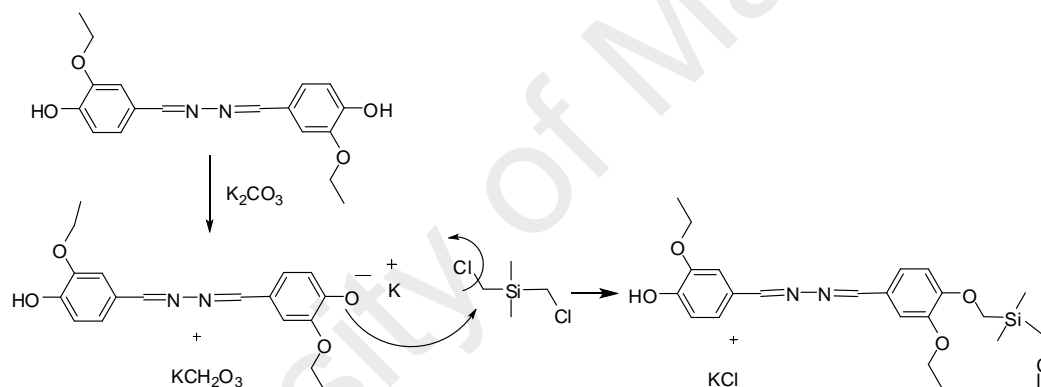


Figure 3.13 : Mechanism of the Williamson etherification of copolymers

### 3.2.4 Characterization of copolymers

The synthesized carbosilane copolymers (**Pa1-Pa6**) were characterized by FTIR,  $^1H$  NMR,  $^{13}C$  NMR and GPC to study the molecular weight of these copolymers. The results are in agreement with the proposed structures.

#### 3.2.4.1 FTIR

Polycarbosilanes are the result of etherification between bisphenol azine monomers and bis-halidmethyl silane in presence of  $K_2CO_3$ . The FTIR spectra of the polycarbosilanes showed same characteristic bands as the monomers since the

functional moieties are similar for copolymers and monomers except for the appearance of a new absorption band at  $1282\text{-}1268\text{ cm}^{-1}$  which is attributed to  $\text{O-CH}_2\text{Si}$  group as well another new absorption band of the  $\text{Si-CH}_3$  group in the range of  $780\text{-}810\text{ cm}^{-1}$ .

Figure 3.14 shows the spectrum of copolymer **Pa3**.

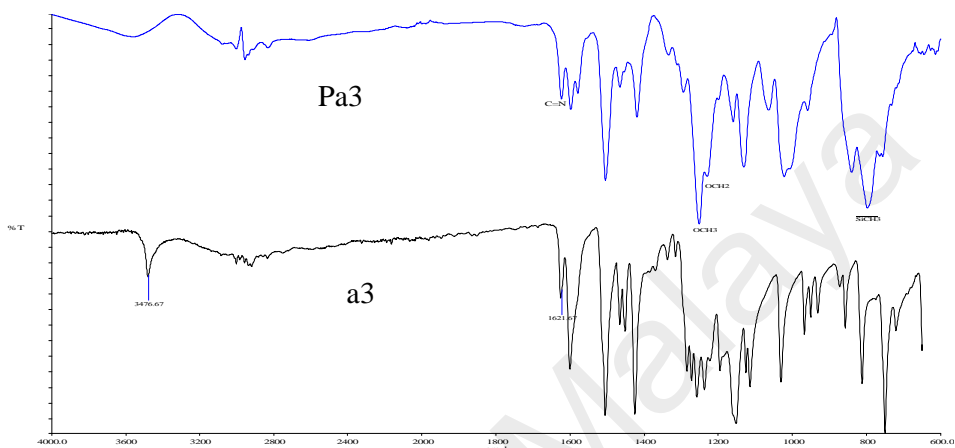


Figure 3.14 : FTIR spectrum of copolymer **Pa3**

#### 3.2.4.2 $^1\text{H NMR}$

The  $^1\text{H NMR}$  spectral analysis presents the structural particularities of the synthesized copolymers. By comparing with the monomer peaks, all the copolymers showed similar shift range with the monomers with obvious distortion peaks due to the repeating units in the main chain of the copolymers. New broad peaks appearing between  $0.17\text{-}1.31\text{ ppm}$  ( $6\text{H}$ ) can be assigned to the methyl protons of the  $\text{Si-CH}_3$  while the protons of the  $\text{O-CH}_2\text{Si}$  group showed a chemical shift at  $3.3\text{-}3.7\text{ ppm}$  ( $2\text{H}$ ) which is considered the best indicator to confirm the copolymer. Furthermore, all copolymers showed small peak in the ranges of  $0.82\text{-}1.18\text{ ppm}$  and  $9.56\text{-}9.85\text{ ppm}$ , which are most possibly attributed to terminal group  $\text{SiCH}_2\text{Cl}$  and  $\text{OH}$  phenol, respectively. Figure 3.15 displays  $^1\text{H NMR}$  spectrum of copolymer **Pa2**.

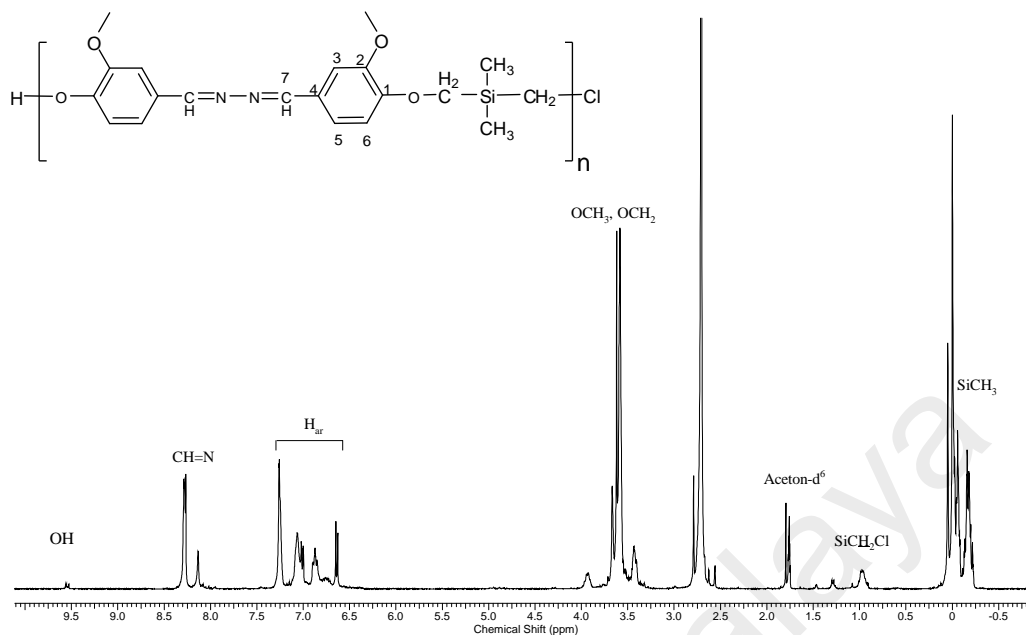


Figure 3.15 :  $^1\text{H}$  NMR spectrum of copolymer **Pa2**

### 3.2.4.3 $^{13}\text{C}$ NMR

The  $^{13}\text{C}$  NMR spectral analysis further confirms the presumed structures. By comparing with the monomer peaks, all the copolymers showed similar shift range with the monomers with obvious distortion peaks of some compounds due to the repeating units of monomers in the main chain of the copolymers. The best identification for formation of the copolymers was appearance a new peak in the region of -7.17-1.71 associated to Si-CH<sub>3</sub> beside another new peak in range of 59.7-66.07 ppm which is attributed to OCH<sub>2</sub>-Si. A small peak that appears at the range 19.3-28.84 ppm supports the  $^1\text{H}$  NMR for SiCH<sub>2</sub>Cl. Figure 3.16 shows the  $^{13}\text{C}$  NMR spectrum of copolymer **Pa3**.

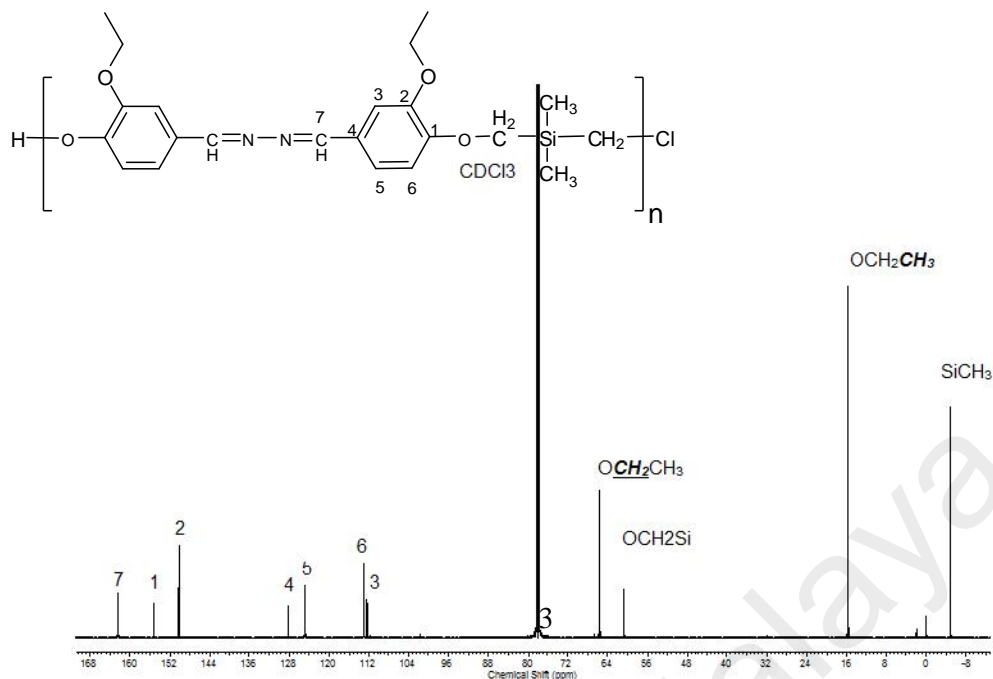


Figure 3.16:  $^{13}\text{C}$  NMR spectrum of copolymer **Pa3**

#### 3.2.4.4 Gel permeation chromatography (GPC)

GPC analyses for all the polycarbosilanes, their colours and yields are summarized in Table 3.7. The number average molecular weights ( $M_n$ ) of the copolymers are from 2322 to 9805 and the degrees of polymerization (DP) are from 7-23. All the copolymers show narrow molecular weight distribution (PDI). Figure 3.17 shows the raw GPC chromatogram of copolymer **Pa3**

Table 3.7: Percentage yield and characteristics of the synthesized copolymers

No.	Yield (%)	Color	$M_w$	Poly dispersity	Degree of polymerization
<b>Pa1</b>	51.91	Yellow	2322	1.47	7
<b>Pa2</b>	76.1	Yellow	7836	1.2	20
<b>Pa3</b>	69.7	Yellow	9805	2.1	23
<b>Pa4</b>	74.6	Brown	8528	1.39	19
<b>Pa5</b>	73.6	Red	3600	1.04	8
<b>Pa6</b>	72.8	Red	4763	1.31	12

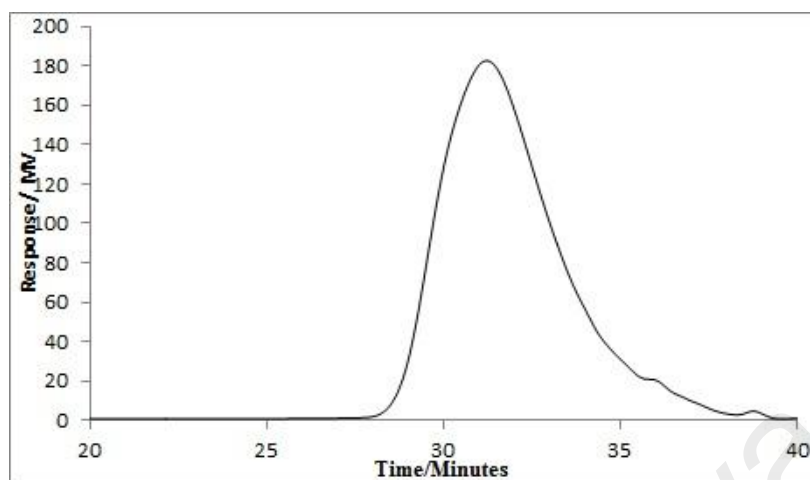


Figure 3.17 : Raw GPC chromatogram of copolymer **Pa3**

The molecular weights of the copolymers containing substituted group O-R (**Pa2**, **Pa3** and **Pa4**) are higher than those of (**Pa5**) and (**Pa6**) containing the nitro group as well the copolymer (**Pa1**), which has the lowest molecular weight of 2322 Da. These differences of molecular weights may be due to the effect of the withdrawing or donating group by resonance and inductive effects. This concept leads us to suggest that the substituent at ortho position plays an important role in increasing or decreasing the molecular weight of the copolymers. The inductive and resonance withdrawing groups such as NO<sub>2</sub> in **Pa5** and **Pa6** show lower molecular weight than the donating group as in **Pa2**, **Pa3** and **Pa4**. These differences could be due to the increase in the electron drift from electron-donating group through  $\pi$ -bond of benzene ring causing the phenoxide to become electron rich while in **Pa5** and **Pa6** the electron will be attracted away from phenoxide ion as NO<sub>2</sub> is electron-withdrawing group and thus subsequently the phenoxide group becomes electron poor. Figure 3.18 displays the suggested mechanism whereby the substituted group of monomer **a2** contains OCH<sub>3</sub> is an electron-donating group.

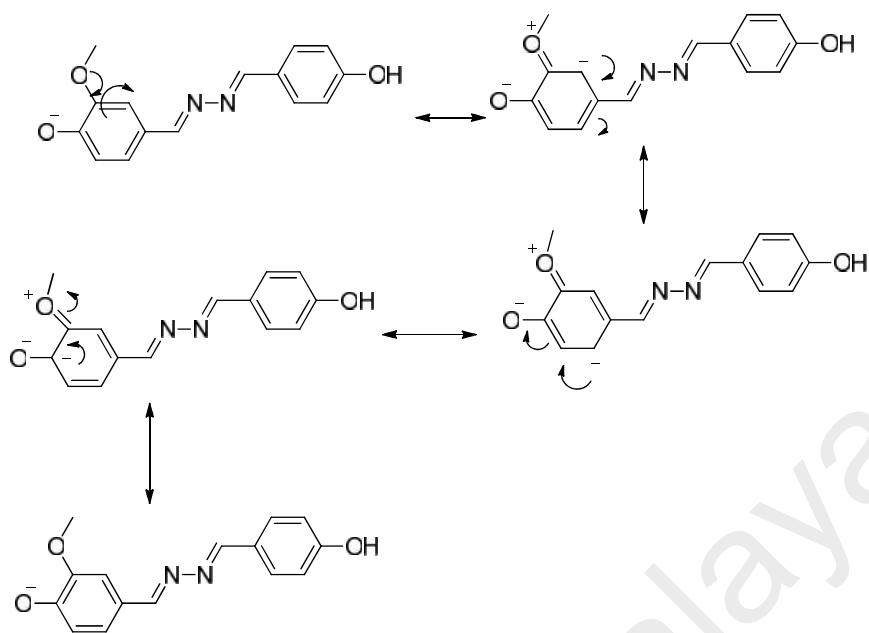


Figure 3.18 : The suggesting mechanism of donating substituent group of copolymer Pa2

Likewise, unsubstituted copolymer **Pa1** exhibits the lowest molecular weight, as a result of the high conjugation present in the monomer. Figure 3.19 displays the suggesting mechanism for **Pa1**. The mechanism shows the long term resonance of the electrons which reduce the negative charge on phenoxide group.

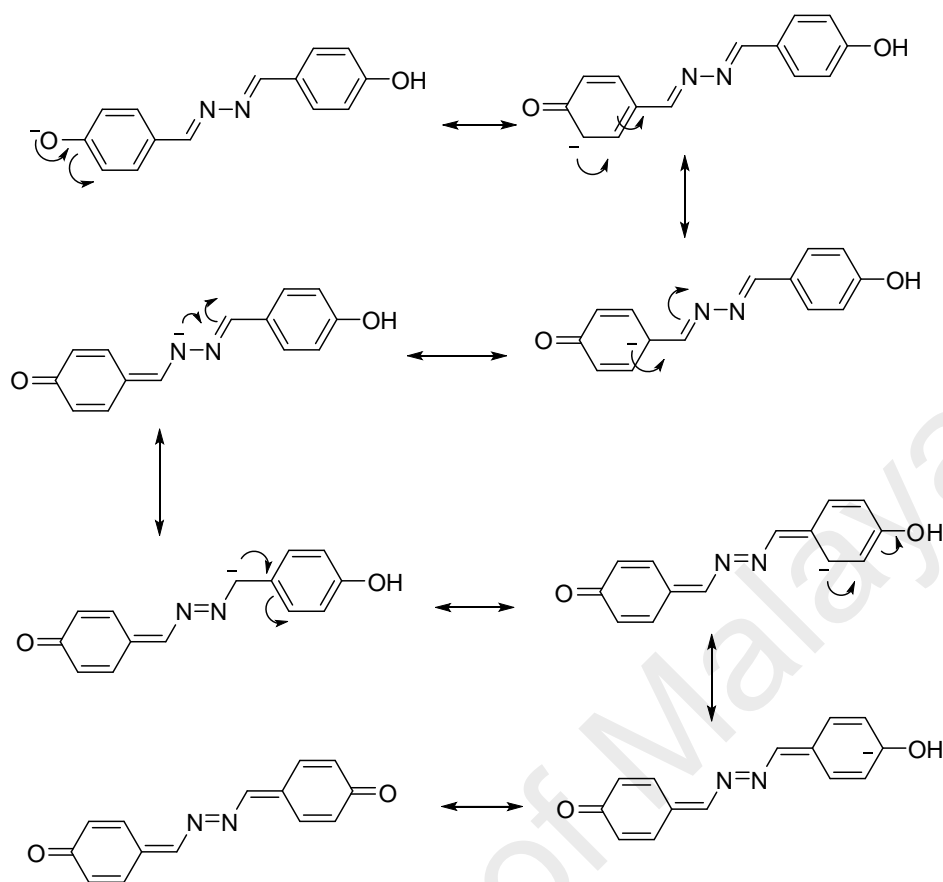


Figure 3.19 : The suggesting mechanism of copolymer **Pa1**

### 3.3 Physical properties

In this section some of physical properties such as thermal stability, optical and electrochemical properties were investigated where the results of these properties could lead to the best copolymer for selected applications.

#### 3.3.1 Thermal properties

Typical TGA thermograms of copolymers are depicted in Figure 3.20 and the detailed thermal data are summarised in Table 3.8.

The polycarbosilane structure displays good thermal stability and a single decomposition step. Temperatures at 10% weight loss are recorded in the range of 258.6-344.4°C, while major weight loss of about 50% in the region of 323.6-490.9°C. The values temperature of copolymers containing substituted groups in the benzene ring

are higher than this without substituted group (**Pa1**) due to higher bond energy values of this group leading to high stability of the copolymers[156]. This may be explained by invoking bond energy values. The residual weight remaining at 700°C is around 17.7-40.7%. Enhancement of thermal stability observed in these polycarbosilane may be attributed to the delocalization characteristic of the azine linkage and the silicon moieties on the main chain. As a result of high decomposition temperature, these polymers have good thermal properties for industrial processing and for possible use in organic LEDs[157].

In addition, the glass transition temperatures ( $T_g$ ) of the copolymers **Pa1-Pa6** were achieved by DSC under nitrogen atmosphere. No detectable phase transition is observed. The undetectable phase transition for the other copolymers with different substituted groups may lie in the rigidity of the main chains and carbonosilane moieties.

Table 3.8 : Thermal properties of copolymers

Copolymer	Temperature (°C) corresponding to				Char yield (%) at 700°C
	Onset	10% Wt loss	50% Wt loss	DTp	
<b>Pa1</b>	276.23	258.6	323.66	276.57	17.7
<b>Pa2</b>	393.13	330.4	422.5	354	32
<b>Pa3</b>	383.67	344.4	477.1	351.5	18.5
<b>Pa4</b>	316.68	302.5	490.9	332.59	40.7
<b>Pa5</b>	306.04	301.4	413.4	311.47	40.1
<b>Pa6</b>	335.8	283.86	370.6	327	25.05

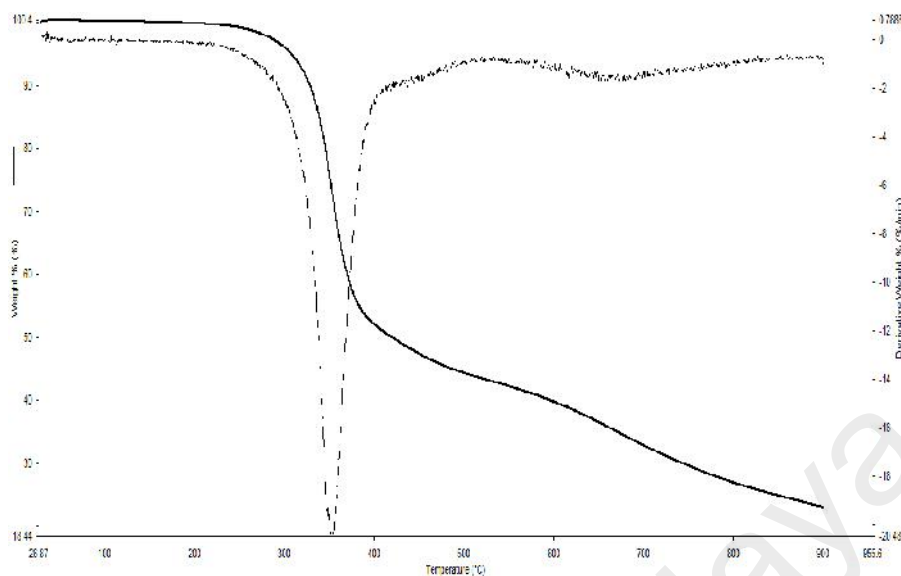


Figure 3.20 : TGA curves of copolymer (**Pa2**) with its derivative

### 3.3.2 Optical properties

Fundamental photophysical properties of the new polycarbosilanes were investigated by UV-vis and fluorescence spectroscopies. Figure 3.21 shows the UV-vis absorption of the selected copolymers (**Pa1**, **Pa3** and **Pa5**) in solution ( $1 \times 10^{-6}$  M in DMF) at room temperature and their detailed photophysical data are summarized in Table 3.9.

From the UV-vis spectra, all the copolymers containing bisphenol azine exhibit single clear absorption peak, i.e. single absorbance maximum band in the range of 318-352 nm corresponding to  $\pi-\pi^*$  and  $n-\pi^*$  transitions of the aromatic ring and the azomethine group [158], as well as from the conjugation of the aromatic ring and the nonbonding electrons (O-CH<sub>3</sub>, OH, N=C). In **Pa2**, **Pa3** and **Pa4** longer wavelength absorption maximum (344.7-351.3 nm) is observed due to the effect of electron-donating substituents (OCH<sub>3</sub> and OCH<sub>2</sub>CH<sub>3</sub>) which increase the density of electron at the azomethine group, decrease the  $n-\pi^*$  transition energy and produce bathochromic shifts of the long wavelength absorption maximum. In **Pa5** and **Pa6** the electron-

withdrawing substituent ( $\text{NO}_2$ ) decreases the electron density at the azomethine group, and increases the  $n \rightarrow \pi^*$  transition energy to produce hypsochromic shifts as report by Valenti N. *et al*[159].

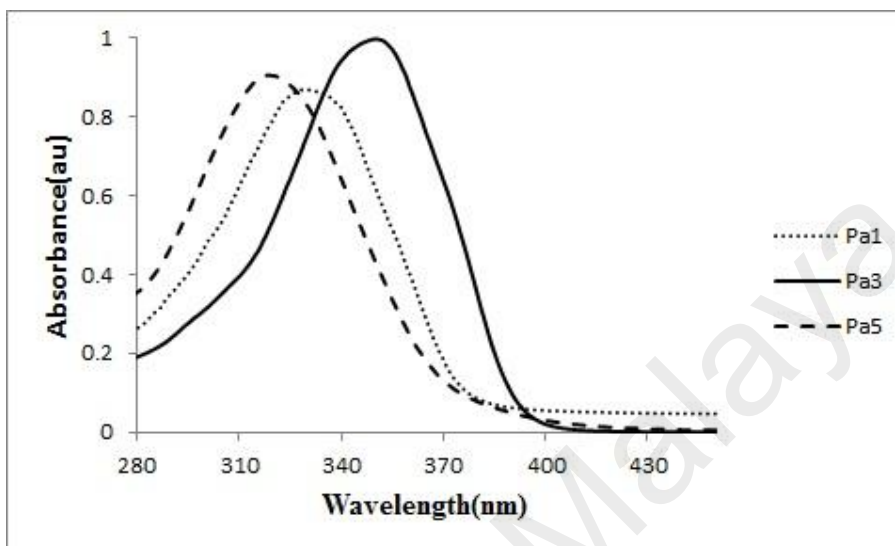


Figure 3.21 : UV-Vis absorption spectral traces of the selected copolymers (**Pa1**, **Pa3**, and **Pa5**)

Figure 3.22 depicts photoluminescence spectra of selected copolymers **Pa1**, **Pa3** and **Pa4** in DMF ( $1 \times 10^{-6}$  M) and the emission spectra of copolymers are identical due to the similarity of the main chain unit. The fluorescence emission maxima of copolymers are the range of 415-422 nm which may be categorized as blue emission. The PL emission maxima which are bathochromically shifted may be ascribed to the electronic effect that lowers the HOMO energy level and reduces the energy gap[38].

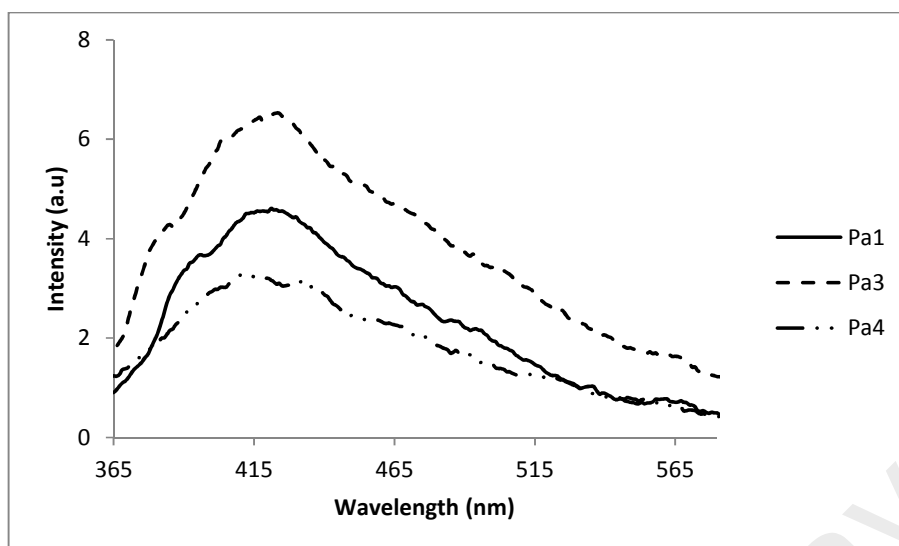


Figure 3.22 : Photoluminescence emission spectral of copolymers **Pa1**, **Pa3** and **Pa4**

Table 3.9 : UV-Vis Absorption and PL emission spectral data of copolymers

Copolymer	Absorption UV-vis, <sub>abs</sub> , max (nm)	PL <sub>abs</sub> , max (nm)
<b>Pa1</b>	331.8	416
<b>Pa2</b>	350.9	422
<b>Pa3</b>	351.3	420
<b>Pa4</b>	344.7	416
<b>Pa5</b>	318.6	418
<b>Pa6</b>	321.6	419

### 3.3.3 Electrochemical properties

Cyclic voltammetry (CV) analysis on the resulting polycarbosilane was carried out to evaluate electrochemical properties as well as to estimate the HOMO and LUMO energy levels, which are important for determining the band gaps.

The experiments were achieved in a 0.1 M tetrabutylammonium perchlorate (TBAP) as a supporting electrolyte in an anhydrous acetonitrile (CH<sub>3</sub>CN) using a thin film coated on an indium-tin-oxide (ITO) glass substrate as working electrode at room temperature. The CV curves were referenced to an AgCl/Ag reference electrode and the

scan rate was  $50 \text{ mV s}^{-1}$  in a potential range of  $-2.0 \text{ V}$  to  $+2.0 \text{ V}$ . Figure 3.23 shows a CV curve of the copolymer **Pa2** which is typical for all the copolymers, all the copolymers showed irreversible redox processes with onset oxidation (p-doping) and reduction (n-doping). The oxidation (p-doping) started at 0.84, 0.91, 0.89, 0.93, 1.11 and 1.03 V for compounds **Pa1-Pa6** respectively. On sweeping the thin film cathodically, the reduction processes n-doping started at -0.53, -0.61, -0.66, -0.64, -0.88 and -0.74 V for the compounds **Pa1-Pa6** respectively.

The highest occupied molecular orbital (HOMO) and lowest unoccupied molecular orbital (LUMO) energy levels as well as the electrochemical energy gaps ( $E_g$ ) of the corresponding copolymers can be determined using the oxidation onset ( $E_{\text{onset}}$ ) following the equations:

$$\text{LUMO} = -E_{\text{red}} - 4.71 \text{ eV} \quad \text{and} \quad \text{HOMO} = -E_{\text{ox}} - 4.71 \text{ eV}$$

$$\text{Thus } E_g = -(E_{\text{HOMO}} - E_{\text{LUMO}}) \quad \text{Equation 3.1}$$

where  $E_{\text{red}}$  and  $E_{\text{ox}}$  are the onset potentials for reduction and oxidation relative to the  $\text{Ag}/\text{Ag}^+$  reference electrode [160]. The HOMO energy levels of the copolymers were calculated to be -5.69, -5.61, -5.60, -5.61, -5.82 and -5.74 eV while; the LUMO energy levels were estimated to be -4.01, -4.10, -4.05, -4.07, -3.83 and -3.97 for (**Pa1-Pa6**) respectively. The results as summarised in Table 3.10 show that the synthesized copolymers containing  $\text{NO}_2$  substituted group has the lowest HOMO energy value among all the copolymers (**Pa1-Pa6**). The presence of electron-withdrawing group ( $\text{NO}_2$ ) may play an important role to lower the HOMO energy level. This observation on electrochemical behaviour of the copolymers (**Pa1-Pa6**) can be well explained on the basis of their structure-property relationship. It is a well-recognised matter that an electron-withdrawing substituent attached with a conjugated molecular system can decrease electron density of the conjugated molecular system. As a result, the

molecule will be stabilised and it is necessary to apply higher potential to oxidize the molecule. This results in a shift of the HOMO energy level to lower energy[161], while copolymers containing electron-donating group (**Pa2**, **Pa3** and **Pa4**) possess lower oxidation range and subsequently have less band gap values. This is due to the increment of electron density of the aromatic ring as reported by Kaya and Kamaci[162]. The electron-donating group may extend the conjugation of the copolymers, hence lowers the energy levels between HOMO and LUMO. Similar observation has been reported by Liu G. *et al*[163] where they observed that the band gaps of diarylethenes containing an electron-donating group were less than those of diarylethenes containing an electron-withdrawing group.

The results, as summarised in Table 3.10, show that the synthesized copolymers have electrochemical band gap of less than 2.00 eV. The HOMO energy level of the copolymers (**Pa1-Pa6**) is comparable with the most widely used hole-transporting material 4,4'-bis(1-naphthylphenylamino)biphenyl (NBP)[164]. As a result of this property, they can potentially be applied in heterojunction solar cells and organic light emitting diodes[165-167].

Table 3.10 : Electrochemical data of the copolymers

<b>Copolymer</b>	$E_{red}^a$ (V)	$E_{ox}^a$ V	$E_{LUMO}^b$ (eV)	$E_{HOMO}^b$ (eV)	$E_g^c$ (eV)
<b>Pa1</b>	-0.53	0.98	-4.01	-5.69	1.68
<b>Pa2</b>	-0.61	0.91	-4.10	-5.61	1.51
<b>Pa3</b>	-0.66	0.89	-4.05	-5.60	1.55
<b>Pa4</b>	-0.64	0.3	-4.07	-5.61	1.54
<b>Pa5</b>	-0.88	1.11	-3.83	-5.82	1.99
<b>Pa6</b>	-0.74	1.03	-3.97	-5.74	1.77

<sup>a</sup> Onset oxidation (p-doping) and reduction (n-doping) potentials versus Ag/Ag<sup>+</sup>.

<sup>b</sup> Estimated from the onset oxidation and reduction potentials by using  $E_{HOMO} = -E_{ox} - 4.71$  eV and  $E_{LUMO} = -E_{red} - 4.71$ eV [168].

<sup>c</sup> Electrochemical band gaps determined using  $E_g = -(E_{HOMO} - E_{LUMO})$ .

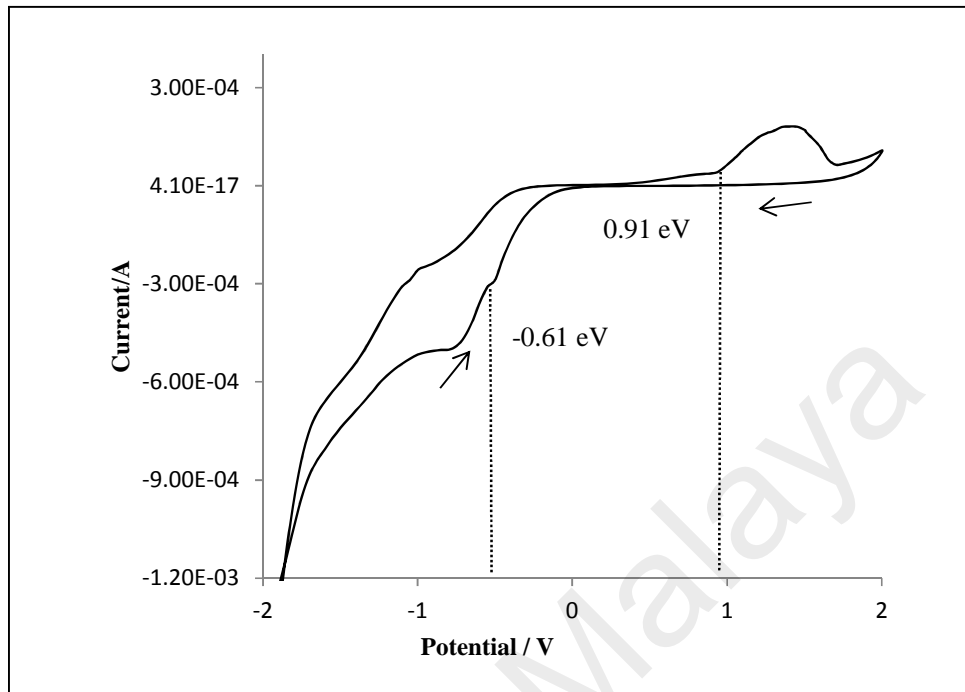


Figure 3.23: Cyclic voltammogram of **Pa2** in CH<sub>3</sub>CN at scan rate 50 mV s<sup>-1</sup>.

University of Malaya

## **CHAPTER 4 : CARBOSILANE COPOLYMERS BASED ON BISPHENOL BIS-SCHIFF BASE MONOMERS**

### **4.1 Introduction**

After successfully synthesized new polycarbosilane based on bisphenol azine monomers in the main backbone as mentioned earlier in Chapter 3, in this chapter synthesis of a new series of copolymers that containing silicon moiety with higher conjugated structure of bisphenol containing bis-Schiff base monomers is presented. The study of some of their physical properties which shed light into the applications of these new copolymers is also discussed.

### **4.2 Results and discussion**

In Chapter 3, we prepared the carbosilane copolymers based on full conjugated bisphenol azine monomers and study some of their properties. In this chapter, the azine was replaced by 1,4-phenylene and 1,5-naphthalene moieties, where seven monomers with higher conjugation and different substituted groups were synthesized and successfully polymerized with bis(chloromethyl) dimethylsilane by Williamson reaction in the presence of low equivalent of  $K_2CO_3$  and DMF as reaction media. The synthesized materials were characterized and identified by FTIR,  $^1H$  NMR,  $^{13}C$  NMR as well as the GPC was utilized to measure the molecular weight of synthesized copolymers.

#### **4.2.1 Synthetic route of bisphenol bis-Schiff base monomers (Schiff base formation)**

The Schiff base formation mechanism is another variation on the theme of nucleophilic addition to the carbonyl group. In this type of reaction, the amine will be the nucleophile. Mechanistically, the formation of Schiff base is shown in Figure 4.1.

The mechanism of Schiff base starts by reacting the amine with the carbonyl group to produce a compound called carbinolamine. The carbinolamine is unstable and loses water by either acid or base catalysed pathways, followed by acid catalysed dehydration. In fact, the carbinolamine dehydration is the rate-determining step of formation of Schiff base and for this reason the reaction is catalysed by acids. However, the concentration of acid cannot be too high because amines are basic compounds. In case of protonation of amine, the amine becomes non-nucleophilic which makes the equilibrium being pulled to the left and prevents formation of the carbinolamine. Therefore, mildly acidic pH is preferred for the synthesis of Schiff base compounds which is usually between pH4 and pH5[169].

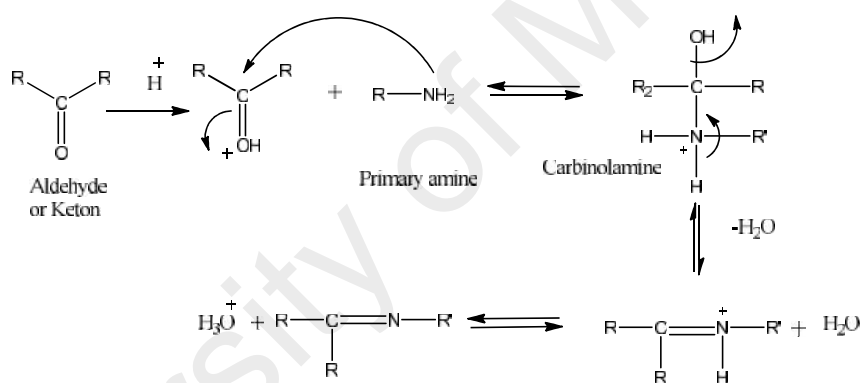


Figure 4.1 : Reaction mechanism of Schiff base

The dehydration of carbinolamines is also catalysed by base. This reaction is somewhat analogous to the E2 elimination of alkyl halides except that it is not a concerted reaction. It proceeds in two steps through an anionic intermediate.

#### 4.2.1.1 Synthesis of Schiff base monomers containing 1,4-phenylene

Schiff base monomers were prepared by condensation reaction of 4-hydroxy benzaldehyde and its derivatives with 1,4-diaminophenylene in hot methanolic solution as illustrated in Figure 4.2 to yield the Schiff base monomers containing different substituted groups. The monomers gave good yield and very good solubility in

DMF and DMSO at room temperature. Table 4.1 shows the substituted groups, yields, melting points and formulae of monomers (**b1-b4**)

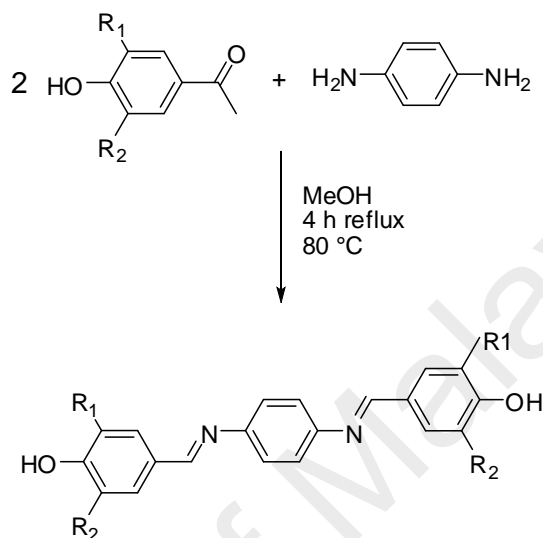


Figure 4.2 : Synthetic route of Schiff base monomers containing 1,4-phenylene group

Table 4.1 : Details of the synthesized bisphenol bis-Schiff base monomers containing 1,4-phenylene group

Monomers.	R <sub>1</sub>	R <sub>2</sub>	Yield (%)	Mp. (°C)	Formula
<b>b1</b>	H	H	275-277	82.9	C <sub>20</sub> H <sub>16</sub> N <sub>2</sub> O <sub>2</sub>
<b>b2</b>	H	OCH <sub>3</sub>	198-199	84.6	C <sub>22</sub> H <sub>20</sub> N <sub>2</sub> O <sub>4</sub>
<b>b3</b>	H	OCH <sub>2</sub> CH <sub>3</sub>	172-176	80.1	C <sub>24</sub> H <sub>24</sub> N <sub>2</sub> O <sub>4</sub>
<b>b4</b>	OCH <sub>3</sub>	OCH <sub>3</sub>	215-216	79.41	C <sub>24</sub> H <sub>24</sub> N <sub>2</sub> O <sub>6</sub>

#### 4.2.1.2 Characterization of Schiff base monomers containing 1,4-phenylene

##### 4.2.1.2.1 FTIR

The FTIR spectra displayed the first impression for the synthesized monomers (**b1-b4**) regarding the nature of functional moieties attached to the monomers. The main IR bands and their assignments are tabulated in Table 4.2. There are similarities in the

IR spectra of the monomers (**b1-b4**), except for some slight variations in the shifts and intensities of vibration peaks due to the different substituted groups attached to the benzene ring. The O-H stretching bands of bisphenol monomers appear within the frequencies of 3489-3579  $\text{cm}^{-1}$ . The characteristics frequencies of all monomers that appeared in the range of 3031-3067  $\text{cm}^{-1}$  are assignable to C-H stretching band and the characteristics frequencies in the range of 2921-2944  $\text{cm}^{-1}$  are assignable to C-H aliphatic stretching band. Strong intensity absorption peaks in the frequencies of 1618-1624  $\text{cm}^{-1}$  region are assignable to the imine group (C=N). On the other hand, the ether group absorbs strongly in the frequencies range of 1254-1273  $\text{cm}^{-1}$ . With disappearance of the carbonyl group of 4-hydroxybenzaldehyde and their derivatives and the amine of 1,4-phenylenediamine in the frequencies of 1720-1800  $\text{cm}^{-1}$  and two sharp N-H stretching peaks in the frequencies of 3350  $\text{cm}^{-1}$  respectively, and appearance of a new peak due to formation of imine group at 1618-1624  $\text{cm}^{-1}$  as well the other expected peak such as OH at 3617-3479  $\text{cm}^{-1}$  confirm that the IR spectra are in agreement with the proposed structure.

Table 4.2 : Some of the important FTIR spectra data of monomers

Monomer	O-H	C-H <sub>ar</sub>	C-H <sub>aliph</sub>	C=N	C=C <sub>ar</sub>	O-C
<b>b1</b>	3489	3067	-	1618	1525-1505	1258
<b>b2</b>	3528	3058	2934	1619	1508-1593	1273
<b>b3</b>	3579	3043	2944	1624	1505-1585	1267
<b>b4</b>	3519	3031	2921	1622	1502-1579	1254

= stretching, aliph= aliphatic, ar= aromatic

#### 4.2.1.2.2 $^1\text{H}$ NMR

The structures and purities of the synthesized Schiff base monomers (**b1-b4**) are confirmed by using  $^1\text{H}$  NMR analysis techniques. The  $^1\text{H}$  NMR spectrum and

structure of **b2** Schiff base monomer with its numbering are shown in Figure 4.4. The data for all monomers are tabulated in Table 4.3.

Similar to azine monomers, no protons of the aldehyde, CHO and amino, NH<sub>2</sub> are observed in all of the compounds, instead appearance of a sharp singlet peak in the region of 8.48-8.50 ppm with an integration equivalent to two protons corresponding to the azomethine proton H<sub>7</sub>. The H<sub>3</sub> proton shows singlet peak at the region of 7.21-7.77 ppm. For H<sub>5</sub> a doublet for the two protons at the range of 7.21-7.77 ppm with a coupling constant of 8.1 MHz is observed. In the region of 6.88-6.90 ppm, the doublet signal for two protons are assigned to the H<sub>6</sub> proton with coupling constant of 8.1 MHz. High intensity sharp peak that appears in the region of 7.25-7.27 ppm is attributed to 4 protons of phenyl ring. The signal observed in the region of 3.48-3.81 ppm correspond to methoxy group protons attached to aromatic ring[151]. A singlet peak in the range of 9.06-10.13 ppm is attributed to proton of OH group. All the monomers showed similar <sup>1</sup>H NMR spectral properties as described for monomer **b2** with slight differences due to the different group that is attached to the aromatic group (Chapter 2, Section 2.2).

Table 4.3: <sup>1</sup>H NMR data of monomers (**b1-b4**)

Type of proton	Chemical shift (ppm)
O-CH <sub>3</sub>	3.48-3.81
CH <sub>2</sub> CH <sub>3</sub>	1.36
Ph-H 9 <sup>th</sup> position	7.25-7.27
Ar-H 2 <sup>th</sup> position	6.88
Ar-H 3 <sup>th</sup> position	7.21-7.77
Ar-H 5 <sup>th</sup> position	7.21-7.77
Ar-H 6 <sup>th</sup> position	6.88-6.90
C=N (7 <sup>th</sup> position)	8.48-8.50
Ar-OH (1 <sup>th</sup> position)	9.06-10.13

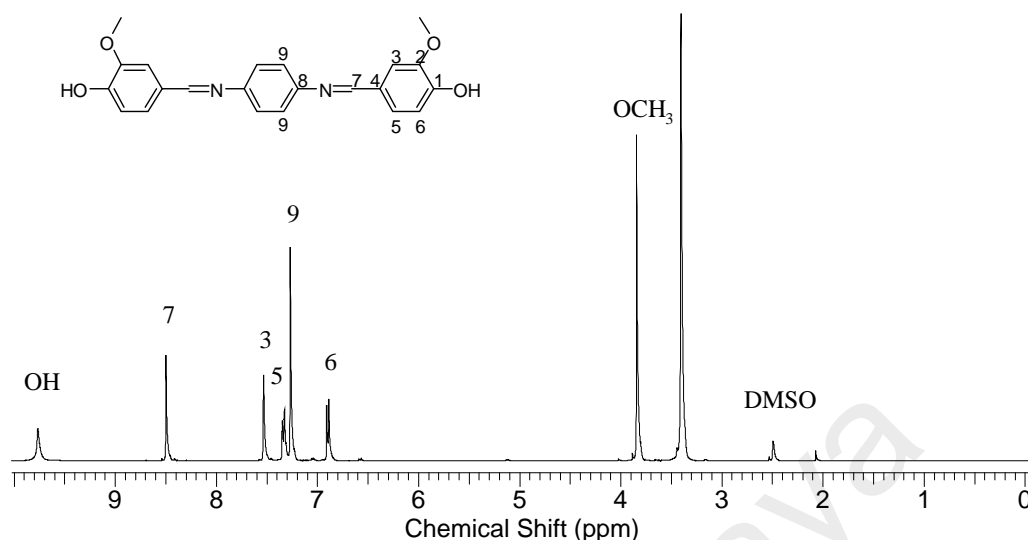


Figure 4.3 :  $^1\text{H}$  NMR spectrum of monomer **b2**

#### 4.2.1.2.3 $^{13}\text{C}$ NMR

The  $^{13}\text{C}$  NMR results correspond well with the  $^1\text{H}$  NMR results and thus confirm the proposed structure. The  $^{13}\text{C}$  NMR spectrum of **b2** monomer and its structure are shown in Figure 4.5. The data for all monomers (**b1-b4**) are tabulated in Table 4.4.

The most significant peak of  $^{13}\text{C}$  NMR for bis-Schiff base monomers containing 1,4-phenylene is observed in the region of 159.9-161.4 ppm which is attributed to the azomethine (C=N) carbon atom. The  $\text{C}_1$  group which is attached to OH phenol appears down field in the region of 149.75-159.71 ppm. In addition,  $\text{C}_2$  appear in the region of 148.6-149.8 ppm due to the de-shielding effect of the methoxy group that is attached to the benzene ring. In case of compound **b1** the  $\text{C}_2$  appears down field in the region of 106.72 ppm where there is no substituted group at this position for this compound. The peak attributable to the  $\text{C}_8$  carbon is observed in the region of 139.69-149.82 ppm.  $\text{C}_4$  and  $\text{C}_5$  are assignable in the regions of 127.24-128.54 and 106.72-131.16 ppm respectively. High intensity peak appearing in the region of 122.33-122.59 ppm is attributed to  $\text{C}_9$  which contains 4 carbon atoms of the phenyl group. The peaks in the range of 116.19-148.6 ppm and 106.72-131.16 ppm consist of carbons  $\text{C}_6$  and  $\text{C}_3$  respectively. The intense peak in the region of 56.06-69.36 ppm is due to the methoxy

group (OCH<sub>3</sub>) attached to the benzene ring. All the monomers showed similar <sup>13</sup>C NMR spectral properties as described for monomer **b2** with some differences due to the different group that is attached to the aromatic group (Chapter 2, Section 2.2).

Table 4.4 : <sup>13</sup>C NMR data of monomers (**b1-b4**)

Type of carbon	Chemical shift (ppm)
OCH <sub>2</sub> , O-CH <sub>3</sub>	56.06-69.36
CH <sub>3</sub>	15.25
Ph-C 9 <sup>th</sup> position	122.33-122.59
Ar-C 2 <sup>th</sup> position	148.6-149.82
Ar-C 3 <sup>th</sup> position	106.72-131.16
Ar-C 5 <sup>th</sup> position	106.72-131.16
Ar-C 6 <sup>th</sup> position	116.19-148.6
Ar-C (4 <sup>th</sup> position)	127.24-128.54
Ph-N (8 <sup>th</sup> position)	139.69-149.82
C=N (7 <sup>th</sup> position)	159.90-161.4
Ar-OH (1 <sup>th</sup> position)	149.75-159.71

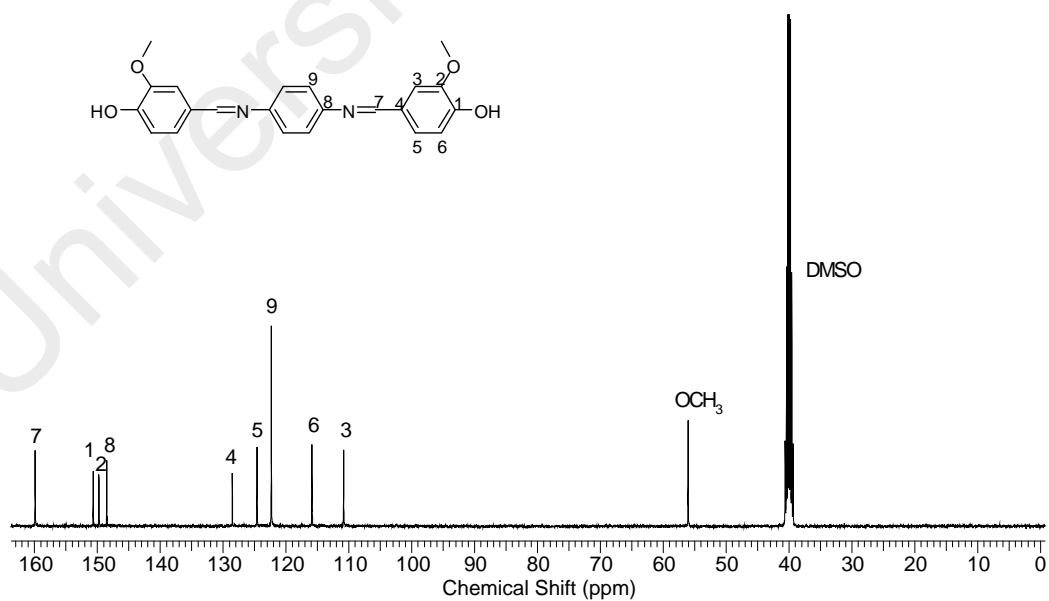


Figure 4.4 : <sup>13</sup>C NMR spectrum of monomer **b2**

#### 4.2.1.3 Synthesis of bis-Schiff base monomers containing 1,5-naphthalene

Another four compounds of bisphenol Schiff base monomers by using 1,5-naphthalenediamine (**b5-b8**) were synthesized by condensation reaction with 4-hydroxybenzaldehyde and its derivatives. In this synthesis some drops of glacial acetic acid were utilized as catalyst and methanol was using as solvent under 90°C for 6 h refluxing. Figure 4.6 displays the synthetic route of the monomers containing the naphthalene group. All the monomers formed showed good yield and good solubility in DMSO and DMF. Table 4.5 shows the substituted groups, yields, melting points and formula of monomers (**b5-b8**).

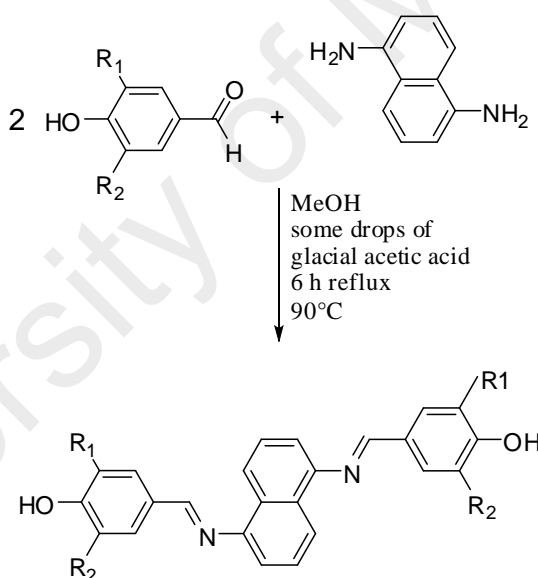


Figure 4.5 : Synthetic route of bis-Schiff base monomers containing 1,5-naphthalene

Table 4.5 : Details of the synthesized bisphenol bis-Schiff base monomers containing 1,5-naphthalene group

Code No.	R <sub>1</sub>	R <sub>2</sub>	Yield (%)	Mp. (°C)	Formula
<b>b5</b>	H	OCH <sub>3</sub>	76.4	195-197	C <sub>26</sub> H <sub>22</sub> N <sub>2</sub> O <sub>4</sub>
<b>b6</b>	H	OCH <sub>2</sub> CH <sub>3</sub>	81.4	207-208	C <sub>28</sub> H <sub>26</sub> N <sub>2</sub> O <sub>4</sub>
<b>b7</b>	OCH <sub>3</sub>	OCH <sub>3</sub>	76.2	281-282	C <sub>28</sub> H <sub>26</sub> N <sub>2</sub> O <sub>6</sub>
<b>b8</b>	H	H	83.3	267-268	C <sub>24</sub> H <sub>18</sub> N <sub>2</sub> O <sub>2</sub>

#### 4.2.1.4 Characterization of Schiff base containing 1,5-naphthalene

##### 4.2.1.4.1 FTIR

The main infrared bands for the synthesized monomers (**b4-b8**) and their assignments are tabulated in Table 4.6. There are similarities in the IR spectra of the monomers (**b5-b8**), except for some slight variations in the shifts and intensities of vibration peaks due to different substituted groups attached to the benzene ring. The O-H stretching bands of bisphenol monomers appear within the frequencies of 3398-3456 cm<sup>-1</sup>. The characteristics frequencies of all the monomers that appeared in the range of 3014-3066 cm<sup>-1</sup> are assignable to C-H stretching band and the characteristics frequencies in the range of 2939-2979 cm<sup>-1</sup> are assignable to C-H aliphatic stretching band. Strong intensity absorption peaks in the frequencies of 1618-1632 cm<sup>-1</sup> region are assignable to the imine group (C=N). The ether group absorbs strongly in the range of 1258-1269 cm<sup>-1</sup>. With disappearance of the carbonyl group of 4-hydroxybenzaldehyde and the amine of 1,5-naphthalenediamine in the frequencies of 1720-1800cm<sup>-1</sup> and two sharp N-H stretching peaks in the frequencies of 3350 cm<sup>-1</sup> respectively, and appearance of a new peak due to formation of imine group at 1618-1632 cm<sup>-1</sup> as well the other expected peak such as OH at 3389-3456 cm<sup>-1</sup> confirm that the IR spectra are in agreement with the proposed structure.

Table 4.6 : Some of the important FTIR spectra data of monomers

Monomer	O-H	C-H <sub>ar</sub>	C-H <sub>aliph</sub>	C=N	C=C <sub>ar</sub>	O-C
<b>b5</b>	3456	3014	2939	1624	1522-1579	1258
<b>b6</b>	3412	3054	2979	1632	1511-1600	1267
<b>b7</b>	3389	3066	2961	1618	1506-1590	1269
<b>b8</b>	3423	3036	-	1626	1513-1592	1261

= stretching, aliph= aliphatic, ar= aromatic

#### 4.2.1.4.2 <sup>1</sup>H NMR

The <sup>1</sup>H NMR spectrum and structure of the bisphenol bis-Schiff base monomer **b5** are shown in Figure 4.7. The data for all monomers are tabulated in Table 4.7.

Disappearance the protons of aldehyde, CHO and amino, NH<sub>2</sub> and appearance a sharp singlet peak in the region of 8.52-8.58 ppm with an integration equivalent to two protons corresponding to the imine proton H<sub>7</sub> confirm the formation of bisphenol Schiff base compound. Besides, the doublet peak that appears in the region of 8.12-8.14 ppm with coupling constant of 8.2 MHz is attributed to H<sub>11</sub>. The H<sub>3</sub> proton shows singlet peak in the region of 7.37-7.68 ppm. The triplet peak appears in the region of 7.50-7.52 ppm and doublet peak appears in the region of 7.43-7.44 ppm, attributed to H<sub>10</sub> and H<sub>9</sub> respectively. For H<sub>5</sub> the doublet is observed for the two protons in the range of 7.17-7.37 ppm with coupling constants of 8.1 MHz. In the region of 6.94-6.95 ppm, the doublet signal for two protons is assigned to the H<sub>6</sub> proton with coupling constant of 8.1 MHz. The signal observed in the region of 3.85-4.89 ppm corresponds to the methoxy protons attached to the aromatic ring. A singlet peak in the range of 9.18-9.82 ppm is attributed to the proton of OH group. All the other monomers showed similar <sup>1</sup>H NMR spectral properties as described for monomer **b5** with some differences due to the different group that is attached to the aromatic group (Chapter 2, Section 2.3).

Table 4.7 :  $^1\text{H}$  NMR data of monomers (**b5-b8**)

Type of proton	Chemical shift (ppm)
O-CH <sub>2</sub> , O-CH <sub>3</sub>	3.85-4.89
CH <sub>2</sub> CH <sub>3</sub>	1.38
Ar-H 3 <sup>th</sup> position	7.37-7.68
Ar-H 5 <sup>th</sup> position	7.17-7.37
Ar-H 6 <sup>th</sup> position	6.94-6.95
Naph-H 9 <sup>th</sup> position	7.43-7.44
Naph-H 10 <sup>th</sup> position	7.50-7.52
Naph-H 11 <sup>th</sup> position	8.12-8.14
C=N 7 <sup>th</sup> position	8.52-8.58
Ar-OH 1 <sup>th</sup> position	9.18-9.82

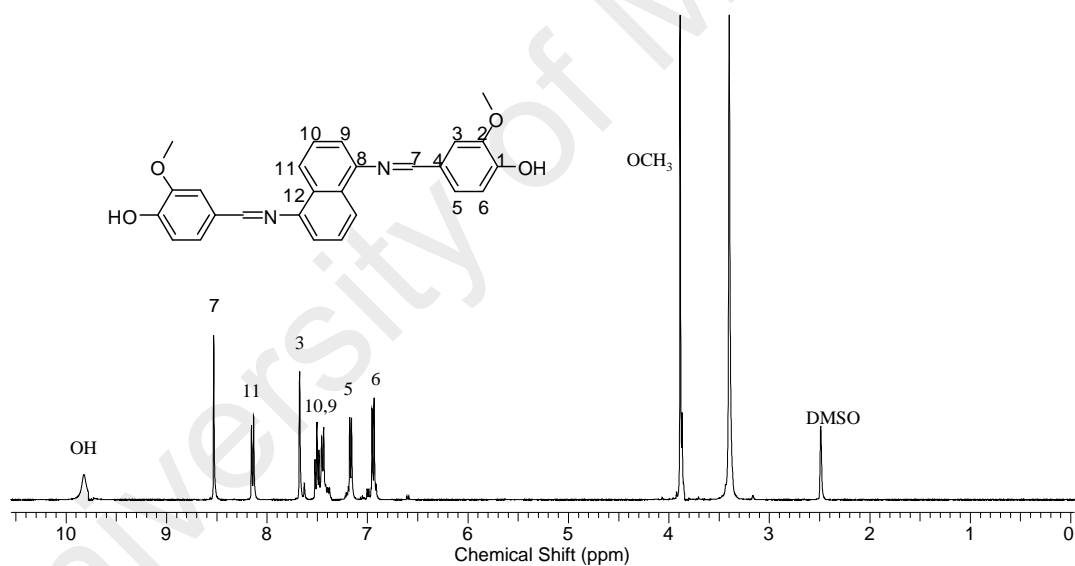


Figure 4.6 :  $^1\text{H}$  NMR spectrum of compound **b5**

#### 4.2.1.4.3 $^{13}\text{C}$ NMR

The  $^{13}\text{C}$  NMR spectrum and structure of the bisphenol bis-Schiff base monomer **b5** are shown in Figure 4.8. The data for all monomers (**b5-b8**) are tabulated in Table 4.8. The most significant peak of  $^{13}\text{C}$  NMR for bisphenol bis-Schiff base monomers containing 1,5-naphthalene is observed in the region of 161.0-161.2 ppm which is attributed to the azomethine (C=N) carbon atom. The C<sub>1</sub> which is attached to

OH phenol appears down field in the region of 149.2-150.1 ppm. In addition, C<sub>2</sub> appears in the region of 148.6-149.31 ppm. The peak attributable to the C<sub>8</sub> carbon is observed in the region of 139.9-148.2 ppm. The peak that appears in the region of 129.0-129.1 ppm is assignable to C<sub>4</sub>. The peaks in the region of 128.0-128.63 ppm and the region of 126.1-126.52 ppm represent to C<sub>12</sub> and C<sub>10</sub> respectively. Five peaks in the range of 110.9-124.37 ppm are attributed to C<sub>3</sub>, C<sub>9</sub>, C<sub>5</sub>, C<sub>6</sub> and C<sub>11</sub>. For compound **b5**, position C<sub>6</sub> is shifted down field due to it being attached to OCH<sub>3</sub> which contains atom with high electronegativity. The intense peak in the region of 55.67-64.44 ppm is due to methoxy group (OCH<sub>3</sub>) attached to the benzene ring. All the other monomers containing 1,5-naphthalene showed similar <sup>13</sup>C NMR spectral properties as those described for monomer **b5** with some differences due to the different group that is attached to the aromatic group (Chapter 2, Section 2.3).

4Table 4.8 : <sup>13</sup>C NMR data of monomers (**b5-b8**)

Type of carbon	Chemical shift (ppm)
O-CH <sub>2</sub> , O-CH <sub>3</sub>	56.63-64.44
CH <sub>2</sub> CH <sub>3</sub>	15.26
Ar-C 3 <sup>th</sup> position	107-112.61
Ar-C 5 <sup>th</sup> position	107-121
Ar-C 6 <sup>th</sup> position	115.57-148.6
Ar-C 4 <sup>th</sup> position	129-129.1
Naph-C 8 <sup>th</sup> position	139.9-148.2
Naph-C 9 <sup>th</sup> position	113.55-114
Naph-C 10 <sup>th</sup> position	126.1-126.52
Naph-C 11 <sup>th</sup> position	121.46-124.64
Naph-C 12 <sup>th</sup> position	128-128.63
Ar-C 2 <sup>th</sup> position	148.6-149.31
C=N 7 <sup>th</sup> position	161-161.2
Ar-OH 1 <sup>th</sup> position	149.2-150.1

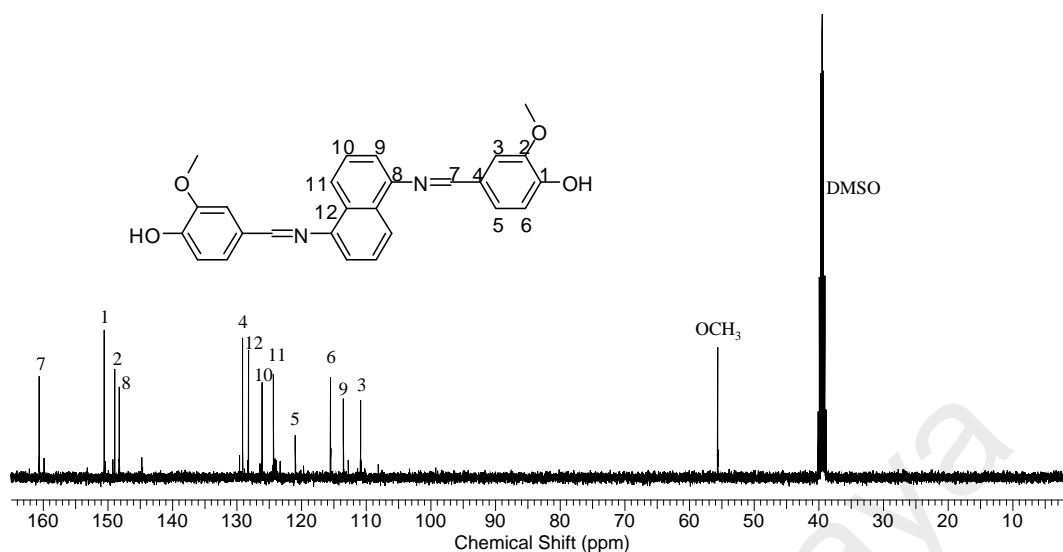
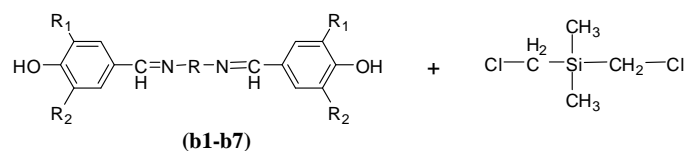


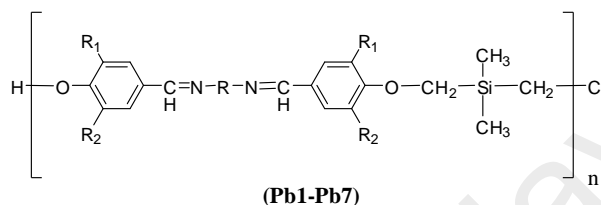
Figure 4.7 :  $^{13}\text{C}$  NMR spectrum of monomer **b5**

#### 4.2.2 Carbonosilane bisphenol bis-Schiff base copolymers

A new series of polycarbosilane containing bisphenol bis-Schiff base (**Pb1-Pb7**) were synthesized through the polycondensation reaction of bis(chloromethyl) dimethylsilane and the synthesized Schiff monomers (**b1-b7**). The same synthetic route as that of polycarbosilane containing bisphenol azine was utilized to synthesize the new copolymers except for some modifications as illustrated in Figure 4.8. The etherification took longer time and a higher temperature compared to the polycarbosilane containing bisphenol azine. Table 4.9 shows the substituted groups and the yield of the copolymers.



(A)



(A) Dry DMF, Dry K<sub>2</sub>CO<sub>3</sub>, Reflux 90°C, 72 h, 2 batches of silane compound.

Figure 4.8 : Synthetic route of copolymers (**Pb1-Pb7**)

Table 4.9 : Details of the synthesized copolymers containing bisphenol bis-Schiff base monomers (**Pb1-Pb7**)

Copolymer	R <sub>1</sub>	R <sub>2</sub>	R	Yield (%)
<b>Pb1</b>	H	H	1,4-phenylene	49.32
<b>Pb2</b>	H	OCH <sub>3</sub>	1,4-phenylene	61.4
<b>Pb3</b>	H	OCH <sub>2</sub> CH <sub>3</sub>	1,4-phenylene	64.11
<b>Pb4</b>	OCH <sub>3</sub>	OCH <sub>3</sub>	1,4-phenylene	59.5
<b>Pb5</b>	H	OCH <sub>3</sub>	1,5-naphthalene	56.2
<b>Pb6</b>	H	OCH <sub>2</sub> CH <sub>3</sub>	1,5-naphthalene	57.01
<b>Pb7</b>	OCH <sub>3</sub>	OCH <sub>3</sub>	1,5-naphthalene	51.6

The polymerization of polycarbosilane based on bisphenol bis-Schiff base proves that DMF is the best solvent as results in higher molecular weight. The synthetic route employed is similar to that for polycarbosilane based on azine monomers but in this reaction more time and higher temperature were needed. This may be due to the long term resonance arising from the higher conjugation and leading to less concentration of phenoxide ion on the Schiff base monomers. Using other solvents as

reaction media such as acetone, acetonitrile and pyridine did not display the same results that obtained using DMF. For example, the  $M_w$  for polymerization of **Pb7** in DMF was 7192 whereas, the polymerizations of the same monomers in acetone, acetonitrile and pyridine showed  $M_w = 2951, 4423$  and  $5.384$  respectively.

Figure 4.9 shows the different samples of the polycarbosilane containing bisphenol bis-Schiff base. By comparing with the polycarbosilane containing azine, these copolymers have slightly lower solubility in common organic solvents (THF,  $\text{CHCl}_3$  and DMF) and it is partially soluble in hydroxyl group containing solvents (methanol and ethanol).

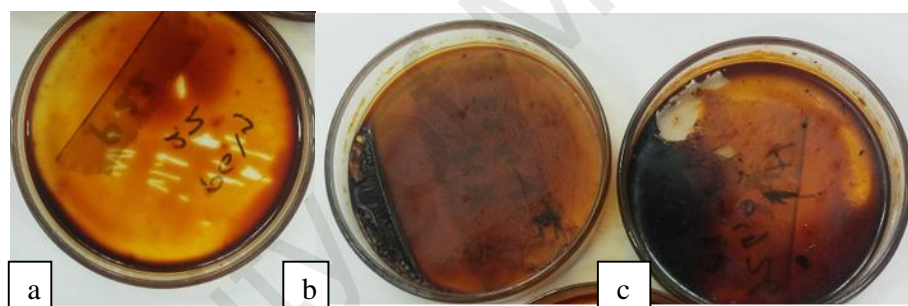


Figure 4.9 : (a) **Pb2** copolymer (b) **Pb4** copolymer (c) **Pb7** copolymer

#### 4.2.3 Characterization of copolymers

The synthesized carbosilane copolymers (**Pb1-Pb7**) were characterized by FTIR,  $^1\text{H}$  NMR,  $^{13}\text{C}$  NMR and GPC to study the molecular weight of these copolymers.

The results are in agreement with the proposed structures

##### 4.2.3.1 FTIR

The FTIR spectra of the polycarbosilanes containing bisphenol bis-Schiff base showed same characteristic bands as the monomers (**b1-b7**) since the functional moieties are similar for copolymers and monomers except for the appearance of a new

absorption band in the range of 1289-1272  $\text{cm}^{-1}$  which is attributed to  $\text{O-CH}_2\text{Si}$  group as well another new absorption band of the  $\text{Si-CH}_3$  group in the range of 777-822  $\text{cm}^{-1}$ .

#### 4.2.3.2 $^1\text{H NMR}$

The  $^1\text{H NMR}$  spectral analysis (Figure 4.10) presents the structural particularities of the synthesized copolymer **Pb2**. By comparing with the monomer peaks, all the copolymers showed similar shifts as those shown by the monomers with obvious distortion peaks due to the repeating units in the main chain of the copolymers. New broad peaks appearing in the range of 0.04-0.26 ppm (6H) can be assigned to the methyl protons of the  $\text{Si-CH}_3$  while the protons of the  $\text{O-CH}_2\text{Si}$  group showed a chemical shift in the range of 3.79-3.89 ppm (2H) which is considered the best indicator to confirm the formation of copolymer. While, the monomer displayed high intense OH group, this peak almost disappeared in the copolymer or appeared only in very small peak which is attributed to terminal group of phenol. All copolymers showed small peak in the range of 0.82-1.18 ppm which is most possibly be attributed to terminal group  $\text{SiCH}_2\text{Cl}$ .

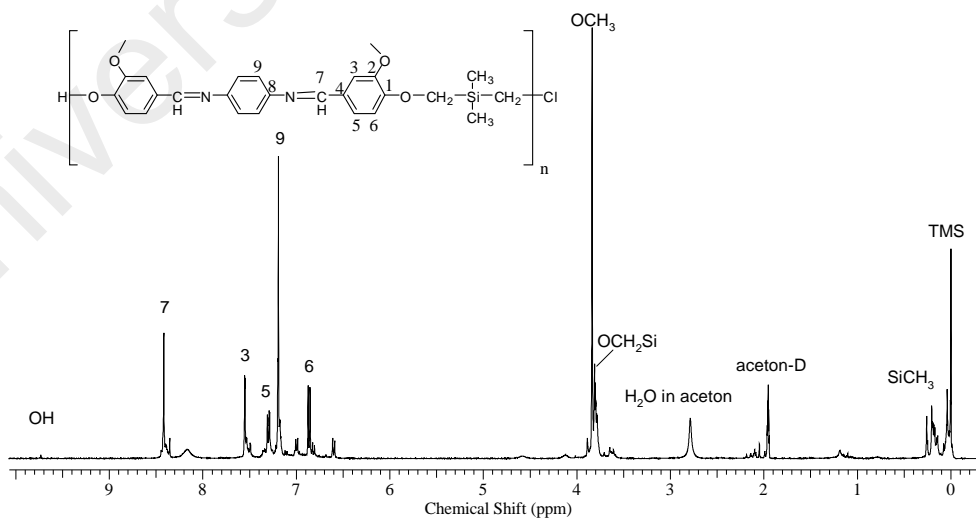


Figure 4.10:  $^1\text{H NMR}$  spectrum of copolymer **Pb2**

#### 4.2.3.3 $^{13}\text{C}$ NMR

The  $^{13}\text{C}$  NMR spectral analysis further confirms the presumed structures. By comparing with the monomer peaks, all the copolymers showed similar shift range with the monomers with obvious distortion peaks of some compounds due to the repeating units of monomers in the main chain of the copolymers. Figure 4.11 shows the  $^{13}\text{C}$  NMR spectrum of Schiff base copolymer **Pb2** with its molecular structure. The best identification for formation the copolymer is appearance of a new peak in the region of -6.68-0.62 ppm associated to  $\text{Si-CH}_3$  beside another new peak in the range of 59.42-66.83 ppm which is attributed to  $\text{OCH}_2\text{-Si}$ . A small peak that appears in the range of 19.3- 28.84 ppm supports the  $^1\text{H}$  NMR for  $\text{SiCH}_2\text{Cl}$ .

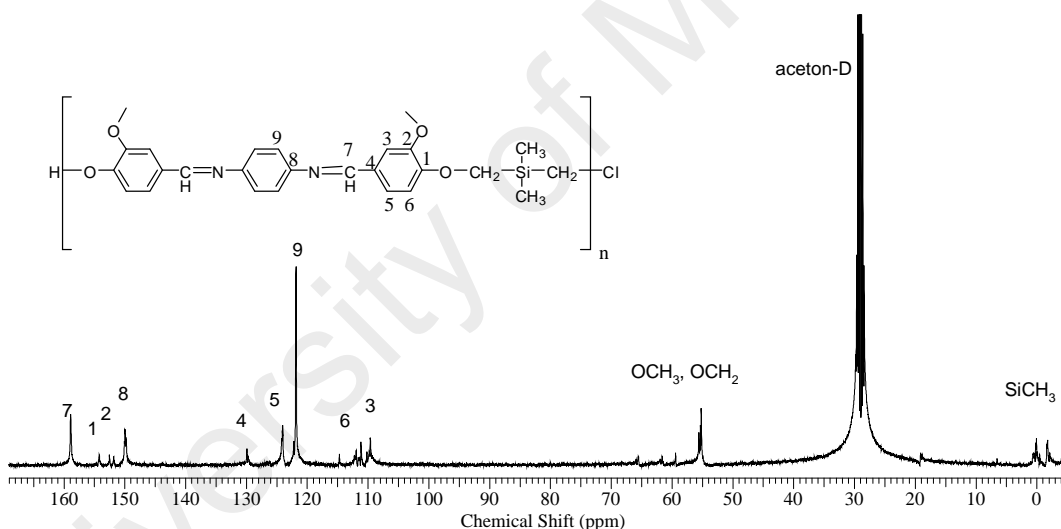


Figure 4.11 :  $^{13}\text{C}$  NMR spectrum of copolymer **Pb2**

#### 4.2.3.4 Gel permeation chromatography (GPC)

GPC analyses for all the polycarbosilanes containing bisphenol bis-Schiff base, percentages, colours and yields are summarized in Table 4.10. The number average molecular weights ( $M_n$ ) of the copolymers vary from 2401 to 7414 and the degrees of polymerization (DP) range from 5-13, where **Pb1** displays the lowest molecular weight, and is agreeable with the result obtained from polycarbosilane containing azine as

discussed earlier in Chapter 3. All the copolymers show narrow molecular weight distribution (PDI) between 1.21-2.04.

Table 4.10 : Yields, colors and characteristics of the synthesized copolymers

Copolymer	Yield (%)	Color	Mol. Wt.	Poly dispersity	Degree of polymerization
<b>Pb1</b>	49.32	Dark brown	2401	1.46	5
<b>Pb2</b>	61.41	Dark brown	6501	1.29	13
<b>Pb3</b>	64.11	Dark brown	7298	1.3	14
<b>Pb4</b>	59.5	Dark brown	6303	1.21	11
<b>Pb5</b>	56.2	Dark brown	6100	1.62	11
<b>Pb6</b>	57.01	Dark brown	7414	1.92	13
<b>Pb7</b>	51.6	Dark brown	7192	2.04	12

### 4.3 Physical properties

#### 4.3.1 Thermal degradation properties of copolymers

Figure 4.12 display the TGA thermogram of copolymer **Pb3** and its derivative which is typically similar for all the other copolymers and the detailed thermal data of the synthesized copolymers are summarized in Table 4.11.

From both Figure 4.13 and Table 4.11, it can be observed that onset decomposition temperatures of all the copolymers are more than 356°C which confirm that the polycarbosilanes containing bisphenol bis-Schiff base display very good thermal stability. From the derivative curve of **Pb3**, the decomposition is shown to occur through a single decomposition step. Temperatures at 10% weight loss are recorded in the range of 324-367°C, while the major weight loss of about 50% in the region of 423-672°C. Obviously, (Table 4.11) for copolymers containing naphthalene moiety, the major weight loss (50%) occurred at very high temperature compared to the copolymers containing bisphenol azine (**Pa1-Pa6**) and bisphenol bis-Schiff base (**Pb1-Pb4**). The copolymers containing naphthalene lost their weight over 623.48°C but those

containing azine and phenylene over than 330°C and 431°C, respectively. This is due to the fact that compounds containing high aromatic content possess high thermal stability and high heat resistance[170, 171]. The residual weight remaining at 700°C was around 31.84-52.61%. Enhancement of thermal stability observed in these polycarbosilane may be attributed to the delocalization characteristic of the Schiff base linkage and the silicon moieties on the main chain.

In addition, the glass transition temperatures ( $T_g$ ) of the copolymers (**Pb1-Pb7**) were achieved by DSC under nitrogen atmosphere. No detectable phase transition was observed in all copolymers. The undetectable phase transition for the copolymers with different substituted groups may lie in the rigidity of the main chains and carbonosilane moieties. As a result of high temperature and one stage decomposition, these copolymers have good thermal properties for industrial processing or for possible use in devices [157].

Table 4.11 : Thermal properties of copolymers (**Pb1-Pb7**)

Copolymers	Temperature (°C) corresponding to				Char yield (%) at 700°C
	Onset	10% Wt loss	50% Wt loss	DTp	
<b>Pb1</b>	368.26	324.23	431.18	381.69	31.84
<b>Pb2</b>	366.36	347.49	446.36	388.31	36.92
<b>Pb3</b>	376.82	354.55	452.72	391.38	44.31
<b>Pb4</b>	369.71	341.71	490.80	389.12	41.23
<b>Pb5</b>	367.36	367.80	672.51	376.72	52.61
<b>Pb6</b>	367.54	355.28	623.48	381.71	47.72
<b>Pb7</b>	356.06	348.37	655.28	358.70	46.06

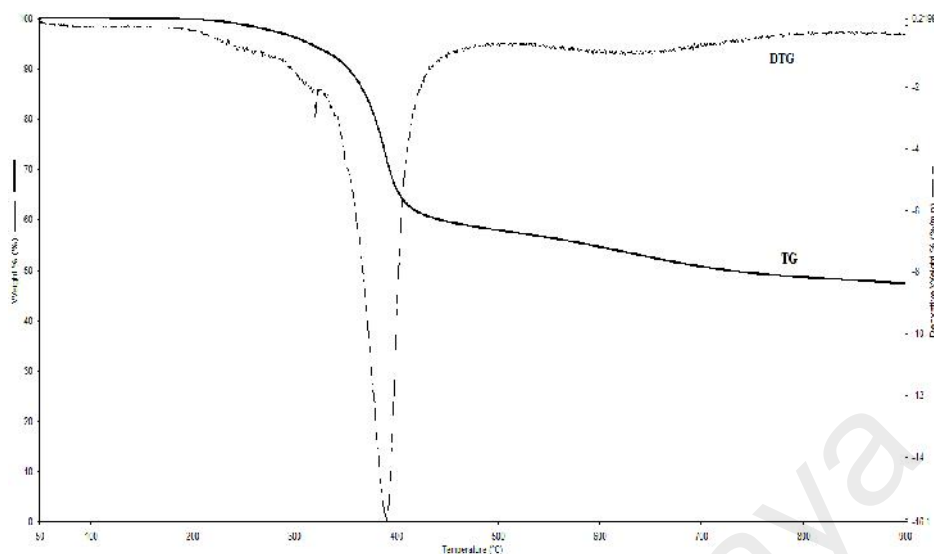


Figure 4.12 : TGA curves for copolymer (**Pb3**) at a heating rate of 10°C/min

### 4.3.2 Optical properties

The UV-vis and fluorescence spectroscopic properties were investigated for all the polycarbosilanes containing bisphenol bis-Schiff base. Figure 4.14 shows the UV-vis absorption emission spectra of the selected copolymers (**Pb2** and **Pb5**) in dilute chloroform solutions ( $1 \times 10^{-6}$  M) at room temperature and their detailed photophysical data are summarized in Table 4.12.

From the UV-vis spectra, the copolymers containing 1,4-phenylene moiety (**Pb1-Pb4**) exhibit similar characteristics, where two absorption peaks are obtained; one at higher energies in the range of 287-289 nm and the other absorbance peak at the lower energies in the region of 348-365 nm. The synthesized copolymers containing 1,5-naphthalene moiety in the main chain (**Pb5-Pb7**) also display similar absorption peaks, where three absorption peaks are obtained; first peak at higher energies with the maximum located in the range of 273-276 nm and second absorbance peak appeared in the region of 312-315 nm and the third appeared at in lowest energies the region of 360-363 nm. According to Jaffe et al. [172], the absorption peak at around 270 nm is attributed to a  $\pi \rightarrow \pi^*$  transition, while the absorption peak that appear at around 310 nm

results from a  $n \rightarrow \pi^*$  transition. The absorption peak at around 365 nm is attributed to  $\pi \rightarrow \pi^*$  transition.

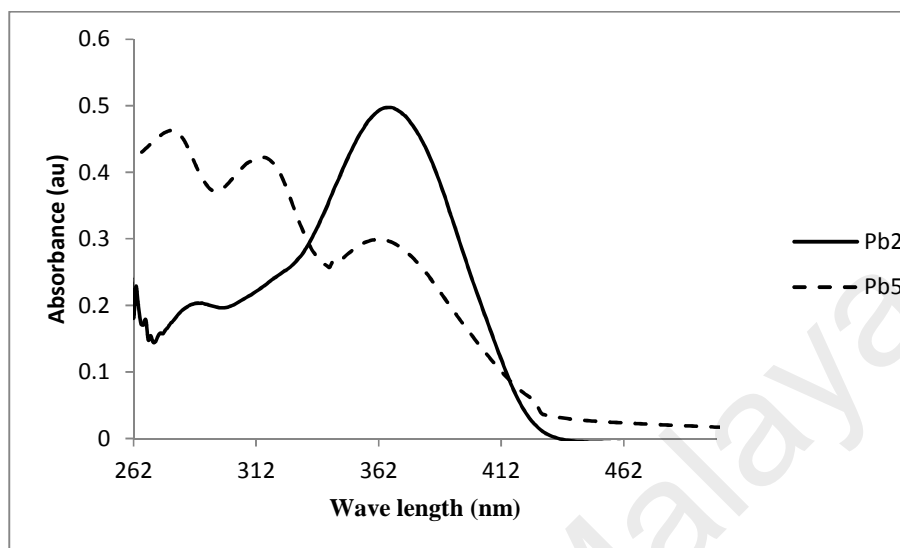


Figure 4.13 : UV-vis absorption spectral traces of the copolymers **Pb2** and **Pb5**

Figure 4.15 depicts PL spectra of selected copolymers, **Pb2**, **Pb5** and **Pb6**, in  $\text{CHCl}_3$  ( $1 \times 10^{-6}$  M) upon excitation of the copolymers at 375 nm Table 4.12 displays the PL data of all the synthesized copolymers. The emission spectra of all copolymers showed similar pattern. The fluorescence emission maxima of copolymers are in the range of 370-620 nm with emission maxima between 416-429 nm which may be categorized as blue emission. The blue emission is due to the conjugation of bisphenol bis-Schiff compounds, resulting in good  $\pi$ -electrons delocalization along bisphenol bis-Schiff base which is a  $p$ -conjugated system as mention in (Chapter 3, Section 3.2)

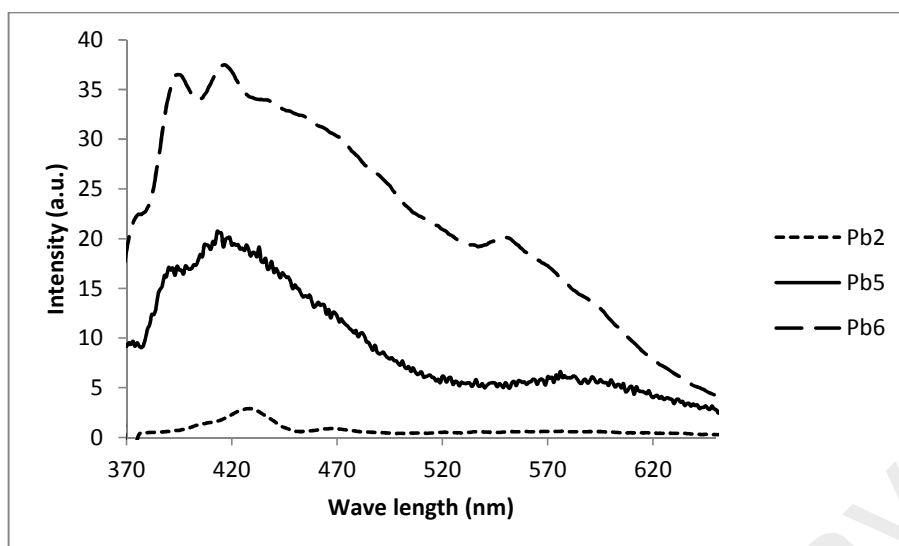


Figure 4.14 : Photoluminescence emission spectral of copolymers **Pb2**, **Pb5** and **Pb6**

Table 4.12 : UV-vis Absorption and photoluminescence emission spectral data of copolymers.

Copolymers	Absorption UV-vis, <sub>abs</sub> max (nm)	PL <sub>abs</sub> max (nm)
<b>Pb1</b>	348, 287	422
<b>Pb2</b>	365, 289	426
<b>Pb3</b>	362, 289	428
<b>Pb4</b>	364, 288	429
<b>Pb5</b>	363, 315, 275	418
<b>Pb6</b>	361, 312, 273	416
<b>Pb7</b>	360, 313, 276	419

### 4.3.3 Electrochemical properties

The electrochemical properties of the polycarbosilane for the copolymers containing bisphenol bis-Schiff base (**Pb1-Pb7**) was carried out by CV to estimate the HOMO, LUMO and band gaps. Same procedures as that mentioned in Section 3.3.3 were achieved to study the electrochemical properties. Figure 4.15 shows a CV curve of the copolymer **Pb3** which is typical for all the copolymers containing bisphenol bis-

Schiff base, all the copolymers showed irreversible redox processes with onset oxidation (p-doping) and reduction (n-doping). The oxidation (p-doping) started at 1.12, 1.13, 1.16, 1.11, 1.24, 1.28 and 1.31 V for compounds **Pb1-Pb7** respectively. On sweeping the thin film cathodically, the reduction processes (n-doping) started at -1.21, -1.28, -1.33, -1.31, -1.29, -1.21 and -1.23 V for the compounds **Pb1-Pb7** respectively.

The highest occupied molecular orbital (HOMO) and lowest unoccupied molecular orbital (LUMO) energy levels as well as the electrochemical energy gaps ( $E_g$ ) of the corresponding copolymers can be determined using Equations 3.1. The HOMO energy levels of the copolymers were calculated to be -5.73, -5.84, -5.87, -5.82, -5.95, -5.99 and -6.02 eV while; the LUMO energy levels were estimated to be -3.50, -3.43, -3.38, -3.40, -3.42, -3.50 and -3.48 for (**Pb1-Pb7**) respectively.

The HOMO and LUMO energy values of polymers **Pb1-Pb7** are in the range -5.73 eV to -6.02 eV and -3.38 eV to -3.50 eV respectively. These HOMO energy values are significantly different from those of copolymers containing bisphenol azine **Pa1-Pa6** (Table 3.10). These variations in electrochemical behaviour of copolymers **Pb1-P7** may be originated from the different molecular structure chain of copolymers where the electrochemical properties of these copolymers may be influenced by the effective conjugation length. Thus, electrochemical behaviours of conjugated polymers can be tuned by varying the above mentioned properties. The presence of 1,4-phenylene and 1,5-naphthalene in the main chain of the copolymers lead to **Pb1-Pb7** possess higher length of conjugated than those of copolymers **Pa1-Pa6**. As a result, the effective conjugation length will increase the oxidation potential of **Pb1-Pb7** and the HOMO energy levels will be shifted to a lower energy level.

The results, as summarized in Table 4.13, show that the synthesized copolymers have electrochemical band gap between 2.23-2.54 eV. As a result of this property, the

HOMO energy level of the copolymers (**Pb1-Pb7**) is comparable with the most widely used hole-transporting material 4,4'-bis(1-naphthylphenylamino)biphenyl (NBP)[164]. Therefore, these copolymers candidate for using as organic light emitting diodes (OLEDs)[167].

Table 4.13 : Electrochemical results of the copolymers (**Pb1-Pb7**)

Copolymer	$E_{red}(V)$	$E_{ox} V$	$E_{LUMO}(eV)$	$E_{HOMO}(eV)$	$E_g(eV)$
<b>Pb1</b>	-1.21	1.12	-3.5	-5.73	2.23
<b>Pb2</b>	-1.28	1.13	-3.43	-5.84	2.41
<b>Pb3</b>	-1.33	1.16	-3.38	-5.87	2.49
<b>Pb4</b>	-1.31	1.11	-3.40	-5.82	2.42
<b>Pb5</b>	-1.29	1.24	-3.42	-5.95	2.53
<b>Pb6</b>	-1.21	1.28	-3.50	-5.99	2.49
<b>Pb7</b>	-1.23	1.31	-3.48	-6.02	2.54

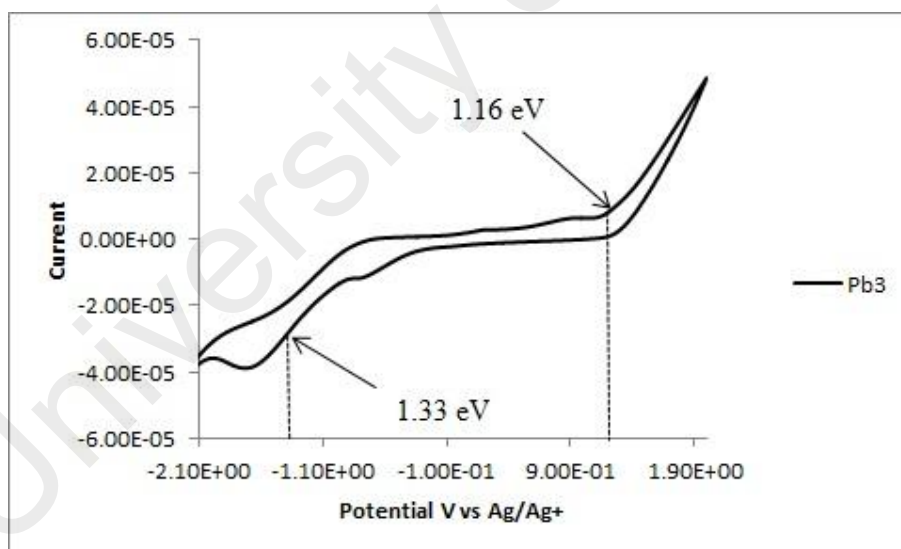


Figure 4.15 : Cyclic voltammogram of **Pb3** in  $CH_3CN$  at scan rate  $50 \text{ mV s}^{-1}$

## CHAPTER 5 : LIQUID CRYSTAL OF SYMMETRICAL DIMERS BASED ON BISPHENOL BIS-SCHIFF BASE

### 5.1 Introduction

In the solid crystal state, the order is usually both orientational and positional, in that the molecules are constrained both to occupy specific sites in a lattice and to point their molecular axes in specific directions. On the other hand, the liquid state diffuses randomly throughout the container with the molecular axes tumbling wildly. When exposed to heating or cooling, materials will pass from isotropic liquid to crystalline solid and vice versa but some materials do not directly pass from these states such as *N*-(4-methoxybenzylidene)-4-butylaniline (MBBA) but adopt an intermediate structure which flows like a liquid but still possesses the anisotropic physical properties similar to crystalline solids. This type of phase is termed liquid crystal phase, liquid crystalline phase, mesophase or mesomorphic phase and the substances called mesomorphs, where liquid crystal represents a state of aggregation that is intermediate between the amorphous liquid and the crystalline solid and material flows like liquids yet possesses some physical behaviours characteristic of solid crystals[173]. Figure 5.1 displays a comparison of the ordering of the crystal, liquid crystal and liquid states.

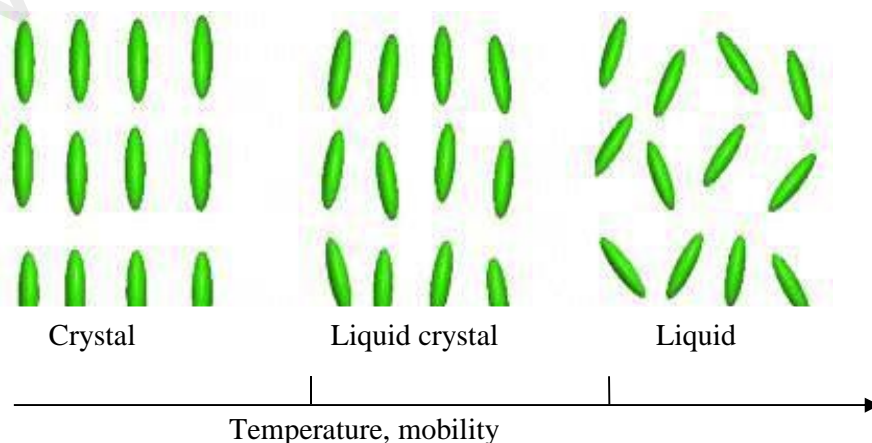


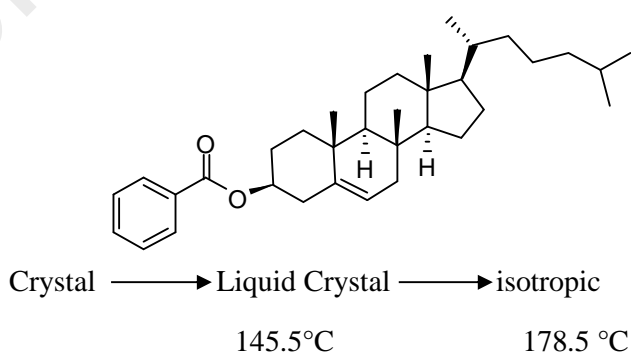
Figure 5.1 : A comparison of the ordering of the crystal, liquid crystal and liquid states.

Liquid crystal has been enormously extended from chemical as well as structural point of view during last two decades. In general, it is accepted that liquid crystals represent a state of higher order than ordinary (isotropic) liquids. Liquid crystalline materials (LCs), which were once just some naturally occurring curious and colourful substances, have now grown to be a major class of technologically and scientifically important materials, in particular as display devices, anisotropic networks, semiconductor materials, organic light emitting diodes (OLEDs) and photoconductors[174, 175]. The most technologically important liquid crystals are thermotropic nematic liquid crystals which are usually composed of rigid rod-shaped (calamitic) or disc-shaped (discotic)[176] and widely used as operating fluid in liquid crystal displays (LCDs). Furthermore, nematic liquid crystals (NLCs) based materials are extremely attractive for photonic applications such as optical information processing, dynamic holography, optical switching and phase conjugation due to their large optical anisotropy, low driving voltage and large electro-optics effects [177-180].

In this chapter, the synthesis and characterization series of a symmetrical dimers of bisphenol bis-Schiff base derivatised from 1,5-naphthalene monomers with different aliphatic ends will be presented and the effect of attaching methoxy group adjacent to the spacer will be investigated. The molecular structures of the titled compounds (**c1-c8**) and (**d1-d8**) were confirmed through FT-IR,  $^1\text{H}$  NMR and  $^{13}\text{C}$  NMR. TGA was performed to evaluate the thermal stability. Studies on the optical properties were achieved through UV-Vis and PL (Photoluminescence) experiments. In order to establish the liquid crystalline behaviour, Differential Scanning Calorimetry (DSC) (for the determination of the phase transition temperatures and enthalpy values) and polarising optical microscopy (POM) (for the texture observations and their changes) have been used.

## 5.2 Historical development of liquid crystals

The liquid crystalline state has been discovered more than 100 years ago when Austrian botanist physiologist named Friedrich Reinitzer[181] examined the physico-chemical properties of various derivatives of cholesterol which now belong to the class of materials known as cholesteric liquid crystals. He found cholesteryl benzoate changed to a cloudy liquid at 145.5°C and this material suddenly became clear when the temperature rose to 178.5°C. When cooling down this material, violet-blue was observed just before changing into an opaque liquid and finally become a white solid crystal. Otto Lehmann, a German physicist[182] studied precisely this phenomena by taking the samples from Reinitzer and investigated under polarizing microscope. He concluded that cholesteryl benzoate in the temperature range of 145.5–178.5°C should be a new state of matter which behaves as liquid and at the same time shows optical behaviour like that of a crystal. In 1900 Lehmann called the new state of matter “liquid crystal”[182]. This discovery represented the first recorded documentation of the liquid crystal phase. Figure 5.2 displays the structure of cholesteryl benzoate with two distinct melting points.



5.5.2 : Structure of cholesteryl benzoate with two melting points

The area of liquid crystals developed progressively more in the following decades. In 1935, Danial Volander had prepared many compounds that displayed liquid crystalline state[183].

In the late 1940s, George William Gray started to investigate and study these materials in England. Gray and his group succeeded in synthesizing many new materials that showed the liquid crystalline state and gave clear study of how to design molecules that display liquid crystal state. “Molecular structure and the properties of liquid crystals” was the first book authored by him to explain the properties of the new state and his book became a guidebook on the subject[184].

Hans Kelker and Scheurle in 1969 also synthesized successfully a new compound, MBBA that showed nematic phase at room temperature, and was considered as one of the most popular in liquid crystal research[185]. Figure 5.3 shows the chemical structure of MBBA.

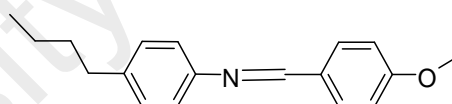


Figure 5.3 : Molecular structure of MBBA

In 1970s, electro-optical liquid crystal display devices became well recognized[186, 187]. George Gray synthesized cyanobiphenyls which are chemically stable substances with low melting temperatures[184]. In beginning 1990, when LCDs was already well established, a French physicist Pierre-Gills de Gennes turned his intention to study liquid crystals, where he was rewarded the Nobel Prize in physics for his finding on the fascinating analogies between superconductors and liquid crystals in addition to magnetic materials[188]. His discovery has deeply influenced the modern

development of liquid crystals science. Today, liquid crystals play a dominant role in display technology.

### **5.3 Types of liquid crystals**

Liquid crystalline phases can be obtained by heating or cooling which are called thermotropic liquid crystals. Meanwhile those obtained by dissolving some substances such as sodium or potassium salts in higher fatty acids into a certain amount of a proper (isotropic) solvent such as water are called lyotropic liquid crystals and are dependent on the concentration of an isotropic solvent. Lyotropic liquid crystals are generally mixtures of two or more compounds, while many of the reported thermotropic liquid crystals are single compounds. Some materials are able to form both thermotropic liquid crystals and lyotropic liquid crystals which are called amphotropic.

The existence of thermotropic liquid crystals is dependent on temperature in certain temperature intervals. Thermotropic liquid crystals which are stable at temperatures above the melting point of the compound are called enantiotropic. Some cases the liquid crystals state are only stable at temperatures below melting point and can be obtained only with decreasing temperature; phase of this kind is called monotropic[189]. Thermotropic liquid crystals are divided to two types based on molecular mass. High molecular mass thermotropic liquid crystals consist of side chain polymers and main chains polymer as well as low molecular mass thermotropic liquid crystals that consist of oligomeric, monomeric and mesogenic substances. Low molecular mass thermotropic liquid crystals are generally further classified to three basic molecular shapes, being called calamitic for rod-like, discotic for disk-like and sanidic for brick- or lath-like molecules. In this thesis only rod-like molecules will be discussed. Figure 5.4 displays the classification of liquid crystals.

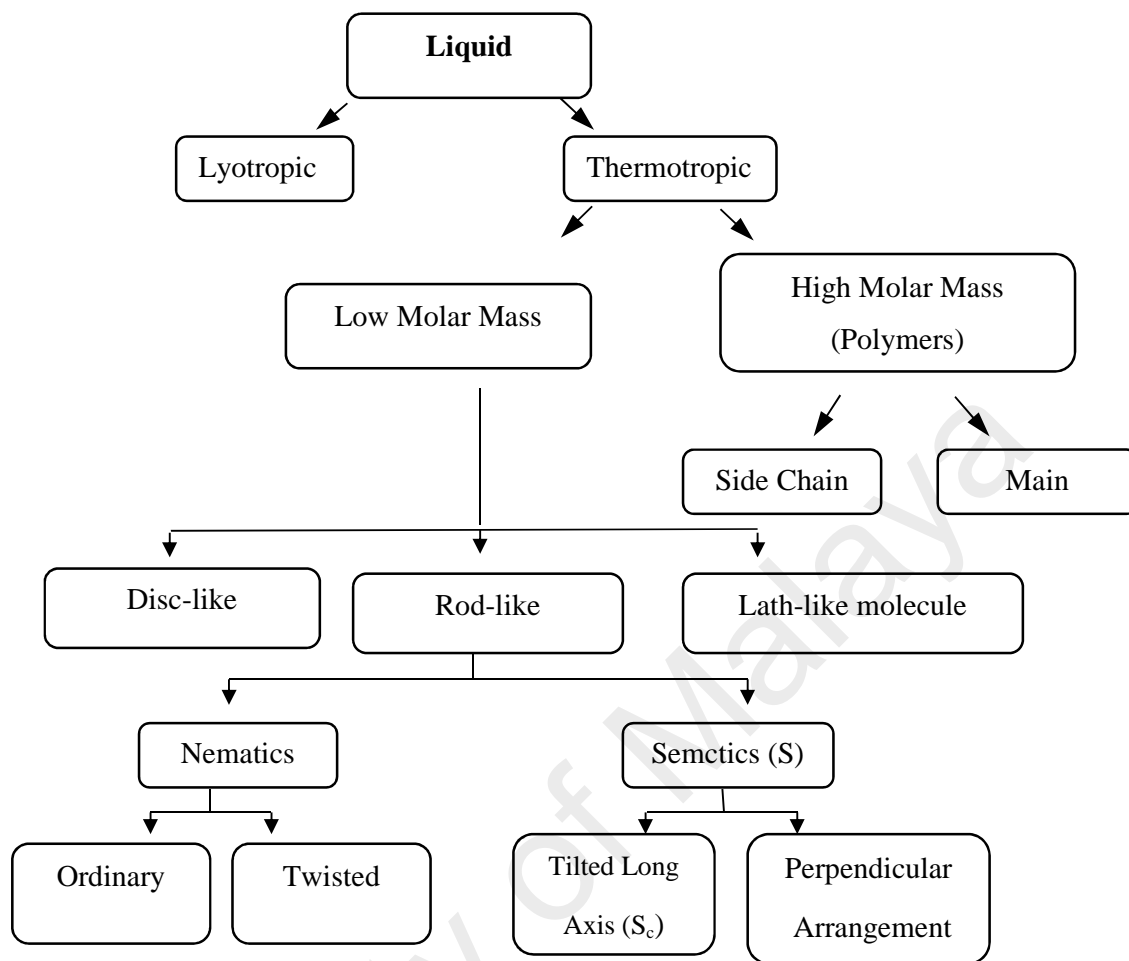


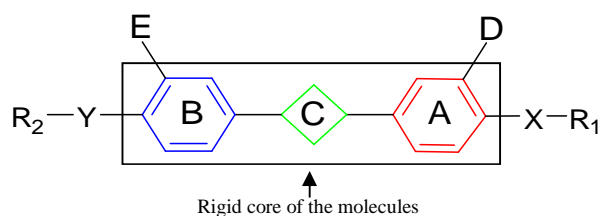
Figure 5.4 : Classification of liquid crystals

### 5.3.1 Calamitic liquid crystals

There are many types of liquid crystal phases which is dependent on the molecular structure of materials. Calamitic mesogens or rod-like molecules are the most important type of molecules that form the thermotropic liquid crystals consisting of rigid cores, often incorporating phenyl and biphenyl groups, and two flexible endgroup which are mostly alkyl or alkoxy chains[190]. The basic structure of typical calamitic liquid crystals is shown in Figure 5.5. The rigid groups A, B normally consist of aromatic rings such as benzene, naphthalene, biphenyl, terphenyl and cyclohexane. In addition, heterocyclic compounds have been used as a core group such as pyridine[191] and benzothiazole [192]. The linking group C connects the core groups A and B

together where this group plays a very important role for the rigidity of the liquid crystal, contribution to the phase transition and physical properties. There are many linking groups reported such as Schiff base (-C=N-)[193], azo (-N=N-)[194], ester (-COO-)[195], and acetylene (-C≡C-)[196]. Generally, the chemical stability of liquid crystal depends much on the linking group where Schiff base linking group is less stable than ester, azo and azoxy linking group but the latest three linking groups are quite susceptible to temperature change, moisture and ultraviolet (UV) radiation[197]. The side groups or sometimes called the flexible spacers are  $R_1$  and  $R_2$  linked directly to the core or through other groups X and Y.

The liquid crystalline phases might not form based on the rigid core alone. Thus, certain flexibility is required to ensure reasonably low melting points and to stabilize the molecular alignment within the mesophase structure [198]. The flexibility spacers,  $R_1$  and  $R_2$ , could be polar (e.g.,  $\text{CH}_3$ ) or nonpolar (e.g., CN, F) to provide the flexibility of the liquid crystal molecules. The flexibility allows one molecule to place itself easily between other molecules when it moves around where the flexibility with rigidity of molecules must be in balance in order to display the properties of liquid crystals[197]. E and D are the lateral moieties which are involved in the modification of phase morphology and the physical properties of materials. Common lateral groups are alkoxy, alkyl, nitro, cyano and halides such as fluoro, chloro and  $\text{OCF}_3$ .



A and B: Core groups, C: Linking group,  $R_1$  and  $R_2$ : Side groups, E and D: Lateral groups

Figure 5.5 : Basic structure of typical calamitic liquid crystals

There are three classes of calamitic liquid crystals: nematic, cholesteric and smectic as well there are many sub-classifications of smectic liquid crystals in accordance with the directional arrangement and positional of the molecules.

#### **5.3.1.1. Nematic Phase**

The nematic phase (N) is one of the most common and simplest liquid crystal phases where the molecules maintain a preferred orientational direction as they diffuse throughout the sample. This is the least ordered mesophase which have fluidity similar to that of ordinary isotropic liquid state but the nematic phase can easily aligned by an external magnetic or electric field. These alignment have the optical properties of uniaxial crystals and this property is extremely useful in LCDs[199, 200]. Figure 5.6 shows the orientation of molecules where the orientation of molecules is parallel with their axes. The long axes of the molecules point on the average in the same direction, which is defined by a unit vector commonly known as ‘the director’ ( $n$ )[201].

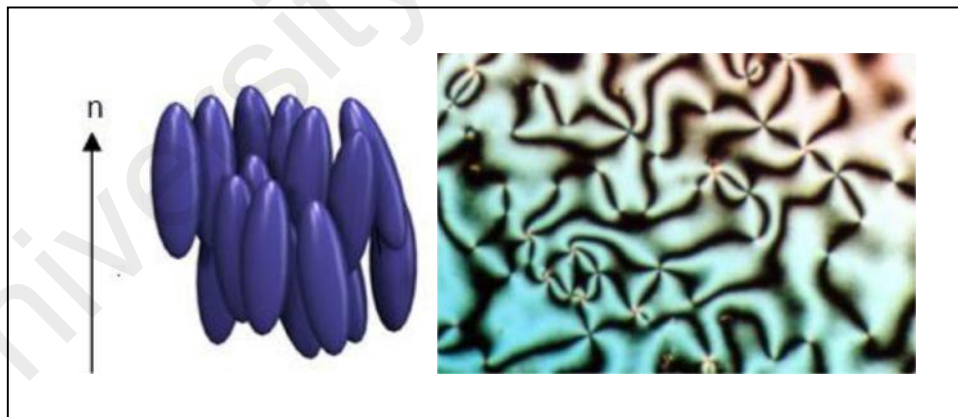


Figure 5.6 : Texture and molecular arrangement of nematic liquid crystals

#### **5.3.1.2 Smectic phase**

The smectic phase (S) is usually found at lower temperatures than nematic phase. In this phase, the arrangement of molecules will be in planar sheets. Within each layer, the molecules are aligned, but they possess only one-dimensional translational

order. The smectic phase is classified into many subclasses, each of which has slightly different properties. The most common sub categories of these phases are the smectic A ( $S_A$ ) phase and smectic C ( $S_C$ ) phase. These phases show orientational order like that as in nematic phase but there is also positional order since the centres of mass of the molecules are arranged in layers. If the director is perpendicular to the plane of the layer, the phases is divided as smectic A but if the director is tilted at some angle between 0 and 90°, the phase is called smectic C [173, 202, 203]. Figure 5.7 displays the molecular arrangements of smectic A and smectic C.

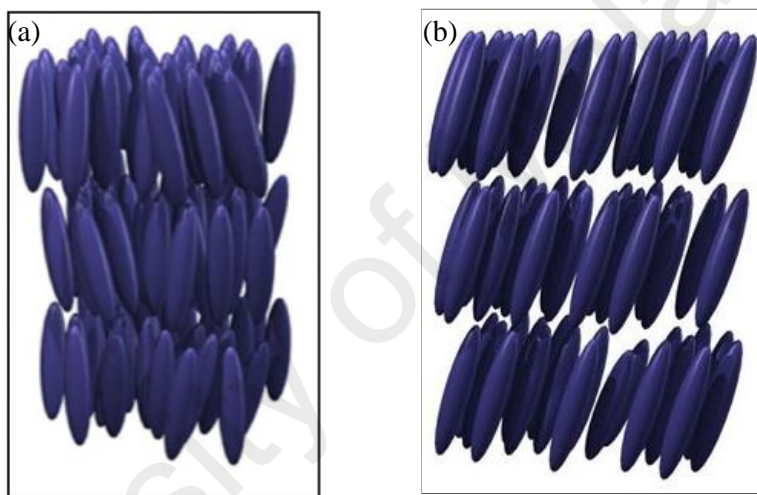


Figure 5.7 : Molecular arrangements of (a) smectic A (b) smectic C

#### 5.4 Structure-mesomorphic properties relationship

The mesomorphic behaviors depend directly on the design of chemical structure of the molecules, where slight change in the architecture of the liquid crystal molecules brings about considerable change in its mesomorphic properties. In this research, the influence of some groups on the physical properties of liquid crystal molecules will be discussed.

#### 5.4.1 Influence of mesogenic core on mesomorphic properties

The core group is the most fundamental structural feature of a liquid crystal material. The core unit can be defined as the rigid group that can be connected to any lateral groups and any linking units. The liquid crystal phase is generated because of the anisotropy of the polarisability resulting from the conjugated core unit and that the higher the polarisability anisotropy the higher the liquid crystal stability[204].

Fornasieri *et al.* in 2003[205] had synthesized three series of thermotropic liquid crystals and he studied the effect of the structure of the mesogenic core group and the length of the hydrocarbon spacer on the mesomorphic properties. The structure consists of a mesogenic core connected to a perfluorinated chain through thioester linking group and hydrocarbon chain containing a terminal double bond. A biphenyl (B1), monophenyl (Ph1) and phenyl benzoate (PhB1) groups were used as the core unit attached to a chain of hydrocarbon with different length to study their influence on the liquid crystal behaviours as shown in Figure 5.8. The liquid crystal behaviour was strongly reduced due to the effect of increasing of the hydrocarbon chain, while the influence of increasing the number of aromatic rings in the core structure caused an increase in the transition temperatures. In addition, the monophenyl allyoxy derivative displayed interesting smectogenic property near room temperature. The compounds containing biphenyl shifted the mesophase to the higher temperatures without any change of temperature range, while the compounds containing phenyl benzoate moiety stabilized the mesophase at wider range (181°C).

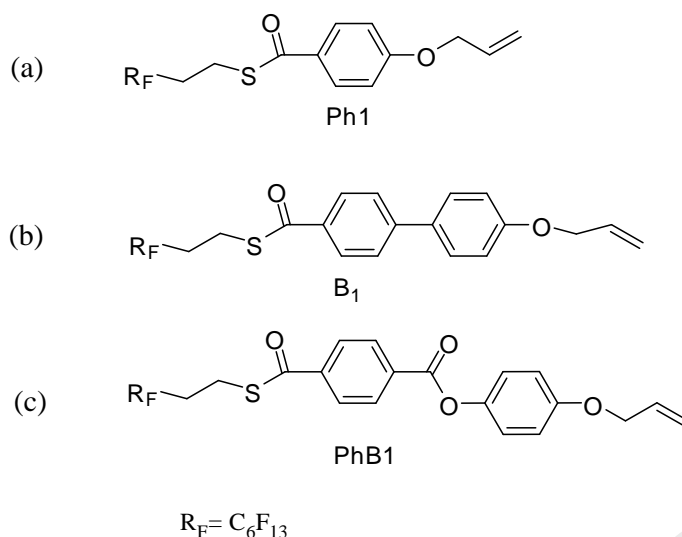


Figure 5.8 : The structures of thermotropic liquid crystals with core unit of (a) monophenyl, (b) biphenyl and (c) phenyl benzoate[205].

#### 5.4.2 Influence of terminal unit on mesomorphic properties

The branch of the chain displays an apparent influence on the liquid crystal phase behaviour as it helps in introducing chirality into the molecule. However, phase stability and the melting point are being reduced as a result of the disruption in the molecular packing[206]. Besides, the formation of liquid crystal is influenced by the position of the end chains as well. In addition, by increasing the terminal chain length, the smectic tendency increases and subsequently eliminates the nematic phase as is observed in this research (see Section 5.6.4). The reason for the appearance of the smectic phase is due to the long chains becoming intertwined and attracted, which facilitates the lamellar packing required for smectic phase generation[204, 207].

Matsunaga *et al.*[208] studied the effects of terminal substituents of 4-(4-X-substituted benzylideneamino)phenyl-4-Y-substituted benzoates on mesomorphic properties (Figure 5.9). X and Y were chosen from nitro, methoxy, chloro, bromo, fluoro, methyl, trifluoromethyl and dimethylamino groups. They found that the order of group (X or Y) efficiency in promoting the nematic-isotropic transition temperature is

markedly affected by the nature of the group (X or Y) located at the other end. The trifluoromethyl series gives  $N(CH_3)_2 > CH_3O > CH_3 > Cl = Br > NO_2 > F$  whereas the methoxy and methyl series gives  $NO_2 > CH_3O > N(CH_3)_2 > Cl = Br > CH_3 > F > CF_3$ , suggesting that the dipole-dipole interaction contributes significantly to the stabilization of the nematic phase.

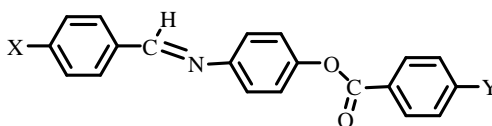
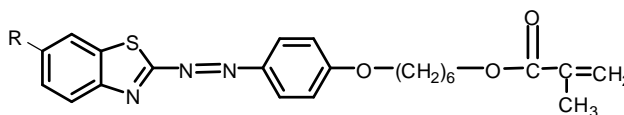


Figure 5.9 : Studied compound [208]

Very recently, Karim et al.[209] studied the effect of different substituents R (where R= -H, -CH<sub>3</sub>, -OCH<sub>3</sub>, and -OC<sub>2</sub>H<sub>5</sub>) at the sixth position on benzothiazole chromophore (Figure 5.10) on mesomorphic, thermal and optical properties. All synthesized compounds showed mesomorphic behaviours and exhibited lamellar structure. The compound with -H substituent revealed only smectic mesophase whereas the compounds with -CH<sub>3</sub>, -OCH<sub>3</sub>, and -OC<sub>2</sub>H<sub>5</sub> groups exhibited nematic and smectic mesophases. They thus concluded that the formation of the mesophases was greatly influenced by the sixth position electron pushing substituents on the benzothiazole ring as well as the terminal methacrylate group. The optical study on these compounds showed that the compound with a methoxy substituent exhibited higher fluorescent emission compared to other compounds.



M1: R=H

M2 : R= CH<sub>3</sub>

M3 : R= OCH<sub>3</sub>

M<sub>4</sub> : R= OCH<sub>2</sub>H<sub>5</sub>

Figure 5.10 : Azo benzothiazole compound[209]

### 5.4.3 Influence of linking unit on mesomorphic properties

Linking units are important to extend the length and polarisability anisotropy of the molecular core of liquid crystal in order to improve the stability of liquid crystal phase.

Prajapati et al. (2004) have studied the influence of different linking units on mesomorphism[210]. Figure 5.11 shows that Compound 3 consists of azomethine (-CH=N-) linking unit while Compound A has an ester (-COO-) linking unit. Compound 3 had been observed to have higher smectic phase as well higher thermal stability than compound containing ester by 77°C and 34°C, respectively. Furthermore, the Schiff base linking unit is coplanar as compared to the ester linking group which makes the packing of the molecules to be more efficient. For this reason the thermal stability of smectic phase of compound A is less than compound 3. In addition, linking unit enhances most of the liquid crystalline properties whenever all the rings are fully conjugated. This will enhance the longitudinal polarisability and extends the molecular length[204], where the linking units such as azomethine or ethylene that contain double bond can thus result in a high liquid crystal transition[210]. However, the ester linking unit does not link the system through a multiple bond. Hence the thermal stability of mesogenic of a system linked through Schiff base group is higher.

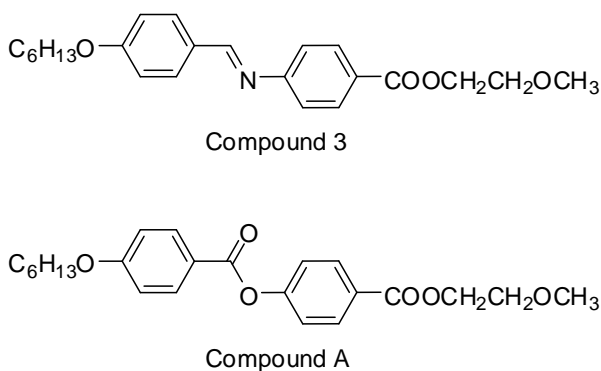


Figure 5.11 : Synthesis of compounds containing azomethine and ester

#### 5.4.4 Influence of lateral unit on mesomorphic properties

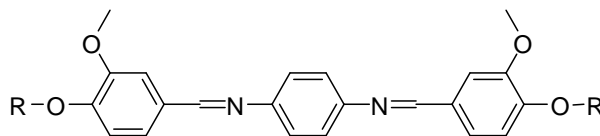
Lateral group replaces the hydrogen atoms in positions 2, 3 and 4 of the phenyl ring by any polar substituted groups such as cyano, chloro, hydroxy, methoxy and fluoro groups. These groups can modify the physical properties of the liquid crystal, where the lateral moiety broadens the molecules, thus reducing lateral attractions and lowering the nematic and smectic phase stability.

#### 5.5 Liquid crystals with Schiff bases

Schiff base materials have received much attention as liquid crystal after the publication of Kelker's work on MBBA in 1970[211-214]. This material contains Schiff base as linking group and possesses a useful functional group due to convenience of its low temperature of phase transition and its rich polymorphism. In addition, Schiff bases are able to maintain the linearity of the molecular structure and provide a stepped core structure and also have high thermal stability. For these reasons, Schiff bases have received attention as liquid crystal display devices such as STN-LCD (supertwisted nematic LCD), TN-LCD (twisted nematic-LCD) and TFT-LCD (thin film transistor-LCD) having improved electro-optical properties [215, 216].

Yeap, G.-Y, *et al.*[217] synthesized a series of symmetrical dimers N,N'- bis (3-methoxy-4-alkoxybenzylidene)-1,2-phenylenediimine compounds with a different length of symmetrical chains of alkyl (C4-C18) to investigate their liquid crystal properties. Figure 5.12 shows that all the symmetrical dimers were nematogenic phase except the dimers containing butyl and hexyl chains as well as the longest octadecyl dimer in which the mesogenic properties were absent. Many studies were reported by Yeap and co-workers on the compounds containing Schiff bases as liquid crystals [218-221]. They also revealed that the compounds containing Schiff base linking groups were

useful structural components for designing mesomorphism in two and three aromatic rings liquid crystals.



$R = C_4H_9, C_6H_{11}, C_8H_{17}, C_{10}H_{21}, C_{12}H_{25}, C_{14}H_{29}, C_{16}H_{33}, C_{18}H_{37}$

Figure 5.12 : Structure of symmetrical dimer containing bis-Schiff base linking group[217].

In addition, a vast number of Schiff bases containing naphthalene moiety as liquid crystal have been studied, where naphthalene moiety displays excellent mesomorphism if the molecular structure is designed properly[126, 222-226]. Prajapati *et al.* [227] synthesized homologous series of Schiff base cinnamates containing naphthalene group and the liquid crystal properties were studied as well the influence of an ethylene linking moiety on the mesomorphic properties. They found that all the synthesized Schiff base compounds containing naphthalene of this homologous series showed liquid crystal properties. The presence of naphthalene group at the terminal position broadened the transition temperature of the mesophase due to high polarizability of the molecule. Also, the existence of naphthalene group increased the nematic liquid crystal phase range and decreased the smectic liquid crystal phase range due to the packing influence. Figure 5.13 shows the synthesized Schiff base compounds containing naphthalene.

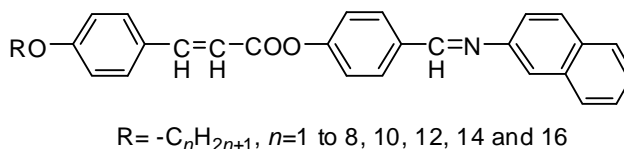
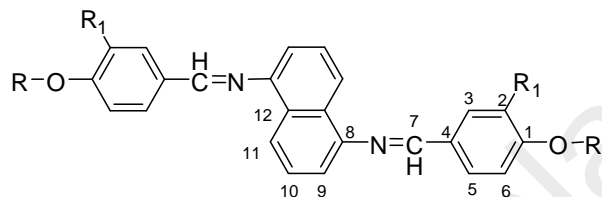


Figure 5.13 : A series of Schiff base compound containing naphthalene group[227].

## 5.6 Experimental

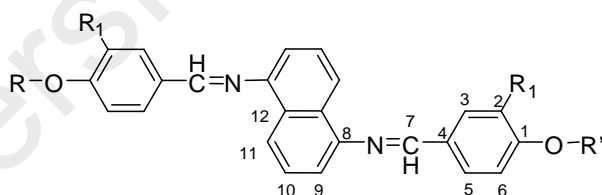
### 5.6.1 Synthesis of symmetrical dimers

The syntheses of the two symmetrical series (**c1-c8**) and (**d1-d8**) were performed using the same procedure and the details as below. Figure 2.1 shows the structures of the symmetrical dimers.



(**c1-c8**)

Sample code	c1	c2	c3	c4	c5	c6	c7	c8
R <sub>1</sub>	H	H	H	H	H	H	H	H
R=R'	C <sub>4</sub> H <sub>9</sub>	C <sub>6</sub> H <sub>13</sub>	C <sub>8</sub> H <sub>17</sub>	C <sub>10</sub> H <sub>21</sub>	C <sub>12</sub> H <sub>25</sub>	C <sub>14</sub> H <sub>29</sub>	C <sub>16</sub> H <sub>33</sub>	C <sub>18</sub> H <sub>37</sub>



(**d1-d8**)

Sample code	d1	d2	d3	d4	d5	d6	d7	d8
R <sub>1</sub>	OCH <sub>3</sub>	OCH <sub>3</sub>	OCH <sub>3</sub>	OCH <sub>3</sub>	OCH <sub>3</sub>	OCH <sub>3</sub>	OCH <sub>3</sub>	OCH <sub>3</sub>
R=R'	C <sub>4</sub> H <sub>9</sub>	C <sub>6</sub> H <sub>13</sub>	C <sub>8</sub> H <sub>17</sub>	C <sub>10</sub> H <sub>21</sub>	C <sub>12</sub> H <sub>25</sub>	C <sub>14</sub> H <sub>29</sub>	C <sub>16</sub> H <sub>33</sub>	C <sub>18</sub> H <sub>37</sub>

Figure 5.14 : General structures of the symmetrical dimers of series (**c**) and (**d**)

### 5.6.2 Synthesis of the symmetrical dimers containing 4,4'-(naphthalene 1,5-diyldis(azan-1-yl-1-ylidene))bis(methan-1-yl-1-ylidene) diphenol (b8)

A new symmetrical dimers, *N,N'*-bis(4-alkoxybenzylidene)-1,5-naphthalene diimines were synthesized by condensation reaction in a round bottomed flask by dissolving compound 1 (1 g,  $2 \times 10^{-3}$  mol) in a *N,N'*-dimethylformamide (DMF) solution containing  $K_2CO_3$  (0.75 g,  $5.4 \times 10^{-3}$ ) as proton acceptor. The stirring solution was heated up to 80°C. After 20 min, 1-bromoalkane (RBr, R= C4 to C18) (0.74 g,  $4.6 \times 10^{-3}$  mol) was added dropwise and the mixture thus obtained was heated for 24 h before being cooled down to room temperature. The obtained solution was then poured into 100 mL of water, and the precipitate formed was filtered off and dried. The product was recrystallized with ethyl acetate to yield yellow–brown solid product. DMF solvent had been used to obtain good yield, shorter time and easier separation of the final product.

#### Synthesis of *N,N*-bis(4-butoxybenzylidene)naphthalene-1,5-diimine (c1)

Yellowish-brown, yield 79.8%, MP: 137-138°C, IR, : 3071-3031  $cm^{-1}$  (C-H<sub>ar</sub>), 2922-2861  $cm^{-1}$  (C-H<sub>aliph</sub>), 1620  $cm^{-1}$  (C=N) and 1262  $cm^{-1}$  (O-CH<sub>2</sub>), <sup>1</sup>H NMR, (ppm, CDCl<sub>3</sub>, 400 MHz): 0.83 (t, 6H, CH<sub>3</sub>), 1.41-1.79 (m, 8H, CH<sub>2</sub>), 3.99 (t, 4H, J=6.5 x(2), O-CH<sub>2</sub>), 6.94 (d, 4H, J=8.8, H<sub>2,6</sub>), 7.00 (d, 2H, J=7.3, H<sub>9</sub>), 7.39 (t, 2H, J=7.8 x(2), H<sub>10</sub>), 7.88 (d, 4H, J=8.8, H<sub>3,5</sub>), 8.14 (d, 2H, J=8.5, H<sub>11</sub>), 8.40 (s, 2H, H<sub>7</sub>). <sup>13</sup>C NMR, (ppm, CDCl<sub>3</sub>, 100 MHz): 14.14 (2C, CH<sub>3</sub>), 22.71-29.32 (4C, C<sub>aliph</sub>), 68.21 (2C, O-CH<sub>2</sub>), 113.42 (2C, C<sub>9</sub>), 114.88 (4C, C<sub>2,6</sub>), 121.78 (2C, C<sub>11</sub>), 125.77 (2C, C<sub>4</sub>), 129.44 (2C, C<sub>10</sub>), 129.50 (2C, C<sub>12</sub>), 131.12 (4C, C<sub>3,5</sub>), 149.53 (2C, C<sub>8</sub>), 159.76 (2C, C<sub>1</sub>), 162.13 (2C, C<sub>7</sub>).

#### Synthesis of *N,N*-bis(4-(hexyloxy)benzylidene)naphthalene-1,5-diimine (c2)

Yellow solid, yield 83.3%, Mp: 133-134°C, IR, : 3078-3025  $cm^{-1}$  (C-H<sub>ar</sub>), 2934-2858  $cm^{-1}$  (C-H<sub>aliph</sub>), 1619  $cm^{-1}$  (C=N) and 1261  $cm^{-1}$  (O-CH<sub>2</sub>), <sup>1</sup>H NMR, (ppm, CDCl<sub>3</sub>, 400 MHz): 0.85 (t, 6H, CH<sub>3</sub>), 1.28-1.79 (m, 16H, CH<sub>2</sub>), 3.97 (t, 4H, J=6.5x (2), O-CH<sub>2</sub>),

6.94 (d, 4H, J=8.8, H<sub>2,6</sub>), 7.00 (d, 2H, J=7.3, H<sub>9</sub>), 7.39 (t, 2H, J=7.8x(2), H<sub>10</sub>), 7.88 (d, 4H, J=8.8, H<sub>3,5</sub>), 8.14 (d, 2H, J=8.5, H<sub>11</sub>), 8.40 (s, 2H, H<sub>7</sub>). <sup>13</sup>C NMR, (ppm, CDCl<sub>3</sub>, 100MHz): 14.14 (2C, CH<sub>3</sub>), 22.71-31.68 (8C, C<sub>aliph</sub>), 68.33 (2C, O-CH<sub>2</sub>), 113.4 (2C, C<sub>9</sub>), 114.82 (4C, C<sub>2,6</sub>), 121.60 (2C, C<sub>11</sub>), 125.87 (2C, C<sub>4</sub>), 129.43 (2C, C<sub>10</sub>), 129.49 (2C, C<sub>12</sub>), 130.75 (4C, C<sub>3,5</sub>), 149.51 (2C, C<sub>8</sub>), 159.74 (2C, C<sub>1</sub>), 162.03 (2C, C<sub>7</sub>).

#### **Synthesis of *N,N*-bis(4-(octyloxy)benzylidene)naphthalene-1,5-diimine (c3)**

Yellow crystal, yield 80.6%, Mp: 108-109°C, IR, : 3074-3041 cm<sup>-1</sup> (C-H<sub>ar</sub>), 2940-2852 cm<sup>-1</sup> (C-H<sub>aliph</sub>), 1614 cm<sup>-1</sup> (C=N) and 1235 cm<sup>-1</sup> (O-CH<sub>2</sub>), <sup>1</sup>H NMR, (ppm, CDCl<sub>3</sub>, 400 MHz): 0.84 (t, 6H, CH<sub>3</sub>), 1.23-1.79 (m, 24H, CH<sub>2</sub>), 3.97 (t, 4H, J=6.6x(2), O-CH<sub>2</sub>), 6.94 (d, 4H, J=8.8, H<sub>2,6</sub>), 6.99 (d, 2H, J=7.3, H<sub>9</sub>), 7.39 (t, 2H, J=7.8x(2), H<sub>10</sub>), 7.88 (d, 4H, J=8.8, H<sub>3,5</sub>), 8.14 (d, 2H, J=8.5, H<sub>11</sub>), 8.41 (s, 2H, H<sub>7</sub>). <sup>13</sup>C NMR, (ppm, CDCl<sub>3</sub>, 100 MHz): 14.21 (2C, CH<sub>3</sub>), 22.77-31.82 (12C, C<sub>aliph</sub>), 68.34 (2C, O-CH<sub>2</sub>), 113.41 (2C, C<sub>9</sub>), 114.82 (4C, C<sub>2,6</sub>), 121.60 (2C, C<sub>11</sub>), 125.87 (2C, C<sub>4</sub>), 129.43 (2C, C<sub>10</sub>), 129.50 (2C, C<sub>12</sub>), 130.75 (4C, C<sub>3,5</sub>), 149.51 (2C, C<sub>8</sub>), 159.75 (2C, C<sub>1</sub>), 162.03 (2C, C<sub>7</sub>).

#### ***N,N*-bis(4-(decyloxy)benzylidene)naphthalene-1,5-diimine (c4)**

Yellow crystal, yield 87.66%, Mp: 98- 99°C, IR, : 3076-3028 cm<sup>-1</sup> (C-H<sub>ar</sub>), 2936-2843 cm<sup>-1</sup> (C-H<sub>aliph</sub>), 1618 cm<sup>-1</sup> (C=N) and 1252 cm<sup>-1</sup> (O-CH<sub>2</sub>), <sup>1</sup>H NMR, (ppm, CDCl<sub>3</sub>, 400 MHz): 0.88 (t, 6H, CH<sub>3</sub>), 1.28-1.85 (m, 32H, CH<sub>2</sub>), 4.03 (t, 4H, J=6.6x(2), O-CH<sub>2</sub>), 7.01 (d, 4H, J=8.8, H<sub>2,6</sub>), 7.06 (d, 2H, J=7.1, H<sub>9</sub>), 7.46 (t, 2H, J=8.3x(2), H<sub>10</sub>), 7.95 (d, 4H, J=8.8, H<sub>3,5</sub>), 8.21 (d, 2H, J=8.3, H<sub>11</sub>), 8.47 (s, 2H, H<sub>7</sub>). <sup>13</sup>C NMR, (ppm, CDCl<sub>3</sub>, 100 MHz): 14.24 (2C, CH<sub>3</sub>), 22.79-32.01 (16C, C<sub>aliph</sub>), 68.33 (2C, O-CH<sub>2</sub>), 113.42 (2C, C<sub>9</sub>), 114.82 (4C, C<sub>2,6</sub>), 121.61 (2C, C<sub>11</sub>), 125.87 (2C, C<sub>4</sub>), 129.43 (2C, C<sub>10</sub>), 129.51 (2C, C<sub>12</sub>), 130.75 (4C, C<sub>3,5</sub>), 149.51 (2C, C<sub>8</sub>), 159.74 (2C, C<sub>1</sub>), 162.03 (2C, C<sub>7</sub>).

### Synthesis of *N,N*-bis(4-(docecyloxy)benzylidene)naphthalene-1,5-diimine (c5)

Yellow crystal, yield 86.9%, Mp: 108-109°C, IR, : 3077-3025 cm<sup>-1</sup> (C-H<sub>ar</sub>), 2921-2854 cm<sup>-1</sup> (C-H<sub>aliph</sub>), 1622 cm<sup>-1</sup> (C=N) and 1251 cm<sup>-1</sup> (O-CH<sub>2</sub>), <sup>1</sup>H NMR, (ppm, CDCl<sub>3</sub>, 400 MHz): 0.81 (t, 6H, CH<sub>3</sub>), 1.20-1.79 (m, 40H, CH<sub>2</sub>), 3.97 (t, 4H, J=6.5x(2), O-CH<sub>2</sub>), 6.94 (d, 4H, J=8.8, H<sub>2,6</sub>), 7.00 (d, 2H, J= 7.1, H<sub>9</sub>), 7.39 (t, 2H, J=7.9x(2), H<sub>10</sub>), 7.88 (d, 4H, J=8.5, H<sub>3,5</sub>), 8.14 (d, 2H, J=8.3, H<sub>11</sub>), 8.40 (s, 2H, H<sub>7</sub>). <sup>13</sup>C NMR, (ppm, CDCl<sub>3</sub>, 100 MHz): 14.23 (2C, CH<sub>3</sub>), 22.80-32.02 (20C, C<sub>aliph</sub>), 68.35 (2C, O-CH<sub>3</sub>), 113.41 (2C, C<sub>9</sub>), 114.82 (4C, C<sub>2,6</sub>), 121.60 (2C, C<sub>11</sub>), 125.86 (2C, C<sub>4</sub>), 129.43 (2C, C<sub>10</sub>), 129.49 (2C, C<sub>12</sub>), 130.75 (4C, C<sub>3,5</sub>), 149.50 (2C, C<sub>8</sub>), 159.74 (2C, C<sub>1</sub>), 162.03 (2C, C<sub>7</sub>).

### Synthesis of *N,N*-bis(4-(tetradecyloxy)benzylidene)naphthalene-1,5-diimine (c6)

Yellow shine solid, yield 84.5%, Mp: 107-108°C, IR, : 3063-3028 cm<sup>-1</sup> (C-H<sub>ar</sub>), 2905-2835 cm<sup>-1</sup> (C-H<sub>aliph</sub>), 1623 cm<sup>-1</sup> (C=N) and 1248 cm<sup>-1</sup> (O-CH<sub>2</sub>), <sup>1</sup>H NMR, (ppm, CDCl<sub>3</sub>, 400 MHz): 0.81 (t, 6H, CH<sub>3</sub>), 1.20-1.77 (m, 48H, CH<sub>2</sub>), 3.97 (t, 4H, J=6.6x(2), O-CH<sub>2</sub>), 6.94 (d, 4H, J=8.5, H<sub>2,6</sub>), 7.00 (d, 2H, J=7.1, H<sub>9</sub>), 7.39 (t, 2H, J=7.9 x(2), H<sub>10</sub>), 7.89 (d, 4H, J=8.5, H<sub>3,5</sub>), 8.14 (d, 2H, J=8.3, H<sub>11</sub>), 8.41 (s, 2H, H<sub>7</sub>). <sup>13</sup>C NMR, (ppm, CDCl<sub>3</sub>, 100 MHz): 14.24 (2C, CH<sub>3</sub>), 22.79-32.02 (24C, C<sub>aliph</sub>), 68.34 (2C, O-CH<sub>2</sub>), 113.41 (2C, C<sub>9</sub>), 114.82 (4C, C<sub>2,6</sub>), 121.59 (2C, C<sub>11</sub>), 126.86 (2C, C<sub>4</sub>), 129.42 (2C, C<sub>10</sub>), 129.49 (2C, C<sub>12</sub>), 130.75 (4C, C<sub>3,5</sub>), 149.51 (2C, C<sub>8</sub>), 159.75 (2C, C<sub>1</sub>), 162.03 (2C, C<sub>7</sub>).

### Synthesis of *N,N*-bis(4-(hexadecyloxy)benzylidene)naphthalene-1,5-diimine (c7)

Yellow solid, yield 84.8%, Mp: 107-108°C, IR, : 3077-3033 cm<sup>-1</sup> (C-H<sub>ar</sub>), 2921-2845 cm<sup>-1</sup> (C-H<sub>aliph</sub>), 1619 cm<sup>-1</sup> (C=N) and 1244 cm<sup>-1</sup> (O-CH<sub>2</sub>), <sup>1</sup>H NMR, (ppm, CDCl<sub>3</sub>, 400 MHz): 0.82 (t, 6H, CH<sub>3</sub>), 1.21-1.79 (m, 56H,CH<sub>2</sub>), 3.97 (t, 4H, J=6.6x(2), O-CH<sub>2</sub>), 6.94 (d, 4H, J=8.8, H<sub>2,6</sub>), 7.01 (d, 2H, J=7.1, H<sub>9</sub>), 7.39 (t, 2H, J=7.8x(2), H<sub>10</sub>), 7.89 (d, 4H,

J=8.6, H<sub>3,5</sub>), 8.14 (d, 2H, J=8.4, H<sub>11</sub>), 8.40 (s, 2H, H<sub>7</sub>). <sup>13</sup>C NMR, (ppm, CDCl<sub>3</sub>, 100 MHz): 14.22 (2C, CH<sub>3</sub>), 22.79-32.02 (28C, C<sub>aliph</sub>), 68.33 (2C, O-CH<sub>2</sub>), 113.41 (2C, C<sub>9</sub>), 114.82 (4C, C<sub>2,6</sub>), 121.60 (2C, C<sub>11</sub>), 125.86 (2C, C<sub>4</sub>), 129.42 (2C, C<sub>10</sub>), 129.48 (2C, C<sub>12</sub>), 130.75 (4C, C<sub>3,5</sub>), 149.50 (2C, C<sub>8</sub>), 159.75 (2C, C<sub>1</sub>), 162.02 (2C, C<sub>7</sub>).

### Synthesis of *N,N*-bis(4-(octadecyloxy)benzylidene)naphthalene-1,5-diimine (**c8**)

Yellow solid, yield 85.4%, Mp: 106-107°C, IR, : 3081-3023 cm<sup>-1</sup> (C-H<sub>ar</sub>), 2922-2849 cm<sup>-1</sup> (C-H<sub>aliph</sub>), 1621 cm<sup>-1</sup> (C=N) and 1256 cm<sup>-1</sup> (O-CH<sub>2</sub>), <sup>1</sup>H NMR, (ppm, CDCl<sub>3</sub>, 400 MHz): 0.82 (t, 6H, CH<sub>3</sub>), 1.22-1.81 (m, 64H, CH<sub>2</sub>), 3.97 (t, 4H, J=6.7x(2), O-CH<sub>2</sub>), 6.95 (d, 4H, J=8.7, H<sub>2,6</sub>), 7.00 (d, 2H, J=7.3, H<sub>9</sub>), 7.39 (t, 2H, J=7.9x(2), H<sub>10</sub>), 7.89 (d, 4H, J=8.5, H<sub>3,5</sub>), 8.15 (d, 2H, J=8.4, H<sub>11</sub>), 8.41 (s, 2H, H<sub>9</sub>). <sup>13</sup>C NMR, (ppm, CDCl<sub>3</sub>, 100 MHz): 14.22 (2C, CH<sub>3</sub>), 22.79-32.02 (32C, C<sub>aliph</sub>), 68.33 (2C, O-CH<sub>2</sub>), 113.41 (2C, C<sub>9</sub>), 114.82 (4C, C<sub>2,6</sub>), 121.59 (2C, C<sub>11</sub>), 125.86 (2C, C<sub>4</sub>), 129.43 (2C, C<sub>10</sub>), 129.48 (2C, C<sub>12</sub>), 130.74 (4C, C<sub>3,5</sub>), 149.51 (2C, C<sub>8</sub>), 159.75 (2C, C<sub>1</sub>), 162.02 (2C, C<sub>7</sub>).

### 5.6.3 Synthesis of the symmetrical dimers containing 4,4'-(naphthalene-1,5-diylbis(azan-1-yl-1-ylidene))bis(methan-1-yl-1-ylidene)bis(2-methoxyphenol) (**b5**)

Same procedure was used to prepare another symmetrical series of dimers (**d1-d8**) containing (**b5**) compound.

#### Synthesis of *N,N*-bis(4-butoxy-3-methoxybenzylidene)naphthalene-1,5-diimine (**d1**)

Yellow solid compound, yield 79.6%, Mp: 152-153°C, IR, : 3066-3023 cm<sup>-1</sup> (C-H<sub>ar</sub>), 2936-2884 cm<sup>-1</sup> (C-H<sub>aliph</sub>), 1622 cm<sup>-1</sup> (C=N), 1277 cm<sup>-1</sup> (O-CH<sub>3</sub>) and 1262 cm<sup>-1</sup> (O-CH<sub>2</sub>), <sup>1</sup>H NMR, (ppm, CDCl<sub>3</sub>, 400 MHz): 0.83 (t, 6H, CH<sub>3</sub>), 1.46-1.86 (m, 8H, CH<sub>2</sub>), 3.94 (s, 6H, OCH<sub>3</sub>), 4.03 (t, 4H, J=6.8x(2), O-CH<sub>2</sub>), 6.88 (d, 2H, J=8.1, H<sub>6</sub>), 7.00 (d, 2H, J=7.3, H<sub>5</sub>), 7.3 (d, 2H, J=8.3, H<sub>9</sub>), 7.40 (t, 2H, J=7.9x(2), H<sub>10</sub>), 7.68 (s, 2H, H<sub>3</sub>), 8.14 (d, 2H, J=8.3, H<sub>11</sub>), 8.38 (s, 2H, H<sub>7</sub>). <sup>13</sup>C NMR, (ppm, CDCl<sub>3</sub>, 100 MHz): 14.21

(2C, CH<sub>3</sub>), 22.76-29.38 (4C, C<sub>aliph</sub>), 56.23 (2C, OCH<sub>3</sub>), 69.18 (2C, OCH<sub>2</sub>), 109.62 (2C, C<sub>3</sub>), 111.87 (2C, C<sub>9</sub>), 113.56 (2C, C<sub>6</sub>), 121.35(2C, C<sub>5</sub>), 124.49 (2C, C<sub>11</sub>), 125.89 (2C, C<sub>10</sub>), 129.44 (2C, C<sub>12</sub>), 129.28 (2C, C<sub>4</sub>), 149 (2C, C<sub>8</sub>), 149.26 (2C, C<sub>2</sub>), 152.03 (2C, C<sub>1</sub>), 160.3 (2C, C<sub>7</sub>).

**Synthesis of *N,N*-bis(4-(hexyloxy)-3-methoxybenzylidene)naphthalene-1,5-diimine (d2)**

Yellow solid compound, yield 82.1%, Mp: 142-143°C, IR, : 3061-3026 cm<sup>-1</sup> (C-H<sub>ar</sub>), 2942-2868 cm<sup>-1</sup> (C-H<sub>aliph</sub>), 1621 cm<sup>-1</sup> (C=N), 1273 cm<sup>-1</sup> (O-CH<sub>3</sub>) and 1267 cm<sup>-1</sup> (O-CH<sub>2</sub>), <sup>1</sup>H NMR, (ppm, CDCl<sub>3</sub>, 400 MHz): 0.8.28 (t, 6H, CH<sub>3</sub>), 1.42-1.89 (m, 12H, CH<sub>2</sub>), 3.96 (s, 6H, OCH<sub>3</sub>), 4.01 (t, 4H, J=6.8x (2), O-CH<sub>2</sub>), 6.89 (d, 2H, J=8.1, H<sub>6</sub>), 6.99 (d, 2H, J=7.3, H<sub>5</sub>), 7.33 (d, 2H, J=8.3, H<sub>9</sub>), 7.41 (t, 2H, J=7.9x(2), H<sub>10</sub>), 7.69 (s, 2H, H<sub>3</sub>), 8.15 (d, 2H, J=8.3, H<sub>11</sub>), 8.40 (s, 2H, H<sub>7</sub>), <sup>13</sup>C NMR, (ppm, CDCl<sub>3</sub>, 100 MHz): 14.19 (2C, CH<sub>3</sub>), 22.66-29.67 (6C, C<sub>aliph</sub>), 56.28 (2C, OCH<sub>3</sub>), 69.26 (2C, OCH<sub>2</sub>), 109.63 (2C, C<sub>3</sub>), 111.89 (2C, C<sub>9</sub>), 113.58 (2C, C<sub>6</sub>), 121.35(2C, C<sub>5</sub>), 124.48 (2C, C<sub>11</sub>), 125.90 (2C, C<sub>10</sub>), 129.44 (2C, C<sub>12</sub>), 129.28 (2C, C<sub>4</sub>), 149 (2C, C<sub>8</sub>)149.27 (2C, C<sub>2</sub>), 152.02 (2C, C<sub>1</sub>), 160.2 (2C, C<sub>7</sub>).

**Synthesis of *N,N*-bis(4-(octyloxy)-3-methoxybenzylidene)naphthalene-1,5-diimine (d3)**

Yellow solid compound, yield 82.9%, Mp: 128-129°C, IR, : 3059-3011 cm<sup>-1</sup> (C-H<sub>ar</sub>), 2946-2894 cm<sup>-1</sup> (C-H<sub>aliph</sub>), 1622 cm<sup>-1</sup> (C=N), 1272 cm<sup>-1</sup> (O-CH<sub>3</sub>) and 1259 cm<sup>-1</sup> (O-CH<sub>2</sub>), <sup>1</sup>H NMR, (ppm, CDCl<sub>3</sub>, 400 MHz): 0.83 (t, 6H, CH<sub>3</sub>), 1.46-1.91 (m, 16H , CH<sub>2</sub>), 3.95 (s, 6H, OCH<sub>3</sub>), 4.04 (t, 4H, J=6.8x (2), O-CH<sub>2</sub>), 6.88 (d, 2H, J=8.1, H<sub>6</sub>), 7.00 (d, 2H, J=7.3, H<sub>5</sub>), 7.4 (d, 2H, J=8.3, H<sub>9</sub>), 7.41 (t, 2H, J=7.9x(2), H<sub>10</sub>), 7.69 (s, 2H, H<sub>3</sub>) 8.14 (d, 2H, J=8.3, H<sub>11</sub>), 8.38 (s, 2H, H<sub>7</sub>). <sup>13</sup>C NMR, (ppm, CDCl<sub>3</sub>, 100 MHz): 14.21 (2C, CH<sub>3</sub>), 22.79-31.91 (8C, C<sub>aliph</sub>), 56.23 (2C, OCH<sub>3</sub>), 69.18 (2C, OCH<sub>2</sub>), 109.68 (2C,

C<sub>3</sub>), 111.87 (2C, C<sub>9</sub>), 113.56 (2C, C<sub>6</sub>), 121.35(2C, C<sub>5</sub>), 124.49 (2C, C<sub>11</sub>), 125.89 (2C, C<sub>10</sub>), 129.40 (2C, C<sub>12</sub>), 129.66 (2C, C<sub>4</sub>), 149.49 (2C, C<sub>8</sub>), 149.90 (2C, C<sub>2</sub>), 151.68 (2C, C<sub>1</sub>), 160.06 (2C, C<sub>7</sub>).

**Synthesis of *N,N*-bis(4-(decyloxy)-3-methoxybenzylidene)naphthalene-1,5-diimine (d4)**

Yellow solid compound, yield 86.1%, Mp: 122-123°C, IR, : 3067-3015 cm<sup>-1</sup> (C-H<sub>ar</sub>), 2948-2874 cm<sup>-1</sup> (C-H<sub>aliph</sub>), 1621 cm<sup>-1</sup> (C=N), 1274 cm<sup>-1</sup> (O-CH<sub>3</sub>) and 1262 cm<sup>-1</sup> (O-CH<sub>2</sub>). <sup>1</sup>H NMR, (ppm, CDCl<sub>3</sub>, 400 MHz): 0.84 (t, 6H, CH<sub>3</sub>), 1.36-1.81 (m, 20H, CH<sub>2</sub>), 3.96 (s, 6H, OCH<sub>3</sub>), 4.07 (t, 4H, J=6.8x (2), O-CH<sub>2</sub>), 6.94 (d, 2H, J=8.1, H<sub>6</sub>), 7.04 (d, 2H, J=7.3, H<sub>5</sub>), 7.34 (d, 2H, J=8.3, H<sub>9</sub>), 7.43 (t, 2H, J=7.9x(2), H<sub>10</sub>), 7.70 (s, 2H, H<sub>3</sub>), 8.16 (d, 2H, J=8.3, H<sub>11</sub>), 8.40 (s, 2H, H<sub>7</sub>). <sup>13</sup>C NMR, (ppm, CDCl<sub>3</sub>, 100 MHz): 14.22 (2C, CH<sub>3</sub>), 22.78-36.57 (10C, C<sub>aliph</sub>), 56.22 (2C, OCH<sub>3</sub>), 69.16 (2C, OCH<sub>2</sub>), 109.59 (2C, C<sub>3</sub>), 111.85 (2C, C<sub>9</sub>), 113.57 (2C, C<sub>6</sub>), 121.58 (2C, C<sub>5</sub>), 124.51 (2C, C<sub>11</sub>), 125.90 (2C, C<sub>10</sub>), 129.40 (2C, C<sub>12</sub>), 129.65 (2C, C<sub>4</sub>), 149.49 (2C, C<sub>8</sub>), 149.89 (2C, C<sub>2</sub>), 151.86 (2C, C<sub>1</sub>), 160.07 (2C, C<sub>7</sub>).

**Synthesis of *N,N*-bis(4-(dodecyloxy)-3-methoxybenzylidene)naphthalene-1,5-diimine (d5)**

Yellow solid compound, yield 81.2%, Mp: 118-119°C, IR, : 3071-3024 cm<sup>-1</sup> (C-H<sub>ar</sub>), 2958-2879 cm<sup>-1</sup> (C-H<sub>aliph</sub>), 1620 cm<sup>-1</sup> (C=N), 1271 cm<sup>-1</sup> (O-CH<sub>3</sub>) and 1260 cm<sup>-1</sup> (O-CH<sub>2</sub>), <sup>1</sup>H NMR, (ppm, CDCl<sub>3</sub>, 400 MHz): 0.85 (t, 6H, CH<sub>3</sub>), 1.34-1.88 (m, 24H, CH<sub>2</sub>), 3.94 (s, 6H, OCH<sub>3</sub>), 4.05 (t, 4H, J=6.8x (2), O-CH<sub>2</sub>), 6.89 (d, 2H, J=7.9, H<sub>6</sub>), 7.03 (d, 2H, J=7.3, H<sub>5</sub>), 7.33 (d, 2H, J=8.3, H<sub>9</sub>), 7.42 (t, 2H, J=8.3x(2), H<sub>10</sub>), 7.69 (s, 2H, H<sub>3</sub>), 8.14 (d, 2H, J=8.3, H<sub>11</sub>), 8.39 (s, 2H, H<sub>7</sub>). <sup>13</sup>C NMR, (ppm, CDCl<sub>3</sub>, 100 MHz): 14.21 (2C, CH<sub>3</sub>), 22.78-32.89 (12C, C<sub>aliph</sub>), 56.22 (2C, OCH<sub>3</sub>), 69.17 (2C, OCH<sub>2</sub>), 109.62 (2C, C<sub>3</sub>), 111.86 (2C, C<sub>9</sub>), 113.57 (2C, C<sub>6</sub>), 121.58 (2C, C<sub>5</sub>), 124.50 (2C, C<sub>11</sub>), 125.90 (2C,

C<sub>10</sub>), 129.40 (2C, C<sub>12</sub>), 129.65 (2C, C<sub>4</sub>), 149.49 (2C, C<sub>8</sub>), 149.90 (2C, C<sub>2</sub>), 151.86 (2C, C<sub>1</sub>), 160.08 (2C, C<sub>7</sub>).

**Synthesis of *N,N*-bis(4-(tetradecyloxy)-3-methoxybenzylidene)naphthalene-1,5-diimine (d6)**

Yellow solid compound, yield 84.01%, Mp: 117-118°C, IR, : 3075-3028 cm<sup>-1</sup> (C-H<sub>ar</sub>), 2960-2877 cm<sup>-1</sup> (C-H<sub>aliph</sub>), 1619 cm<sup>-1</sup> (C=N), 1269 cm<sup>-1</sup> (O-CH<sub>3</sub>) and 1258 cm<sup>-1</sup> (O-CH<sub>2</sub>), <sup>1</sup>H NMR, (ppm, CDCl<sub>3</sub>, 400 MHz): 0.86 (t, 6H, CH<sub>3</sub>), 1.39-1.95 (m, 28H, CH<sub>2</sub>), 3.95 (s, 6H, OCH<sub>3</sub>), 4.13 (t, 4H, J=6.8x (2), O-CH<sub>2</sub>), 6.88 (d, 2H, J=8.3, H<sub>6</sub>), 7.03 (d, 2H, J=7.3, H<sub>5</sub>), 7.32 (d, 2H, J=8.3, H<sub>9</sub>), 7.42 (t, 2H, J=7.9x(2), H<sub>10</sub>), 7.68 (s, 2H, H<sub>3</sub>) 8.14 (d, 2H, J=7.9, H<sub>11</sub>), 8.38 (s, 2H, H<sub>7</sub>). <sup>13</sup>C NMR, (ppm, CDCl<sub>3</sub>, 100 MHz): 14.22 (2C, CH<sub>3</sub>), 22.76-29.68 (14C, C<sub>aliph</sub>), 56.25 (2C, OCH<sub>3</sub>), 69.21 (2C, OCH<sub>2</sub>), 109.63 (2C, C<sub>3</sub>), 111.89 (2C, C<sub>9</sub>), 113.59 (2C, C<sub>6</sub>), 121.37(2C, C<sub>5</sub>), 124.54 (2C, C<sub>11</sub>), 125.91 (2C, C<sub>10</sub>), 129.46 (2C, C<sub>12</sub>), 129.28 (2C, C<sub>4</sub>), 149.69 (2C, C<sub>8</sub>), 149.86 (2C, C<sub>2</sub>), 152.33 (2C, C<sub>1</sub>), 160.9 (2C, C<sub>7</sub>).

**Synthesis of *N,N*-bis(4-(hexadecyloxy)-3-methoxybenzylidene)naphthalene-1,5-diimine (d7)**

Yellow solid compound, yield 83.9%, Mp: 117-118°C, IR, : 3078-3028 cm<sup>-1</sup> (C-H<sub>ar</sub>), 2966-2881 cm<sup>-1</sup> (C-H<sub>aliph</sub>), 1622 cm<sup>-1</sup> (C=N), 1268 cm<sup>-1</sup> (O-CH<sub>3</sub>) and 1258 cm<sup>-1</sup> (O-CH<sub>2</sub>). <sup>1</sup>H NMR, (ppm, CDCl<sub>3</sub>, 400 MHz): 0.86 (t, 6H, CH<sub>3</sub>), 1.24-1.90 (m, 32H, CH<sub>2</sub>), 3.99 (s, 6H, OCH<sub>3</sub>), 4.10 (t, 4H, J=6.8x (2), O-CH<sub>2</sub>), 6.94 (d, 2H, J=8.3, H<sub>6</sub>), 7.05 (d, 2H, J=7.3, H<sub>5</sub>), 7.36 (d, 2H, J=7.8, H<sub>9</sub>), 7.47 (t, 2H, J=7.8x(2), H<sub>10</sub>), 7.73 (s, 2H, H<sub>3</sub>) 8.16 (d, 2H, J=8.3, H<sub>11</sub>), 8.44 (s, 2H, H<sub>7</sub>). <sup>13</sup>C NMR, (ppm, CDCl<sub>3</sub>, 100 MHz): 14.20 (2C, CH<sub>3</sub>), 22.78-32.01 (16C, C<sub>aliph</sub>), 56.23 (2C, OCH<sub>3</sub>), 69.19 (2C, OCH<sub>2</sub>), 109.68 (2C, C<sub>3</sub>), 111.90 (2C, C<sub>9</sub>), 113.54 (2C, C<sub>6</sub>), 121.58(2C, C<sub>5</sub>), 124.47 (2C, C<sub>11</sub>), 125.89 (2C,

C<sub>10</sub>), 129.42 (2C, C<sub>12</sub>), 129.70 (2C, C<sub>4</sub>), 149.51 (2C, C<sub>8</sub>), 149.94 (2C, C<sub>2</sub>), 151.88 (2C, C<sub>1</sub>), 160.04 (2C, C<sub>7</sub>).

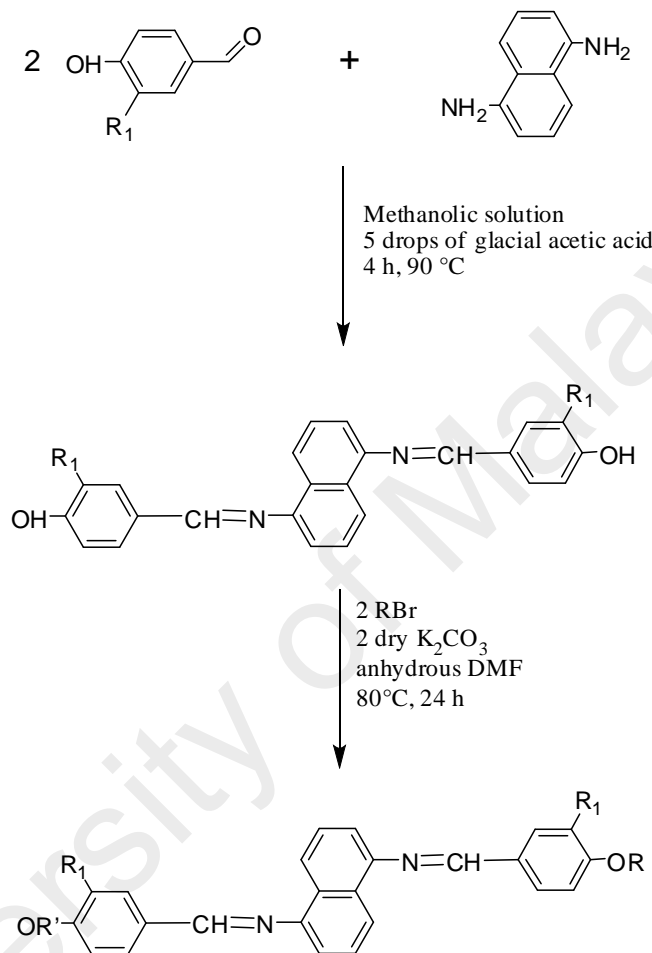
### Synthesis of *N,N*-bis(4-(octadecyloxy)-3-methoxybenzylidene)naphthalene-1,5-diimine (**d8**)

Yellow solid compound, yield 82.8%, Mp: 112-113°C, IR, : 3077-3029 cm<sup>-1</sup> (C-H<sub>ar</sub>), 2966-2879 cm<sup>-1</sup> (C-H<sub>aliph</sub>), 1621 cm<sup>-1</sup> (C=N), 1275 cm<sup>-1</sup> (O-CH<sub>3</sub>) and 1259 cm<sup>-1</sup> (O-CH<sub>2</sub>), <sup>1</sup>H NMR, (ppm, CDCl<sub>3</sub>, 400 MHz): 0.87 (t, 6H, CH<sub>3</sub>), 1.39-2.01 (m, 36H, CH<sub>2</sub>), 3.96 (s, 6H, OCH<sub>3</sub>), 4.11 (t, 4H, J=6.9x (2), O-CH<sub>2</sub>), 6.91 (d, 2H, J=8.3, H<sub>6</sub>), 7.06 (d, 2H, J=7.8, H<sub>5</sub>), 7.39 (d, 2H, J=7.8, H<sub>9</sub>), 7.49 (t, 2H, J=7.9x(2), H<sub>10</sub>), 7.71 (s, 2H, H<sub>3</sub>), 8.18 (d, 2H, J=8.3, H<sub>11</sub>), 8.48 (s, 2H, H<sub>7</sub>). <sup>13</sup>C NMR, (ppm, CDCl<sub>3</sub>, 100 MHz): 14.23 (2C, CH<sub>3</sub>), 22.76-32.96 (18C, C<sub>aliph</sub>), 56.23 (2C, OCH<sub>3</sub>), 69.19 (2C, OCH<sub>2</sub>), 109.86 (2C, C<sub>3</sub>), 111.94 (2C, C<sub>9</sub>), 113.96 (2C, C<sub>6</sub>), 121.05 (2C, C<sub>5</sub>), 124.63 (2C, C<sub>11</sub>), 126.10 (2C, C<sub>10</sub>), 129.89 (2C, C<sub>12</sub>), 129.28 (2C, C<sub>4</sub>), 149.64 (2C, C<sub>8</sub>), 149.89 (2C, C<sub>2</sub>), 151.87 (2C, C<sub>1</sub>), 162.01 (2C, C<sub>7</sub>).

## 5.7 Results and discussion

A new symmetrical dimers *N,N'*-bis(4-alkoxybenzylidene)1,5-naphthalenediimine and *N,N'*-bis(3-methoxy-4-alkoxybenzylidene)1,5-naphthalenediimine with high yield were synthesized through the condensation reaction of bisphenol bis-Schiff base and 2 moles of bromoalkyl by using DMF as solvent and K<sub>2</sub>CO<sub>3</sub> as catalyst. Figure 5.14 shows the synthetic route of symmetrical dimers. Spectroscopic methods (FT-IR, <sup>1</sup>H NMR, and <sup>13</sup>C NMR) have been employed to elucidate the structures of the target compounds. The series (**c1-c8**) will be discussed in this research which is almost similar to the series of (**d1-d8**). In the terms of solubility, the new series of symmetrical dimers have good solubility with the most solvents such as CHCl<sub>3</sub>, acetone and DMF, whereas the naphthalene monomers dissolve in DMSO only. Some physical properties were

studied to investigate the thermal degradation and optical properties of series (c) as well the mesophase properties and the influence of the structure were investigated for both series.



Series (c)  $R_1=H$ ,  $R=R'=C_4H_9$  (c1),  $C_6H_{13}$  (c2),  $C_8H_{17}$  (c3),  $C_{10}H_{21}$  (c4),  $C_{12}H_{25}$  (c5),  $C_{14}H_{29}$  (c6),  $C_{16}H_{33}$  (c7),  $C_{18}H_{37}$  (c8).

Series (d)  $R_1=OCH_3$ ,  $R=R'=C_4H_9$  (d1),  $C_6H_{13}$  (d2),  $C_8H_{17}$  (d3),  $C_{10}H_{21}$  (d4),  $C_{12}H_{25}$  (d5),  $C_{14}H_{29}$  (d6),  $C_{16}H_{33}$  (d7),  $C_{18}H_{37}$  (d8).

Figure 5.15 : Synthetic route of symmetrical dimers

## 5.7.1 Characterization of the symmetrical dimers

### 5.7.1.1 FTIR

FTIR data showed that the diagnostic bands, which can be assigned to the stretching of aliphatic groups, were present within the frequencies of 2835-2940  $\text{cm}^{-1}$  with relative intensities ranging from weakest absorption for **c1** to the strongest for **c8**. This characteristic is in accordance with the length of symmetrical terminal alkyl groups attached to the central core in which **c1** is the shortest member having only terminal butyl groups. The presence of the aromatic rings was inferred within the frequencies of 3081-3023  $\text{cm}^{-1}$ . The band appearing within the frequencies of 1614-1623  $\text{cm}^{-1}$  can be attributed to the stretching of azomethine moiety (CH=N). The strong absorption band observed in the fingerprint region of 1235-1261  $\text{cm}^{-1}$  is indicative of the C-O stretching of the aromatic ether (Ar-O-R). The representative IR spectra of compound **c2**, **c4** and **c6** are shown in Figure 5.16.

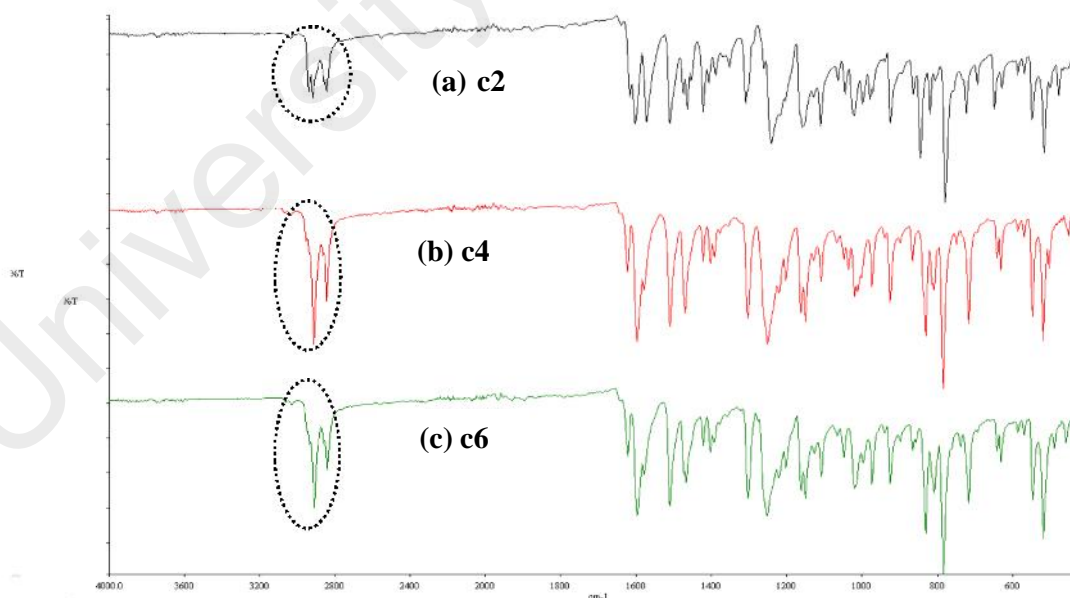


Figure 5.16: FT-IR spectra of the symmetrical dimers (a) **c2**, (b) **c4** and (c) **c6**

### 5.7.1.2 <sup>1</sup>H NMR

The molecular structure for all the compounds were further confirmed by high resolution <sup>1</sup>H and <sup>13</sup>C spectroscopies.

From Table 5.1 the triplet peak that appeared at the region of  $\delta = 0.81-0.88$  ppm was assigned to the six proton of methyl (-CH<sub>3</sub>) of the alkyl chain. The multiplet peak owing to the presence of methylene protons was observed within the range of  $\delta = 1.20-1.85$  ppm. For the longer homologous series (**c1-c8**), the presence of indistinguishable overlapping multiplet was observed for methylene protons. The triplet peak that appeared at region of 3.97-4.03 ppm was assigned to the methylene protons of ether (Ar-O-CH<sub>2</sub>-). The peak that appeared as doublet at the region of 6.94-7.01 ppm is attributed to the four aromatic protons of position 2<sup>th</sup> and 6<sup>th</sup> on the phenyl ring. The doublet peak appeared at the region of 6.99-7.01 ppm was assigned to two protons of naphthalene group for the position number 9<sup>th</sup>. The intense triplet peak at the region of 7.39-7.46 ppm is due to the two protons of the naphthalene moiety for the position 10<sup>th</sup>. The peaks appeared at the region of 7.88-7.95 ppm are associated to the four protons for the position 3<sup>th</sup> and 5<sup>th</sup> in phenyl ring. The peaks that appeared as doublet at the region of 8.14-8.21 ppm is attributed to the two aromatic protons of position 11<sup>th</sup> of the naphthalene group. A sharp singlet peak was observed at low field within the region of 8.40-8.47 ppm, which can be ascribed to the two protons of azomethine linking group, in which the deshielding effect is caused by the inductive effect of N atom which reduces the electron density on the adjacent C atom.

The new peak observed at the region of 0.81-1.85 ppm is due to the flexible chain of alkyl groups that are attached to the phenyl groups. The other new peak that appeared at the region of 3.97-4.03 ppm represents the ether group (Ar-O-CH<sub>2</sub>) which is the best indication for the confirmation of the target compounds. Figure 5.17 displays

$^1\text{H}$  NMR spectra of **b8** and Figure 5.18 shows  $^1\text{H}$  NMR spectra of the symmetrical dimers of **c2**.

Table 5.1 :  $^1\text{H}$  NMR chemical shifts of dimers (c1-c8)

Type of proton	Chemical shift (ppm)
$\text{CH}_3$	0.81-0.88 (t)
$-\text{CH}_2-$	1.20-1.85 (m)
$\text{OCH}_2$	3.79-4.03 (t)
Ar-H ( $2^{\text{th}}, 6^{\text{th}}$ position)	6.94-7.01 (d)
naph-H ( $9^{\text{th}}$ position)	6.99-7.06 (d)
naph-H ( $10^{\text{th}}$ position)	7.39-7.46 (t)
Ar-H ( $3^{\text{th}}, 5^{\text{th}}$ position)	7.88-7.95 (d)
naph-H ( $11^{\text{th}}$ position)	8.14-8.21 (d)
C=N ( $7^{\text{th}}$ position)	8.40-8.47 (s)

Note: s=singlet, d=doublet, t=triplet, m=multiplet.

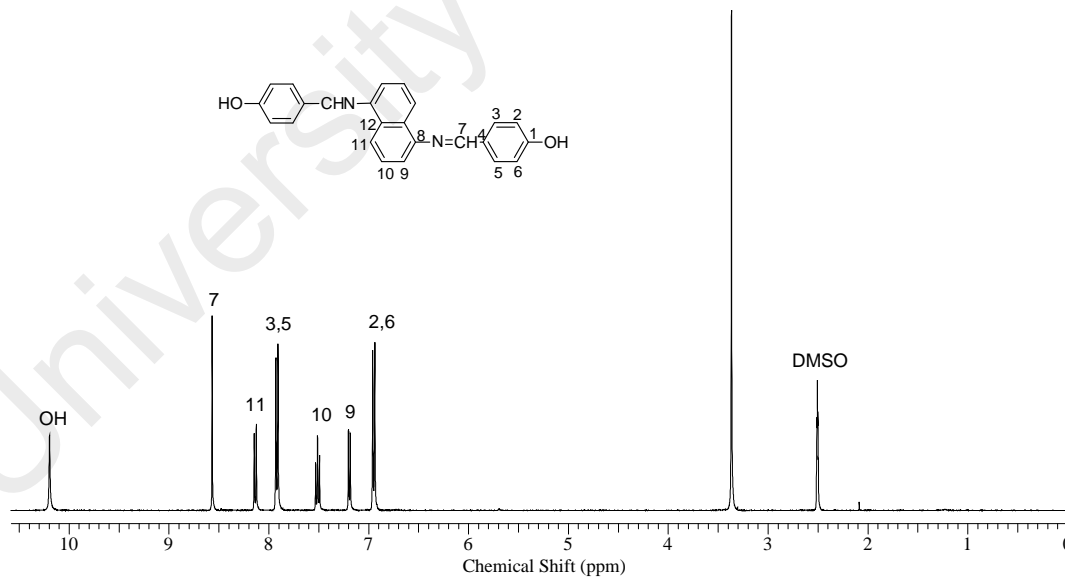


Figure 5.17 :  $^1\text{H}$  NMR spectrum of monomer containing naphthalene **b8**

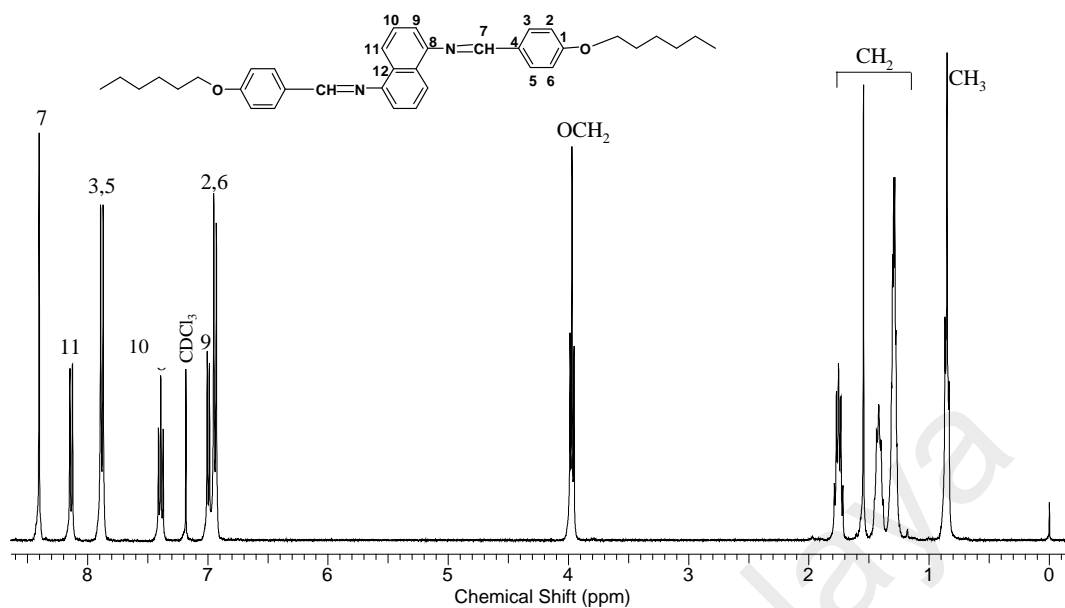


Figure 5.18 :  $^1\text{H}$  NMR spectrum of dimer containing naphthalene **c2**

#### 5.7.1.3. $^{13}\text{C}$ NMR

The molecular structures of compounds **c1-c8** were further substantiated by  $^{13}\text{C}$  NMR spectroscopy. Table 5.2 shows the spectrum data of  $^{13}\text{C}$  NMR for series **c1-c8**. The peak attributable to the methyl carbon ( $\text{CH}_3$ ) was observed at the region of 14.14-14.24 ppm. The following peaks at the region of 22.71-32.08 ppm were assigned to the methylene carbons of the symmetrical aliphatic groups, where the number of peaks and the intensities increase with increasing methylene groups. The carbon of ether group that is attached to the phenyl group ( $\text{Ar-O-CH}_2$ ) appeared in the region of 68.21-68.35 ppm. The phenyl and naphthalene carbons gave rise to different peak in the region of 113.40-159.67 ppm. The appearance of peak in the region of 162.02-162.13 ppm was subsequently assigned to the azomethine carbon  $\text{C}_7$ . A representative  $^{13}\text{C}$  NMR spectrum and complete structural assignments of the monomer **b8** and **c2** are shown in Figure 5.19 and 5.20 respectively. All the compounds in series **d1-d8** showed  $^1\text{H}$  NMR and  $^{13}\text{C}$  NMR of similar characteristic peaks as discussed for series **c1-c8**.

Table 5.2 :  $^{13}\text{C}$  NMR chemical shifts of compounds (c1-c8)

Type of carbon	Chemical shift (ppm)
$\text{CH}_3$	14.14-14.24
$-\text{CH}_2-$	22.71-32.08
$\text{OCH}_2$	68.21-68.35
naph-C (9 <sup>th</sup> position)	113.40-113.42
Ar-C (2 <sup>th</sup> ,6 <sup>th</sup> position)	114.82-114.88
naph-C (11 <sup>th</sup> position)	121.59-121.78
Ar-C (4 <sup>th</sup> position)	125.77-125.87
naph-C (10 <sup>th</sup> position)	129.42-129.44
naph-C (12 <sup>th</sup> position)	129.48-129.50
Ar-C (3 <sup>th</sup> ,5 <sup>th</sup> position)	130.74-131.12
Ar-C (1 <sup>th</sup> position)	149.50-149.53
naph-C (8 <sup>th</sup> position)	159.74-159.76
$\text{C}=\text{N}$ (7 <sup>th</sup> position)	162.02-162.13

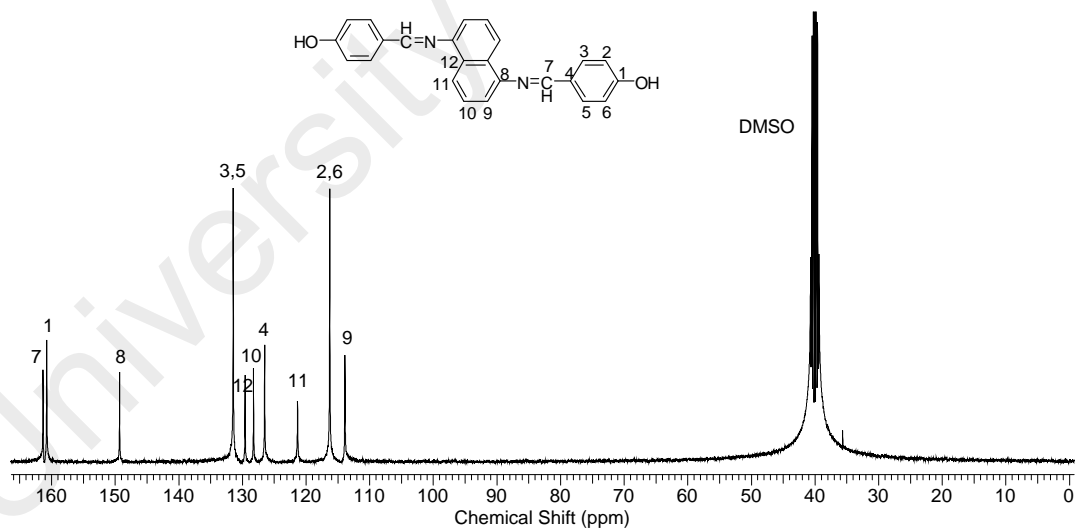


Figure 5.19 :  $^{13}\text{C}$  NMR spectrum of dimer containing naphthalene **b8**

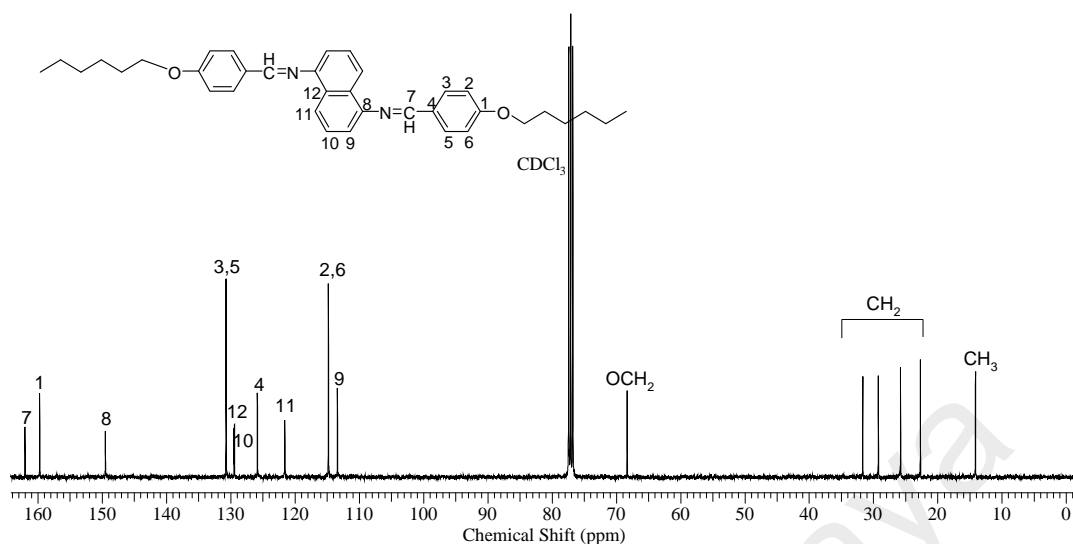


Figure 5.20 :  $^{13}\text{C}$  NMR spectrum of dimer containing naphthalene **c2**

### 5.7.2 Thermal degradation properties

The thermal stabilities of the compounds in series **c** in its various forms were examined through TGA within a temperature range of 50-900°C under nitrogen atmosphere at heating rate of 20°C/min. The detailed thermal data for all compounds are summarized in Table 5.3.

All the compounds displayed excellent decomposition temperatures ( $T_d$ )[228], with decomposition temperatures ( $T_d$ ) of approximately 400°C and the anaerobic char yields at 900°C for all the compounds were in the range 2.4-15.8 wt%. The  $T_d$  values at 10 wt% loss for the compounds occurred at 411-430°C which may attributed to the decomposition of alkyl flexible chains. This process is followed by a rapid weight loss of 80 wt% of the initial weight between 490-565°C due to the decomposition of rigid mesogenic chains containing aryl and naphthalene groups.

The TGA thermograms of **c2**, **c4**, **c6** and **c7** are depicted in Figure 5.21 (a). All the compounds exhibited a one-stage decomposition behaviour at elevated temperatures as shown in Figure 5.21 (b). The high thermal stability obtained could be attributed to

the rigidity and symmetry of the compounds[229]. Generally, compounds containing naphthalene moiety improve the thermal stability due to the rigidity of this group[230].

Table 5.3 : Thermal analysis data of the symmetrical dimers (**c1-c8**).

Sample code	10% weight loss temperature (°C)	80% weight loss temperature (°C)	Char yield (%)
<b>c1</b>	420	549	15.3
<b>c2</b>	417	555	14.9
<b>c3</b>	430	565	15.8
<b>c4</b>	425	558	14.6
<b>c5</b>	422	551	8.1
<b>c6</b>	418	496	2.4
<b>c7</b>	424	490	8.5
<b>c8</b>	427	489	4.9

As a result of the excellent decomposition temperature, these compounds show good thermal stability for industrial processing. Decomposition of the compounds was almost complete at around 900°C with no further weight loss observed after that.

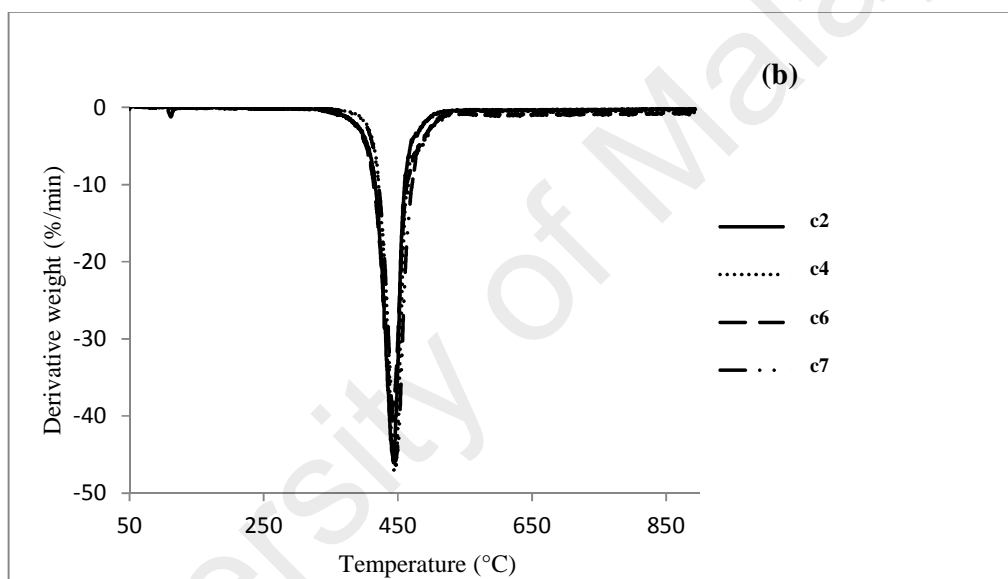
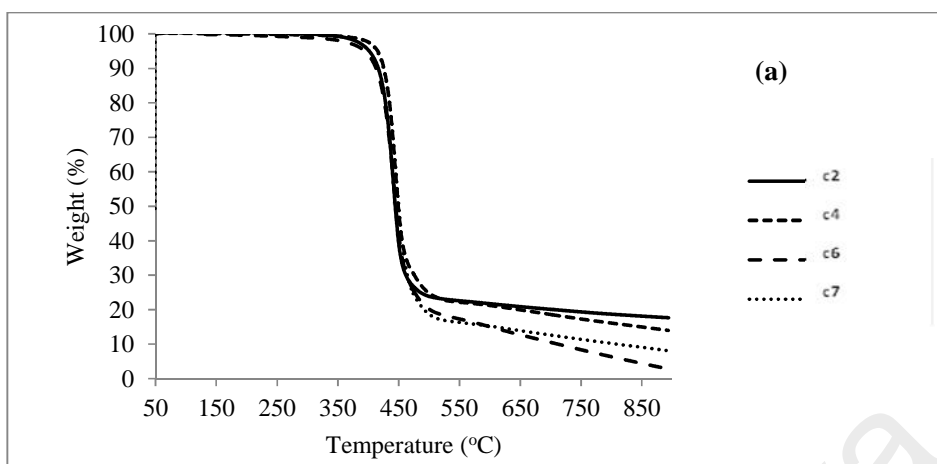


Figure 5.21 : (a) Thermograms of **c2**, **c4**, **c6** and **c7**, (b) DTG of **c2**, **c4**, **c6** and **c7**.

### 5.7.3 Optical properties

Fundamental photophysical properties of the new compounds were investigated by UV-Vis and fluorescence spectroscopies. The results are summarized in a Table 5.4. The dilute solutions of these compounds in THF exhibited strong absorption peaks in the range of 281-283 nm and weak absorption in the range 362-363 nm, assignable to the (n-\*) transition resulting from the conjugation between the aromatic rings and nitrogen atoms and transition from the characteristic ( $\pi$ -\*) transitions of naphthalene

chromophore. Figure 5.22 shows the UV-Vis absorption spectra for compounds **c3**, **c5** and **c7**. Figure 5.23 shows that the compounds exhibited strong fluorescence emission in a red shift region with a fluorescence maximum wavelength at 518-523 nm. Although several different azomethines have been described in the literature, only a few azomethines have been reported to exhibit fluorescence together with the liquid crystalline properties[231, 232].

Table 5.4 : UV-vis absorption and PL emission spectral data of the symmetrical dimer  
(**c1-c8**)

Sample code	Absorption abs (nm)	PL emission max (nm)
<b>c1</b>	283 , 362	516
<b>c2</b>	283 , 362	517
<b>c3</b>	283 , 362	518
<b>c4</b>	281 , 362	517
<b>c5</b>	281 , 363	517
<b>c6</b>	282 , 362	519
<b>c7</b>	283 , 363	518
<b>c8</b>	283 , 363	518

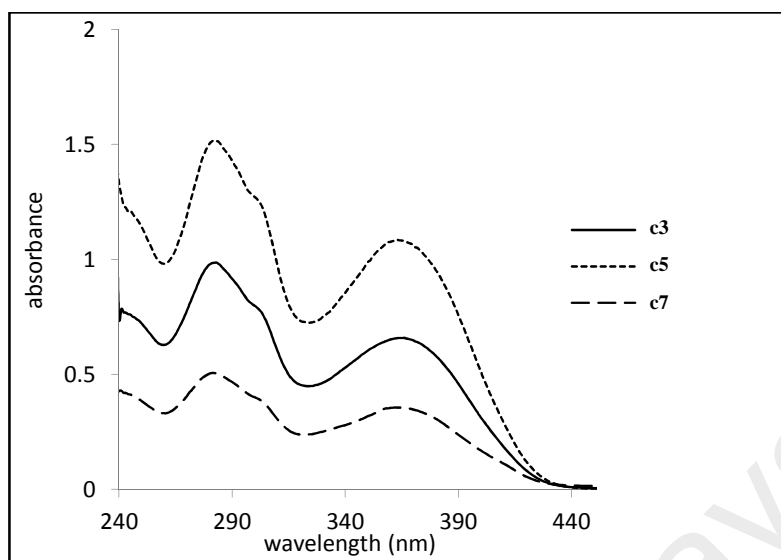


Figure 5.22 : UV-Vis absorption spectra of compounds **c3**, **c5** and **c7**.

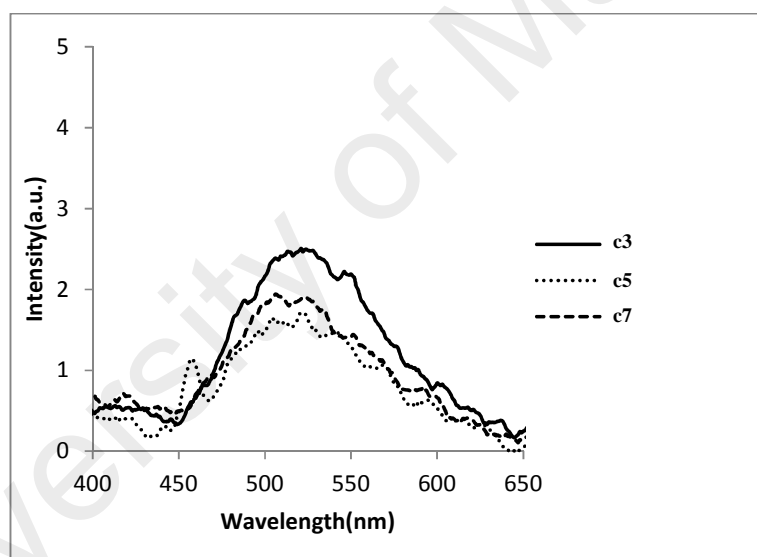


Figure 5.23 : PL spectra of compounds **c3**, **c5**, and **c7** in THF solution

#### 5.7.4 Thermal behavior and textural observation

Two series of symmetrical dimers (**c** and **d**) had been synthesized in order to investigate the liquid crystal properties and study the effect of a methoxy group at the core adjacent to the spacer where the liquid crystal behaviour of these compounds are determined by mesogenic group, the linking unit and the flexibility of the terminal moiety.

The thermal properties including the transition temperature and changes of enthalpy ( $\Delta H$ ) were achieved by Differential Scanning Calorimetry analysis technique for both series. Transition temperatures obtained from the DSC are in agreement with the OPM results. Deviations are within  $\pm 1^\circ\text{C}$ . For the homologous series (**c**), two different liquid crystal phases were observed i.e. the nematic and smectic C with Schliere textures of both phases obtained upon heating and cooling as shown in Figure 5.26. The phase transition temperatures and corresponding enthalpy changes of all compounds are tabulated in Table 5.5.

Table 5.5 : Phase transitions, Temperature and transition enthalpy changes for compounds (**c1–c8**) and (**d6** and **d7**)

Compounds	Transition temperatures, $^\circ\text{C}$ (corresponding enthalpy changes, $\text{kJ mol}^{-1}$ )
<b>c1</b>	Cr 268 (54) I
<b>c2</b>	Cr 134 (36) N 222 I (2)
<b>c3</b>	Cr 111 (58) N 198 I (2)
<b>c4</b>	Cr 102 (58) N 181 I (2)
<b>c5</b>	Cr 105 (70) SmC 119 N (1) 167 I (2)
<b>c6</b>	Cr 107 (97) SmC 133 N (1) 157 I (3)
<b>d6</b>	Cr 112 (101) I
<b>c7</b>	Cr 110 (45) SmC 137 N (2) 158 I (3)
<b>d7</b>	Cr 154 (111) I
<b>c8</b>	Cr 103 (73) I

Note: Cr, crystal; SmC, smectic C; N, nematic; I, isotropic.

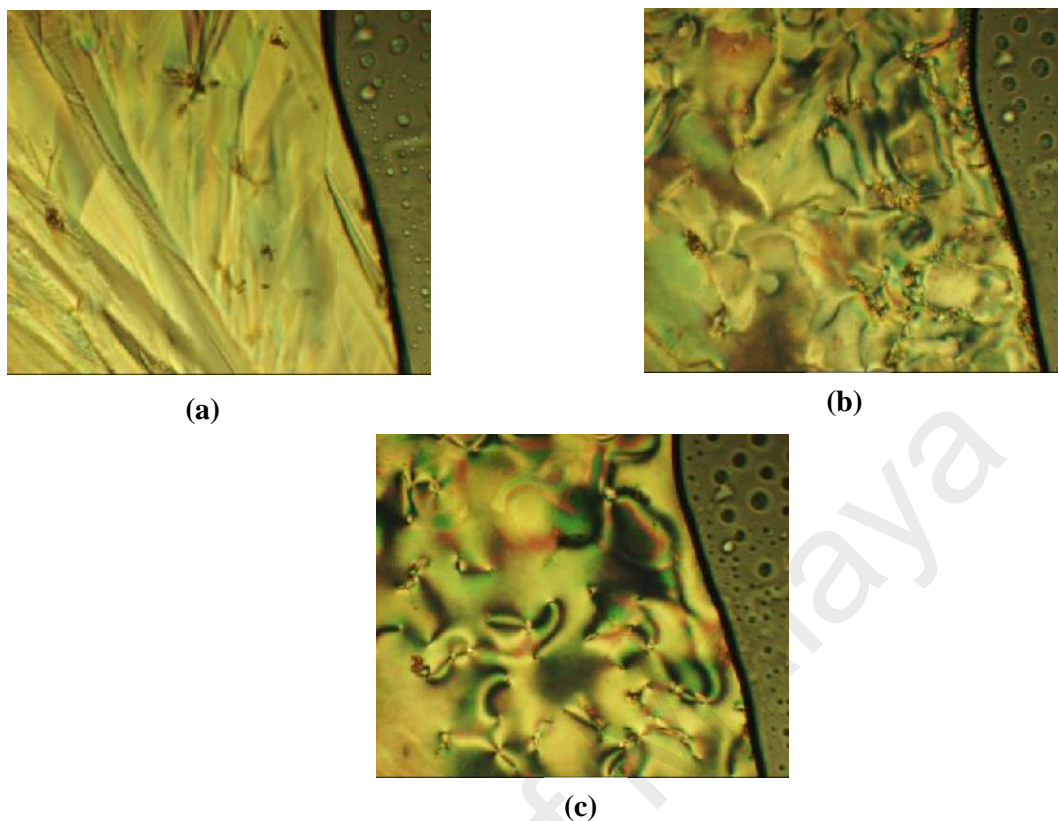


Figure 5.24 : **(a)** The crystal texture on cooling taken at 79°C, **(b)** schlieren texture of smectic C at 128°C while **(c)** is showing schlieren texture for nematic phase on cooling at 158°C for compound **c6**.

During heating and cooling just one transition temperature was observed for compound **c1** which contains only a four carbon chain where this compound does not show liquid crystalline behaviour. The absence of liquid crystalline behaviour may be attributed to the presence of a strong intermolecular attraction among the short-chain molecules leading to restricted thermal motion.

When the alkyl chain length is increased to six carbon atoms as represented in compound **c2**, two transitions phase were observed during the heating process, where at 134°C is the first transition from crystal to liquid crystalline phase and followed by the transition from liquid crystalline phase to isotropic phase at 222°C. Compounds **c3**, **c4** and **c5** showed similar peaks to compound (**c2**) during heating and cooling process (i.e.

two transition phase) with different range of temperatures. Figure 5.25 shows the two transition phase of compound **c4** from DSC thermogram.

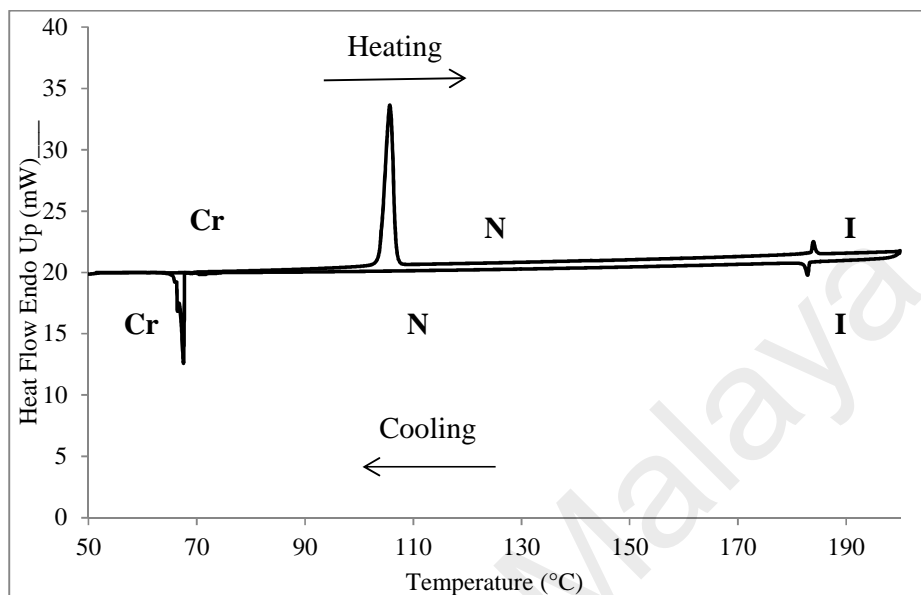


Figure 5.25 : DSC trace of compound **c4**

As for heating cycle of compound **c6**, three peaks are obtained. A sharp peak is observed at 110°C with change of enthalpy ( $45 \text{ kJ mol}^{-1}$ ) indicating that the transition phase is from crystal to nematic phase followed by small peak at 137°C with change of enthalpy ( $1 \text{ kJ mol}^{-1}$ ) indicating the transition phase is from smectic phase to nematic phase and the last peak appeared at 158°C with change of enthalpy ( $3 \text{ kJ mol}^{-1}$ ) indicating the transition is from the nematic phase to isotropic phase. Smectic C is suggested based on the molecular structure that we observed from OPM. Figure 5.26 shows the representative DSC thermogram of compound **c6**.

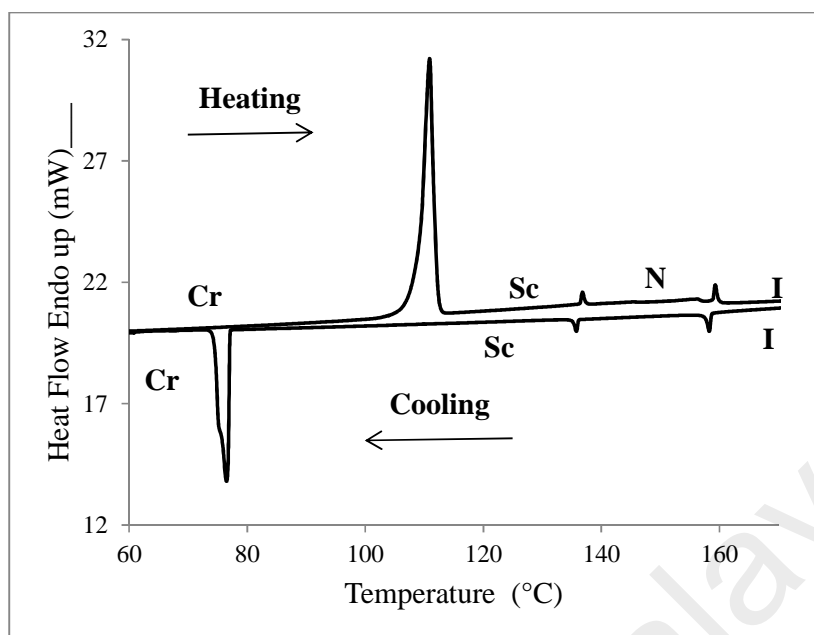


Figure 5.26 : DSC trace of compound **c6**

Figure 5.27 displays the thermotropic behavior as a function of alkyl chain length for series **c**, starting with  $C_4H_9$  and ending with  $C_{18}H_{36}$ . In order to visualize the effect of the methoxy group, two representatives for structure type **d** are also included, i.e. compounds **d6** and **d7**.

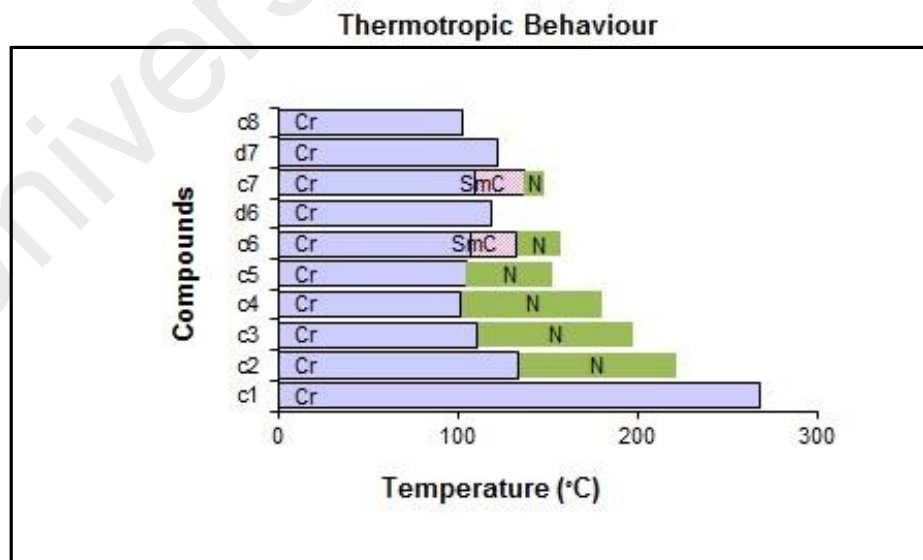


Figure 5.27 : Thermotropic behaviors as a function of alkyl chain length for series (**c**) and (**d**).

As shown in Figure 5.28 series (**d**), on the other hand, did not exhibit any transition phase by DSC. Figure 5.28 displays the DSC trace of compound **d6** where just two peaks are observed in this compound during heating cycle and cooling cycle which indicates that the phase transition is from crystal phase to isotropic phase in heating cycle and vice versa in cooling cycle.

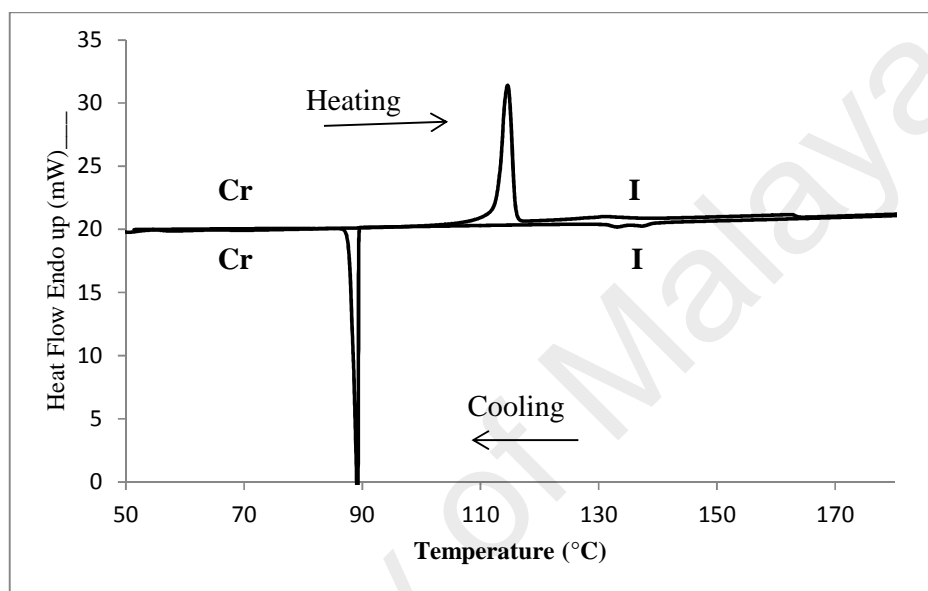


Figure 5.28 : DSC trace of compound **d6**

Based on the results we can conclude that the core of the compounds is very rigid, leading to dense molecular packing, thus resulting in high melting points with large enthalpy changes. Also, increasing chain length for the series **c** reduces the melting temperature but decreases the clearing point.

Compound **c1** having the shortest chain length ( $C_4$ ) does not exhibit liquid crystal property. Earlier works on other symmetrical dimers[197], have shown that in compounds of short-chain molecules, there exist strong intermolecular attractions which lead to restricted thermal motion. This causes the molecules to be highly positioned resulting in absence of liquid crystal property. A chain length of six carbon atoms, however, provides sufficient flexibility of the compound to access the liquid crystalline

state, which was identified as a nematic phase. Starting with a C<sub>12</sub> chain length an additional more ordered, smectic, mesophase emerges, where the smectic tendency increases by increasing the terminal chain due to the long chains becoming intertwined and attracted, which facilitates the lamellar packing required for smectic phase generation and eventually eliminates the nematic phase [204]. The molecular structure of the compounds suggests a tilted smectic C phase rather than the smectic A phase. The OPM texture confirms this expectation. The two liquid crystal phases are obtained from the series (i.e nematic and smectic) may be attributed to the fact that naphthalene moiety displays rich mesomorphism[233]. From a chain length of C<sub>18</sub> the liquid crystal state disappears. The absence of liquid crystalline phase in **c8** may be attributed to the influence of increasing the alkyl length chain which weakened the rigidity of the long molecular axis and for that reason the linearity of the molecule is affected. Consequently, the molecules do not fit readily into the parallel molecular arrangement liquid crystal phase due to the more significant bending conformation which leads to decreasing in the phase stability and lower transition temperatures are observed in compound **c8**[234].

Introducing the methoxy group causes the compounds to lose their liquid crystalline behavior. In addition, they show higher melting points compared to the analog compounds in series **c**. Moreover, the trend for melting temperatures for series **c** is reverted, leading to rising melting temperatures with increasing chain length instead. The methoxy groups, therefore, are considered as effective obstacles for liquid crystal phases. The influence of methoxy moiety on *ortho* position of the aromatic ring causes a disruption in the liquid crystal stability.

During the heating process for the compounds **c1** to **c8**, it is important to observe that the clearing points decrease gradually with increasing the length of alkyl chains.

This observation agrees with previously reported homologous series of *p,p*-biphenylene esters of *p*-alkoxy and *p*-carbalkoxybenzoic acids[235], as well as complies to the homologous series of *N,N*-bis(3-methoxy-4-alkoxybenzylidene)-1,4-phenylene diimine[217] in which the shortest chain homologue of the alkyl chains has the greatest thermal stability. Generally, in this type of the compounds, the stability of the mesophase will be influenced by at least four diversified ways[236]. First, the alkyl chain will behave as a diluent, increasing the mean separation between molecules and so likewise the separation between them which in turn reduces the anisotropy of the intermolecular forces and subsequently results in lower stability of the mesophase. Second, by increasing the length of the molecule will cause an increase in its geometrical anisotropy. Third, by increasing the size of the polar terminal groups can lead to reducing the attractions between the molecules. Fourth, the total polarizability should increase with increasing the size of molecule. The first and third factors explain that increasing the size of the alkyl chain leads to decrease in mesophase stability which causes the liquid transition temperature to decrease with increasing size of the alkyl chain.

## CHAPTER 6 : CONCLUSIONS AND SUGGESTION FOR FUTURE STUDIES

### 6.1 Conclusions

A series of new polycarbosilanes containing bisphenol Schiff base monomers with different substituted groups (electron-donating and/or withdrawing) and different conjugation number was successfully synthesized by polycondensation reaction using bis(chloromethyl) dimethylsilane. The purity and chemical structures of the prepared monomers and copolymers have been identified by FTIR,  $^1\text{H}$  NMR,  $^{13}\text{C}$  NMR, 2D NMR, X-ray crystallography and GPC. All the results were in agreement with the proposed structure. The monomers showed good solubility in DMSO and DMF and the copolymers exhibited excellent solubility in common organic solvents (THF,  $\text{CHCl}_3$  and DMF) but copolymers containing bisphenol azine were insoluble in hydroxyl-group containing solvents ( $\text{CH}_3\text{OH}$  and  $\text{C}_2\text{H}_5\text{OH}$ ) while copolymers containing bisphenol bis-Schiff base were partially soluble. The molecular weights of the copolymers as measured by GPC were higher when synthesized by monomers containing electron-donating group than monomers containing electron-withdrawing groups and monomers without substituted groups were the less due to the long term resonance.

All the copolymers exhibited good thermal stability with one stage decomposition which is really good for practical processing or for possible use in devices. Copolymers containing 1,5-naphthalene in the main chain exhibited higher thermal stability than those containing azine and 1,4-phenylene due to their high aromatic content. Also, the copolymers containing substituted groups in the benzene ring possess higher thermal degradation due to higher bond energy values of this group leading to high stability of the copolymers. The char yields for all the copolymers at  $700^\circ\text{C}$  were between 17.7-52.61%.

The optical properties of the synthesized polycarbosilane were investigated by UV-vis and photoluminescence spectroscopies. All the copolymers containing bisphenol azine exhibited single clear absorption peak in the range of 318-352 nm corresponding to  $\pi-\pi^*$  and  $n-\pi^*$  transitions of the aromatic ring and the azomethine group as well as from the conjugation of the aromatic ring and the nonbonding electrons (O-CH<sub>3</sub>, OH). In **Pa2**, **Pa3** and **Pa4** longer wavelength absorption maximum (344.7-351.3 nm) is observed due to the presence of electron-donating substituents (OCH<sub>3</sub> and OCH<sub>2</sub>CH<sub>3</sub>) which possess higher wavelength, where these groups increase the density of electron at the azomethine group, decrease the  $n-\pi^*$  transition energy and produce bathochromic shifts of the long wavelength absorption maximum. For copolymers containing electron-withdrawing substituent (Pa5 and Pa6), the bands are shifted to lower wavelength (318-321 nm) due to decrease in electron density at the azomethine group, and consequently increases the  $n-\pi^*$  transition energy to produce hypsochromic shifts. Absorption peaks for copolymers containing 1,4-phenylene and 1,5-naphthalene appeared as two peaks in the region of 287-365 nm and three peaks in the region of 273-363 nm respectively. The fluorescence emission maxima of the all copolymers are in the range of 370-620 nm with emission between 415-429 nm which may be categorized as blue emission. The blue emission is due to the conjugation of bisphenol Schiff base compounds, resulting in good  $\pi$ -electrons delocalization along bisphenol Schiff base which is a  $p$ -conjugated system.

From cyclic voltammetric studies the HOMO and LUMO energy levels of copolymers **Pa1-Pa6** were found to be in the range of -5.60 to -5.82 eV and -3.83 to -4.10 eV respectively and the obtained HOMO-LUMO values were influenced by the substituents groups located in the benzene ring. The synthesized copolymers containing electron-withdrawing group have lower HOMO energy values, while copolymers containing electron-donating groups have higher HOMO energy values. On the other

hand, the HOMO and LUMO energy values of the copolymers **Pb1-Pb7** were in the range -5.73 eV to -6.02 eV and -3.38 eV to -3.50 respectively. The variations in electrochemical behaviours of copolymers **Pb1-Pb7** originated from the different molecular structure chain of copolymers where the electrochemical properties of these copolymers may be influenced by the effective conjugation length. The conjugation lengths will increase the oxidation potential of **Pb1-Pb7** and the HOMO energy levels will be shifted to a lower energy level. The HOMO-LUMO energy levels of polymers confirmed that the newly synthesized polycarbosilane are conjugated p-type polymers and they could be potential candidate as hole-transporting materials in organic light emitting diodes (OLED) and heterojunction solar cell.

Two new series of homologous symmetrical dimers N,N-bis(4-alkoxy- benzylidene)-1,5-naphthalenediimine grouped as series **c** and N,N-bis(3-methoxy-4-alkoxy-benzylidene)-1,5-naphthalenediimine grouped as series **d** with different lengths of terminal alkyl groups of even parity ranging from butyl to octadecyl were synthesized and characterized. The mesomorphic properties of these compounds were investigated via differential scanning calorimetry and optical polarizing microscopy. A diversified phase-transition behaviour was observed for the members of series **c** which could be attributed to the possible molecular conformations. Compounds with chain length in a range of C<sub>6</sub>H<sub>13</sub> to C<sub>12</sub>H<sub>33</sub> showed smectic C phase while C<sub>14</sub>H<sub>29</sub> and C<sub>16</sub>H<sub>33</sub> displayed smectic and nematic phase. The dimers containing butyl and octadecyl moiety did not display mesogenic properties. Meanwhile, series **d** did not exhibit any liquid crystalline phase due to the effect of methoxy group on molecule. All of the compounds in the first series (**c1-c8**) have high thermal stability and did not show significant decomposition below 400°C in nitrogen atmosphere. UV-vis results showed strong peak at 281-283 nm and weak peak at 362–363 nm and fluorescence intensity of the resultant compound was in the red region at 516-518 nm.

## 6.2 Suggestion for further research

The copolymers synthesized by polycondensation in this work only possess low molecular weights. Further investigation is required on the successful synthesized new types of polysilane by reacting same monomers with propargyl bromide to obtain diacetylene monomers followed by reacting with dichlorodimethylsilane by Greignard reaction to produce new copolymers of polysilylacetylene with high molecular weight and narrow polydispersity. The logical continuation of this work would be to scale up the production of the monomers and copolymers for various practical applications.

It is also interesting to synthesize new copolymers by adding dichlorodimethylsilane to the synthesized monomers to prepare polysiloxane and explore the novel mesomorphic and optical properties of the new copolymers.

## REFERENCES

1. Duerinckx, F. and Szlufcik, J., *Defect passivation of industrial multicrystalline solar cells based on PECVD silicon nitride*. Solar Energy Materials & Solar Cells, 2002. **72**: p. 231-246.
2. Semenov, V.V., *Preparation, properties and applications of oligomeric and polymeric organosilanes*. Russian Chemical Reviews, 2011. **80**(4): p. 313.
3. Uhlig, W., *Synthesis, functionalization, and cross-linking reaction of organosilicon polymers using silyl triflate intermediates*. Progress Polymer Science, 2002. **27**: p. 255-305.
4. Ohshita, J., Kangai, S., Tada Y., Yoshida, H., Sakamaki K., Kunai A., and Kunugi Y., *Synthesis of diarylenenaphthylene and diaryleneanthrylene containing organosilicon polymers and their applications to organic EL devices*. J. Organometallic Chemistry, 2007. **692**: p. 1020-1024.
5. Maeda, H., Nishimura, K-I, Mizuno, K., Yamaji, M., Oshima, J., and Tobita, S., *Synthesis and Photochemical Properties of Stilbenophanes Tethered by Silyl Chains. Control of (2 + 2) Photocyclo addition, Cis-Trans Photoisomerization, and Photocyclization*. Organic Chemistry, 2005. **24**: p. 9693-9701.
6. Nicola, C., Roberto, C., Lamberto, N., Francesco, P., and Giacomo, R., *Electrochemical synthesis of intrinsically conducting polymers of 3-alkylpyrroles*. Synthetic Metals, 1998. **92**(2): p. 139-147.
7. Liming, D. and William, W.J., *Morphology and electrical properties of polyacetylene-polyisoprene conducting copolymers*. Polymer, 1997. **38**(4): p. 775-783.
8. Brbdas, J.L., Silbey, R., Boudreaux, D.S., and Chance, R.R., *Chain-length dependence of electronic and electrochemical properties of conjugated systems: polyacetylene, polyphenylene, polythiophene, and polypyrrole*. J. American Chemical Society, 1983. **105**: p. 6555-6559
9. Bai, Y., Xu, Y., Wang, J., Gao, M., and Wang, J., *Interface effect on the electropolymerized polypyrrole films with hollow micro/nanohorn arrays*. J. American Chemical Society, 2014. **6**: p. 4693-4704.
10. Hsieh, B.R., Yu, Y., Forsythe, E.W., Schaaf, G.M., and Feld, W.A., *A New family of highly emissive soluble poly(p-phenylene vinylene) derivatives. A step toward fully conjugated blue-emitting poly(p-phenylene vinylenes)*. J. American Chemical Society, 1998. **120**: p. 231-232.
11. Foot, P.J.S. and Simon, R., *Electrochromic properties of conducting polyanilines*. Journal of Physics D: Applied Physics 1989. **22**: p. 1598-1608.
12. Mark, J.E., Allcock, H.R., and West, R., *Inorganic Polymers* 2nd ed, 2004, New York Oxford University press.

13. Grunlan, M.A., Regan, K.R., and Bergbreiter, D.E., *Liquid/liquid separation of polysiloxane-supported catalysts*. Chemical Communications Issue, 2006, **16**: p. 1715-1717.
14. Jovanovic, J.D., Govedaricab, M.N., Dvornica, P.R., and Popovic, I.G., *The thermogravimetric analysis of some polysiloxanes*. Polymer Degradation and Stability, 1998. **61**(1): p. 87-93.
15. Stamatialis, D.F., Papenburg, B.J., Girones, M., Saiful, S., Bettahalli, S.N.M., Schmitmeier, S., and Wessling, M., *Medical applications of membranes: Drug delivery, artificial organs and tissue engineering*. J. Membrane Science, 2008. **308**: p. 1–34.
16. Liua, L. and Sheardown, H., *Glucose permeable poly (dimethyl siloxane) poly (N-isopropyl acrylamide) interpenetrating networks as ophthalmic biomaterials*. Biomaterials, 2005. **26**(3): p. 233-244.
17. Giordano, G. and Refojo, M., *Silicone oils as vitreous substitutes*. Progress of Polymer Science., 1998. **23**: p. 509-532.
18. Paluszkiewicz, C., Gumuła, T., Podporska, J., and Błazewicz, M., *Structure and bioactivity studies of new polysiloxane-derived materials for orthopedic applications*. J. Molecular Structure, 2006. **792**: p. 176-181.
19. Colas, A. and Courts, J., *Silicone biomaterials: history and chemistry & medical application of silicone*. 2<sup>nd</sup> ed. 2005: Elsevier.
20. Thein-Han, W.W., Shah, J., and Misra, R.D.K., *Superior in vitro biological response and mechanical properties of an implantable nanostructured biomaterial: Nanohydroxyapatite–silicone rubber composite*. Acta Biomaterialia, 2009. **5**: p. 2668-2679.
21. Shansong, M., Mei, T., Shunqing, T., and Changren, Z., *Improvement of blood compatibility of silicone rubber by the addition of hydroxyapatite*. J. Material Science Letter, 2003. **22**(5): p. 343-344.
22. Fallahi, D., Mirzadeh, H., and Khorasani, M.T., *Physical, mechanical, and biocompatibility evaluation of three different types of silicone rubber*. J. Applied Polymer Science, 2003. **88**: p. 2522-2529.
23. Jeram, E.M. and Striker, R.A., *High Strength Organopolysiloxane Composition*, 1976. US Patent, 3,884,866.
24. Kumar, A., Abbott, N.L., Biebuyck, H.A., Kim, E., and Whitesides, G.M., *Patterned Self-Assembled Monolayers and Meso-Scale Phenomena*. Accounts of Chemical Research, 1995. **28**(5): p. 219-226.
25. Sarmiento, V.H.V., Schiavetto, M.G., Hammer, P., Benedetti, A.V., Fugivara, C.S., Suegama, P.H., Pulcinelli, S.H., and Santilli, C.V., *Corrosion protection of stainless steel by polysiloxane hybrid coatings prepared using the sol–gel process*. Surface and Coatings Technology, 2010. **204**(16-17): p. 2689-2701.

26. Liang, Y., Wang, H., Wang, D., Liu, H., and Feng, S., *The synthesis, morphology and liquid-crystalline property of polysiloxane-modified perylene derivative*. Dyes and Pigments, 2012. **95**: p. 260-267.
27. Fahem, Z. and Bauhofer, W., *Thiol-ene polymer based fast photo-curable gate insulator for organic field effect transistors*. Microelectronic Engineering, 2013. **105**: p. 74-76.
28. Apfel, M.A., Finkelmann, H., Janini, G.M., Laub, R.J., Luehmann, B.H., Price, A., W. L. Roberts, Shaw, T.J., and Smith, C.A., *Synthesis and properties of high-temperature mesomorphic polysiloxane (MEPSIL) solvents: biphenyl- and terphenyl-based nematic systems*. Analytical Chemistry, 1985. **57**(3): p. 651-658.
29. Neyer, A., Kopetz, S., Rabe, E., Kang, W.J., and Tombrink, S., *Electrical-optical circuit board using polysiloxane optical waveguide layer* Electronic Components and Technology. Conference, 2005. **7**: p. 246- 250.
30. Chen, J., Xie, Z., Lam, J.W.Y., Law, C.C.W., and Tang, B.Z., *Silole-Containing Polyacetylenes. Synthesis, Thermal Stability, Light Emission, Nanodimensional Aggregation, and Restricted Intramolecular Rotation*. Macromolecules, 2003. **36**(4): p. 1108-1117.
31. Chen, J., Law, C.C.W., Lam, J.W.Y., Dong, Y., Lo, S.M.F., Williams, I.D., Zhu, D., and Tang, B.Z., *Synthesis, Light Emission, Nanoaggregation, and Restricted Intramolecular Rotation of 1,1-Substituted 2,3,4,5-Tetraphenylsiloles*. Chemistry of Materials, 2003. **15**(7): p. 1535-1546.
32. Tamao, K., Uchida, M., Izumizawa, T., Furukawa, K., and Yamaguchi, S., *Silole Derivatives as Efficient Electron Transporting Materials*. J. American Chemical Society, 1996. **118**: p. 11974-11975.
33. Ohshita, J., Kunai, A., Kai, H., Ohta, N., Adachi, A., Takata, A., Komaguchi, K., Sakamaki, K., Iida, T., Shiotani, M., and Okita, K., *Effects of Conjugated Substituents on the Optical, Electrochemical, and Electron-Transporting Properties of Dithienosiloles*. Organometallics, 2001. **20**: p. 4800-4805.
34. Geramita, K., McBee, J., Shen, Y., Radu, N., and Tilley, T.D., *Synthesis and characterization of perfluoroaryl-substituted siloles and thiophenes: a series of electron-deficient blue light emitting materials*. Chemistry of Materials, 2006. **18**(14): p. 3261–3269.
35. Yamaguchi, S., Endo, T., Uchida, M., Izumizawa, T., Furukawa, K., and Tamao, K., *Toward new materials for organic electroluminescent devices: synthesis, structures, and properties of a series of 2, 5-Diaryl-3,4-diphenylsiloles*. Chemistry - A European Journal, 2000. **6**: p. 1683-1692.
36. Toal, S.J. and Trogler, W.C., *Polymer sensors for nitroaromatic explosives detection*. J. of Material Chemistry, 2006. **16**: p. 1871-1883.

37. Sohn, H., Huddleston, R.R., Powell, D.R., and West, R., *An electroluminescent polysilole and some dichlorooligosiloles*. American Chemical Society, 1999. **121**: p. 2935-2936.
38. Rulkens, R., Lough, A.J., and Manners, I., *Anionic ring-opening oligomerization and polymerization of silicon-bridged [1]ferrocenophanes: characterization of short-chain models for poly(ferrocenyliane) high polymers*. American Chemical Society, 1994. **116**: p. 791-198.
39. Fossum, E. and Matyjaszewski, K., *Polysilane-Poly(ferrocenyliane) Random Copolymers*. *Macromolecules*, 1996. **28**: p. 401-402.
40. Kepler, R.G., Zeigler, J.M., Harrah, L.A., and Kurtz, S.R., *Photocarrier generation and transport in  $\sigma$ -bonded polysilanes*. *Physical Review B*, 1987. **35**(6): p. 2818-2822.
41. Kobayashi, T., Hatayama, K., Suzuki, S., Abe, M., Watanabe, H., Kijima, M., and Shirakawa, H., *Preparation of substituted network polysilanes and their electrical conductivities*. *Organometallics*, 1998. **17**: p. 1646-1648.
42. Hasegawa, T., Iwasa, Y., Koda, T., Kishida, H., Tokura, Y., Wada, S., Tashiro, H., Tachibana, H., Matsumoto, M., and Miller, R.D., *Nonlinear optical spectroscopy on polysilanes: Dependence of exciton states on polymer backbone conformations*. *Synthetic Metals*, 1995. **71**(1-3): p. 1679-1680.
43. Burkhar, C.A., *Polydimethylsilanes*. American Chemical Society, 1949. **71**: p. 963.
44. SU, K., Remsen, E.E., Zank, G.A., and Sneddon, L.G., *Synthesis, characterization, and ceramic conversion reactions of borazine-modified hydridopolysilazanes: new polymeric precursors to SiNCB ceramic composites*. *Chemistry of Materials*, 1993. **5**: p. 547-556.
45. Weinmann, M., Schuhmacher, J., Kummer, H., Prinz, S., Peng, J., Seifert, H.J., Christ, M., Muller, K., Bill, J., and Aldinger, F., *Synthesis and thermal behavior of novel Si-B-C-N ceramic precursors*. *Chemistry of Materials*, 2000. **12**: p. 623-632.
46. Krüger, C.R. and Rochow, E.G., *Polyorganosilazanes*. *J. of Polymer Science*, 1964. **2**(7): p. 3179-3189.
47. Vabreek, W., *Production of shaped articles of homogenous mixture of silicon carbide and nitride* 1974, p.78-101.
48. Winter, G., Vabreek, W., and mansmann, M., *Production of Shaped Articles of Silicon Carbide and Silicon Nitride*, 1974, US. patent, 3,892,583.
49. Bianconi, P.A. and Weidman, T.W., *Poly(n-hexylsilylene): synthesis and properties of the first alkyl silicon [RSi]<sub>n</sub> network polymer*. American Chemical Society, 1988. **110**(7): p. 2342-2344.

50. Bianconi, P.A., Schilling, F.C., and Weidman, T.W., *Ultrasound-mediated reductive condensation synthesis of silicon-silicon-bonded network polymers*. *Macromolecules*, 1989. **4**(22): p. 1697-1704.
51. Smith, D.A., Freed, C.A., and Bianconi, P.A., *Functionalization of polysilyne networks for enhanced surface properties*. *Chemistry of Materials*, 1993. **5**(3): p. 245-247.
52. Wilson, W.L. and Weidman, T.W., *Radiative recombination and vibronic relaxation in  $\pi$ -delocalized silicon-backbone-network polymers: Energy thermalization in poly(*n*-hexylsilyne)*. *Physical Review B*, 1993. **48**(4): p. 2169-2174.
53. Hornak, L.A. and Weidman, T.W., *Propagation loss of index imaged poly(cyclohexylsilyne) thin film optical waveguides*. *Applied Physical Letters*, 1993. **62**(9): p. 913-915.
54. Hornak, L.A., Weidman, T.W., and Kwock, E.W., *Polyalkylsilyne photodefined thin-film optical waveguides*. *J. of Applied Physics*, 1990. **67**(5): p. 2235 - 2239.
55. Kunz, R.R., Bianconi, P.A., Horn, M.W., Paladugu, R.R., Shaver, D.C., Smith, D.A.M., and Freed, C.A., *Polysilyne resists for 193 nm excimer laser lithography*. *J. of Vacuum Science & Technology B*, 1991. **9**: p. 1447-1466.
56. Walree, C.A.v., Cleij, T.J., Jenneskens, L.W., and Vlietstra, E.J., *Structural, photophysical, and conductive properties of *n*-Hexyl substituted hybrid polysilylene-polysilyne networks*. *Macromolecules*, 1996. **29**(23): p. 7362-3737.
57. Pitcher, M.W., Joray, S.J., and Bianconi, P.A., *Smooth continuous films of stoichiometric silicon carbide from poly(methylsilyne)*. *Advance Materials*, 2004. **16**(8): p. 706-709.
58. Watanabe, A., Nagai, Y., and Matsuda, M., *Amorphous silicon structure of heat-treated poly(*n*-propylsilyne) studied by far-infrared spectroscopy*. *Chemistry Physical Letters*, 1993. **207**(2): p. 132-136.
59. Watanabe, A., Komatsubara, T., Ito, O., and Matsuda, M., *SiC/SiO<sub>2</sub> micropatterning by ultraviolet irradiation and heat treatment of a poly(phenylsilyne) film*. *J. of Applied Physics*, 1995. **77**(6): p. 2796-2800.
60. Manhart, S.A., Adachi, A., Sakamaki, K., Okita, K., Ohshita, J., Ohno, T., Hamaguchi, T., Kunai, A., and Kido, J., *Synthesis and properties of organosilicon polymers containing 9,10-diethynylanthracene units with highly hole-transporting properties*. *Organometallic Chemistry*, 1999. **592**(1): p. 52-60.
61. Nguyen, P., Gómez-Elipé, P., and Manners, I., *Organometallic polymers with transition metals in the main chain*. *Chemical Reviews*, 1999. **99**(6): p. 1515-1548.
62. Wong, W.-Y., Poon, S.-Y., Shi, J.-X., and Cheah, K.-W., *Synthesis, optical properties, and photoluminescence of organometallic acetylide polymers of*

- platinum functionalized with Si and Ge-bridged bis(3,6-diethynyl-9-butylcarbazole)*. J. of Inorganic and Organometallic Polymers and Materials, 2007. **17**(1): p. 189-200.
63. Ohshita, J. and Kunai, A., *Polymers with alternating organosilicon and -conjugated units*. Acta Polymer, 1999. **49**(8): p. 379-403.
64. Ohshita, J., Nada, D., Tada, Y., Kimura, Y., Yoshida, H., Kunai, A., and Kunugi, Y., *Sonogashira coupling of diethynylsilane and dibromoarene in wet solvent for the formation of poly[(ethynylenearylene)-co-(diethynylenesilylenearylene)]*. J. of Organometallic Chemistry, 2005. **260**(17): p. 3951–3956.
65. Wang, R., Fang, L., and Xu, C., *Synthesis, characterization, and thermal properties of new silarylene–siloxane–acetylene polymers*. European Polymer, 2010. **46**(3): p. 465-471.
66. Han, W.J., Ye, L., Hu, J.D., and Zhao, T., *Synthesis and kinetics of non-isothermal degradation of acetylene terminated silazane*. Chinese Chemical Letters, 2011. **22**(2): p. 139-142.
67. Homrighausen, C.L. and Keller, T.M., *High-temperature elastomers from silarylene-siloxane-diacetylene linear polymers*. J. of Polymer Science Part A: Polymer Chemistry, 2002. **40**(1): p. 88-94.
68. Yan, M., Tan, Y., Zhang, Z., Hu, J., and Xi, Z., *Synthesis and thermal properties of conjugated poly[(silylene)diacetylene silazanes]*. European Polymer, 2006. **42**(11): p. 3068-3077.
69. Noll, W., *Chemistry and technology of silicones* 1986, New York: Academic press INC p.113.
70. Tacke, R., *Organosilicon and bioorganosilicon chemistry: structure, bonding, and synthetic application* 1985, New York: John Wiley.
71. Yajima, S., Hayashi, J., Omori, M., and Okamura, K., *Development of a silicon carbide fibre with high tensile strength*. Letters to Nature, 1976. **261**: p. 683-685.
72. Yajima, S., Hayashi, J., and Omori, M., *Continuous silicon carbide fiber of high tensile strength*. Chemistry Letters, 1975. **2**(391-397).
73. Yajima, S., Hasegawa, Y., Okamura, K., and Matsuzawa, T., *Development of high tensile strength silicon carbide fibre using an organosilicon polymer precursor*. Letters to Nature, 1978. **273**: p. 525 - 527.
74. Bunsell, A.R. and Berger, M.-H., *Fine diameter ceramic fibres*. Journal of the European Ceramic Society, 2000. **20**: p. 2249±2260.
75. Soraru, G.D., Babonneau, F., and Mackenzie, J.D., *Structural evolutions from polycarbosilane to SiC ceramic*. Materials Science, 1990. **25**(9): p. 3886-3893.

76. Interrante, L.V., Liu, Q., Rushkin, I., and Shen, Q., *Poly(silylenemethylenes) — a novel class of organosilicon polymers*. J. of Organometallic Chemistry, 1996. **521**(1–2): p. 1-10.
77. Lienhard, M., Rushkin, I., Verdecia, G., Wiegand, C., Apple, T., and Interrante, L.V., *Synthesis and characterization of the new fluoropolymer poly(difluorosilylenemethylene); an analogue of poly(vinylidene fluoride)*. American Chemical Society, 1997. **119**: p. 12020-12021.
78. Sacarescu, G., Sacarescu, L., Ardeleanu, R., Marcu, M., and Voiculescu, N., *Polysilaanthracene synthesis*. European Polymer, 2000. **36**(10): p. 2089-2093.
79. Aleksander Filarowski, A.K., Tadeusz Głowiak, *Proton transfer equilibrium in the intramolecular hydrogen bridge in sterically hindered Schiff bases*. Molecular Structure, 2002. **615**: p. 97-108.
80. Rospenk, M., Król-Starzomska, I., Filarowski, A., and Koll, A., *Proton transfer and self-association of sterically modified Schiff bases*. Physical Chemistry, 2003. **287**: p. 113-124.
81. Koll, A. and Wolschann, P., *Mannich Bases as Model Compounds for Intramolecular Hydrogen Bonding II [1]. Structure and Properties in Solution*. J. of Chemistry and Material Science, 1999. 130 : p. 983-1001.
82. Shan, S.-o. and Herschlag, D., *The change in hydrogen bond strength accompanying charge rearrangement: Implications for enzymatic catalysis*. Biochemistry, 1996. **93**: p. 14474-14479.
83. Kim, K.S., Oh, K.S., and Lee, J.Y., *Catalytic role of enzymes: Short strong H-bond-induced partial proton shuttles and charge redistributions*. Biochemistry, 2000. **97** p. 6373-6378.
84. Fujiwara, T., Lee, J.-K., Zgierski, M.Z., and Lim, E.C., *Intramolecular charge transfer in the excited state of 4-dimethylaminobenzaldehyde and 4-dimethylaminoacetophenone*. Chemical Physics Letters, 2009. **481**: p. 78-82.
85. Lambi, E., Gegiou, D., and Hadjoudis, E., *Thermochromism and Photochromism of N-salidenebenzylamin and N-salicylidene-2-amino methylpyridine*. Photochemistry and Photobiology, 1995. **86**: p. 241-246.
86. Y., O.M. and Feher, G., *Proton transfer in reaction centers from photosynthetic bacteria*. Annu. Review Biochemistry, 1992. **61**: p. 861-896.
87. Zhang, N., Fan, Y.-h., Zhen Zhang, J.Z., Zhang, P.-f., Wang, Q., Liu, S.-b., and Bi, C.-f., *Syntheses, crystal structures and anticancer activities of three novel transition metal complexes with Schiff base derived from 2-acetylpyridine and l-tryptophan*. Inorganic Chemistry Communications, 2012. **22**: p. 68-72.
88. Vicini, P., Geronikaki, A., Incerti, M., Busonera, B., Poni, G., Cabras, C.A., and Colla, P.L., *Synthesis and Biological Evaluation of Benzo[d]isothiazole, Benzothiazole and Thiazole Schiff Bases*. Bioorganic & Medicinal Chemistry, 2003. **11**: p. 4785-4789.

89. Gwaram, N.S., Ali, H.M., Abdulla, M.A., Buckle, M.J.C., Sukumaran, S.D., Chung, L.Y., Othman, R., Alhadi, A.A., Yehye, W.A., Hadi, A.H.A., Hassandarvish, P., Khaledi, H., and Abdelwahab, S.I., *Synthesis, Characterization, X-ray Crystallography, Acetyl Cholinesterase Inhibition and Antioxidant Activities of Some Novel Ketone Derivatives of Gallic Hydrazone-Derived Schiff Bases*. *Molecules*, 2012. **17**: p. 2408-2427.
90. Odabaolu, M., Albayrak, Ç., Özkanca, R., Aykan, F.Z., and Lonecke, P., *Some polyhydroxy azo-azomethine derivatives of salicylaldehyde: Synthesis, characterization, spectroscopic, molecular structure and antimicrobial activity studies*. *Molecular Structure*, 2007. **840**: p. 71-89.
91. Jin, X., Wang, J., and Bai, J., *Synthesis and antimicrobial activity of the Schiff base from chitosan and citral*. *Carbohydrate Research*, 2009. **344**: p. 825-829.
92. Wadher, S.J., Puranik, M.P., Karande, N.A., and Yeole, P.G., *Synthesis and biological evaluation of Schiff base of Dapsone and their derivative as antimicrobial agents*. *J. of PharmaTech research*, 2009. **1**: p. 22-33.
93. Azas, N., Rathelot, P., Djekou, S., Delmas, F., Gellis, A., Giorgio, C.D., Vanelle, P., and Timon-David, P., *Ntiparasitic activity of highly conjugated pyrimidine-2,4-dione Derivatives*. *Il Farmaco*, 2003. **58**: p. 1263-1270.
94. S.N.Pandeya, Sriram, D., Nath, G., and Clercq, E.D., *Synthesis, antibacterial, antifungal and anti-HIV evaluation of Schiff and Mannich bases of isatin derivatives with 3-amino-2-methylmercaptoquinazolin-4(3H)-one*. *Pharmaceutica Acta Helvetiae*, 1999. **74**: p. 11-17.
95. Hng, T.-V., Mahmood, W.A.K., and Adnan, R., *Synthesis and mesomorphic properties of symmetrical dimers N,N-(3-methoxy-4-alkoxybenzylidene)-1,4-phenylenediamine*. *Molecular Crystals and Liquid Crystals*, 2006. **452**: p. 49-61.
96. Yeap, G.Y., Ha, S.T., Lim, P.L., Boey, P.L., Ito, M.M., Sanehisa, S., and Vill, V.S., *Synthesis, physical and mesomorphic properties of Schiff's base esters containing ortho-, meta- and para-substituents in benzylidene-4'-alkanoxyanilines*. *Molecular Crystals and Liquid Crystals*, 2006. **452**: p. 63-72.
97. So, B.-K., Kim, W.-J., Lee, S.-M., Jang, M.-C., Song, H.H., and Park, J.-H., *Novel bent-shaped liquid crystalline compounds: III. Synthesis of Schiff base liquid crystal dimmers*. *Dyes and Pigments*, 2007. **75**: p. 619-623.
98. Yilmaz-Canli, N., Bilgin-Eran, B., and Nesrullajev, A., *Synthesis, mesomorphic and physical properties of two new analogs of Schiff's base with an alkenic terminal chains*. *Molecular Structure*, 2011. **990**: p. 79-85.
99. R, G. and W, S., *Polymeric Schiff base complexes as solid phases in gas chromatography*. *J. of Chromatography*, 1982. **122**: p. 9-63.

100. Niu, H.-J., Huang, Y.-D., Bai, X.-D., and Li, X., *Novel poly-Schiff bases containing 4,4' -diamino-triphenylamine as hole transport material for organic electronic device*. *Materials Letters*, 2004. **58**(24): p. 2979-2983.
101. DN, D. and CL, T., *Schiff bases and their applications*. Science and Research, 1982. **41**: p. 6-501.
102. Bhuiyan, M.D.H., Teshome, A., Gainsford, G.J., Ashraf, M., Clays, K., Asselberghs, I., and Kay, A.J., *Synthesis, characterization, linear and non-linear optical (NLO) properties of some Schiff's bases*. *Optical Materials*, 2010. **32**: p. 669-672.
103. Adams, R., Bullock, J.E., and Wilson, W.C., *Contribution to the structure of benzidine*. American Chemical Society, 1923. **45**(2): p. 521-527.
104. Steinkopf, W. and Eger, N., *Thiophene series. XLII. Reactions of 3,4-dibromothiophene-2,5-dialdehyde*. *Liebigs Annalen Chemistry*, 1938. **533**: p. 270-278.
105. Marvel, C.S. and Hill, H.W., *Polyazines*. American Chemical Society, 1950. **72**(10): p. 4819-4820.
106. D'Alelio G.F., Crivello J.V., R.K., S., and Huemmer, T.F., *Polymeric Schiffbases. I. The synthesis and evaluation of polymeric Schiff bases prepared by Schiff base exchange reactions*. *Macromolecular Science Chemistry*, 1967. **A1**: p. 1161-1249.
107. D'Alelio, G.F., Crivello, J.V., and Dehner, T.R., Schoenig, R.K. *Polymeric Schiff bases. VII. Some parameters in the evaluation of the thermal stability of poly(p-xylylidene-p-phenylenediamine)*. *Macromolecular Science Chemistry*, 1967. **A1**(7): p. 1331-1364.
108. Burroughes, J.H., Bradley, D.D.C., Brown, A.R., Marks, R.N., Mackay, K., Friend, R.H., Burns†, P.L., and Holme, A.B., *Light-emitting diodes based on conjugated polymers*. *Nature*, 1990. **347**(6293): p. 539-541.
109. Nalwa, H.S., *Handbook of Conductive Molecules and Polymers*, 1997, New York: John Wiley and Sons: 728-739.
110. Skotheim, T.A., Elsenbaumer, R.L., and Reynolds, J.R., *Handbook of conducting polymers*. 2<sup>nd</sup> ed. 1998, New York.
111. Li, X., Li, C., and Li, S., *Synthesis, characterization and electrical properties of soluble conjugated poly-Schiff bases*. *Synthetic Metals*, 1993. **60**(3): p. 285-288.
112. Lee, Y.K. and Jang, S.M., *Synthesis and electrical conductivity of polyazomethines-I*. *Chemical Abstract*, 1986. **10**(2): p. 125-133.
113. El-Shekeil, A.G., Khalid, M.A., and Al-Yusuf, F.A., *A Comparative Study of Some Undoped Aromatic Polyazomethines*. *Macromolecular Chemistry and Physics*, 2001. **202**(15): p. 2971-2979.

114. Yang, C.-J. and Jenekhe, S.A., *Conjugated Aromatic Polyimines. 2. synthesis, structure, and properties of new aromatic polyazomethines*. *Macromolecules*, 1995. **28**(4): p. 1180-1196.
115. Yang, C.J. and Jenekhe, S.A., *Conjugated aromatic poly(azomethines). 1. Characterization of structure, electronic spectra, and processing of thin films from soluble complexes*. *Chemistry of Materials*, 1991. **3** (5): p. 878-887.
116. Li, W. and Wan, M., *Electrical and magnetic properties of conjugated schiff base polymers*. *J. of Applied Polymer Science*, 1996. **62**(6): p. 941-950.
117. El-Shekeil, A.G., Al-Saady, H.A., and Al-Yusufy, F.A., *Synthesis and characterization of some soluble conducting polyazomethine polymers*. *Polymer International*, 1997. **44**(1): p. 78-82.
118. El-Shekeil, A.G., Al-Saady, H.A., and Al-Yusufy, F.A., *Synthesis and characterization of some soluble conducting polyazomethine polymers*. *New Polymeric Materials*, 1998. **5**(2): p. 131-140.
119. D'Sa, J.T., Rao, V.J., Patel, K.C., and Patel, R.D., *Magnetic and electrical properties of chelate polymers*. *Macromolecular Chemistry*, 1978. **68**(1): p. 17-21.
120. Grigoras, M. and Catanescu, C.O., *Imine oligomers and polymers*. *J. of Macromolecular Science, Part C: Polymer Reviews*, 2004. **C44**(2): p. 131-173.
121. Sprung, M.A., *A Summary of the Reactions of Aldehydes with Amines*. *Chemistry Reviews*, 1940. **26** (3): p. 297-338.
122. Suematsu, K., Nakamura, K., and Takeda, J., *Polyimine, a C= N Double Bond Containing Polymers: Synthesis and Properties*. *Polymer*, 1983. **15**(1): p. 71-79.
123. Simionescu, C.I., Cianga, I., Duca, M.I.A., Cocarla, I., and Grigoras, M., *Synthesis and electrochemical polymerization of some monomers with Schiff base or vinylene structures and thiophene moieties*. *European Polymer*, 1999. **35** p. 587-599.
124. Simionescu, C.I., Grigoras, M., Cianga, I., Diaconu, I., and Farcas, A., *Chemical synthesis of some Schiff base-type polymers containing pyrrole units*. *Polymer Bulletin*, 1994. **32**(3): p. 257-264.
125. Simionescu, C.I., Grovu-Ivanoiu, M., Grigoras, C.M., Duca, A., and Cocarla, I., *Electrochemical polymerization of some monomers with schiff's base structure. A voltammetric study*. *Macromolecules Chemistry*, 1996. **239**(1): p. 1-12.
126. Simionescu, C.I., Grigoras, M., Cianga, I., and Olaru, N., *Synthesis of new conjugated polymers with Schiff base structure containing pyrrolyl and naphthalene moieties and HMO study of the monomers reactivity*. *European Polymer*, 1998. **34**(7): p. 891-898.

127. Tanaka, S., Sato, M., and Kariyama, K., *Electrochemical polymerization of dithienylethylene, -butadiene, and hexatriene*. . Macromolecular Chemistry, 1985. **186**: p. 1685-1694.
128. Destri, S., Porzio, W., and Dubitsky, Y., *Design preparation and properties of regularly alternating conjugated low molecular weight copolymers based on thienylene-azomethine moieties*. Synthetic Metals, 1995. **75**(1): p. 25-36.
129. Grigoras, M., Stoica, G., Cianga, I., and Simionescu, C.I., *Synthesis and characterization of some pyrrole-based aldimine monomers*. Revue roumaine de chimie, 1997. **42**(10): p. 993-998.
130. Morgan, P.W., Kwolek, S.L., and Pletcher, T.C., *Aromatic azomethine polymers and fibers*. Macromolecules, 1987. **20**: p. 729-739.
131. Hattori, K., Kagawa, K., Iguchi, M., and Matsumoto, K., *Molecular composite material composed of polyazomethine and thermoplastic polymer* Chemistry abstract, 1996. **126**: p. 144987.
132. Hattori, T. and Kagawa, K., *Molecular composite material composed of liquid crystal polymer and thermoplastic polymer and method for producing the blend in 5 565530*, U.S. Patent, Editor 1997. p. 212872.
133. Hattori, K., Kagawa, K., M. Iguchi, M., and Matsumoto, K., *Polymer composites materials of liquid crystalline polyazomethines, polycarbonate, and polyarylates and their manufacture*. Chemistry Abstract, 1997. **22**: p. 128-138.
134. Wiff, D.R., Lenke, G.M., and Fleming, P.D., *In situ thermoset molecular composites*. J. of Polymer Science Part B: Polymer Physics, 1994. **32**(16): p. 2255-2265.
135. Cerrada, P., Oriol, L., Pinol, M., and Serrano, J.L., *Copper-containing semiflexible hydroxypolyazomethines: metallomesogenic units inducing enhanced mechanical properties*. American Chemical Society, 1997. **119**(32): p. 7581-7582.
136. Jain, S.R., Murthy, K.N., and Thanoo, B.C., *Ignition delay studies on hypergolic fuel grains*. Defence Science, 1988 **38**: p. 273-286.
137. Al-Mehana, W.N.A., Yahya, R., Sonsudin, F., and Loa, K.M., *(E,E)-1,2-Bis[3-(prop-2-yn-1-yloxy)-benzylidene]hydrazine*. Acta Crystallographica Section E, 2012. **E68** p. o2087.
138. Al-Mehana, W.N.A., Yahya, R., and Lo, K.M., *(E,E)-1,2-Bis[4-(prop-2-yn-1-yloxy)-benzylidene]hydrazine*. Acta Crystallographica Section E, 2011. **E67**: p. o2900.
139. Al-Mehana, W.N.A., Shakir, R.M., Yahya, R., Halim, S.N.A., and Tiekink, E.R.T., *(E,E)-1,2-Bis[3-methoxy-4-(prop-2-yn-1-yloxy)benzylidene]hydrazine*. Acta Crystallographica Section E, 2011. **E67** p. o1659.

140. Griffiths, P.R. and Haseth, J.A.d., *Fourier transform infrared spectrometry*. 2<sup>nd</sup> ed. 2007, Hoboken, New Jersey: John Wiley & Sons.
141. Smith, I.C.P. and Blandford, D.E., *Nuclear magnetic resonance spectroscopy*. Analysis Chemistry, 1995. **67**(12): p. 509-518.
142. Steven, M.P., *Polymer chemistry*. 3<sup>rd</sup> ed. 1999, New York: Oxford university press.
143. Rabek, J.F., *Experimental methods in polymer chemistry : physical principles and applications*, 1980, New York: Wiley-Interscience.
144. Michalski, J., Kucharska, E., Sa, siadek, W., Lorenc, J., and Hanuz, J., *Intra- and inter-molecular hydrogen bonds, conformation and vibrational characteristics of hydrazo-group in 5-nitro-2-(2-phenylhydrazinyl)pyridine and its 3-, 4- or 6-methyl isomers*. Spectrochimica Acta Part A: Molecular and Biomolecular Spectroscopy, 2013. **112**: p. 263-275.
145. Stuart, B.H., *Infrared spectroscopy: fundamentals and application*, 2000, Sydney, Australia John Wiley &son, Ltd. 632-654.
146. Subramaniana, N., Sundaraganesanc, N., and Jayabharathi, J., *Molecular structure, spectroscopic (FT-IR, FT-Raman, NMR, UV) studies and first-order molecular hyperpolarizabilities of 1,2-bis(3-methoxy-4-hydroxy benzylidene) hydrazine by density functional method*. Spectrochimica Acta Part A: Molecular and Biomolecular Spectroscopy, 2010. **76**: p. 259-269.
147. Wang, C., Shieh, S., LeGoff, E., and Kanatzidis, M.G., *Synthesis and Characterization of A New Conjugated Aromatic Poly(azomethine) Derivative Based on the 3',4'-Dibutyl- -Terthiophene Building Block*. Macromolecules, 1996. **29**(9): p. 3147-3156.
148. Iwan, A., Rannou, P., Janeczek, H., Palewicz, M., Hreniak, A., Bilski, P., Oswald, F., and Pocięcha, D., *Liquid-crystalline phases formed by symmetrical azines with different terminal chains: Thermal, optical and electrical study*. Synthetic Metals, 2010. **160**: p. 859-865.
149. Mihai, I., Ivanoiu, M., Vacareanu, L., and Grigoras, M., *Polyazomethines with Triphenylamine Groups Synthesized by Suzuki Polycondensation Reactions*. Designed Monomers and Polymers, 2012. **15**: p. 41-52.
150. Robert M. Sclverstein, F.X.W., *Spectrometric Identification Of Organic Compounds*, ed. sixth 1998, New York: Jon Wiley & Sons Inc. . 90-91.
151. Issam, A.M. and Ismail, J., *New aromatic poly(azomethine urethane)s containing o-tolidine moiety in the polymer backbone*. Designed Monomers and Polymers, 2006. **9**(3): p. 237-246.
152. Reddy, K.R., Raghu, A.V., Jeong, H.M., and Siddaramaiah, *Synthesis and characterization of pyridine-based polyurethanes*. Designed Monomers and Polymers, 2009. **12**: p. 109-118.

153. Qu, Y. and Sun, X.-M., *(E,E')*-4-Hydroxy-3-methoxybenzaldehyde azine. *Acta Crystallographica Section E*, 2005. **E61**: p. o3828-o3830.
154. Al-mehana, W.N.A., Yahya, R., Sonsudin, F., Al-Mehanac, I.N.A., and Loa, K.M., 2,20-Diethoxy-4,40-[(E,E)-hydrazinediylidenebis(methanylylidene)] *diphenol*. *Acta Crystallographica Section E*, 2012. **E68**: p. o2990.
155. Brown, W.H., Foote, C.S., Iverson, B.L., and Eric V. Anslyn (2009): (pp 420-422), t.e., *Organic chemistry*. 5<sup>th</sup> ed, 2009, United States of America.
156. Blanksby, S.J. and Ellison, G.B., *Bond dissociation energies of organic molecules*. *Accounts of Chemical Research*, 2003. **36**(4): p. 255-263.
157. Radhakrishnan, S., Subramanian, V., and Somanathan, N., *Structure–optical, thermal properties studies on thiophene containing benzothiazole groups*. *Organic Electronics*, 2004. **5**(5): p. 227-235.
158. Kaya, I. and Kamaci, M., *Synthesis, optical, electrochemical, and thermal stability properties of poly(azomethine-urethane)s*. *Progress in Organic Coatings*, 2012. **74**: p. 204-214.
159. Valenti, N., Mijin, D., Ušumli, G., Marinković, A., and Petrović, S., *Solvent and substituent effect on electronic spectra of N-(4-substituted phenyl)-2,3-diphenylpropanamides*. *Arkivoc*, 2006. **891**: p. 81-90.
160. He, Q.-Y., Lai, W.-Y., Ma, Z., Chen, D.-Y., and Huang, W., *Novel blue light-emitting hyperbranched polyfluorenes incorporating carbazole kinked structure*. *European Polymer Journal*, 2008. **44**: p. 3169-3176.
161. Vishnumurthy, K.A., Sunitha, M.S., Safakath, K., Philip, R., and Adhikari, A.V., *Synthesis, electrochemical and optical studies of new cyanopyridine based conjugated polymers as potential fluorescent materials*. *Polymer*, 2011. **52**(19): p. 4174–4183.
162. Kaya, I. and Kamaci, M., *Synthesis, optical, electrochemical, and thermal stability properties of poly(azomethine-urethane)s*. *Progress in Organic Coatings*, 2012. **74**(1): p. 204-214.
163. Liu, G., Pu, S., Wang, X., Liu, W., and Yang, T., *Effects of substitution on the optoelectronic properties of photochromic diarylethenes bearing a pyrrole moiety*. *Dyes and Pigments*, 2011. **90**(1): p. 71-81.
164. Fu, H.-Y., Sun, X.-Y., Gao, X.-d., Xiao, F., and Shao, B.-X., *Synthesis and characterization of benzothiazole derivatives for blue electroluminescent devices*. *Synthetic Metals*, 2009. **159**(3-4): p. 254-259.
165. Stylianakis, M.M., Mikroyannidis, J.A., Dong, Q., Pei, J., Liu, Z., and Tian, W., *Synthesis, photophysical and photovoltaic properties of star-shaped molecules with triphenylamine as core and phenylethenylthiophene or dithienylethylene as arms*. *Solar Energy Materials & Solar Cells*, 2009. **93**: p. 1952-1958.

166. Tamilavan, V., Song, M., Kang, J.-W., and Hyun, M.H., *Facile synthesis of 1-(2,6-diisopropylphenyl)-2,5-di(2-thienyl)pyrrole-based narrow band gap small molecules for solar cell applications*. *Synthetic Metals*, 2013. **176**: p. 96-103.
167. Zhang, X.H., Lai, W.Y., Gao, Z.Q., Wong, T.C., Lee, C.S., Kwong, H.L., Lee, S.T., and Wu, S.K., *Photoluminescence and electroluminescence of pyrazoline monomers and dimers*. *Chemical Physics Letters*, 2000. **320**(1-2): p. 77-80.
168. Lai WY, H., QY, Zhu R, Chen QQ, Huang W, *Kinked star-shaped flourene/triazatruxene co-oligmer hybrids with enhanced functional properties for high performance , solution processed, blue organic light-emitting modes*. *Advance Function matererials*, 2008. **18**: p. 76-265.
169. Graham, W.T.S. and Fryhle, C.B., *Organic chemistry. (pp 477-497). United States of America: John Wiley & Sons Inc.* 2000.
170. Chen, B.K., Tsay, S.Y., and Shih, I.C., *Synthesis of copolyimide containing fluorine and naphthalene with synergizing effect on dielectric constants*. *Polymer Bulletin*, 2005. **54**(1): p. 39-46.
171. Pan, G., Du, Z., Zhang, C., Li, C., Yang, X., and Li, H., *Synthesis, characterization, and properties of novel novolac epoxy resin containing naphthalene moiety*. *Polymer*, 2007. **48**(13): p. 3686-3693.
172. Jaffé, H.H., Yeh, S.-J., and Gardner, R.W., *The electronic spectra of azobenzene derivatives and their conjugate acids*. *J. Molecular Spectroscopy*, 1958. **2**(1-6): p. 120-136.
173. Collings, P.J. and Hird, M., *Introduction to liquid crystal: chemistry and physics* 1997: Taylor & Francis.
174. N. A. Shurpo, M.S.V., N. V. Kamanina, *Technical Physics Letters*, 2010. **36**( 4): p. 319-321.
175. Petti, L.R., M.; Fiore, A.; Manna, L.; Mormile, P., *Optically induced light modulation in an hybrid nanocomposite system of inorganic CdSe/CdS nanorods and nematic liquid crystals*. *Optical Materials*, 2010. **32**(9): p. 1011-1016.
176. D. Demus, J.G., G.W. Gray, et al., *Handbook of Liquid Crystals*. 1998 Wiley-VCH., **2a** (Chapter 3).
177. F. Simoni, O.F., *Effects of light on molecular orientation of liquid crystals*. *Physica B*, 1999. **11**: p. 439-487.
178. L. Sirleto, L.P., P. Mormile, G.C. Righini, G. Abbate, *Fast integrated electrooptical switch and beam deflector based on nematic liquid crystal waveguides*,. *Fiber Integrated Optics*, 2002. **21**: p. 435-449.
179. I. C. Khoo, S.S., B. D. Guenther, Min-Yi Shih, P. Chen, and W. V. Wood, *Optically induced space-charge fields, dc voltage, and extraordinarily large nonlinearity in dye-doped nematic liquid crystals*. *Optical Letters*, 1998. **23**(4): p. 253-255.

180. Peccianti, M. and Assanto, G., *Nematicons*. Physics Reports. 1997, **516**: p. 147-208.
181. Reinitzer, F., *Beiträge zur kenntniss des cholesterins*. Monatshefte für Chemie und verwandte Teile anderer Wissenschaften, 1988. **9**(1): p. 421-441.
182. Lehmann, O., *Fliebende kristalle*. Physical chemistry, 1989. **4**(462-468).
183. Sluckin, T.J., Dunmur, D.A., and Stegemeyer, H., *Crystals that flow: classic papers from the history of liquid crystals* 2004: Taylor & Francis.
184. Gray, G.W., *Molecular Structure and the Properties of Liquid Crystals* 1962: Academic Press.
185. Kelker, H. and Scheurle, B., *A Liquid-crystalline (Nematic) Phase with a Particularly Low Solidification Point*. Angewandte Chemie International Edition in English, 1969. **8**(11): p. 884-885.
186. Vanne, K.C., *Liquid crystals: A survey and bibliography of their optical and electro-optical applications* Optics & Laser Technology, 1973. **5**(4): p. 87-91.
187. Castellano, J.A., *Fundamentals of liquid crystals and other liquid display technologies*. Optics & Laser Technology 1975. **7**(6): p. 259-265.
188. Gennes, P.-G.d. and Prost, J., *The physical of liquid crystals.*, 1993, 2nd ed Oxford University Press.
189. Bahadur, B., *Liquid crytals application and uses*. 1990, World Scientific Publishing.
190. Dierking, I., *Texture of liquid crystals*. 2003, United Kingdom: Wiley-Vch Verlag.
191. Chia, W.-L., Shen, S.-W., and Lin, H.-C., *Novel synthesis of liquid crystalline compounds of 5-substituted 2-(4-alkylphenyl)pyridines*. Tetrahedron Letters, 2001. **42**: p. 2177-2179.
192. Koh, T.M., Ha, S.T., Lee, T.L., Lee, S.L., Yeap, G.Y., Lin, H.C., and Subramaniam, R.T., *Synthesis and mesomorphic evaluation of new calamitic liquid crystals containing benzothiazole core*. Chinese Chemical Letters, 2011. **22**: p. 619-622.
193. Rao, G.K., Kumar, A., Singh, M.P., Kumar, A., and Biradar, A.M., *Influence of pendent alkyl chains on Heck and Sonogashira C–C coupling catalyzed with palladium(II) complexes of selenated Schiff bases having liquid crystalline properties*. Organometallic Chemistry, 2014. **753**, : p. 42-47.
194. Lutfor, M.R., Hegde, G., Kumar, S., Tschierske, C., and Chigrinov, V.G., *Synthesis and characterization of bent-shaped azobenzene monomers: Guest–host effects in liquid crystals with azo dyes for optical image storage devices*. Optical Materials, 2009. **32**: p. 176-183.

195. Levert, E., Lacelle, S., Zysman-Colman, E., and Soldera, A., *Influence of molecular structure on phase transitions in liquid crystal binary mixtures: The role of the orientation of the central ester*. J. Molecular Liquids, 2013. **183**: p. 59-63.
196. Vasconcelos, U.B., Schrader, A., Vilela, G.D., Borges, A.C.A., and Merlo, A.A., *Buchwald protocol applied to the synthesis of N-heterotolan liquid crystals*. Tetrahedron, 2008. **64**: p. 4619-4626.
197. Khoo, C., *Liquid crystals* 2007, New Jersey: John Wiley & Sons, p144-156.
198. Singh, S., *Liquid Crystal fundamental*. 3rd ed, 2001, New York: Plenum Press.
199. Castellano, J.A., *Liquid Gold: The Story of Liquid Crystal Displays and the Creation of an Industry*. 2005: World Scientific
200. Ma, J., Ye, X., and Jin, B., *Structure and application of polarizer film for thin-film-transistor liquid crystal displays*. Displays, 2001. **32**: p. 49-57.
201. Chandrasekher, S., *Liquid crystals* 1992, New York: Cambridge University Press.
202. Kamp, P.V.D., *The Physics of Liquid Crystals* 1974, Oxford Clarendon Press. 1-224.
203. Kumar, S., *Liquid Crystals: Experimental Study of Physical Properties and Phase Transitions*, 2001, New York: Cambridge University Press.
204. Priestley, E.B., Wojtowicz, P.J., and Sheng, P., *Introduction to liquid crystals* 1997, Princeton. New Jersey: Plenum Press.
205. Fornasieri, G., Guittard, F., and Gribaldi, S., *Influence of the structure of the mesogenic core on the thermotropic properties of v-unsaturated fluorinated liquid crystals*. Liquid Crystals, 2003. **30**: p. 251-257.
206. Singh, S., *Kiquid crystal fundamental* 3rd ed., 2001: World Scientific Publishing Co. Pte. Ltd.
207. Yeapa, G.-Y., Haa, S.-T., Lima, P.-L., Boeya, P.-L., Itob, M.M., Sanehisab, S., and Youheib, Y., *Synthesis, physical and mesomorphic properties of schiff base esters containing ortho-,meta- and para-substituents in benzylidene-4'-alkanoyloxyanilines*. Liquid Crystals and Molecules Crystals, 2006. **33**: p. 205-211.
208. Matsunaga, Y., Echizen, T., Hashimoto, K., and Nakamura, S.M., *Effects of terminal substituents on mesomorphic properties. 4-(4-x-substituted benzylideneamino) phenyl 4-y-substituted benzoates*. Molecular Crystals and Liquid Crystals Science and Technology. Section A, 1998. **325**(1): p. 197-207.
209. Karim, M.R., Sheikh, M.R.K., Salleh, N.M., Yahya, R., Hassan, A., and Hoque, M.A., *Synthesis and characterization of azo benzothiazole chromophore based liquid crystal macromers: Effects of substituents on benzothiazole ring and*

*terminal group on mesomorphic, thermal and optical properties* Materials Chemistry and Physics, 2013. **140**: p. 543-552.

210. Prajapati, A.K., Thakkar, V., and Bonde, N., *New Mesogenic Homologous Series of Schiff Base Cinnamates Comprising Naphthalene Moiety*. Molecular Crystals and Liquid Crystals, 2004. **393**: p. 41-48.
211. Yeap, G.-Y., Ooi, W.-S., Nakamura, Y., and Cheng, Z., *Synthesis and Mesomorphic Properties of Schiff Base Esters  $p$  -  $n$  - Octadecanoyloxybenzylidene-  $p$  -Cyano-,  $p$  -Hydroxy-,  $p$  -Nitro, And  $p$  -Carboxyanilines*. Molecular Crystals and Liquid Crystals, 2002. **381**: p. 169-178.
212. So, B.-K., Kim, W.-J., Lee, S.-M., Jang, M.-C., Song, H.H., and Park, J.-H., *Novel bent-shaped liquid crystalline compounds: III. Synthesis of Schiff base liquid crystal dimers*. Dyes and Pigments, 2007. **75**(3): p. 619-623.
213. Mohan, M.L.N.M., Goud, B.V.S., Kumar, P.A., and Pisipati, V.G.K.M., *Design and fabrication of an automated technique: measurement of spontaneous polarization in two new Schiff base ferroelectric liquid crystals* Materials. Research Bulletin, 1999. **34**: p. 2167-2175.
214. Paschke, R., Liebsch, S., Tschierske, C., Oakley, M.A., and Sinn, E., *Synthesis and Mesogenic Properties of Binuclear Copper(II) Complexes Derived from Salicylaldimine Schiff Bases*. Inorganic Chemistry, 2003. **42**(25): p. 8230-8240.
215. Pelzl, G., *Symmetry and Chirality in Liquid Crystals*. In: Handbook of Liquid Crystals, Demus, D., Goodby, J., Garg, G. W., Spicess, H.-W, & Vill, V. (Eds), Wiley: Weinheim, 2000. **2**: p. 128.
216. Madhusudana, N.V., Shashidhar. R., & Chandrasekhar, S. , *Molecular Crystals and Liquid Crystals*, 1971. **13**: p. 61.
217. Yeap, G.-Y., Hng, T.-C., Mahmood, W.A.K., Adnan, R., Ito, M.M., and Youhei, Y., *Synthesis and mesomorphic properties of symmetrical dimers  $N,N'$  -bis(3-methoxy-4-alkoxybenzylidene)-1,4-phenylenediamine*. Molecular Crystals and Liquid Crystals, 2006. **452**(1): p. 49-61.
218. Ooi, Y.-H., Yeap, G.-Y., and Takeuchi, D., *Synthesis, mesomorphic properties and structural studies on 1,3,5-trisubstituted benzene-based star-shaped derivatives containing Schiff base ester as the peripheral arm*. Molecular Structur, 2013. **1501**: p. 361-375.
219. Yeap, G.-Y., Heng, B.-T., Faradiana, N., Zulkifly, R., Ito, M.M., Tanabe, M., and Takeuchi, D., *Synthesis, molecular structures and phase transition studies on benzothiazole-cored Schiff bases with their Cu(II) and Pd(II) complexes: Crystal structure of (E)-6-methoxy-2-(4-octyloxy-2-hydroxybenzylidene amino)benzothiazole*. Molecular Structure, 2012. **1012**: p. 1-11.
220. Yeap, G.-Y., Mohammad, A.-T., and Osman, H., *Synthesis, spectroscopic and mesomorphic studies on heterocyclic liquid crystals with 1,3-oxazepine-4,7-*

dione, 1,3-oxazepane-4,7-dione and 1,3-oxazepine-1,5-dione cores. *Molecular Structur*, 2010. **982**(1-3): p. 33-44.

221. Yeap, G.-Y., Ooi, Y.-H., Kubo, K., and Ito, M.M., *Synthesis and mesomorphic properties of 4-(4-bromopropoxy)-40-(4-alkyloxybenzylidene)anilines*. *Chinese Chemical Letters*, 2012. **23**: p. 769-772.
222. Leube, H.F. and Finkelmann, H., *Optical investigations on a liquid-crystalline side-chain polymer with biaxial nematic and biaxial smectic A phase*. *Die Makromolekulare Chemie*, 1991. **192**(6): p. 1317-1328.
223. Kozmíka, V., Kuchař, M., Svoboda, J., Novotná, V., Glogarová, M., Baumeister, U., Dielec, S., and Pelzl, G., *Laterally substituted naphthalene-2,7-diol-based bent-shaped liquid crystals*. *Liquid Crystals*, 2005. **32**(9): p. 1151-1160.
224. Lee, S.K., Naito, Y., Shia, L., Tokita, M., Takezoe, H., and Watanabe, J., *Mesomorphic behaviour in bent-shaped molecules with side wings at different positions of a central naphthalene core*. *Liquid Crystals*, 2007. **34**(8).
225. Lee, S.K., Tokita, M., Shimbo, Y., Kang, K.-T., Takezoe, H., and Watanabe, J., *Ferroelectric and Antiferroelectric Behavior in Chiral Bent-shaped Molecules with an Asymmetric Central Naphthalene Core*. *Bulletin of the Korean Chemical Society*, 2007. **28**(12): p. 2241-2248.
226. Lee, S.K., Tokita, M., Takezoe, H., and Watanabe, J., *Effect of Molecular Structure on Smectic Phase Structures in Two Homologous Series of Bent-Shaped Molecules with Asymmetric Central Naphthalene Core*. *Ferroelectrics*, 2008. **365**(1): p. 1-11.
227. Prajapatia, A.K., Thakara, V., and Bondea, N., *New Mesogenic Homologous Series of Schiff Base Cinnamates Comprising Naphthalene Moiety*. *Molecular Crystals and Liquid Crystals*, 2003. **393**(1): p. 41-48.
228. Giménez, R., Millaruelo, M., Piñol, M., Serrano, J.L., Viñuales, A., Rosenhauer, R., Fischer, T., and Stumpe, J., *Synthesis, thermal and optical properties of liquid crystalline terpolymers containing azobenzene and dye moieties*. *Polymer*, 2005. **46**(22): p. 9230-9242.
229. Asir, S., Demir, A.S., Icil, H., *The synthesis of novel, unsymmetrically substituted, chiral naphthalene and perylene diimides: Photophysical, electrochemical, chiroptical and intramolecular charge*, *Dyes and Pigments*, 2010. **84** p. 1-13.
230. Pan, G., Du, Z., Zhang, C., Li, C., Yang, X., and Li, H., *Synthesis, characterization, and properties of novel novolac epoxy resin containing naphthalene moiety*. *Polymer*, 2007. **48**: p. 3686-3693.
231. Iwan, A., Janeczek, H., Jarzabek, B., and Rannou, P., *Mesomorphic behavior of symmetrical and unsymmetrical azomethines with two imine groups*. *Materials*, 2009. **2**: p. 38-61.

232. Iwan, A., Janeczek, H., Rannou, P., and Kwiatkowski, R., *Mesomorphic and optical properties of undoped and doped azomethines*. *Molecular Crystal*, 2009. **148**: p. 77-87.
233. Prajapati, A.K., Pandya, H.M., and Bonde, N.L., *Naphthyl azomesogens with lateral chloro groups*. *J. Chemical Science*, 2004. **116**(4): p. 227-233.
234. Perez, F., Jundeinstein, P., Bayle, J.-P., Roussel, F., and Fung, B.M., *The effect of a lateral aromatic branch on the orientational ordering of laterally alkoxy substituted nematics*. *Liquid Crystals*, 1997. **22**(6): p. 711-719.
235. Dewar, M.J.S. and Schroeder, J.P., *P-alkoxy- and p-carbalkoxybenzoates of diphenols. A new series of liquid crystalline compounds I*. *J. Organic Chemistry*, 1965. **30**(7): p. 2296-2300.
236. Dewar, M.J.S. and Goldber, R.S., *Effects of central and terminal groups on nematic mesophase stability*. *J. Organic Chemistry*, 1970. **35**: p. 2711-2715.